Dissertation zur Erlangung des Grades Doktor der Naturwissenschaften

- Dr. rer. nat. -

am Fachbereich Human- und Gesundheitswissenschaften

der Universität Bremen

Brain maturation throughout adolescence: An EEG study

vorgelegt von:

Annika Susann Wienke, M.Sc.

Bremen, Januar 2018

Universität Bremen*

* EXZELLENT.

Institut für Psychologie und Kognitionsforschung

Gutachter

PD Dr. Birgit Mathes,
Institut für Psychologie und Kognitionsforschung, Universität Bremen

Prof. Dr. Canan Başar-Eroğlu,
Institut für Psychologie und Kognitionsforschung, Universität Bremen

Datum des Promotionskolloquiums

26.Februar 2018

Contents

Abstract

Objective

Adolescence is characterised by a genuine interest in new experiences and an increased sense of responsibility. The aim of this study was to investigate changes in brain maturation that underlie task-relevant behaviour and the relation of these changes to novel impressions during the transition from childhood into adolescence and then young adulthood. We hypothesized that, with development, improved target detection abilities and reduced distractibility will be characterised by an increased involvement of frontal brain regions within the fronto-parietal brain network during novel processing and target detection.

Methods

In a cross-sectional study, a classical visual oddball task (*n = 159*) and a novelty visual oddball task (*n = 84*) were utilized in combination with EEG measurements to investigate brain maturation between late childhood and young adulthood (8 to 30 years of age). Developmental changes of late ERP components and concurrent delta (0.5–4 Hz) and theta (4–7 Hz) oscillations were analysed using regression models. Pre-stimulus amplitude and post-stimulus amplitude modulation, inter-trial phase coherence of local maxima and inter-electrode spatial phase coherence were assessed.

Results and Discussion

A general decline in reaction time and late ERP latency (novelty N2, P3a and P3b) with age was observed and may depend on task performance.

The frontal novelty N2 amplitude decreased while the P3a amplitude increased with age. This opposing developmental trend may relate to a compensatory mechanism for immature P3a-related cognitive functions, such as attention control.

The pre-stimulus amplitudes of delta and theta oscillations decreased while post-stimulus amplitude enhancements and inter-trial phase coherence increased with age. Both effects seem to underlie maturation of the P3b amplitude, even though this cannot be observed directly in ERP amplitude measurements.

Post-stimulus theta inter-electrode spatial phase coherence originating from frontal electrode sites increased with age during novel and target stimulus processing, indicating prolonged maturation of the fronto-parietal network that underlies target detection and novel processing.

Conclusion

Functional brain networks involving the frontal cortex, such as the fronto-parietal network, mature until young adulthood, thereby affecting slow-wave oscillations on a local and global scale alongside late frontal ERP components.

Brain maturation during adolescence may lead to a reduction of spontaneous slow-wave oscillations and an enhancement of amplitude modulation and regional and inter-regional precision of timing of event-related oscillations within the P3 time-window. Thus, brain maturation underlying task-related behaviour and reduced distractibility is versatile.

Significance

Combined analysis of developmental trajectories of late ERPs, concurrent changes in spontaneous and task-modulated brain oscillations and their embedding within functional brain networks (e.g., the fronto-parietal network) is important to estimate how brain maturation relates to abilities of cognitive control during the transition into adolescence and young adulthood. It is critical to extend our understanding of healthy brain maturation as excessive brain plasticity during adolescence raises the sensitivity to the environment and learning experiences, and its outcome may have long-term positive or negative impact on personal opportunities in life and mental health.

Zusammenfassung

Grundlagen

Das genuine Interesse an neuen Erfahrungen und gesteigerter Verantwortung prägt das Entwicklungspotenzial junger Menschen in der Adoleszenz. Ziel dieser Studie war es, Veränderungen in der Gehirnentwicklung, die dem Aufgaben-relevanten Verhalten zugrunde liegen, sowie deren Beziehung zu neuartigen Eindrücken während des Übergangs vom Kindes- zum Jugend- und jungen Erwachsenenalter zu untersuchen. Wir stellten die Hypothese auf, dass verbesserte Fähigkeiten zur Zieldetektion und reduzierte Ablenkbarkeit während der Entwicklung von einer erhöhten Aktivierung von frontalen Gehirnarealen innerhalb des fronto-parietalen Gehirnnetzwerks während der Verarbeitung neuartiger Reize und der Zielerfassung charakterisiert werden.

Methoden

In einer Querschnittsstudie wurden ein klassisches visuelles Oddball-Paradigma (*n = 159*) und ein visuelles Novelty-Oddball-Paradigma (*n = 84*) in Kombination mit EEG-Messungen untersucht, um die Gehirnentwicklung von der späten Kindheit bis zum jungen Erwachsenenalter (8 bis 30 Jahre) zu untersuchen. Regressionsmodelle wurden verwendet, um Entwicklungsverläufe von späten EKP-Komponenten und gleichzeitig auftretender Delta- (0,5-4 Hz) und Theta-Oszillationen (4-7 Hz) zu analysieren. Dabei wurden die Amplitude des Vorreiz-EEGs, die Veränderung der Amplitude nach einem Reiz sowie die zeitliche Konsistenz des neuronalen Antwortmusters zwischen Reizen und Elektrodenpositionen untersucht.

Ergebnisse und Diskussion

Es konnte ein allgemeiner Rückgang der Reaktionszeit und der späten EKP-Latenz (novel N2, P3a und P3b) mit zunehmendem Alter beobachtet werden. Diese Effekte könnten von kognitiven Fähigkeiten, die zur Aufgabenbewältigung nötig sind, abhängen.

Die frontale novel N2-Amplitude nimmt mit dem Alter ab, während die P3a-Amplitude mit dem Alter zunimmt. Dieser gegenläufige Entwicklungstrend könnte im Zusammenhang mit einem Mechanismus zur Kompensation der nicht vollständig ausgereiften kognitiven

Funktionen stehen, die im Zusammenhang mit der P3a stehen (beispielsweise die Aufmerksamkeitskontrolle).

Die Baseline-bezogenen Amplituden der Delta- und Theta-Oszillationen nahmen mit dem Alter stetig ab, wohingegen die Amplitudenverstärkungen und die zeitliche Konsistenz des neuronalen Antwortmusters zwischen Reizen während der Reizverarbeitung einen Anstieg verzeichneten.

Beide Effekte scheinen entwicklungsbedingte Veränderungen der P3b-Komponente hervorzubringen, auch wenn dies nicht direkt in den EKP-Amplituden beobachtet werden kann. Die räumliche Phasenkohärenz, ausgehend von frontalen Elektroden, der Theta Oszillationen nahm während der Verarbeitung von Zielreizen und neuartigen Reizen mit dem Alter zu. Dies deutet auf eine bis in das junge Erwachsenenalter andauernde Reifung des fronto-parietalen Netzwerks, welches beiden Verarbeitungsprozessen unterliegt, hin.

Schlussfolgerung

Funktionelle Netzwerke des Gehirns, die den frontalen Kortex einbeziehen, wie das fronto-parietale Netzwerk, reifen bis in das junge Erwachsenenalter und beeinflussen dadurch langwellige Oszillationen auf lokaler und globaler Ebene sowie späte frontale EKP-Komponenten.

Die Reifung des Gehirns während der Adoleszenz kann zu einer Verringerung der spontanen langwelligen Oszillationen und einer Verbesserung der Amplitudenmodulation sowie der regionalen und interregionalen Präzision des Timings ereigniskorrelierter Oszillationen innerhalb des P3-Zeitfensters führen.

Somit ist die Gehirnreifung, die dem aufgabenbezogenen Verhalten und der reduzierten Ablenkbarkeit zugrunde liegt, vielseitig.

Bedeutung

Es bedarf der kombinierten Analyse von Entwicklungsverläufen spät auftretender EKP-Komponenten mit zeitgleich auftretenden Veränderungen von spontanen und aufgabenmodulierten Gehirnoszillationen und deren Einbettung in funktionale Gehirnnetzwerke (z. B. dem fronto-parietalen Netzwerk) zur Abschätzung, wie sich die Gehirnreifung auf kognitive Kontrollfähigkeiten während des Übergangs in die Adoleszenz und bis in das junge Erwachsenenalter auswirkt.

Die erhöhte Plastizität des Gehirns, wie sie während der Adoleszenz auftritt, verstärkt die Sensibilität für Umwelt- und Lernerfahrungen und wirkt sich langfristig entweder positiv oder negativ auf die persönlichen Chancen im Leben und die psychische Gesundheit aus. Es ist daher von großer Bedeutung, unser Verständnis einer gesunden Gehirnentwicklung zu erweitern.

"If our brains were simple enough for us to understand them, we'd be so simple that we couldn't."

— Ian Stewart, 1994 —

SECTION I.

Theoretical Background

1. Introduction

The phase of adolescence is important for a person's health, social inclusion, performance and potential (e.g. Nuechterlein, Ventura, Subotnik, & Bartzokis, 2014; Pantelis et al., 2009). It covers the second decade of life and poses new challenges for adolescents. Associated with this phase are the separation from the parental home and the existence in a social group of peers (Blakemore, 2008). Adolescents more often put themselves in new and high-risk situations than children and adults (Steinberg, 2013). Dealing with new impressions is at the heart of adolescence, thereby distinguishing it from childhood and adulthood.

The new challenges that young people seek and encounter can have a positive impact on personality development. Ideally, adolescents learn to take on self-responsibility and a stable role in society during the transition into adulthood. This is not, however, axiomatic (Kaiser & Gruzelier, 1999; Nuechterlein et al., 2014; Pantelis et al., 2009).

A pathologically increased search for rewarding and intensive new experiences can have addictive effects. Negative developmental patterns can also be observed when adolescents face new challenges that they are not able to master. Schizophrenic disorders are often discussed in the context of early predisposition and high psychological stress during adolescence.

The aforementioned change in the behaviour of adolescents is accompanied by fundamental changes in the neuronal networks of the brain (Luna, Padmanabhan, & O'Hearn, 2010; Uhlhaas et al., 2009). Neural networks reflect the connection, and thus the cooperation (i.e. the communication) of different brain areas. In the adolescent phase, the involvement of the frontal cortex in neural networks especially improves. The frontal brain areas are an important controlling authority for decision-making and action control and thus are seminal for a self-determined life.

Currently, it is assumed that changes in neuronal networks are triggered by new developmental tasks and in turn require the mastering of these developmental tasks to

ensure the neuronal changes. The interest in new experiences during the adolescent phase probably plays a major role here (Lourenco & Casey, 2013). Mental disorders, such as addictions and schizophrenia, are associated with disorders in the maturation of the neuronal networks of the frontal cortex (McGlashan & Hoffman, 2000; Paus, Keshavan, & Giedd, 2008).

2. Adolescence

Adolescence is a time full of physical, emotional and intellectual changes. New strategies and skills are gained through one's own reasoning and decisions, risk-taking and the questioning of others. The human brain particularly undergoes major reorganisational steps (see review Segalowitz, Santesso, & Jetha, 2010). Structural changes are combined with functional alterations. The aim of adolescence is to become independent and for adolescents to stand on their own feet within the social community.

2.1. Definition adolescence

Youth is a developmental phase between childhood and adulthood, although the boundaries are not clearly defined. It is evident that this phase represents a break between childhood and adulthood (Jensen & Nutt, 2015; Steinberg, 2014).

Granville Stanley Hall was the first to describe the time between childhood and adulthood as a discrete developmental stage in 1904: "These years are the best decade of life. No age is so responsive to all the best and wisest adult endeavour. In no psychic soil, too, does seed, bad as well as good, strike such deep root, grow so rankly or bear fruit so quickly or so surely." (Hall, 1904, Preface)

Hall described that the character and personality are taking form; however, everything is plastic and pliable. Further, he equated the beginning of adolescence with the initiation of puberty (Hall, 1904).

Until today, a concrete demarcation between childhood and adulthood remains unclear. It can be described as a stage of life when adolescents are no longer children, yet not quite

fully independent and still less mature than adults. The goal of adolescence can be classified as becoming an independent individual by the separation from the parental home and the existence in a social group of peers (Blakemore, 2008).

Puberty refers to the physical and hormonal changes that lead to sexual maturity. Puberty represents a universal phase in life. Thus, considering puberty as the beginning of adolescence enables quantification as obvious physical consequences can be observed.
Attaining a stable and independent role in society marks the end of adolescence. This includes moving out of the parents' home, achieving financial independence by starting to work full-time as well as starting one's own family, often initiated through marriage (Dahl, 2004; Steinberg, 2014).

Assessing the time between puberty and adult-like stages in life leads to the observation that the overall time of adolescence has been increasing over the last decades.
A decline in the onset of puberty is evident. Physicians have documented girls' menarches for decades. The age of girls' menarche is not the onset of puberty, but it is rather close to the age of sexual maturity that takes place about three years before the first physical changes can be observed. For boys, during the beginning of puberty, which occurs about three years before its completion, a deepening of the voice is observed and also well-documented over time.

A decreasing trend for both male and female puberty of three to four months per decade can be detected over the last decades. Hormones stimulate changes in physical appearance, reproductive capabilities and libido during puberty. Modern nutrition and life-style seem to have an influence on the hormonal balance and thus cause this effect. Presently, first signs of puberty can be seen in many ten-year-old girls, while boys are constantly delayed by about one to two years of puberty onset (Dahl, 2004; Steinberg, 2014).

Today's society leads to an increase in the age of adult-like events taking place in young people's lives. The age of marriage increases for men and women by about a year per decade. Other events like finishing education, relying on financial support, housing of the parents and delaying parenthood are observed in several countries around the world (Steinberg, 2010). Counting the years from onset of adolescence until adulthood, an increase of the phase of adolescence from seven to fifteen years from 1950 to 2010 can be measured and it still continues to lengthen. In 2004 Dahl counted about the second decade of life to youth (Dahl, 2004).

This holds true while scientific research is indicating a prolonging that stretches into the middle of the third decade of life (Steinberg, 2014). Therefore in this thesis, no clear line is drawn between adolescence and young adulthood and both are referred to as the time between about 10 to 25 years of age.

2.2. Behavioural aspects - The appeal of the novel

At the end of childhood basic abilities are consolidated especially relating to sensory, motoric and language skills (Ahnert, 2013; Gogtay et al., 2004; Sowell et al., 2003). However, adolescence is the time to develop the ability of higher-order cognitive abilities, like planning and decision-making, and self-regulation in order to control thoughts, emotions and actions (Blakemore & Choudhury, 2006; Demetriou, Christou, Spanoudis, & Platsidou, 2002). In order to become an independent and stable person in social community adolescents need new experience and situations to exercise their abilities. The motivation to seek out novel and exciting experiences is said to increase shortly after puberty (Lerner & Steinberg, 2004). Novel objects and new experience bring along excitation and rewarding emotions (Horvitz, 2000; Wittmann, Bunzeck, Dolan, & Düzel, 2007). During adolescence the brain is exceptionally prone to rewarding stimulation and is more responsive to arousal making the adolescent seek for sensation (Cohen, J. R. et al., 2010; Dahl, 2004; Galvan et al., 2006; Galvan, Hare, Voss, Glover, & Casey, 2007; Spear, 2000; Steinberg, 2014). At the same time, the adolescent brain is primed to learning and change through experience – also described by its plasticity - during this period of life (Lerner & Steinberg, 2004).

A system that gets easily aroused is highly influenceable and not stable yet holds the danger of risks and brings vulnerability along (Arnett, 1992; DiClemente, Hansen, & Ponton, 1996; Jensen & Nutt, 2015; Steinberg, 2014).

Risk-taking

Risk-taking is a commonly observed behaviour during adolescence. Adolescents are more likely pursuing novel situations and their possible reward even though potential risk and danger is to be expected (Arnett, 1992; Jensen & Nutt, 2015; Steinberg, 2008, 2014).

Zuckerman (1994, p. 27) defined sensation seeking as a personality trait characterised by the "seeking of varied, novel, complex, and intense sensations and experiences, and the willingness to take physical, social, legal, financial risks for the sake of such experiences."

Sensation seeking and impulsivity seem to be distinct personality traits; however, they increase during adolescence. Together with the increase of strong arousal of emotions they seem to influence risky behaviour (Steinberg, 2008).

As example of increased adolescent risk-taking behaviour, the level of conducted crimes peaks during adolescence along several decades up to now as depicted in Figure 1A. At about the same time, the number of unintentional drowning increases dramatically peaking during the late teen years depicted in Figure 1D. Typically, adolescents are able to swim growing up in western civilisation and are normally even at their height of their physical strength in life (Birbaumer & Schmidt, 2010; Myers, 2008). Drowning of juveniles is rather occurring at night, inebriated, in unknown waters and under the influence of peers, and therefore, rather illustrates the serenity of juvenile risk-taking.

Adolescents fail to consider possible long-term consequences of reckless behaviour (Arnett, 1999; Steinberg, 2013). They act impulsively; often the situation is worsened by peers driving, even pressuring, each other into reckless behaviour, and the influence of drugs (Gardner & Steinberg, 2005; Steinberg, 2014; Steinberg et al., 2008). It is only with increasing age that adolescences become better able to evaluate dangerous situations appropriately (Steinberg, 2008, 2013).

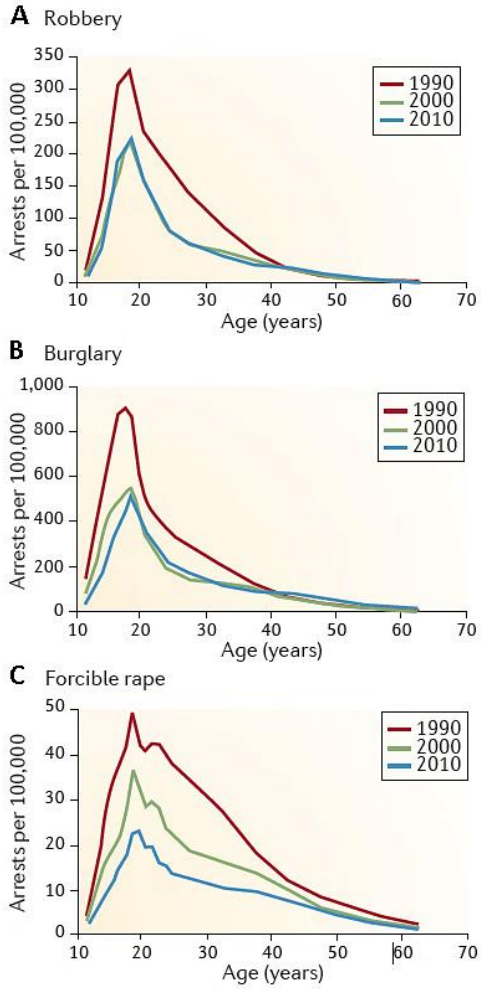

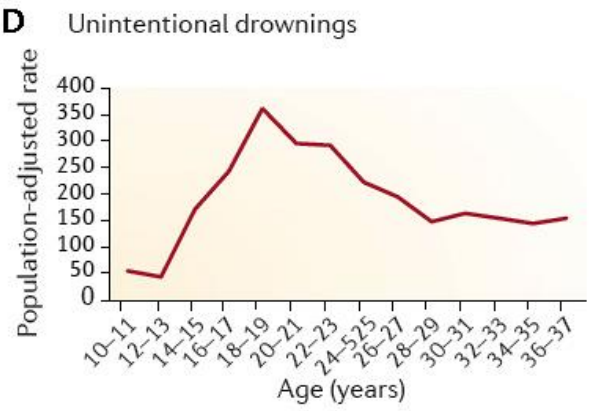

Figure 1: Left: (A-C) Age-crime relationship. (A) Robbery, (B) burglary and (C) forcible rape are depicted over the age for the years 1990 (red), 2000 (green) & 2010 (blue).
Right: (D) Age-Risk-taking relationship. Unintentional drownings over the age.
(Steinberg, 2013)

Peer influence

Adolescents are highly susceptible to peers and peer pressure, as social acceptance, praise and attention come along with rewarding stimulation (Steinberg, 2014). Risk-taking behaviour increases in the presence of peers (Gardner & Steinberg, 2005). Alcohol and illicit drug consumption (Chassin, Fora, & King, 2004), automobile accidents (Simons-Morton, Lerner, & Singer, 2005), and commitment of crimes (Zimring, 1998) are just a few examples, in which peer influence has a pernicious effect. In a study, Gardner and Steinberg (2005) could demonstrate that only in the presence of peers adolescents exhibited increased risk–taking behaviour while driving in a video game in comparison to adults (see Figure 2).

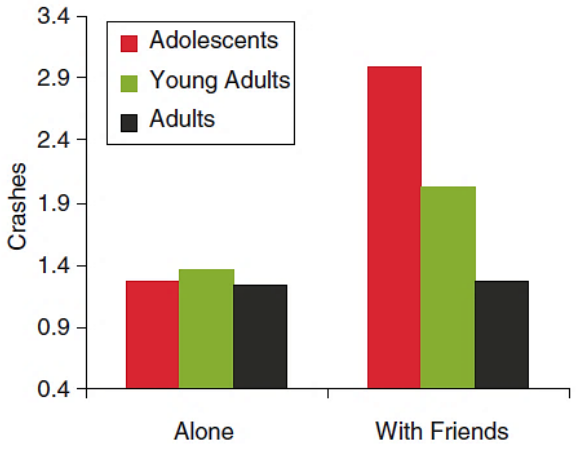

Figure 2: Age-Risk-taking and peer influence. Car crashes during driving game, when playing alone and when playing with friends for adolescents (red), young adults (green) and adults (black) (Gardner & Steinberg, 2005).

Addiction

High susceptibility to rewards can give rise to and promote addictive behaviour, which is defined by a compulsive engagement in the rewarding stimulus (Steinberg, 2014). Addiction can be related to various types of behaviour and substances (Silveri, Tzilos, Pimentel, & Yurgelun-Todd, 2004). It is known, that adolescents are more vulnerable to most forms of addiction, like gambling, shopping, internet use, substances like tobacco, alcohol, drugs (Steinberg, 2014). It has been shown that adolescents react more strongly to rewarding stimuli, avoid reward delays and are less sensitive to losses compared to adults (Steinberg, 2014). It is also reported that relative reward preference is exaggerated during adolescence (Galvan et al., 2006).

Disorders

Adolescents are less emotionally stable, especially in the early and mid-phase of youth (Jensen & Nutt, 2015). At the same time, they are more responsive to arousal, which can also mean stress and anxiety (Steinberg, 2014). Adolescents are more prone to negative information (Carstensen & Mikels, 2005) even though they seem to have less ability to process negative information (Jensen & Nutt, 2015). Consequently, these effects make them more vulnerable for disorder. Steinberg (2014) emphasizes disorders, which most often have their onset in adolescence and categorizes them as follows:

- Mood disorders (e.g. depression & bipolar disorder)

- Substance-abuse disorders (e.g. alcohol or drug dependence)
- Most anxiety disorders (e.g. obsessive-compulsive disorder or anxiety disorders)
- Eating disorder (anorexia or bulimia)
- Schizophrenia

Two model system

Risk-taking behaviour in general can be observed as an inverted U-shaped pattern along age peaking during adolescence. A two model system underlying this behaviour is discussed in literature. A combination of relatively higher tendency to seek rewards and sensations (Galvan et al., 2006; Stephenson, Hoyle, Palmgreen, & Slater, 2003) is accompanied by a still maturing self-control system, like impulse control, during youth (Lerner & Steinberg, 2004; Steinberg, 2014). However, both models are developing on different time tables leading to an inverted U-shaped trajectory of risk-taking behaviour as depicted in Figure 3 (Steinberg, 2010). Thus, a protraction in harm-avoidance system relative to approach system may be reflected (Ernst, Pine, & Hardin, 2006).

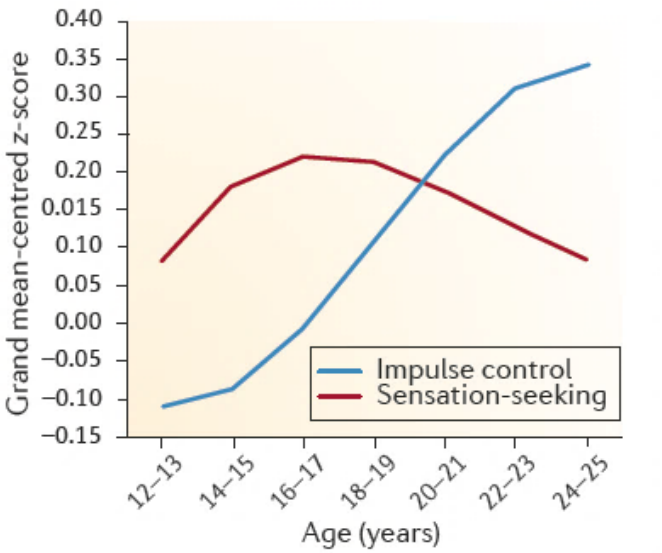

Figure 3: Development of sensation-seeking (red) and impulse control (blue) over age (Steinberg, 2013).

Summary

Human cognitive performance is reaching its peak with the transition to adulthood. In many cognitive achievements, adolescents reach the level of adults. However, they are still worse

when it comes to focusing on a task and planning for the future despite disruptions (Crone, 2009). Fatigue, stress or emotional arousal has greater influence on task performance during youth (Shulman et al., 2016). They are still developing a leaner and more efficient adult mental system (Steinberg, 2014).

The observed changes in behaviour during adolescence are considered to be biologically normative (Steinberg, 2010). Full understanding of underlying developmental mechanisms may help to reinforce physical and psychological well-being of this age-group.

2.3. Processing of novel stimuli in adolescents

Attention describes the ability to direct consciousness to certain aspects of the environment or one's own behaviour, and to selectively process these, while suppressing stimuli that appear less important for the moment (Simons, 2000).

New stimuli draw the attention from the current situation to the processing of the new information and thus interrupt the current focus or the current action. The impulse for this is presumably automatic (orientation reaction) and serves to quickly assess whether the new stimulus is relevant to react to. Attention can be further strengthened by consciously focusing on certain stimuli, whereby personal motivation plays a decisive role (Simons, 2000).

Research results suggest that on neuronal level control of attention in adults is primarily responsible for frontal activation of the cortex, both consciously and unconsciously. The frontal cortex probably assumes the central assessment and evaluation of the stimulus and delegates appropriate response patterns (Windmann, Wehrmann, Calabrese, & Gunturkun, 2006). This is achieved by the activation of global networks, affecting distant brain regions (Naghavi & Nyberg, 2005).

In the phase of youth, the frontal cortex is not yet fully matured and integrated into global networks, which is likely to limit the ability to control attention (Crone, 2009; Naghavi & Nyberg, 2005). At the same time, novel stimuli for young people appear to be particularly exciting and to have a rewarding character (Lerner & Steinberg, 2004; Spear, 2000). This is due to the development of personality and new abilities in this phase, which is shaped by new impressions and the deliberate testing of new situations. This process apparently promotes the motivation to turn to new stimuli.

Figure 4 describes how attention (A) of adolescents, which, caused by the automatic orientation reaction, overcomes the unconscious, not fully mature control of the attention (represented by a still perforated wall), in order to turn to the new object on the right. This process is additionally reinforced by the conscious heightened motivation to turn to this new object in adolescents through the rewarding character of this process (Heim & Keil, 2012).

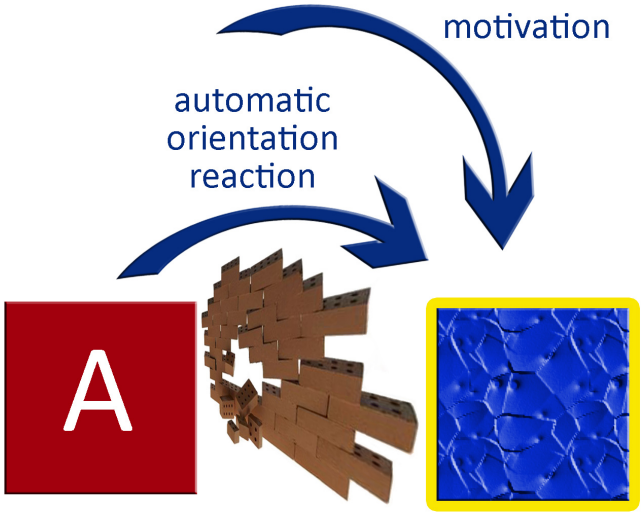

Figure 4: Model for shifting of attention during adolescence when presented a novel stimulus. The attention (A) is shifted from the left object to the new object on the right. The orientation reaction overcomes the still not fully developed control of attention (represented as a perforated wall), whereby this process is further strengthened by the motivation to consciously turn to something new.

2.4. Brain maturation as foundation of adolescence

Despite physical changes during puberty, major changes within the brain mark the period of adolescence, which extends well beyond puberty and into the third decade of life (Steinberg, 2014).

Three major phases determine brain maturation during adolescence and serve as an explanatory approach for the behavioural observations of adolescence described in the previous sections (Jensen & Nutt, 2015):

Phase 1: Around onset of puberty, the limbic system of the brain becomes easily aroused.

Phase 2: Starting in pre-adolescence, the prefrontal cortex slowly becomes better organized.

Phase 3: The brain becomes better interconnected, especially with respect to connections between frontal brain areas and the limbic system.

These three phases reflect the maturational processes described in the dual systems model, depicted in Figure 5. This model is based on the cognitive control system and the socioemotional, incentive-processing system that matures along different developmental courses (Steinberg, 2013).

In phase 1, young adolescents become emotionally volatile. Concurrently, reward-seeking behaviour increases due to their easily aroused limbic system. The limbic system is associated with emotional processing and the processing of social information. It is further involved in memory processing, reward anticipation, prediction of punishment and sexual behaviour. In this brain area, emotions are integrated with experiences. The easily aroused limbic system is reflected in the socioemotional, incentive-processing system, showing a heightened responsiveness with increasing age during adolescence. Around the age of 16 years, the system peaks and begins to attenuate, reaching a moderate activation level in adulthood (Jensen & Nutt, 2015; Steinberg, 2013; van Duijvenvoorde, Peters, Braams, & Crone, 2016).

The limbic system is in constant contact with the prefrontal cortex. Emotional information is evaluated and interpreted through the prefrontal cortex in order to assess an adequate response to the emotion. The prefrontal cortex thus controls the majority of behaviour (Jensen & Nutt, 2015).

During phase 1, cognitive abilities, like the control of behaviour, are reflected in the cognitive control system and they are not entirely mature yet. This system increases slowly and steadily until adulthood (Steinberg, 2013).

Maturational processes in the brain of phases 2 and 3 allow for faster information flow across distant brain areas. In parallel, advanced thinking abilities are strengthened. This includes the maturation of the cognitive control system, which is associated with prefrontal brain areas (Steinberg, 2013). Differentiation of cognitive control abilities and the underlying cerebral network is described in more detail in section 2.7.

Together, the interplay of both systems and their differing developmental trajectories explain adolescent behaviour. Increasing sensation-seeking, risk-taking, impulsive antisocial acts and the susceptibility to peer influence are observed in this age period (Casey et al., 2010; Chein, J., Albert, O'Brien, Uckert, & Steinberg, 2011). Adolescent behaviour seems to relate more to the anticipation of reward, despite the risk, than to the perception of the risk itself (Smith, Chein, & Steinberg, 2014).

With maturation of the cognitive control system, self-regulation increases (Steinberg, 2013).

The following section describes these developmental changes in more detail on the cellular level.

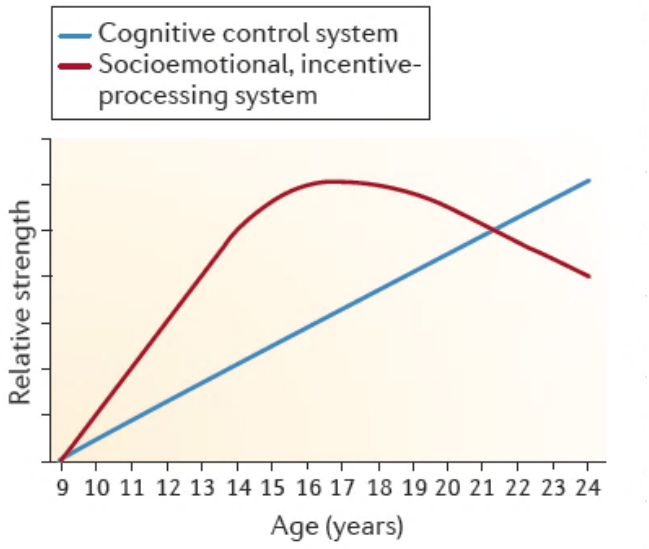

Figure 5: The dual systems model. Hypothetical developmental trajectories of cognitive control system (blue) and socioemotional, incentive-processing system (red) over age (Steinberg, 2013).

2.5. Structural changes of the brain during maturation

At the approximate age of 13 years, the human brain reaches its full size (Hedman, van Haren, Schnack, Kahn, & Hulshoff Pol, 2012), while internal development continues into early adulthood (Segalowitz, Santesso, & Jetha, 2010). The aforementioned changes of limbic and prefrontal brain areas are thought to especially have a basis on the structural changes during brain maturation (Jensen & Nutt, 2015).

The brain possesses a continuous plasticity throughout the life span. During adolescence, this plasticity is highly utilized to strengthen important neuro-circuits and to get rid of unimportant connections (Hedman et al., 2012). These processes are related to a decrease of grey matter volume during this time. Due to so-called 'synaptic pruning', unimportant synapses and neuropil (dendrites, dendritic spines, axon terminals and possibly associated glial cells) are eliminated. In parallel, the so-called 'arborisation' leads to the formation of new neural pathways, thereby enabling a heightened capacity of learning (cf. Paus et al., 2008). Additionally, an increase in white matter across all brain regions - either by increased myelination or increased axon size - enables faster signal transmission (Giedd, 2004; Giedd et al., 1999; Paus, 2010).

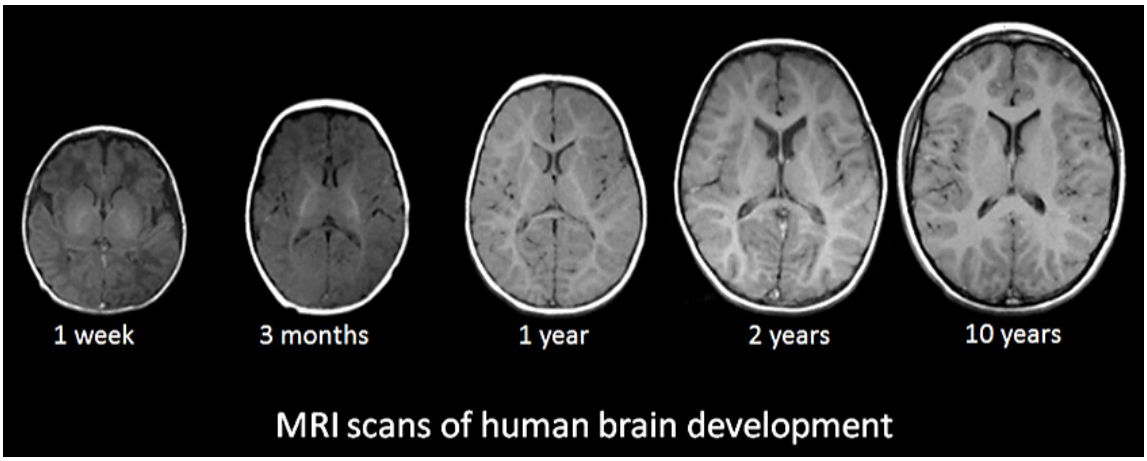

Figure 6: Size ratios of a child brain for various age levels. The brain grows only a little from the second year of age onwards.
(The NIH MRI Study of Normal Brain Development: http://pediatricmri.nih.gov)

2.6. General changes in brain networks

Recent studies indicate that cerebral development during adolescence general results in less-diffused neuronal networks. Fewer regions are recruited with increased response intensity throughout the processing of tasks. In addition, the higher interconnectivity of brain regions leads to an increase in the specificity and efficiency of brain functions (Durston & Casey, 2006; Durston et al., 2006). This effect can be especially attributed to the fronto-parietal network (FPN) with its widespread connections (Klingberg, 2014). Additionally, Amso, D. and Scerif (2015) stated that brain maturation is particularly slow in the FPN.

Figure 7 depicts the reorganisational steps of brain maturation in the first decades of life. During childhood, brain areas related to sensory and motoric processing mature first, especially improving local brain networks. With adolescence, the frontal brain becomes more involved in widespread brain networks taking a lead role in coordination of higher-order cognitive functions. Brain-wide networks are then improved and organized in order to facilitate inter-regional the coordination and to become more efficient (Durston & Casey, 2006; Miskovic et al., 2015; Segalowitz, Santesso, & Jetha, 2010; Uhlhaas & Singer, 2011). In general, brain maturation takes place from posterior to anterior brain regions (Blakemore, 2012).

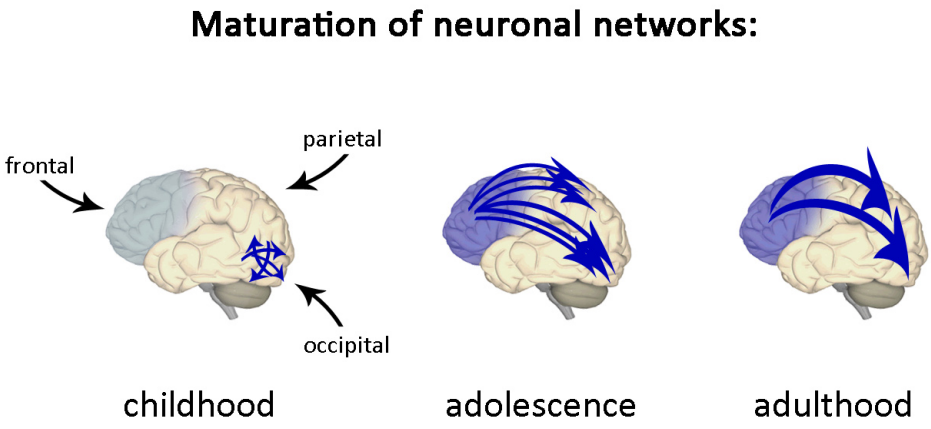

Figure 7: A model for the maturation of neural networks from childhood to adolescence and into adulthood. Blue arrows of different thickness indicate the connectivity strength between different brain areas. The blue marking of the brain illustrates the location of the frontal cortex.
Together, frontal, parietal and occipital cortices form the neural basis for the processing of visually excited shifts of attention. In childhood, the areas for sensory processing are developed first. Through adolescence, the frontal cortex increasingly takes the coordinating role of these network structures.

2.7. The Fronto-Parietal Network

2.7.1. Cognitive control

One of the main features of human cognition is the ability of executive control, which is the regulation of cognitive processes and functions. This includes: problem solving, working memory, inhibitory control, cognitive flexibility, planning, execution and the ability to deal with novelty. Those functions are used to solve interference conflicts during cognitive processing (Chan, Shum, Toulopoulou, & Chen, 2008; Coderre, Conklin, & van Heuven, 2011; Niendam et al., 2012). Thus, cognitive control is not a single mechanism, but it rather includes several functions (Bunge & Crone, 2009; Lahat & Fox, 2013). It can be subdivided into the broad fields of:

- inhibitory control, the ability to inhibit responses, (Rothbart, Ellis, Rueda, & Posner, 2003) and
- self-monitoring, which consists of
  - conflict monitoring, reflection of inference of information (Braver, Barch, Gray, Molfese, & Snyder, 2001) and
  - error or feedback monitoring, as processing and reflection of feedback or error detection (Bunge & Crone, 2009).

The brain is constantly environed from multiple sensory channels by more information than it is able to process. Filtering relevant information is a key challenge achieved by the focus of attention. The limitations of our mental capacity demand the guidance of attention toward important stimuli, while ignoring distractors, to allow faster processing. Attention is crucial for the inflow of information. Higher cognitive top-down control functions are necessary to enable subjective classification of a stimulus' importance and permit for the allocation of resources flexibly (Amso, D. & Scerif, 2015).

2.7.2. Characteristics of the fronto-parietal network

As early as 1990, Posner and Petersen (1990) established a model that proposed that several brain regions are necessary to carry out distinct functions of attentional control. Prefrontal brain areas have been associated with executive functions, specifically cognitive control, for several years (Duncan & Owen, 2000; Luna et al., 2010; Rubia et al., 2001). A growing base of evidence indicates the role of the fronto-parietal network (FPN) in attentional control processes (Amso, D. & Scerif, 2015; Dosenbach, Fair, Cohen, Schlaggar, & Petersen, 2008; Naghavi & Nyberg, 2005). In a review, Naghavi and Nyberg (2005) summarized a strong overlap of network activation involving the dorsolateral prefrontal and bilateral parietal cortices during tasks involving visual perception, attention, working memory and episodic retrieval. Naghavi and Nyberg (2005) further suggested a generally independent spatial attention network, which integrates additional brain regions upon specific task requirements. The FPN serves as one cerebral subsystem of cognitive control, which initiates and modulates cognitive control abilities in order to select among competing or conflicting alternatives (Dosenbach et al., 2008; Zanto, Rubens, Thangavel, & Gazzaley, 2011).

The control system needs to be highly adaptive for the ability to implement a wide variety of tasks in order to cope with various situations in life. Executive functions share subordinated networks that are associated with cognitive control (Niendam et al., 2012). In accordance with this view, studies found involvement of the FPN in different complex mental processes (Cole, Repovs, & Anticevic, 2014; Duncan, 2010; Fehr, 2013; Niendam et al., 2012). Therefore, the FPN, in comparison to other brain networks, especially spans extensively throughout the entire brain with systematic and structured connectivity patterns (Zanto & Gazzaley, 2013). The flexibility is achieved through brain regions that serve as flexible hubs, which are connection points or gateways that link different brain regions. This suggests communication with a variety of systems in the brain, regardless of the processing of sensory or motor modality (Chein, J. M. & Schneider, 2005; Cole et al., 2014; Fedorenko, Duncan, & Kanwisher, 2013; Zanto & Gazzaley, 2013). These brain regions rapidly update their patterns of global functions in order to direct the connectivity according to current task demands (Cole et al., 2013).

2.7.3. The conflict monitoring approach

The FPN integrates both bottom-up and top-down processes during attentional control (Luna et al., 2010). Primary sensory areas process the detection of salient events. Bottom-up representations of perceptual features are utilized in order to facilitate access to and integration between other large-scale networks of attention and working memory resources. The bottom-up representations are influenced and processed by sensory areas in the occipital and temporal cortex (Bledowski, Prvulovic, Goebel, Zanella, & Linden, 2004). The insular cortex facilitates the modulation of autonomic reactions to salient stimuli. The ACC is suggested to play a major role in conflict detection and resolution. It reacts upon stimulus novelty (Berns, Cohen, & Mintun, 1997) and to violations of regularity in a stimulus sequence (Ursu, Clark, Aizenstein, Stenger, & Carter, 2009). The ACC is thought to recruit higher-order processes in diverse cortical regions such as those associated with the PFC (Posner & Rothbart, 2007). Botvinick, Braver, Barch, Carter, and Cohen (2001) postulated the conflict monitoring theory, which places the ACC in the central role for response coordination to the occurrence of conflict. The ACC is proposed to signal the occurrence of conflict and trigger compensatory adjustments in cognitive control (Botvinick, Cohen, & Carter, 2004). The increased activations during cognitive control have been found for the ACC and also the DLPFC (e.g. Greene, Nystrom, Engell, Darley, & Cohen, 2004) and therefore, a strong coordination of both structures is indicated as well as the proposition of an involvement of the ACC in the FPN.

Cognitive control is suggested to be linked to motivation in order to guide decision-making processes (Rubenstein & Rakic, 2013; Somerville & Casey, 2010).

2.7.4. Top-down control

Top-down task-selective signals are generated in the premotor & dorso-lateral prefrontal cortex (dlPFC) (Ptak, 2012). The frontal and parietal cortices and the thalamus serve as control regions for top-down implementation (Scolari, Seidl-Rathkopf, & Kastner, 2015). Taken together, imaging studies constitute the general role of the FPN in attentional tasks and furthermore, the FPN might serve as the coordinator for top-down bias as it modulates lower-level sensory systems (Naghavi & Nyberg, 2005).

2.7.5. Alternative to ACC – MFC

The cognitive control employed during response conflict is utilized to inhibit irrelevant stimuli in order to focus on relevant ones; it is also linked to the frontal cortex (van Noordt, Desjardins, Gogo, Tekok-Kilic, & Segalowitz, 2017). Several studies ascribed this ability to the medial frontal cortex (MFC) (e.g. Danielmeier & Ullsperger, 2011; Nigbur, Cohen, Ridderinkhof, & Sturmer, 2012). Cohen, M. X. and Ridderinkhof (2013) further suggested the MFC as a hub for large-scale network formation and information integration in this context, which is in contrast to the conflict monitoring approach described above that focuses on the ACC as the central hub.

2.7.6. Role of slow-wave oscillations in the fronto-parietal network

Both network models take into account theta oscillations (located over medial frontal scalp sites and source localized to the frontal cortex) for cognitive control functions, as during a variety of tasks where medial frontal theta is exhibited (Cohen, M. X. & Ridderinkhof, 2013; for an overview: van Noordt et al., 2017). Medial frontal theta is suggested to function as a mechanism for integration of information from memory, for the bias of sensory gating toward relevant stimuli or stimulus features and for modification of task-sets in the face of dynamic environmental contingencies (Buzsaki & Draguhn, 2004; Klimesch, 1999). In this context, frontal theta oscillations are related to control and influence of posterior brain sites and may functions as a main communication tool within the FPN (Cohen, M. X. & van Gaal, 2013; de Borst et al., 2012; Kawasaki, Kitajo, & Yamaguchi, 2014; Lee, T. G. & D'Esposito, 2012; Sauseng et al., 2006).

Thus, theta activity plays, in general, an important role in the transfer, integration and coordination of information over wide-spanning brain regions (Kayser, Ince, & Panzeri, 2012; von Stein, Chiang, & Konig, 2000; von Stein & Sarnthein, 2000) and for connection of different brain areas (Lopes da Silva, 2013). Theta activity is, therefore, involved in the whole process from perception to action (Fuster, 2006).

Studies showed that, in general, elicited slow-wave activities are important for cognitive control processing. This also includes the delta frequency band. It exhibits a similar activation pattern as medial frontal theta oscillations, linking delta to cognitive control and the focus of attention (Harmony et al., 1996; Mathewson et al., 2012; van Noordt et al.,

2017; Yordanova, J., Falkenstein, Hohnsbein, & Kolev, 2004). Through these mechanisms, the FPN can be associated with the P3 component occurring in Oddball tasks, which has been involved in attentional processing of novel and/or task-relevant cues and mainly consists of slow-wave oscillatory activity patterns (Polich, 2007; Prada, Barceló, Herrmann, & Escera, 2014).

2.7.7. Association of working memory and the fronto-parietal network

Working memory is one of the forms of executive function. It can be seen as a fundamental cognitive capacity that contributes critically to many high-level cognitive functions (Naghavi & Nyberg, 2005). Lee, T. G. and D'Esposito (2012) suggested the prefrontal cortex (PFC) as the source of top-down signalling, since transcranial magnetic stimulation inducing disruptive signals of the theta frequency band led to the impairment of cognitive performance during a working memory task. Kawasaki et al. (2014) also supported the idea of theta oscillations playing a main role in large-scale communication and information transfer among distant task-relevant regions as they discovered fronto-parietal theta phase synchronization during a visual working memory task.
In addition, other frequency bands also play a role in long distance top-down information processing, e.g., long distance alpha oscillations were involved during working memory processing (Zanto et al., 2011).

2.7.8. Role of alpha oscillations in the fronto-parietal network

Modulations of alpha oscillations are often found to correlate with theta oscillations during tasks that involve cognitive control (van Noordt et al., 2017). An established perspective on alpha oscillations describes their function at rest. At rest, the default mode network becomes activated and alpha oscillations highly synchronize and are suggested to reflect an idling state of the brain (Jann et al., 2009). Upon attentional focus due to external demands, alpha oscillations are reduced in power. In most tasks requiring cognitive control, an enhancement of frontal theta oscillations was accompanied by an inverse modulation of alpha, especially over posterior sites, when demands on attention and behavioural control were required (van Noordt et al., 2017). Sadaghiani et al. (2012) suggested alpha and theta oscillations mechanisms operate as a support gate in the service of cognitive control.

2.7.9. Summary

Further research is necessary to elucidate the association between frontal theta, delta and posterior alpha oscillations in the context of response preparation and higher-order cognitive control of behaviour (van Noordt et al., 2017).

Long-range theta connectivity plays an extraordinary role in the fronto-parietal processing of cognitive control and it also enables the investigation of the cognitive control processes during an Oddball experiment.

Prolonged maturation of the frontal cortex until young adulthood in association with the reorganisation of widely distributed neural networks, like the FPN, is proposed by a large number of studies (Blakemore & Choudhury, 2006; Crone, 2009; Luna et al., 2010). In line, developmental improvements of a variety of higher-order cognitive abilities with age are observed (cf. Segalowitz, Santesso, & Jetha, 2010). This highlights the opportunity to investigate brain maturation during adolescence by considering functional network communication of the FPN.

2.8. Changes in behaviour during experimental tasks

An improvement of performance factors is detectable during development. Error rates decrease over childhood and adolescence for appropriate and inappropriate response behaviour in a variety of tasks (Booth et al., 2003; Segalowitz, Santesso, Murphy, et al., 2010; Tamm, Menon, & Reiss, 2002; van Dinteren, Arns, Jongsma, & Kessels, 2014a). Reaction times also decrease during development and exhibit a decelerating trend reaching into young adulthood (Booth et al., 2003; Segalowitz, Santesso, Murphy, et al., 2010; van Dinteren, Arns, Jongsma, & Kessels, 2014b). Especially in tasks assessing higher-order cognitive abilities a general improvement over development and often into young adulthood can be observed (Blakemore & Choudhury, 2006; Casey, Giedd, & Thomas, 2000; Liu, Woltering, & Lewis, 2014). In children and adolescents, immature frontal brain areas and the related FPN might account for the inefficient and slower processing of tasks that employ these structures (Crone, 2009; Polich, 2007; Segalowitz, Santesso, & Jetha, 2010).

3. Method Background: Electric measurement of cognitive functioning

3.1. Electroencephalogram (EEG)

3.1.1. Historical background

The Electroencephalogram (EEG) was invented only about one century ago. In 1875, Richard Caton (1842–1926) became the first researcher who was able to measure cerebral electrical activity on the surface of the heads of mammal. About 50 years later, in 1920, the neurologist Hans Berger (1873–1941) succeeded in the registration of electrical activity of the human brain by non-invasively placing electrodes on the surface of the head (Sanei & Chambers, 2007). This measured electrical activity is called the EEG. Shortly afterwards, Adrian and Matthews (1934), Jasper and Carmichael (1935) and Gibbs, Davis, and Lennox (1935) were able to confirm Berger's observations, thereby gaining support for this rather new method. Berger already observed and described a phenomenon, which was later called the "alpha blockage": The EEG of a human in relaxed, eyes closed state is dominated by slow alpha waves; upon opening of the eyes a block of these slow-waves can be observed. Simultaneously to the block faster waves start prevailing the EEG signal (Adrian & Matthews, 1934). In the following years, Berger postulated his findings on brain waves and pathologies

and he alluded to the linkage between EEG signals and the mental processes taking place in the brain (Khader, Heil, & Rösler, 2009; Luck, 2005; Neundörfer, 1990; Sanei & Chambers, 2007).The growing technical capabilities of the following years allowed for improvement of the technique and eventually led to the acknowledgement of EEG as a powerful utility for both scientific and clinical applications (Lopes da Silva, Gonçalves, & De Munck, 2010; Luck, 2005).

3.1.2. Biophysical basis of EEG measurements

The EEG enables recording of neuronal activity in the form of voltage fluctuations along the scalp. In the process of neuronal activation, ions are exchanged across the membranes of neurons, leading to excitatory or inhibitory postsynaptic membrane potentials with corresponding electrical fields. Through a conglomeration of large cell ensembles aligned in the same spatial orientation, synchronous postsynaptic potentials are summed up, producing electrical field potentials detectable on the scalp surface via electrodes. Potential fluctuations of around 100 µV are measured and they reflect a macroscopic picture of the electrical activity of at least 10,000 neurons, most of them belonging to more superficial cortical layers (Murakami & Okada, 2006); hence, the spatial resolution of the EEG is rather low, as distortions by the skull and scalp tissue dampen the cerebral signal. By contrast, the EEG yields a high temporal resolution as it enables measurement of neuronal activity in the range of milliseconds (Lopes da Silva et al., 2010; Zschocke, 2012).

3.1.3. Technical aspects

Silver/silver-chloride electrodes, in combination with an electrolyte gel containing free chloride ions, are typically used for the EEG recording. This application yields the advantage of a low half-cell potential (around 220 mV) as well as relatively low electrode impedances (Lee, S. & Kruse, 2008).

A standardised way of electrode positioning, the so-called 10-20 system (see Figure 8), exists to ensure comparability between measurements (Jasper, 1958). Due to variable scalp form and size, the positioning of 19 electrodes is related to the reference points, nasion, inion (see Figure 8) and two periauricular points at 10 or 20 % steps of distance from each other (Zschocke, 2012).

With increasing technical improvements, EEG recordings with more electrodes (high-density recordings) became feasible (e.g. 10-10 system of Chatrian, Lettich, & Nelson, 1988). The labelling is related to the underlying cortical regions: from frontal (F), over central (C) and temporal (T), to parietal (P) and occipital (O). Laterality of the electrodes is expressed for the left cerebral hemisphere with uneven numbers and for the right hemisphere with even numbers (compare Figure 8). For most people, the standardized electrode positioning matches these cortical regions (Okamoto et al., 2004).

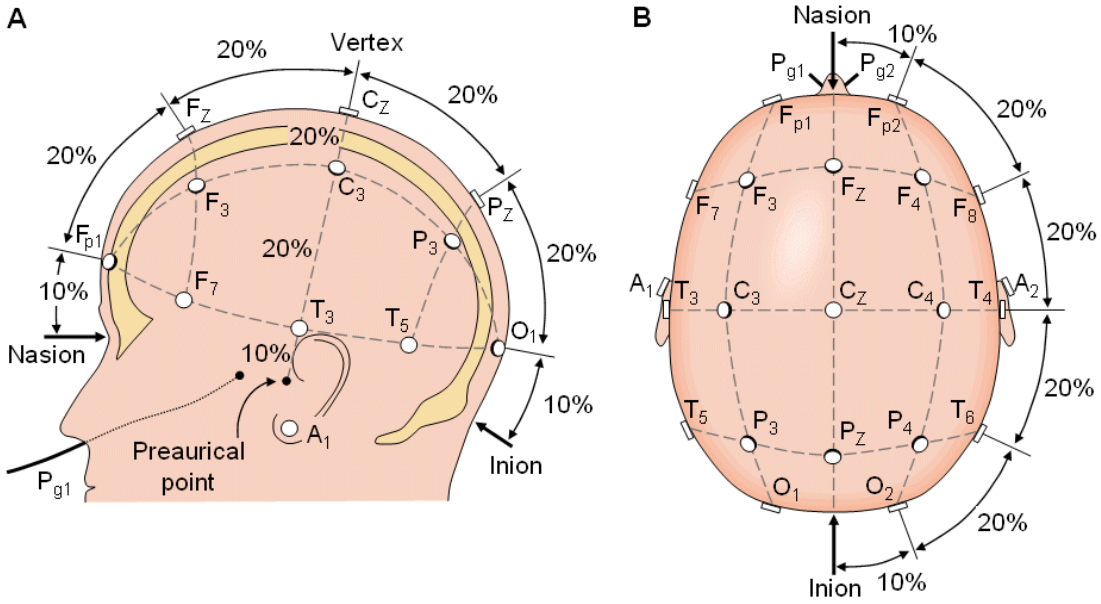

Figure 8: 10-20 system with labelled EEG recording electrodes and reference points. (A) Head displayed from left side. (B) Head shown from above with nose pointing upwards. (Labate, Foresta, Mammone, & Morabito, 2015)

3.2. Brain oscillations measured by EEG

Activity of cortical neurons is reflected in the EEG measurement and exhibits a rhythmic nature. The rhythmic activity of pyramidal cells in the cortex is associated with cortico-thalamic or cortico-hippocampic feedback coupling (Hughes et al., 2004; Zschocke, 2012), while the brainstem and the thalamus are suggested as the main sub-cortical generators of synchronous periodic neuronal activity (Lopes da Silva et al., 2010). Synchronous neural activity measured by EEG is referred to as brain oscillations (Basar, 1998).

The EEG signal is composed of oscillations of varying frequency range. In part, these rhythms can be assigned to certain physical states, e.g. wakefulness or sleep, due to their predominance within these states (Birbaumer & Schmidt, 2010).

Brain oscillations also reflect cognitive processes such as attention, perception, memory or the preparation of motor activity, as these functions are not the result of single-cell activity but instead require the linkage between several neuronal associations that form networks. The linkage between several neuronal associations that form neuronal networks is necessary. Network communication is suggested to be implemented by oscillatory activity patterns (Basar, 1998; Basar, Basar-Eroglu, Karakas, & Schürmann, 2000; Buzsaki & Draguhn, 2004; Herrmann, Strüber, Helfrich, & Engel, 2016).

Cerebral activity can be classified either as spontaneous or evoked activity. Spontaneous activity is assumed to reflect internal, endogenous neural activity. Evoked or event-related cerebral activity is elicited as a result of or response to certain motoric, cognitive behaviour – e.g. attention – or exogenous stimulation (sensory stimulation). The EEG signal can be analysed time-locked to an event in terms of the voltage changes elicited in the time domain or in the frequency domain. The former leads to consideration of so-called event-related potentials (ERPs). In the ERP, several oscillatory patterns of different frequency range are intermingled. The filtering of these oscillations in regard to the event leads to so-called event-related oscillations (EROs; cf. section 3.4) (Basar, 1998).

ERP and ERO are described in more detail in the following sections, as they are the main focus of the analysis of the subsequent studies.

3.3. Event-related Potentials (ERP)

Sensory, cognitive and motor processes are reflected in the EEG pattern by ERPs. ERPs possess rather small amplitudes compared to the random background activity of the spontaneous EEG. The ERP can be filtered through the averaging of several EEG recordings (epochs) as this increases the signal of the specific components by decreasing random background noise. The averaging process can be conducted time-bound either to a presented stimulus or a specific response, leading to either a stimulus- or response-locked ERP, respectively (Birbaumer & Schmidt, 2010; Tong & Thakor, 2009).

The ERP consists of a sequence of several components, which are generated as a consequence of activity changes in cerebral networks before, during and after a sensory, motor or psychological event. These components are distinguished by the polarity of their voltage deflection being positive (P) or negative (N) and their latency onset regarding a specific event (Birbaumer & Schmidt, 2010). Naming reflects either the full latency onset in ms or it is abbreviated in a manner that often reflects the order of components occurring with the same polarity.

Figure 9 displays typical time-courses of ERPs evoked by visual stimuli that were relevant in a within a target detection task with the elicited components P1, N1, P2, N2 and P3 (also referred to as P100, N100, P200, N200 and P300, respectively).

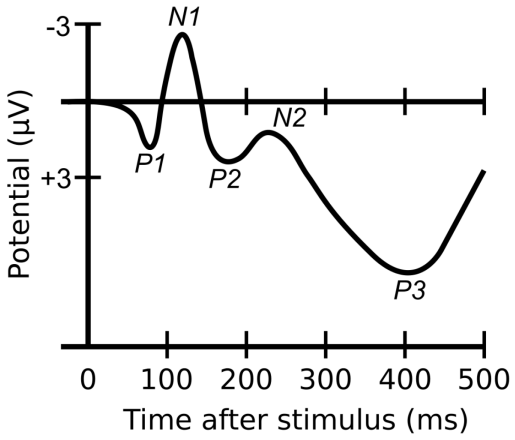

Figure 9: Visual event-related potentials after presentation of a relevant target stimulus (source: https://en.wikibooks.org/w/index.php?title=File:Constudevent.gif).

The characteristics of ERP components (amplitude and latency) vary due to particular conditions, as they are related to specific neurophysiologic and psychological processes. The cognitive processes underlying the ERP components depend on the type of stimulus presentation (e.g. visual or auditory) and cognitive task demands (Luck, 2005).

The ERP components can be divided into two categories: exogenous and endogenous. Exogenous components occur up to 100 ms after stimulus presentation and are influenced by the physical characteristics of the stimulus. Exogenous components are followed by endogenous components; however, an overlap of both is likely, although, earlier components have more exogenous influence. Endogenous components relate to psychological processes, like attentional processes and decision-making (Birbaumer & Schmidt, 2010; Luck, 2005).

In the following sections, ERP components will be introduced that were elicited during visual target detection tasks similar to the experimental design of this thesis. Further details of EEG measurements and analysis will be introduced in subsequent sections.

The P1 represents an early positive component, which is linked to visual perception and the physical properties of a stimulus (Kuba, Kubová, Kremláček, & Langrová, 2007). It can be further modulated by temporal orientation and enhanced processing of target stimuli (Correa, Lupianez, Madrid, & Tudela, 2006). The P1 is suggested to reflect the cost of paying attention to an invalidly-cued location (Coull, 1998).

The N1 reflects designating and allocating resources for information processing before the occurrence of conscious attention and perception (Birbaumer & Schmidt, 2010; Hansen & Hillyard, 1980). It is influenced by the physical properties of the presented stimulus as well as selective and spatial attention. Therefore, the N1 increases in amplitude when the subject is paying more attention (Birbaumer & Schmidt, 2010; Hansen & Hillyard, 1980; Mangun, 1995). As it appears larger in discrimination than in detection tasks, it is suggested to be involved to some extent in discriminative processes (Vogel & Luck, 2000).

The P2 component is related to stimulus evaluation, encoding and comparison of several stimuli (McCarley, Faux, Shenton, Nestor, & Adams, 1991). Thus, the P2 is sensitive to stimuli containing target features, especially for relatively infrequent target stimuli and rather simple stimulus features (Luck, 2005; Luck & Hillyard, 1994). The P2 wave is often difficult to define due to its overlap with other components (Luck, 2005).

The N2 is a commonly observed ERP component in tasks requiring focused attention to stimuli and cognitive control, such as suppression of distractors. Localisation and amplitude modulation depends on task designs suggesting differential ERP components may be reflected within/may compose the N2 complex (Folstein & van Petten, 2008; Hillyard, 1985; Hopf, Schoenfeld, & Heinze, 2005; Schmiedt-Fehr & Basar-Eroglu, 2011).

The most prominent ERP component in research is the P3 component, which is a positive deflection elicited between 300 to 700 ms after presentation of a task-relevant target stimulus. The range can vary depending on various factors such as stimulus modality, task conditions, subject and age. The P3 is associated with cognitive processes like attention, memory and decision-making (Polich, 2007).

3.4. Event-related Oscillations (ERO)

Spatio-temporal integration of neuronal activity is suggested to be controlled through brain oscillations. The integrative function of collaborative brain oscillations seems to be a driving mechanism that enables the realization of the highly organized brain states necessary for perception and action (Basar, Basar-Eroglu, Karakas, & Schürmann, 1999; Basar & Güntekin, 2009; Buzsaki, Logothetis, & Singer, 2013). Brain oscillations, as measured with the EEG, occur in a wide frequency range, and are typically divided into five frequency bands: delta (< 4 Hz), theta (4 – 7 Hz), alpha (7 – 12 Hz), beta (12 – 30 Hz) and gamma (30 – 80 Hz). The boundaries of the bands vary slightly in literature and in addition, individual frequency band differences are detectable (Klimesch, 1996).

3.4.1. Delta Oscillations

Frequencies lower than 4 Hz are labelled as delta. Beginning as early as 1980, Basar suggested phase-locked delta responses as a major processing signal in the cat and human brain (Basar, Basar-Eroglu, Karakas, & Schürmann, 2001).

In general, delta oscillations may serve as systematic activation and coordination of different brain regions in the waking state. Nácher, Ledberg, Deco, and Romo (2013) indicated the role of coherent delta oscillations for large-scale network coordination between frontal and parietal brain areas during decision-making. Long-range delta oscillations were further linked to the fronto-parietal network through cognitive control and the focus of attention (Harmony et al., 1996; Mathewson et al., 2012; van Noordt et al., 2017; Yordanova, J. et al., 2004), while the association with working-memory processes also has been indicated (Mathes, Schmiedt, Schmiedt-Fehr, Pantelis, & Basar-Eroglu, 2012).

Delta oscillations play a role in cognitive processes like attention, recognition and decision-making (Güntekin & Basar, 2014) as well as during emotional processing in the detection and evaluation of (unknown) faces, affective face expressions and pictures (Güntekin & Basar, 2016). Delta oscillations can, in general, be linked to endogenous, cognitive processes (Güntekin & Basar, 2016; Harmony, 2013).

3.4.2. Theta Oscillations

The theta frequency band spans from 4 to 8 Hz. Theta oscillations commonly reach their maximum over frontal brain areas and a relation to cognitive top-down processes is suggested (Basar-Eroglu & Demiralp, 2001; Basar et al., 2001). Basar-Eroglu, Basar, Demiralp, and Schürmann (1992) measured theta oscillations in the hippocampus of the cat brain. Buzsaki (2002) concluded that hippocampal regulation is involved in theta oscillations during signal-detection tasks in the human brain. Furthermore, theta oscillations are thought to be based on the synchronizing influence of the thalamus (Hughes et al., 2004; Steriade, 2000; Steriade, Mccormick, & Sejnowski, 1993). Theta oscillations, as measured with the EEG, may thus predominantly reflect large-scale frontal networks including subcortical brain regions (Cohen, M. X. & Ridderinkhof, 2013; Kawasaki et al., 2014; Sauseng et al., 2006).

Recent studies revealed an increase of theta oscillation in tasks that demand selective attention and/or a controlled mobilisation of memory resources (Bösel, 2001), focused attention towards a stimulus during target detection (Basar-Eroglu & Demiralp, 2001; Mathes, Khalaidovski, Schmiedt-Fehr, & Basar-Eroglu, 2014), as well as a correlation between the increase of these oscillations with memory performance in a concentration-demanding task (Klimesch et al., 2004). The level of difficulty in tasks that require discrimination processes as well as several other memory- and attention-demanding tasks (see review: Bastiaansen & Hagoort, 2003) are related to these types of oscillations. Theta oscillations play a general role in a wide range of behaviour from arousal, attention and memory to the orienting reflex, conditioning and learning (Buzsaki, 2005). Theta rhythms also occur during the recognition of faces and their expressions (Güntekin & Basar, 2007), indicating a linkage to emotional paradigms with the involvement of limbic structures (see review: Basar & Güntekin, 2008).

Delta and theta oscillations, as they relate to the oddball paradigm, are described in more detail in section 3.5.3.

3.4.3. Alpha Oscillations

The alpha frequency band spans from 8 to 12 Hz. The alpha rhythm in the spontaneous EEG is blocked when the idling state is replaced by concentration, attention focusing and alertness (Jann et al., 2009).

Alpha oscillations are associated with sensory processing, anticipation, attention, working memory and the consolidation to long-term memory (Basar et al., 1999; Hanslmayr, Gross, Klimesch, & Shapiro, 2011; Klimesch, 1997).

The alpha frequency band can be sub-divided. The faster oscillations (upper alpha) may be connected to the relaxed state of mind as well as stimulus-related aspects and semantic memory processes (Klimesch, 1996).

The slower oscillations of the lower alpha may be related to the maintenance of attention (Orekhova, Stroganova, & Posikera, 2001), attentional demands (Klimesch, 1999), concept forming (Bösel, 2001) and memory load (Krause et al., 2000). Bösel (2001) suggested an attention shift in two steps: first the mobilization of memory resources (connected to theta activity) followed by a reorganisational constriction of neuronal activity (indicated by lower alpha oscillations). According to this model, lower alpha activity can be seen as an expression of cortical inhibition.

3.4.4. Beta Oscillations

After alpha rhythms are blocked in the spontaneous EEG upon withdrawal from the idling state, beta oscillations dominate (Birbaumer & Schmidt, 2010).

In event-related experimental designs, beta rhythms (12-30 Hz) are systematically varied by sensomotoric stimulation over corresponding cortical areas and by the association and execution of movements (see review: Kilavik, Zaepffel, Brovelli, MacKay, & Riehle, 2013; Neuper & Pfurtscheller, 2001). As beta activity is reduced or inhibited during an imagined or executed movement and as it is increased 300 to 1000 ms after the ended movement, it is correlated with the active facilitation of existing cognitive and motoric states (Engel & Fries, 2010). Beta oscillations are also related to high arousal, multisensory stimulation, cognitive load, attention processes and negative emotional stimulation (see review: Güntekin & Basar, 2014; Wrobel, 2000). Furthermore, beta activity plays an important role in the recognition of faces and their expressions (Güntekin & Basar, 2007; Ozgoren, Basar-Eroglu, & Basar, 2005).

3.4.5. Gamma Oscillations

Gamma oscillations span from 30 to 80 Hz, representing the higher frequencies. They are elicited by the interplay between inhibition and excitation processes in communication between single neurons (Bosman, Lansink, & Pennartz, 2014).

Synchronized gamma activity is suggested as a general dynamic mechanism for local integration processes of spatially allocated neurons and neuron populations (Fell et al., 2001; Herrmann & Demiralp, 2005; Stein & Nicoll, 2003). In the brain, information about an object is processed in parallel and thus the binding of this information is necessary for a coherent object representation, presumably implemented through gamma oscillations (Gray, König, Engel, & Singer, 1989). Herrmann, Munk, and Engel (2004) postulated that gamma oscillations are related to sensory and cognitive functions during perception, attention and memory. Overall, gamma oscillations can be linked to several low-level functions in circuit computations, in addition to higher cognitive functions as they are associated with visual attention, decision-making, response timing, motivation and short- and long-term memory (Bosman et al., 2014).

3.5. Brain responses elicited by the oddball paradigm

Two versions of the oddball paradigm were utilized in the current study. An oddball task consists of two or three stimulus categories presented in a sequence of several repetitions (Polich, 2007).

In the common two-stimulus oddball task, a participant is instructed to react to a rare, infrequent target stimulus but not to a frequently presented non-target stimulus. In the following sections this is referred to as the oddball task for simplification (Polich, 2007).

A variation of the oddball task is the novelty oddball task, which consists of three stimulus classes. In addition to target and non-target stimuli, novel stimuli are embedded in the presentation sequence. Novel stimuli, similar to non-targets, are not task-relevant and they serve as distractors. The distracting effect of novel stimuli is increased by their high salience and by presenting each novel stimulus only once within the entire paradigm. Both target and novel stimuli are presented rarely in comparison to non-targets (Polich, 2007).

The constant presentation of stimuli demands stimulus processing. However, stimulus classes require different attentional resources, and further differ with regard to cognitive control and response preparation. These differences are reflected in the N2 and P3 components and their underlying brain oscillations, which are explained in further detail below.

3.5.1. N2 complex

The three stimulus categories in the novelty oddball task may elicit three variations of the N2 (Bocquillon et al., 2014).

3.5.1.1 Non-target N2

The repeated presentation of an irrelevant non-target stimulus elicits a N2 complex with an anterior distribution. The non-target N2 was suggested to be related to attentional processing. Constant non-target processing in the Oddball task, however, only requires limited attentional capacities. In line with this view, the non-target N2 is reduced in amplitude compared to task-relevant target stimuli, which demand increased attentional processing (Folstein & van Petten, 2008).

3.5.1.2 Novelty N2

In case of a stimulus that differs from the expectation and the repetitive stimuli presented before, an N2 with larger amplitude follows. When no response is demanded upon novel stimulus presentation this amplitude is additionally increased. The N2 complex is distributed over fronto-central brain areas. The novelty N2 is not influenced by task difficulty. By contrast, visually more complex or unfamiliar novel stimuli elicit greater N2; however, this effect is rather related to a salient difference in category between frequent and rare stimuli (Daffner, K. R., Mesulam, et al., 2000). It can be seen as a process of mismatch detection (Folstein & van Petten, 2008).

3.5.1.3 Target N2

Rare target stimuli also deviate from the stimulus sequence, thus elicit an N2 larger than for non-target stimuli. By contrast, this N2 complex is located over posterior brain regions,

sensitive to target probability and appears slightly earlier in time than the novelty N2. The target N2 was suggested to be related to stimulus classification processes (Folstein & van Petten, 2008).

3.5.2. The P3 component

The P3 is suggested to be involved in various functions including attention, memory, and decision-making. It is also involved in the linking of signal perception, detection and recognition to task-relevant action (Basar-Eroglu et al., 1992; Basar-Eroglu, Demiralp, Schürmann, & Basar, 2001; Verleger, Gorgen, & Jaskowski, 2005). It thus reflects more than one specific cognitive function (Mathes et al., 2012).

This section introduces the two observed subcomponents of the P3 and their relation to stimulus classes. Further, theoretical models reflecting cognitive functions of the P3 are introduced.

3.5.2.1 P3a and P3b subcomponents of the P3

The P3 can be subdivided into an anterior P3a and a posterior P3b sub-component. The task design determines to what extent P3a and P3b manifest in the P3 (Polich & Comerchero, 2003).

P3a: The P3a is linked to an automatic shift of attention to salient stimuli. This shift is not dependent on task relevance. Thus, the P3a is elicited as an orienting response implying top-down control (Friedman, Cycowicz, & Gaeta, 2001; Luck, 2005). This view is in line with the evoking of P3a over frontal brain regions and frontal brain areas suggested to be involved in the P3a generation (Polich, 2007).

P3b: In the oddball task, a P3b has a centro-parietal maximum and is elicited upon detection of a task-relevant target stimulus. Memory processes during stimulus evaluation, categorization and response organisation are associated with the P3b. Temporal and parietal brain areas are involved in P3b generation (Polich, 2007).

Frontal activation is associated with attention driven working memory changes and elicits the P3a. The P3b is generated by temporal and parietal lobe activation and relates to the updating of context in the working memory. As depicted in Figure 10, the P3 is composed of

P3a and P3b related aspects, as both seem to be involved in target detection in the classical oddball design (cf. Figure 11) (Polich & Comerchero, 2003).

A circuit pathway between P3a and P3b was suggested, linking frontal and temporal/parietal brain areas (Polich & Comerchero, 2003; Soltani & Knight, 2000). In this way, combined top-down attention switching and bottom-up memory-driven processes guide response organisation and execution (Debener, Makeig, Delorme, & Engel, 2005; Escera, Alho, Winkler, & Näätänen, 1998; Goldstein, Spencer, & Donchin, 2002)

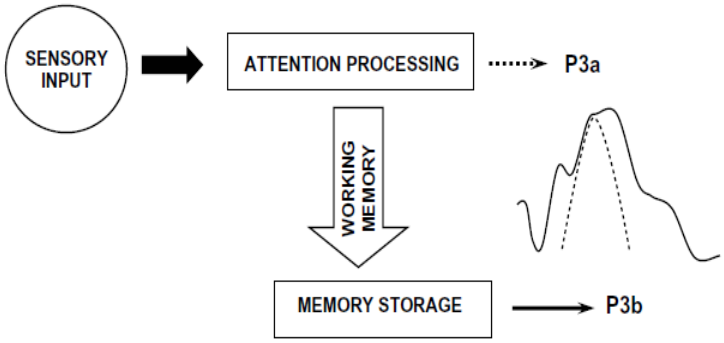

Figure 10: The P3 component consists of P3a and P3b subcomponents. Processing of sensory input demands attentional processing. Attention-driven working memory changes elicit a frontal P3a activation. Through storage of changes in working memory a temporal/parietal P3b is generated (figure & adapted description from Polich & Criado, 2006)

Novelty P3

In a novelty oddball task, the P3b aspect becomes more prominent for target stimuli. Thus, target stimuli elicit a P3b-like component over parietal cortical regions; while novel stimuli elicit a P3a-like component over frontal brain regions that occurs slightly earlier (cf. Figure 11 & Figure 10) (Polich & Criado, 2006). Difficult differentiation between target and non-target stimuli increases the elicited P3a amplitude upon the presentation of a novel stimulus. Novel stimuli serve as distractors; thus, attentional focus on task conductance is related to the P3a (Friedman et al., 2001; Gaeta, Friedman, & Hunt, 2003; Polich, 2007; Polich & Comerchero, 2003). The P3a is generated by frontal lobe activation relating to the hippocampus (Grunwald, Lehnertz, Heinze, Helmstaedter, & Elger, 1998; Knight, R., 1996).

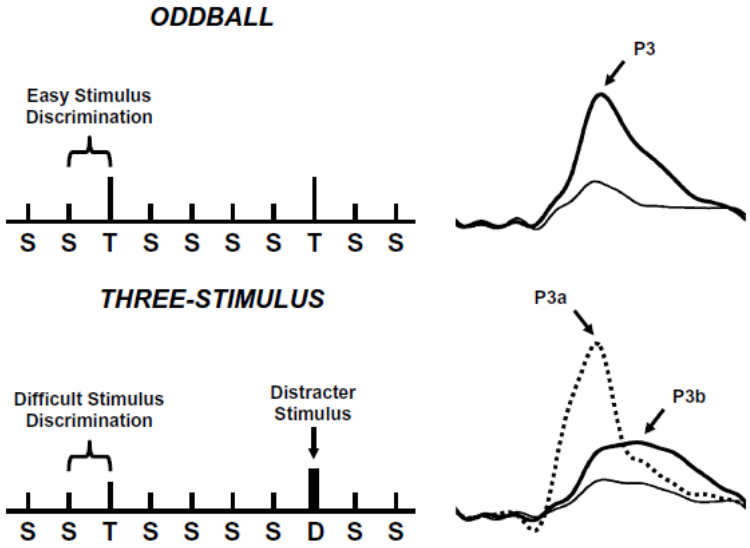

Figure 11: Top: Classical two stimulus Oddball task.
Left: Stimulus sequence of standard (S, frequent) and target (T, rare, demands response) stimuli in random order. Right: Elicited response upon stimulus presentation for S (thin line) and T (bold line) eliciting the P3
Bottom: Novelty three stimulus Oddball task.
Left: Stimulus sequence of S, T and distractors (D) in random order. Right: Elicited response upon stimulus presentation for S (thin line), T (bold line) eliciting a P3b and D (dotted line) eliciting a P3a (figure & description adapted from Polich & Criado, 2006).

3.5.2.2 Task demands

Figure 12 illustrates the necessity of attentional resources that are engaged during an oddball task and the factor of task demands resulting in variations of the characteristics of the P3, namely its amplitude and latency: The level of arousal provides a certain processing capacity for the allocation of attention in order for the fulfilment of the ongoing task. Several parallel-processed tasks or increasing task demands lead to a reduced P3 component (Kahneman, 1973; Polich, 2007).

The P3 latency is considered an indicator of processing requirements for stimulus evaluation and response preparation. With increasing difficulty of stimulus discrimination, the P3 latency increases with concurrent amplitude decreases (Luck et al., 2011). The P3 amplitude is sensitive to the amount of engaged attentional resources. The P3 amplitude is inversely correlated with the appearance frequency of the target stimulus (Duncan-Johnson & Donchin, 1982).

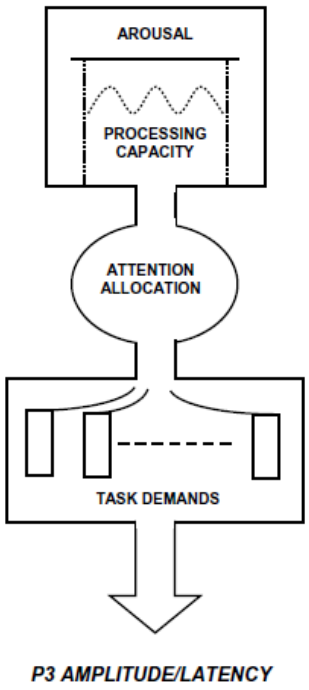

Figure 12: Schematic illustration of how attentional resources affect P3. This model provides a general framework for how attentional resources can affect P3 measures. Overall arousal level determines the amount of processing capacity available for attention allocation to ongoing tasks. More difficult or multiple task demands reduce P3 amplitude and lengthen peak latency (figure & description adapted from Polich, 2007).

3.5.2.3 Context-updating theory of the P3

Several theoretical models attempt to explain the cognitive processes related to the target P3. The context-updating theory and the perception-to-action model are two of these important models that are introduced in the following sections.

In 1981 Donchin laid the foundation for the context-updating theory, suggesting the formation of a mental model of presented stimuli through the engagement of working memory resources. Incoming stimuli are compared to a mental representation based on previously presented stimuli and subsequently classified as identical or deviant. Upon identical incoming and previous stimulus, the model is maintained and only ERPs related to sensory processing are elicited (N1, P2, N2).

By contrast, a new incoming stimulus, like a rare target, leads to attention allocation in order to update the mental model. As depicted in Figure 13, this process elicits an additional component subsequent to the N2: the P3 (Polich, 2007).

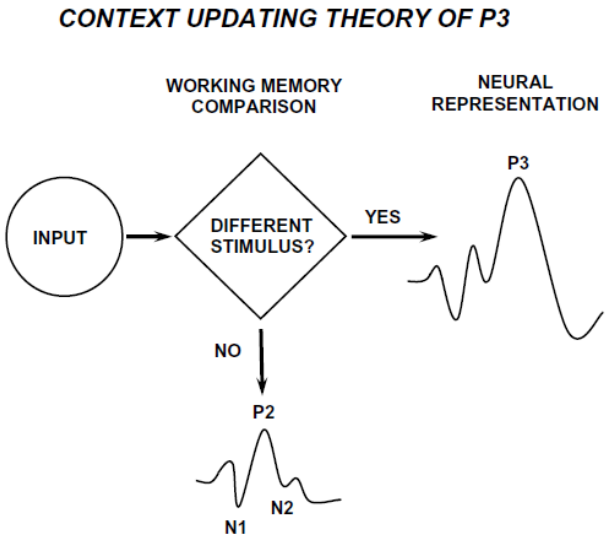

Figure 13: Schematic illustration of the P3 context-updating model. Stimuli enter the processing system and a comparison process of memories is engaged that ascertains whether the current stimulus is the same as the previous stimulus or not (e.g., in the oddball task, whether a standard or a target stimulus was presented). If the incoming stimulus is the same as the previous one, the neural model of the stimulus environment is unchanged, and sensory evoked potentials (N1, P2, N2) are obtained after signal averaging. If the incoming stimulus differs from the previous and the subject allocates attentional resources to the target, the neural representation of the stimulus environment is changed or updated leading to generation of a P3 (P3b) potential in addition to the sensory-evoked potentials. (figure & description adapted from Polich, 2007)

3.5.2.4 Perception-to-action model of the P3

The P3 in the perspective of the context-updating model can be seen as a rather strategic process on stimulus classification, as opposed to serving to organize a response upon target presentation. In 1988, Verleger (1988) proposed that the P3 may reflect strategic processing. Contrary to this proposition, he interpreted the P3 being elicited from the expectation of an occurring target rather than from an unexpected event, as suggested in the previous model. A decision implies a consequence – the response. Thus, the P3 may reflect the mediation process between perceptual analysis and response initiation. Once a stimulus is classified as response-relevant, the P3 could reflect monitoring whether or not this decision is appropriately transformed into action and it could thus serve as a link between perception and action (Verleger, Jaśkowski, & Wascher, 2005).

3.5.3. Event-related oscillations related to the P3 component

The P3 component upon target presentation in an oddball task is based on the oscillatory network activity of the brain. Already in 1992, Basar-Eroglu et al. (1992) investigated oscillations in a target detection task and revealed that the P3 is mainly composed of delta, theta and alpha oscillations, decreasing in proportion respectively. Thus, the overlay of aligned slow-wave delta and theta oscillations plays an important role in the formation of the relatively large and long-lasting positive deflection composing the P3. Simultaneously, the alpha band amplitudes decreased within the P3 time window (Kolev, Demiralp, Yordanova, Ademoglu, & Isoglu-Alkac, 1997). Modern analysis techniques provided additional affirmation for the assumption of superimposed oscillations of different frequency ranges underlying the P3 component (Demiralp, Ademoglu, Istefanopulos, Basar-Eroglu, & Basar, 2001).

Figure 14 displays how the ERP following the presentation of a target or non-target stimulus is composed of an overlay of the frequency bands delta, theta and alpha (here: 8 – 16 Hz). Figure 14 also shows how the oscillations are distributed from anterior to posterior over the central line of the scalp.

For the P3a wave, fronto-central theta oscillations in connection to simultaneous delta oscillations play a major role. The P3b wave is prevailed by delta oscillations with a parietal predominance (Kolev et al., 1997).

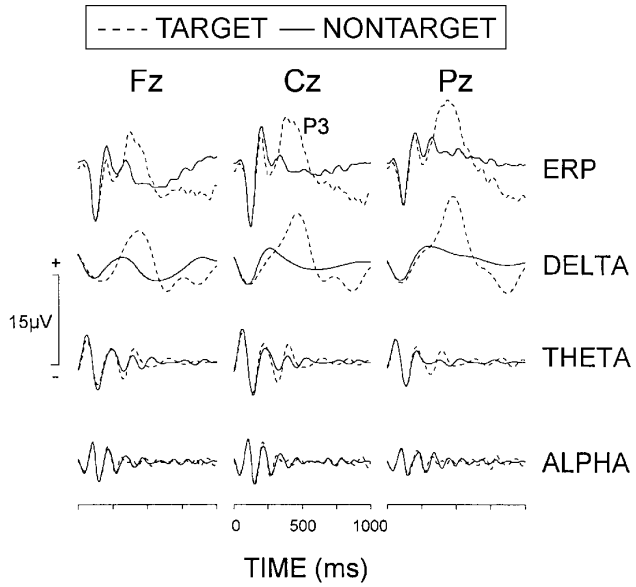

Figure 14: Grand average ERPs from oddball non-target and target stimuli and the reconstructed delta (0.5 – 4 Hz), theta (4 – 8 Hz) and alpha (8 – 16 Hz) frequency components. Stimulus onset occurred at 0 ms (adapted figure & description from Kolev et al., 1997).

3.5.3.1 Delta oscillations

Underlying the P3, delta oscillations are discussed as a part of the processes involved in signal detection and evaluation (Basar-Eroglu et al., 1992). Furthermore, delta oscillations seem to play a major role in decision-making, working memory processes and response initiation involved in target detection (Basar-Eroglu et al., 1992; Basar et al., 2000; Mathes et al., 2012; Verleger, Jaśkowski, et al., 2005). Coherent delta oscillations have also been associated with attentional processing during novelty processing (Isler, Grieve, Czernochowski, Stark, & Friedman, 2008; Polich, 2007; Prada et al., 2014). Through these various functions, delta oscillations can be linked to the fronto-parietal network (Mathewson et al., 2012; Miskovic et al., 2015).

3.5.3.2 Theta oscillations

In an oddball experiment, sustained theta activity can be observed. Theta might be the most consistent element of the P3 component (Basar et al., 1999, 2001). Buzsaki (2002) concluded that hippocampal regulation is involved in theta oscillations during such tasks.

Medial frontal theta oscillations are discussed as a major top-down communication tool in the fronto-parietal network, in order to integrate information from memory and bias sensory gating toward target stimuli (Buzsaki & Draguhn, 2004; Klimesch, 1999). Theta oscillations are related to a variety of cognitive control functions, as theta oscillations are generally associated with attentional processes, such as focused attention towards a detected target stimulus (Basar-Eroglu & Demiralp, 2001; Mathes et al., 2014) or novelty processing (Hajihosseini & Holroyd, 2013).

Theta oscillations play a major role in the P3a subcomponent, as they are elicited upon violation of regularity in a stimulus sequence (Ursu et al., 2009) and stimulus novelty (Berns et al., 1997).

Enhancements of theta oscillations in the oddball task occur slightly earlier in time compared to delta oscillations and also contribute to the earlier N2 complex (Hajihosseini & Holroyd, 2013; Schmiedt-Fehr & Basar-Eroglu, 2011). The N2 complex and concurrent theta activity is also linked to attentional processes, such as attention control, and, further, to inference processing (Braver et al., 2001; Chan et al., 2008; Coderre et al., 2011; Niendam et al., 2012).

3.5.3.3 Alpha oscillations

Alpha oscillations are generally associated with sensory processing, attention and working memory; cognitive processes required during oddball processing (Basar et al., 1999; Hanslmayr et al., 2011; Klimesch, 1997). Alpha oscillations are suggested to be involved in perceptual memory processes indicated by more posterior alpha distribution during target detection (Basar et al., 2000).

3.6. Time-frequency analysis

3.6.1. Mathematical background of time-frequency analysis

Time-frequency analysis enables the investigation of oscillations, as it allows the separation of the frequency bands from an EEG signal. One mathematical form of time-frequency analysis is the wavelet transformation.

Wavelet transformation is a suitable technique for the decomposition of the EEG signal into its amplitude and phase components for specific ranges of frequency, all the while preserving time information in order to enable examination of their changes over a period of time (Cohen, M. X., 2014).

The components are estimated by a convolution of the original signal and a wavelet as represented by Equation 1. The wavelet is generated by complex conjugation of a joint function, the mother wavelet, through scaling (change of oscillation length) and translation.

$$W_z^{\Psi}(b,a) = A_{\psi} \int \Psi^* \left(\frac{t-b}{a}\right) x(t)dt \qquad \textbf{Equation 1}$$

In Equation 1, *x(t)* represents the EGG signal over time of a single epoch. *Ψ** describes the complex conjugate of the scaled and translated wavelet ψ, with *a* standing for the scaling and *b* for the translation parameter. A_{ψ} denotes a wavelet specific normalization parameter.

The resulting wavelet coefficient $W_z^{\Phi}(b,\ a)$ gives a measure of the congruence of the wavelets to the original signal for the given time-frequency-range (*b*, *a*). Curve progression of the mother wavelet is supposed to be chosen in accordance with the curve progression of the original signal. The scale parameter is an inverse of the frequency. Therefore, high scales

(low frequencies) represent large patterns in the EEG signal and vice versa (Herrmann, Rach, Vosskuhl, & Strüber, 2014).

The **Morlet wavelet**, specified in Equation 2, consists of the multiplication of a complex sinusoid wave (first term) with a Gaussian (second term), displayed in Figure 15. The Gaussian function serves as an envelope function with the characteristic of exhibiting the highest sensitivity for a specific time window and frequency range. The wavelet is finite in both time and frequency space, has zero mean amplitude and reflects the sinusoidal features of the biological EEG signal (Herrmann, Grigutsch, & Busch, 2005). Therefore, it is suitable for the analysis of EEG signals and was assessed for analysis in the present study.

$$\Psi(\mathrm{t}) = e^{j\omega_0 t} * e^{-t^2/2} \qquad \textbf{Equation 2}$$

In Equation 2, ω_0 represents the dimensionless angular frequency, which determines the width of the wavelet in time.

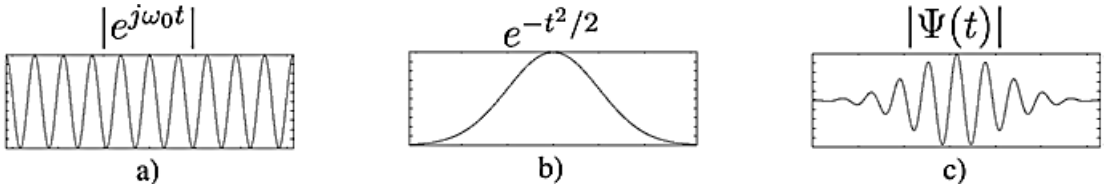

Figure 15: By multiplication of the sinusoidal function (a) with the envelope function (b) the mother wavelet (c) results (Herrmann et al., 2005).

The time resolution depends on the standard deviation of the Gaussian in the time domain and is given by Equation 3.

$$\sigma_t = \frac{n}{2\pi * f_0} \qquad \textbf{Equation 3}$$

In Equation 3, f_0 represents frequency as an inverse of the scale parameter, while *n* refers to the number of wavelet cycles and defines the trade-off between temporal precision and frequency precision The approximate width in time of the centre frequency of the used wavelet is estimated as twice the folding time of the used Morlet wavelet (i.e., the time after which the Gaussian window has dropped to exp(-2) ≈ 14%) (Torrence & Compo, 1998).

The frequency range is inversely related to the standard deviation of the Gaussian in the time domain, as depicted in Equation 4; it is defined by approximately two standard deviations of the wavelet in the frequency domain.

$$\sigma_f = \frac{1}{2\pi * \sigma_t}$$ **Equation 4**

Thus, the time and frequency resolution of the wavelet analysis depends on the choice of the centre frequency f0 and number of wavelet cycles of the Gaussian function. The option to vary the resolution in the time and frequency domains is the main advantage in contrast to the standard short-time Fourier Transform. The choice of the parameters of the wavelet influences a trade-off between temporal and spectral resolution, allowing improvement of the temporal resolution for higher frequencies as well as the improvement of frequency resolution for lower frequency ranges (Herrmann et al., 2014).

3.6.2. Amplitude

For each subject, factor level and single trial the amplitude *A* of the given frequency band over time as the absolute value of the transformed data can be calculated by wavelet transform and averaged over all included trials (Mathes et al., 2012):

$$A(t) = (|W_x|)_{Trials}$$ **Equation 5**

This measure reflects the induced EEG response, which is the oscillatory activity following a sensory stimulation that is not necessarily time-locked to a stimulus (cf. Basar-Eroglu, Strüber, Schürmann, Stadler, & Basar, 1996). Figure 16 depicts the difference between evoked and induced cerebral activity. Evoked activity occurs time-locked to a stimulus onset and adds up when averaged for several trials. By contrast, induced activity is not time-locked to the stimulus occurrence and exhibits a latency or phase jitter when compared for several trials. Induced activity nearly cancels out when averaged across trials (cf. Herrmann et al., 2005).

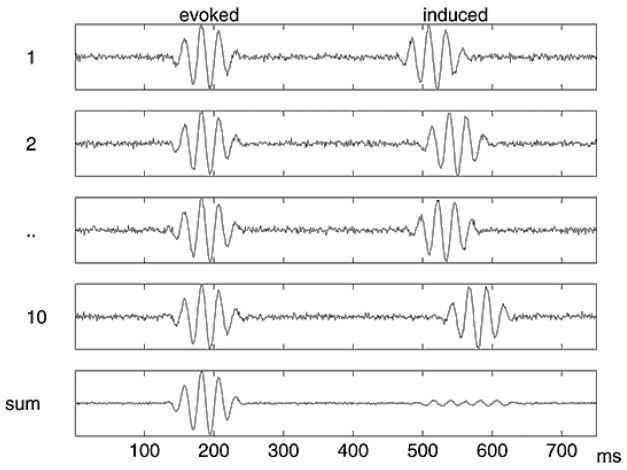

Figure 16: Cerebral oscillatory activity for multiple trials (rows 1-4) after stimulus presentation (0 ms). Evoked activity (left) occurs time-locked to stimulus onset, while induced (right) activity exhibits a latency or phase jitter in regard to stimulus onset. On average evoked activity sums up, while induced activity is nearly cancelled out (figure & adapted description from Herrmann et al., 2005).

3.6.3. Baseline correction

For event-related brain activity, single trial amplitude measures can be baseline-corrected using the Z-transform (as suggested by Uhlhaas et al., 2006) with a time window preceding the stimulus onset. This enables an estimation of the amplitude changes induced by the stimulus onset and it is of particular interest for the investigation of maturational changes of the brain, since the frequency composition of spontaneous brain activity varies with age (Mathes, Khalaidovski, Wienke, Schmiedt-Fehr, & Basar-Eroglu, 2016).

The Z-transform corrects for *1/f* power law scaling in order to allow the comparison of data across frequencies, electrodes, conditions and subjects (with *f* representing frequency). In comparison to other baseline correction methods (e.g. decibel, percentage change), the Z-transform corrects for outliers in a stronger manner by scaling to standard deviation units in relation to the overall power of the baseline time window (Cohen, M. X., 2014).

$$z_{tf} = \frac{activity_{tf} - \overline{baseline_f}}{\sqrt{n^{-1}\sum_{i=1}^{n}\left(baseline_{tf} - \overline{baseline_f}\right)^2}} \qquad \textbf{Equation 6}$$

In Equation 6, *n* indicates the number of time points in the baseline period, *f* the frequency and *t* a time point, while *activity* stands for the signal as it is corrected in relation to the

baseline. The denominator represents the formula for the calculation of the standard deviation.

3.6.4. Event-Related Spectral Perturbation (ERSP)

The amplitude reflects the magnitude of the local synchronization of neural firing patterns (Pfurtscheller & Lopes da Silva, 1999). To estimate the amplitude changes induced by an event (i.e., stimulus onset) the mean baseline log spectrum is subtracted from each spectral estimate, producing a baseline-normalised time-frequency distribution referred to as the post-stimulus amplitude modulation or event-related spectral perturbation (ERSP). The estimated values indicate amplification or attenuation (in dB) at a given frequency and latency relative to the baseline (time window preceding stimulus onset; see Delorme and Makeig (2004) for a detailed description of the method). The chosen baseline should be set by the width in time of the wavelets used for filtering (for more information see (Mathes et al., 2014; Mathes et al., 2012).

3.6.5. Inter-trial Phase Coherence (ITC)

The inter-trial phase coherence (ITC) enables the estimation of phase consistency over trials within a particular time-frequency window, i.e., the phase-locking with respect to an experimental event, e.g., stimulus onset. A value of ITC = 0 represents the absence of consistent EEG phases; values near 1 indicate perfect alignment (see Delorme & Makeig, 2004) for a detailed description of the method).

This measure may reflect the local stability of a functional network (Yordanova, Juliana & Kolev, 2009). Group differences in ITC may occur without changes in amplitude modulations (Busch, Dubois, & van Rullen, 2009; Cohen, M. X., 2014).

3.6.6. Spatial phase coherence (SPC)

Spatial phase coherence (SPC) methods allow the investigation of network communities of the brain measured by EEG. In contrast to other time-frequency EEG measures, which describe local electrode information, SPC calculates inter-electrode information, thus assessing neural activity between different brain regions.

To calculate an SPC index, the phase of the oscillatory signal of different electrode locations needs to be extracted for a defined time window and a frequency band. Thereafter, a phase comparison between different signal locations is conducted in order to determine the coupling intensity.

3.6.6.1 Extraction of phase information of EEG signal

Convolution of an EEG signal with a complex Morlet wavelet as kernel utilizes a dot product (see also of section 3.6.1) and results in a complex number containing a real and an imaginary part. Applying Euler's formula, a representation of this complex number as a vector in the polar space is feasible (see Figure 18). The phase is given by the angle of the vector in relation to the positive real part axis. Therefore, the convolution of a signal and a wavelet gives information about the relative phase depending on kernel and signal at one time point. It can also be used as the basic step for analysis of spatial phase coherence (see Figure 17).

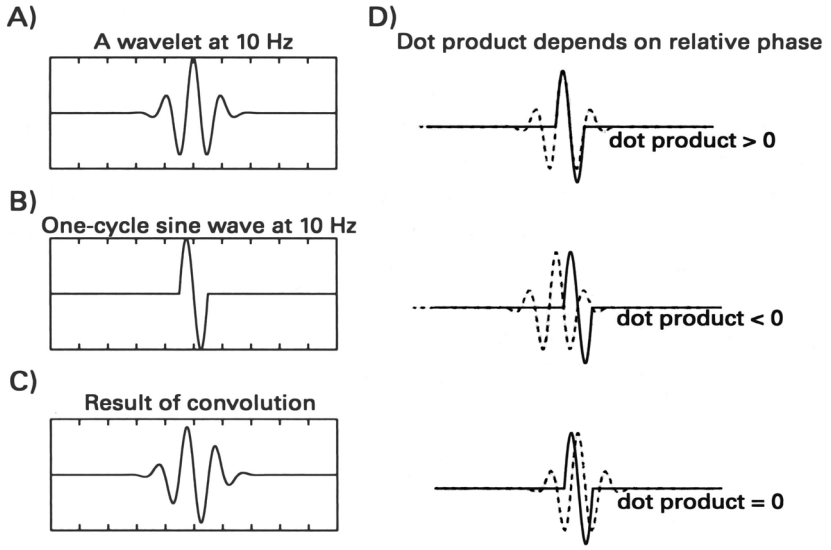

Figure 17: The result of each step of convolution (the dot product between a wavelet and data). The dot product depends on the phase relationship between the kernel and the signal at that time point. (figure & adapted description from Cohen, M. X., 2014)

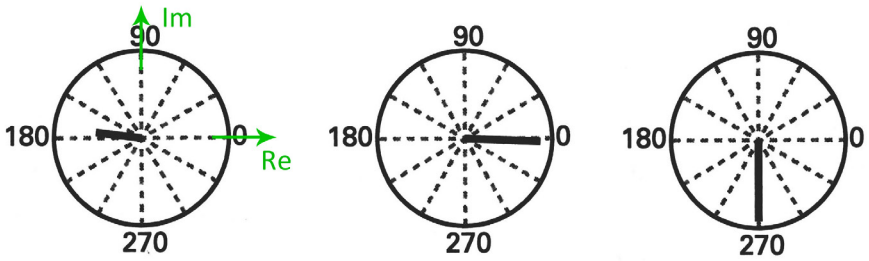

Figure 18: Three different dot products of signals and a complex Morlet wavelet presented as vectors in polar space. Real (Re) and imaginary (Im) axes are indicated by green labelled arrows. (figure adapted from Cohen, M. X., 2014)

As depicted in Figure 18 dot products of signals and wavelets can be presented as vectors with regard to the real and imaginary parts in polar space. The presentation in polar space has the advantageous option to plot several convolution results at once and it therefore helps to visually explain the analysis of spatial phase coherences (see Figure 19).

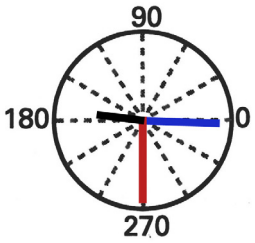

Figure 19: Three different dot products of signals and a complex Morlet wavelet presented as vectors in one polar plane. All three vectors of Figure 18 can be displayed in one single polar plane. (figure adapted from Cohen, M. X., 2014)

The length of the vector in polar space indicates the similarity of the kernel and the signal, however gives no further information about the phase. For more simplistic visualisation of the phase analysis the vectors can be displayed in the polar space with a standardised length of 1.

In order to gain information about not only one time point of the signal but rather a time series over a larger time window a complex Morlet wavelet is applied. The complex Morlet wavelet follows Equation 7, in which t represents time, f is the peak frequency of the wavelet, while s stands for the standard deviation of the Gaussian curve. The first part of the equation is a frequency specific scaling factor of the Gaussian (first exponential of the equation). The second exponential of the equation is a complex sine wave. A complex wavelet can be conceptualized as a corkscrew with three dimensions of time, real and imaginary dimension sliding in time the convolution process over the signal (Cohen, M. X., 2014).

$$\mathbf{cmw} = \left(s\sqrt{\pi}\right)^{-1/2} e^{-t^2/2s^2} \; e^{i2\pi ft} \qquad \textbf{Equation 7}$$

3.6.6.2 Usage of spatial phase coherence

Functionally coupled neural populations synchronise their activity of oscillatory patterns leading to phase-synchronization patterns in the form of systematic phase-delays. Therefore, an analysis of the temporal correlation of spatially distributed EEG electrode signals of a frequency band reveals information about such an underlying neural connectivity through an investigation of their phase-relations.

Phase-based connectivity analysis depends on the distribution of phase angle differences between two electrodes compared for their consistency over several trials (Cohen, M. X., 2014). For comparing phase angle differences, the angles cannot simply be averaged; instead, their vectors must be summed up, resulting in a difference vector. In the following section 3.6.6.5, the phase synchronization index WPLI (weighted phase lag index) based on the PLI (the phase lag index) is explained in more detail.

3.6.6.3 Volume conduction

Neural activity provokes electrical fields that spread through the volume of the brain to the scalp by volume conduction. This enables neurophysiological recordings via electrodes on the scalp. Volume conduction, however, can lead to spurious connectivity results, as the electrical fields can also spread 'laterally' through head tissue towards neighbouring electrodes. In this case, volume conduction causes an instantaneous spread of the signal, leading to a phase lag difference of either zero or π (π in the case of the electrodes positioned on opposite sides of the dipole). Correcting for volume conduction always accounts for the issue of the possible existence of true connectivity with a zero- or π-phase lag caused by cerebral activity.

3.6.6.4 Phase Lag Index (PLI)

The phase lag index (PLI; Stam, Nolte, & Daffertshofer, 2007) estimates for a particular frequency band to what extent the phase difference between signals from two EEG electrodes are non-equiprobable, i.e. whether they are distributed toward the positive or negative sides of the imaginary axis on the complex plane. The sign of the imaginary part of

the cross-spectral density is averaged, irrespective of the magnitude of the phase difference. Figure 20A depicts the phase difference vectors in the polar plane with a standard length set to ± 1. The magnitude of the PLI value is shown as a black arrow. In Figure 20B the pairwise products of all imaginary components with their standardized length are described. Identical signs give a positive product, indicated by a red square, while unequal signs lead to a negative product in blue. The diagonal with the products of identical objects is excluded. For the estimation the order of the components is irrelevant.

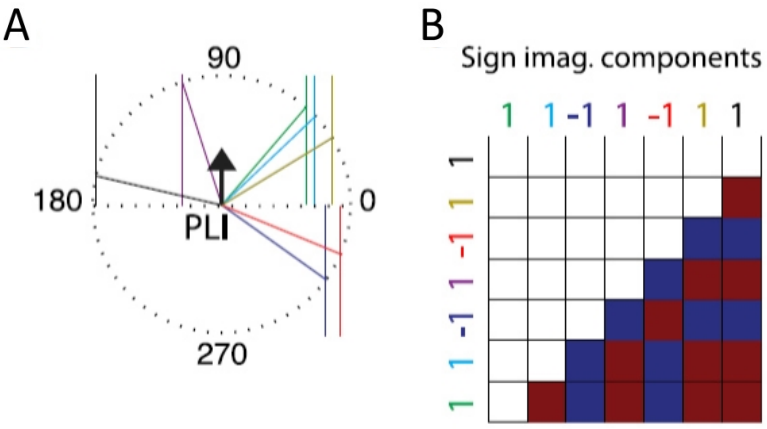

Figure 20: Graphical illustration of the PLI and its estimator. (A) Each coloured line originating from the centre of the circle represents a phase angle difference vector (cross-spectrum) in polar space, scaled to 1. Vertical lines originating from the endpoints of the cross-spectra represent the sign of their corresponding imaginary components. The PLI value is shown as a black arrow. (B) The unbiased PLI-square estimator is defined as the average of all pairwise products of signs. Pairs with identical observations are excluded (diagonal). Red squares indicate equal signs, blue squares indicate unequal signs. Order of 1's and -1's is irrelevant (figure & adapted description after Vinck, Oostenveld, van Wingerden, Battaglia, & Pennartz, 2011).

The PLI is calculated according to Equation 8, in which *imag*(S_{xyt}) indicates the imaginary part of the cross-spectral density (the pairwise product of each cross-spectrum) between activities at two electrodes *x* and *y* at time point (or trial) *t*. The *sgn()* function assigns +1 for positive values, -1 for negative values, and 0 for zero values. All signs of the imaginary components are then added up (compare with Figure 20B), normalized through dividing by the number of cross spectra (*n*) and the calculated absolute value is the PLI.

$$PLI_{xy} = \left| n^{-1} \sum_{t=1}^{n} sgn(imag(S_{xyt})) \right| \qquad \textbf{Equation 8}$$

The PLI is insensitive to volume conduction, as it predominantly considers the phase angle differences dominating on one side of the real axis. Phase lag differences distributed around zero and pi lead to very small PLI values. The index is assigned to values between zero (no spatial connection or volume conducted noise) and one (high spatial connectivity).

Figure 21 depicts some examples for PLI values and their corresponding phase angle distributions.

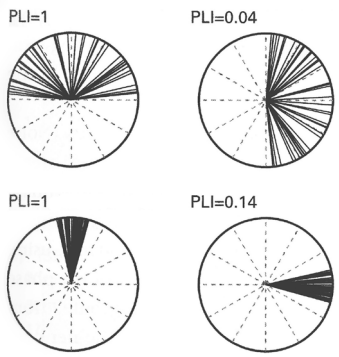

Figure 21: Comparison of PLI under different phase angle distributions. The value is sensitive to the phase angle directions rather than clustering per se. (figure & description adapted from Cohen, M. X., 2014)

The PLI, however, is not an index of the variance of the phase angle differences as seen in Figure 21 & Figure 22.

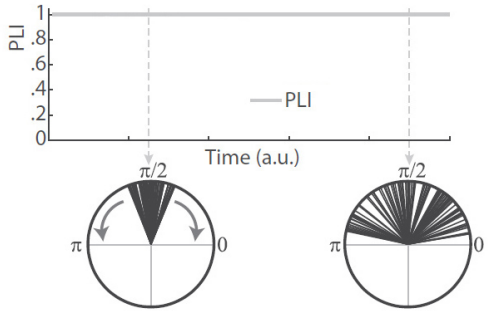

Figure 22: The PLI reflects the proportion of phase angle differences above or below the real (horizontal) axis. The phase angle differences remained above the real axis but the variance increased over time (visualized in the lower polar plots). The top plot shows time courses of connectivity. The PLI remains at 1.0 because it is only sensitive to the proportion of phase angles that point to one side of the real axis, but not to the variance of the phase angle distributions, which increased over time. (figure & description adapted from Cohen, M. X., 2015)

Figure 23 demonstrates that a subtle frequency mismatch between two oscillators (in non-coupled neural populations) will cause the cluster to spin around the polar plane, leading to transient fluctuations in the PLI values as the cluster crosses zero or pi radians.

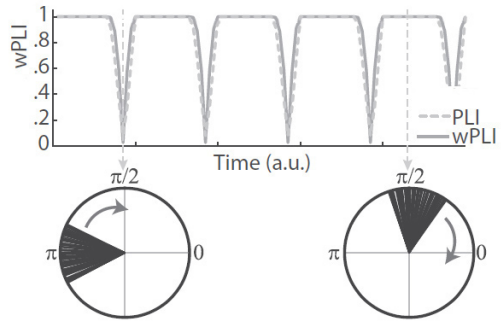

Figure 23: Simulated connectivity had the same clustering but cycled around the polar plane (visualized in the lower polar plots). This phenomenon occurs when there is a subtle frequency mismatch between the two oscillators, and occurs in real neural data. The top plot shows time courses of connectivity. The PLI and WPLI exhibited large fluctuations corresponding to the distribution crossing the real axis 0 or π. (figure & description adapted from Cohen, M. X., 2015)

3.6.6.5 Weighted Phase Lag Index (WPLI)

The weighted phase lag index (WPLI) is an extension of the PLI (Vinck et al., 2011). In addition to the PLI, each phase angle difference is weighted by the magnitude of the imaginary component of the cross-spectrum, i.e., its distance from the real axis. Therefore, as displayed in Figure 24, vectors around zero or pi radians contribute to a lesser extent, while vectors more distant from the real axis have a greater influence on the WPLI.

Equation 9 depicts the equation for the WPLI calculation. A weighting term is appended to Equation 8 of the PLI. For the WPLI, the sign of the imaginary component is additionally scaled by the magnitude of its component before all values are added up (see nominator).

$$\boldsymbol{WPLI_{xy}} = \frac{\boldsymbol{n^{-1}} \sum_{t=1}^{n} \left| \boldsymbol{imag}\left(\boldsymbol{S_{xyt}}\right) \right| \boldsymbol{sgn}(\boldsymbol{imag}(\boldsymbol{S_{xyt}}))}{\boldsymbol{n^{-1}} \sum_{t=1}^{n} \left| \boldsymbol{imag}\left(\boldsymbol{S_{xyt}}\right) \right|} \qquad \textbf{Equation 9}$$

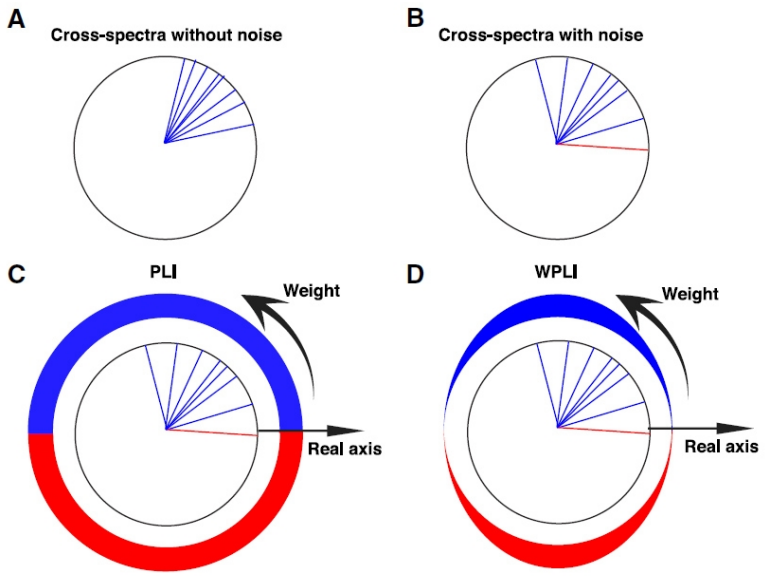

Figure 24: Illustration of the PLI and the WPLI. (A) Cross-spectra without noise. (B) Cross-spectra with noise, causing one of the cross-spectra to rotate across the real axis. (C) PLI weights all cross-spectra equally, and assigns a value of +1 (blue; phase lead) or -1 (red; phase lag) depending on which side of the real axis a cross-spectrum lies. (D) WPLI weights cross-spectra according to the magnitude of the imaginary component of the respective cross-spectrum. Cross-spectra around the real axis contribute to a lesser extent to the WPLI than cross-spectra around the imaginary axis. (figure & description from Vinck et al., 2011)

The WPLI connectivity estimator was further developed through introduction of a debiasing term to correct for some inflation due to sample size, naming it dWPLI (Vinck et al., 2011). Figure 25A depicts the phase difference vectors in the polar plane, this time the magnitude of the imaginary part is considered. In Figure 25B the dWPLI-square estimator is graphically explained. The corrected term of the dWPLI consists of a fraction. The imaginary components including their sign are multiplied pairwise and summed up to estimate the nominator. In contrast, the sign is not considered for calculation of the denominator; pairwise products of only the absolute values of the imaginary components are summed up. Again the diagonal is not taken into consideration. The index of the dWPLI still takes values between zero and one.

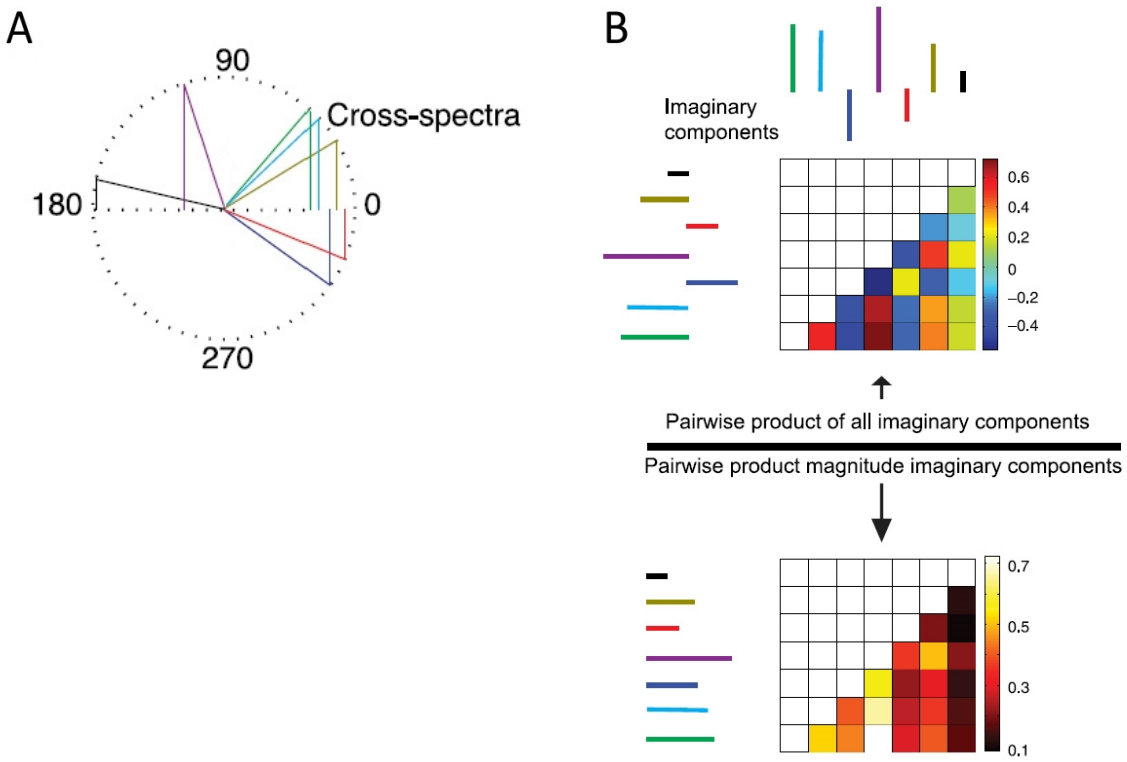

Figure 25: Graphical explanation of the debiased WPLI-square estimator. (A) Each coloured line originating from the centre of the circle represents a phase angle difference vector in polar space, scaled to 1. Vertical lines originating from the endpoints of the cross-spectra represent the magnitude of the corresponding imaginary components. (B) Top (nominator): the debiased WPLI-square estimator's numerator is defined as the sum of all pairwise products of imaginary components that correspond to the imaginary components in (A). Bottom (denominator): the denominator of the debiased WPLI-square estimator is defined as the sum of all pairwise products of the magnitudes of the imaginary components. (figures & description adapted from Vinck et al., 2011)

3.6.6.6 WPLI as tool for the investigation of brain maturation

The WPLI is suitable to investigate moment-to-moment variability of functional brain connectivity without being distorted by spurious volume conduction effects (Bastos & Schoffelen, 2015; Cohen, M. X., 2014, 2015). Contrary to other measures, the WPLI does not require an age-fitting brain model and is suitable for data-driven analysis (Cohen, M. X., 2014). These properties make the WPLI specifically suitable for studying developmental changes in event-related functional brain connectivity, because developmental studies on brain connectivity are still piloting and implicate extensive neural reorganisation (Uhlhaas et al., 2009).

4. Developmental changes in the EEG-signal

Evidence is strong that precise temporal patterns of oscillatory brain activity serve as the fundament of cognitive functions and brain network communication (Basar et al., 1999; Basar & Güntekin, 2009; Buzsaki et al., 2013; Merchant, Harrington, & Meck, 2013; Nobre, Correa, & Coull, 2007). The electroencephalography (EEG) is a suitable non-invasive technique to investigate the precise dynamic of cognitive processes with a high temporal resolution. Throughout the human life, age-related changes affect brain activity. The EEG enables to study developmental changes of oscillatory patterns underlying these changes in brain activity (Basar, 2011; Segalowitz, Santesso, & Jetha, 2010) and, therefore, is employed as the tool to gather data discussed throughout this thesis.

4.1. Developmental changes in spontaneous EEG

Cerebral changes are related to changes in the spectrum of neuronal oscillations; however, it is still unclear whether the cerebral changes cause and/or are caused by changes in the oscillation spectrum.

Absolute & relative power changes of frequency bands

A general decline of absolute EEG power with age is detectable beginning in posterior and shifting towards anterior regions with age, within and across brain regions, and including all bands, but it is most prominent in the slow-wave bands (delta and theta) for childhood and

adolescence (Barry & Clarke, 2009; Cragg et al., 2011; Dustman, Shearer, & Emmerson, 1999; Gasser, Jennen-Steinmetz, Sroka, Verleger, & Mocks, 1988; Gasser, Verleger, Bacher, & Sroka, 1988; Segalowitz, Santesso, & Jetha, 2010). This trend might extend into early adulthood with a slowing tendency (e.g. see life span sample Dustman et al., 1999). Furthermore, slow-wave oscillations also decrease for relative EEG power during development. The faster oscillatory bands however, exhibit a slight (gamma & alpha) and steady (beta) increase of relative EEG power during development (Clarke, Barry, McCarthy, & Selikowitz, 2001; Cragg et al., 2011; Dustman et al., 1999; Gasser, Jennen-Steinmetz, et al., 1988; Gasser, Verleger, et al., 1988; Segalowitz, Santesso, Murphy, et al., 2010).

The EEG signal is thus dominated by slow-wave oscillations in children, e.g. beta oscillations especially are of low power in early childhood (Plowman, Dustman, Walicek, Corless, & Ehlers, 1999).

Relation to other brain changes

Absolute EEG power is reflected by the sum of pyramidal neuronal activity. Excessive reduction in grey matter might, therefore, account for or play an in important role in the steady decrease of absolute EEG power (Whitford et al., 2007). As these developmental changes are not linear or equal between individuals (Segalowitz & Davies, 2004), an increase in intra-individual variance of EEG power can be observed in this age period (Whitford et al., 2007). This variance is not only explained by grey and white matter changes (Whitford et al., 2007), but also by other factors, including developmental variations in the level of neurotransmitters (also see review: Segalowitz, Santesso, & Jetha, 2010; Uhlhaas & Singer, 2011), synaptic density and increased information-processing efficiency (Segalowitz, Santesso, & Jetha, 2010).

Changes within frequency bands

The mean frequency of alpha oscillations increases from childhood to an adult level of around 10 Hz by 10 to 16 years of age (Marcuse et al., 2008). Developmental changes also occur within conventional frequency bands. Splitting of the alpha band into lower alpha (7.5 to 9 Hz) and upper alpha (9.5 to 12 Hz) revealed a power increase in the upper alpha range during early adolescence, while lower alpha oscillations show little or no change (Cragg et al., 2011). There is also evidence for developmental differences between genders, indicating an earlier maturation of EEG power in males during childhood, while females undergo the maturation during adolescence (Cragg et al., 2011).

4.2. Developmental changes in event-related oscillations

Similar to EEG power, decreases the intra- and inter-individual variance of EROs with maturation (Dustman et al., 1999). In relation to pre-stimulus amplitudes, post-stimulus amplitude enhancements of slow-wave oscillations seem to increase with age (Liu et al., 2014; Mathes, Khalaidovski, et al., 2016; Yordanova, J. & Kolev, 1997). The degree of phase-locking of the EROs in tasks including control processing, perception, and learning was found to increase with brain maturation, especially in the theta band (Liu et al., 2014; Müller, Brehmer, von Oertzen, Li, & Lindenberger, 2008; Yordanova, J. & Kolev, 1998). In a study of Yordanova, J. and Kolev (1996), adults showed reduced alpha response amplitudes but stronger phase-locking to target stimuli compared to children. Werkle-Bergner, Shing, Müller, Li, and Lindenberger (2009) observed increasing involvement of gamma oscillations in a discrimination task from childhood to young adulthood. Other studies indicate that also the coupling between oscillatory responses improves during childhood and adolescence (Cho et al., 2015; Hwang, Ghuman, Manoach, Jones, & Luna, 2016; Wang et al., 2014). These findings indicate that maturation of timing and post-stimulus amplitude modulation of EROs affects multiple oscillatory systems and their interrelation across a wide range of frequencies.

Papenberg, Hämmerer, Müller, Lindenberger, and Li (2013) found a correlation of higher variability in medial frontal inter-trial coherence of stimulus-locked theta oscillations with an increased variability of the reaction times (RT) and with lower behavioural performance in a Go/NoGo task. This variability is especially high in children compared with young adults, indicating that variable medial frontal cortical control may be related to performance fluctuations.

Taken together, functional brain communication is characterised by task-related amplitude modulation and precision of response timing, both being enhanced during adolescence. In accordance with the structural changes described in section 2.5, brain communication is thought to become faster, more precise and more efficient with brain maturation (Luna et al., 2010; Segalowitz, Santesso, & Jetha, 2010).

4.3. Developmental changes of event-related potentials

The event-related potential (ERP) reflects the response of the brain to a presented stimulus. In order to increase the signal-to-noise ratio, EEG data from several repeated trials is averaged time-locked to the same stimulus presentation.

Cerebral development is to some extent reflected in the ERP and its concurrent ERO. Commonly, a clear differentiation between effects on the ERP caused by structural changes or by different skills or strategies is not possible (Segalowitz, Santesso, & Jetha, 2010). In general, the results for amplitude and latency changes of ERP components vary across studies, as different tasks and different stimuli affect results (Polich, 2007). Overall, the ability for faster signalling and better-structured neuronal networks lead to increased processing speed (Blakemore & Choudhury, 2006; Whitford et al., 2007).

Developmental effects can be observed for the P3 component in response to target stimuli in an oddball task:

Children show a broader peak at central and parietal regions, which becomes more focalized with age (Stige, Fjell, Smith, Lindgren, & Walhovd, 2007).

A decline of P3 latency over childhood and adolescence is well observed in literature (Polich, Ladish, & Burns, 1990; Rozhkov, Sergeeva, & Soroko, 2009; Sangal, Sangal, & Belisle, 1998; Tsai, Hung, Tao-Hsin Tung, & Chiang, 2012; van Dinteren et al., 2014b; Yordanova, J. & Kolev, 1997). This effect is associated with increases in neural speed, cerebral efficiency (e.g. Courchesne, 1978b) and higher-order cognitive abilities (e.g. Polich, Howard, & Starr, 1983). The age at which P3 latency reaches its minimum varies across studies; however, results indicate a prolongation of a decelerating trend well into adolescence and partly even into young adulthood (Courchesne, 1978b; Mathes, Khalaidovski, et al., 2016; Polich et al., 1990; van Dinteren et al., 2014b).

Developmental trends observed for P3 amplitude during childhood and adolescence strongly vary in the literature. Both an increase (Polich et al., 1990; Tsai et al., 2012; van Dinteren et al., 2014a, 2014b) and a decrease (Courchesne, 1978b; Katsanis, Iacono, & McGue, 1996) of P3 amplitude have been observed. Some studies could not reveal any relation of P3

amplitude to development over adolescence (Johnstone, Barry, Anderson, & Coyle, 1996; Sangal et al., 1998).

Differences in task design (Courchesne, 1983; Polich, 2007) or calculation method (Luck, 2005) across studies might account for this divergent observation. It is likely that changes in P3 maturation are generated through changes in mental processing and underlying cerebral assemblies (Katsanis et al., 1996). However, it is still unclear whether the faster processing in adults compared to children is caused by differences in anatomy, information processing or some combination of the two (Segalowitz, Santesso, & Jetha, 2010). Diverging maturational processes might contribute to P3 amplitude generation and these processes might follow own developmental courses and manifest to different extents across studies.

The following section describes general changes of oscillatory processes during development and how they affect the measurement of event-related potentials, such as the P3 component. These processes might explain the divergent observations for developmental of the P3 amplitude.

4.4. General changes of oscillatory processes affecting event-related potential measures

As described prior, the amplitudes of low frequencies in the spontaneous EEG decline over childhood and adolescence. The age-related patterns of EEG activity affect also task-related modulations of ERO (Raichle & Snyder, 2007).

Figure 26 depicts a model presenting the differences between the EEG patterns for children and adults during processing of a certain event. The EEG signal of children (left side) is characterised by high amplitudes and a high variability in the timing of the cerebral response pattern, indicated by vertical red lines. The adult EEG (right side) constitutes of lower amplitudes and low trial-by-trial variability. Averaging of several trials time-locked to the event may result in similar patterns for the ERP signals of children and adults. In real event-related EEG data the post-stimulus amplitude modulations elicited through cognitive processes further impacts the shape of the mean ERP and ERO signals.

Developmental trends of low frequency amplitude reduction and increasing trial-by-trial precision of response timing are obscured by their opposing character. Thereby, underlying

developmental effects in the frequency domain are not detectable in the time domain, the ERP signal.

Baseline correction enables to set the processing of stimuli in relation to the EEG signal occurring prior to stimulus presentation. This pre-processing step allows describing amplitude modulation in relation to individual EEG baseline patterns. Selective developmental trajectories of ERO during brain maturation may be distinguished by description of pre-stimulus amplitude, post-stimulus amplitude modulation and precision of response timing of a certain frequency band.

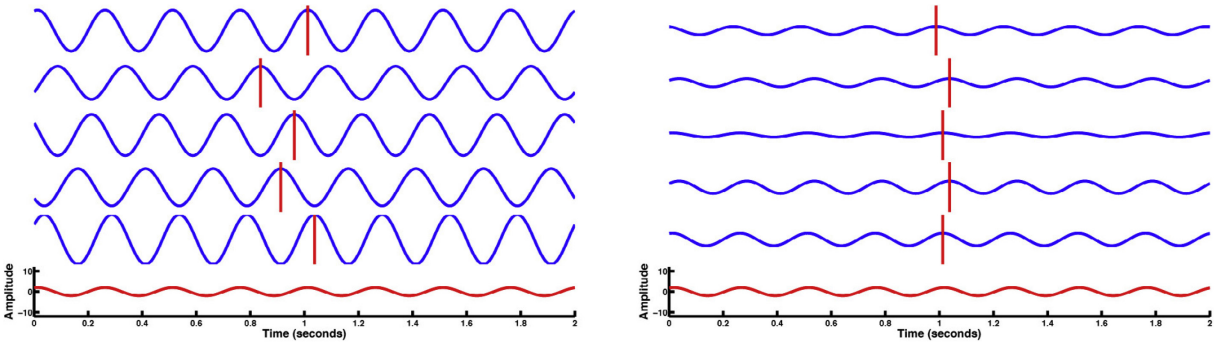

Figure 26: Schema for illustration of developmental changes in cerebral oscillatory characteristics and their subsequent implications for averaged trial data analysis.
Five blue curves of 4 Hz sinus waves represent single trial EEG signals of children (left) and adults (right). Red curves indicate averaged signal over the trials for children and adults demonstrating similar patterns. EEG signals on the left, however, exhibit high amplitudes and low precision of response timing (indicated by red vertical lines), while on the right amplitudes are low and precision of response timing high (Mathes, Khalaidovski, et al., 2016).

5. Conduction of study I & II

5.1. Brief summary

Adolescence is an important phase of life. Its main goal is becoming an independent, responsible and self-reliant adult. Recent studies indicate that brain maturation extends well after childhood and even into young adulthood. In particular, higher-order cognitive functions, like decision-making, control of attention and working memory, all of which are associated with prefrontal brain structures, mature during adolescence and young adulthood (Amso, D. & Scerif, 2015; Anderson, Anderson, Northam, Jacobs, & Catroppa, 2001; Blakemore & Choudhury, 2006). Therefore, the prefrontal cortex plays a crucial role in the coordination of cognition and action through interacting with a decisive number of brain areas. Thus, the maturation of the prefrontal cortex also demands coincident maturation of connecting brain networks. Although in the context of maturational processes of cerebral activity patterns and their neuronal network structures, studies are still scarce. Brain oscillations serve as bases of neuronal communication by integrating information through synchronization across brain regions (Basar, 2011; Buzsaki et al., 2013; Fries, 2015; Klimesch, Freunberger, & Sauseng, 2010). There are few studies on the integration of neuronal activity into global cerebral networks, since only recently necessary novel analytical possibilities have developed that allow more precise and, above all, valid conclusions (Hardmeier et al., 2014). These global activity patterns, however, form the basis of general neuronal processing and are thus central to the research of maturational cerebral processes.

5.2. General aim & hypotheses

The aim of this study was to investigate maturational changes of the prefrontal cortex and prefrontal brain networks throughout late childhood, adolescence and young adulthood. Investigating the maturational course of the prefrontal cortex and underlying neuronal networks, e.g. including the parietal cortex, can be assessed utilizing tasks requiring executive functions. In this study, attention control, as one particular executive function, was necessary during the confrontation with new, unknown and distracting stimuli and continuous tracking or rare, task-relevant stimuli and was, thus, employed to investigate neuro-behavioural maturation.

The spatio-temporal coordination of neural activity within functionally integrated neural networks can be observed via EEG measuring techniques (Basar, 1998). Neural processing takes place in a very fast time range. The EEG method is capable of adequately depicting this, thereby providing the opportunity to investigate the differences in the maturation of young people in more detail than on the pure basis of the behavioural data. EEG techniques already have proven to enable disentangling of different developmental brain changes, especially when related to tasks (Mathes, Khalaidovski, et al., 2016; Yordanova, Juliana & Kolev, 2009).

In this project, investigation of brain maturation was conducted presenting two different visual paradigms combined with EEG measurement. The visual oddball and its extension the novelty oddball paradigm, provide a tool for investigating visual processing, stimulus evaluation, target detection and attention control. Furthermore, behavioural changes during maturation were assessed by error rates and response timing.

The focus of analysis lay on late ERPs, like P3b, N2 and P3a and concurrent slow brain oscillations within the delta and theta frequency band, as they are related to cognitive processes necessary for solving the oddball tasks. Time-frequency analysis and especially spatial phase coherence analysis were utilized to provide new insights into age-dependent connectivity differences of oscillatory brain networks.

We hypothesised that while the posterior P3b amplitude may have reached adult levels in adolescents, behavioural performance still lack behind the adult level (van Dinteren et al., 2014a, 2014b), indicating prolonged brain maturation not reflected within the P3b amplitude. In contrast to posterior P3b, developmental differences of the novelty N2 and

P3a at frontal sites may be observed (Courchesne, 1978b; Oades, Dittmann-Balcar, & Zerbin, 1997). Delayed latencies of the P3a and P3b might also be observed in younger subjects (Oades et al., 1997; van Dinteren et al., 2014b). We predicted that in accordance with the decrease of EEG activity at rest, pre-stimulus amplitude of delta and theta oscillations would decline (Barry & Clarke, 2009); however, post-stimulus task-related modulations in amplitude and ITC would increase during brain development (Müller, Gruber, Klimesch, & Lindenberger, 2009; Werkle-Bergner et al., 2009; Yordanova, Juliana & Kolev, 2009).

Additionally, maturation of frontal brain networks is known to be central during adolescence and mental health in young adulthood (Kaiser & Gruzelier, 1999; Nuechterlein et al., 2014; Pantelis et al., 2009). Large developmental changes of these regions are induced especially between the ages of early and late adolescence (Luna et al., 2010; Segalowitz, Santesso, & Jetha, 2010; Steinberg, 2013; van Dinteren et al., 2014b). The theta frequency band is known to play a role in frontal processing requiring in particular long-range connections within the FPN during the target P3b component and the novelty N2-P3a complex (Basar-Eroglu & Demiralp, 2001; Folstein & van Petten, 2008; Hajihosseini & Holroyd, 2013; Isler et al., 2008; Mathes et al., 2014). We hypothesized a maturational increase of cerebral connectivity strength within frontal theta networks.

The hypothesised increase in task-related coordination of brain responses with age may either be linear, exhibit a peak/trough during adolescence or decelerate when reaching the final maturational sages leading into young adulthood (Uhlhaas et al., 2009; van Dinteren et al., 2014b) and indicators of both possibilities were, therefore, investigated and compared in this project.

Taken together, late ERPs, such as the P3 and concurrent oscillatory activity in the delta and theta frequency bands were found to correlate with top-down processes involved in visual processing and control of attention in general, and also during execution of an oddball and novelty oddball task. Decreased level of local task-related changes of brain activity, reduced task-related connectivity within brain networks accompanied by poorer performance levels in younger participants, indicate that maturational changes of the prefrontal cortex and its connections to other brain regions, like the parietal cortex, relate to the development of higher-order cognitive functions.

SECTION II.

Study I: Visual Oddball Task

1. Aim of the study

The aim of the study was to investigate the maturational course of higher-order cognitive functions from late childhood to young adulthood. Brain maturation is proposed to continue until the third decade of life affecting a diversity of cognitive functions (Paus et al., 2008; van Dinteren et al., 2014b).

In this study, a visual oddball paradigm, which required detection of rare targets randomly embedded in a stimulus sequence of frequent non-targets, was conducted in combination with EEG scalp recording. The oddball task constitutes of a rather simple cognitive task enabling to study underlying cognitive processes and associated behavioural performance over a broad age range.

Processing of target stimuli, in particular, involves cognitive processes eliciting the P3b component and concurrent event-related delta and theta oscillations, which were observed for their age-related differences regarding amplitude, latency, pre- and post-stimulus amplitude modulation, ITC and SPC measures. Brain maturation likely affects a combination of all the assessed measures.

The following sections will provide a comprehensive description of the methods employed in study I containing the recruitment of participants, the paradigm, the procedure of the EEG session, the EEG set-up, the data acquisition and pre-processing and the applied analysis methods. Furthermore, the results of behavioural and EEG data are presented followed by a discussion and integration into current literature of the main findings.

2. Methods

2.1. Participants

This study margined an age span from childhood to adulthood with a range of 8 to 30 years.

176 participants were included in this study. For the analysis, 17 participants had to be excluded due to poor data quality, resulting in a low number of artefact-free epochs (see also section 2.5.1).

From the total of 159 participants included in the analysis, 77 participants were measured by Dr. Ksenia Khalaidovski during her PhD thesis, the results of which were partly published by Mathes, Khalaidovski, et al. (2016). The study attempted to recruit participants with a balanced gender distribution as well as participants that were equally distributed with respect to age range, in order to deduce results from a representative reflection of society.

Participants were primarily students of the University of Bremen. Children and adolescents were recruited through visits to local schools, a youth science club of the Universum® Bremen and through distribution of leaflets with information of the project. Except for three participants, all older pupils were attending a secondary school that aims for a-level graduation (German: Abitur).

Prior to conducting the experiment, a brief description of the study's background, the method (EEG) and the duration of the experiment were given to the participant. In the case when the participant was under 18 years old, the details were also given to the parent. Participants were informed about the option to cancel the experiment at any time without explaining any reason. Afterwards, the participants (and their parents) had ample time to ask any questions. All participants gave written consent of their participation (see

appendix C). For participants below 18 years of age (in accordance with German law), parental consent was also obtained (also shown in appendix C). All participants were paid an allowance for their participation, except for students who instead received credit points for their participation.

Subsequently, a questionnaire was completed (see appendix D) that asked for details about the level of education, birth date, nationality, medical condition and drug use, possible head trauma, visual impairments, and neurological and psychiatric disorders of the participant and his or her relatives. Participants were further asked for self-assessment of physical and mental well-being on a scale from 1 to 10 (where 1 referred to a horrible and 10 to an excellent state), and of their current stress level (in this case, 1 referred to a low and 10 to a high stress level). In order to exclude confounding variables, the participants were asked about their sleeping habits (average hours of sleep and sleep duration the night before testing), daily medication intake and the intake of food on the day of testing, as well as their consumption of caffeinated drinks, their use of nicotine and that of alcohol. Individual head circumference was measured and noted.

All participants were fluent in German and had normal or corrected-to-normal vision. Both right- and left-handed participants were included in the study, determined by the test of Oldfield (1971). Four participants reported to have reading and writing difficulties and one participant stated to have arithmetical weakness. Participants reported that they were free of neurological, psychiatric or other diseases or pathological drug intake. One participant, however, stated having experienced one epileptic seizure during young childhood, but reported having no further seizures as well as being free of medication for one year.

Of the 159 participants, 153 underwent the d2-test after the EEG session. The d2-test was assessed in order to characterise their ability to sustain attention during cognitive tasks (Bates & Lemay, 2004; Chaix et al., 2007).

As an indicating factor for concentration performance, the concentration factor (German: Konzentrationsleistung, KL PR*), in percentage to age-related performance, was utilized, as it represents both errors and processing speed (Bates & Lemay, 2004; Brickenkamp, 2002).

Five participants, mostly of young age, were showing symptoms of fatigue and were thus unable to conduct any further demanding psychological test. Symptoms of fatigue are a factor that has to be taken into consideration for all participants, especially for the younger ages, as the d2-test was always performed after the EEG session.

Test scores could not be assessed for one participant of 8.5 years of age because the comparative calibration scale is intended for children of at least 9 years of age (Brickenkamp, 2002).

Two participants scored poorly on the d2-test (KL PR* < 5 %). No participant was excluded from further analysis due to low scoring on the d2-test, since these two participants were solving the task during the EEG session with an error percentage below 8 %.

Demographic information of participants included for analysis, like age span and its standard deviation as well as gender and handedness, are given in Table 1.

No participant was excluded for having excessively long reaction times (849.79 ms being the slowest individual RT) or too many errors (23.68 % being the highest individual error rate).

Table 1: Characteristics of participants included in analysis of the oddball task

Number of participants	159
Age span:	8 to 30 years
Mean age ± SD:	17.91 ± 4.92
Male/female	69/90
Right-/left-handed	154/5

2.2. Visual Oddball Paradigm

The experimental design consisted of a simple visual oddball paradigm. A scheme of the experimental design is displayed in Figure 27B. A black and white checkerboard with 8x8 checkers (stimulus size: 50°) was presented on a 17“ cathode ray tube screen, positioned 1.5 m in front of the participants. Within one experimental session, a total of 38 target (25 %) and 112 non-target stimuli were pseudo-randomly presented to the participants for 1000 ms each. Inter-stimulus interval (ISI) varied randomly between 1800 and 3000 ms, separating the presentation of targets and non-targets in order to prevent rhythmic adaptation of the subject to the temporal characteristics of the experimental sequence.

Throughout the experiment, a green fixation dot of 0.4° was presented at the centre of the screen. For non-target, the fixation dot was located at the intersection of four squares, while white checkers were positioned on the upper left and lower right. For targets, the checkerboard was shifted diagonally for half the length of one checker, with the fixation dot now occurring in the centre of a white checker. The checkerboard presented during the ISI was inverted in luminance compared to the non-targets, i.e. white checkers were now positioned on the lower left and upper right of the green fixation dot (see Figure 27A).

The stimuli and the ISI are displayed below Figure 27A.

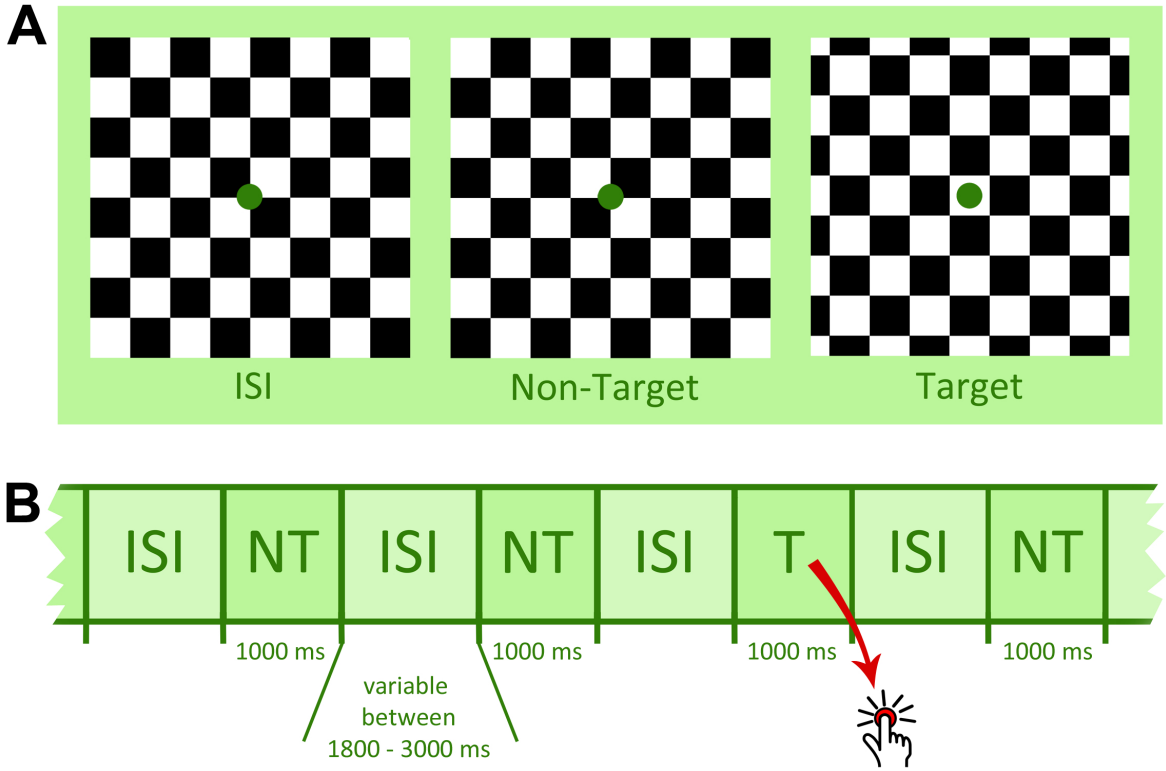

Figure 27: A: Presented stimuli and the inter-stimulus interval (ISI) of the oddball experiment.
B: Scheme of checkerboard changes and the according presentation times of the oddball experiment.
T: target stimulus; NT: non-target stimulus; ISI: inter-stimulus interval

Upon the appearance of a target stimulus, participants were instructed to press a button using their right index finger. Responses between 200 to 3000 ms after the stimulus were classified as correct.

The luminance of the stimuli was kept constant throughout the entire experiment. Stimuli were presented in pseudo-random order. After presentation of a target, an ISI and a non-target stimulus followed.

It should be noted, that visual perception of non-target, ISI, and target stimuli are of equal visual saliency. The reversals of black to white checkers ensure a high level of retinal receptor activation. The pattern reversal is smooth and continuous, as the stimuli are not separated by a break interval between a non-target stimulus and an ISI, with the checkerboard presented during the ISI not being perceived as a separator of both stimuli. Thus, appearance of the target stimuli became very salient.

2.3. Procedure/ EEG session

Participants were seated in the measuring chamber and the EEG cap was put on. After completion of the set-up, participants were allowed to observe their own ongoing EEG signals. This was in place to reduce muscle tensions given that the instructions were combined with direct biological feedback. This especially helped younger participants to raise awareness on how to minimize artefacts.

EEG-Measurements took place in a dimly-lit, soundproof, electromagnetically-shielded room. All stimuli used in the experiment were presented using Presentation R (v. 16.3) on a screen with a refreshing rate of 85 Hz and a resolution of up to 1024 x 768 pixels.

The EEG session started with the measurement of a spontaneous EEG sequence. Participants were instructed to fixate their gaze on a black cross in the centre of a white screen and to close their eyes as soon as the cross disappeared. In this way, the spontaneous EEG with open and closed eyes was recorded for 1 min in each circumstance. During this task, the participants were asked to relax and to minimize muscle tension and movements.

Subsequently, the visual oddball task was explained to the participants. A trial run was conducted to ensure full understanding of the task requirements. The participants were instructed to respond as quickly as possible by pressing a button upon each presentation of a target stimulus. Participants were asked to stay relaxed and to reduce eye blinks, if possible. The EEG experiment lasted approximately 90 minutes.

Following the EEG session, participants answered a questionnaire regarding difficulties or comments on the previous tasks.

2.4. EEG settings

A fitting electrode cap with 30 Ag-AgCl electrodes (F7, F3, Fz, F4, F8, FT7, FC3, FCz, FC4, FT8, T7, C3, Cz, C4, T8, TP7, CP3, CPz, CP4, TP8, P7, P3, Pz, P4, P8, PO3, POz, O1, O2; Easycap, Falk Minow Services) was placed onto the participant's head according to the international 10-10 system (Chatrian et al., 1988). Linked earlobes were used as reference. Impedances were kept below 10 kΩ by the application of electrode gel (Abralyt HiCl, EASYCAP GmbH). Electrodes were placed above and to the right of the right eye to record the electrooculogram (EOG). The EEG was recorded at 500 Hz with band limits of 0.01 - 250 Hz by means of a 32-channel BrainAmp System (Brain Products®) and digitized at a sampling rate of 500 Hz, resulting in a band-pass of 0.1 – 250 Hz.

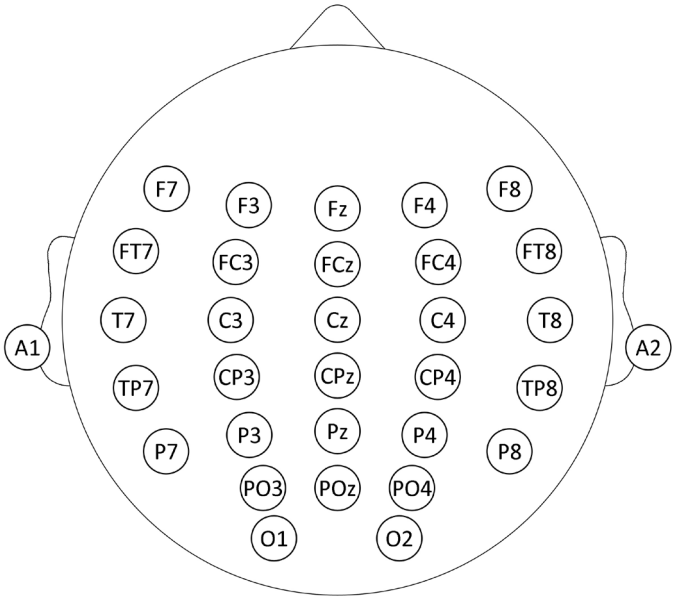

Figure 28: Placement of all EEG electrodes measured according to the 10-10 system.

2.5. EEG data analysis

The pre-processing, segmentation and further data analysis of the EEG data was performed in Matlab® v.7.10 using custom-written scripts based on scripts of EEGLAB®.

2.5.1. EEG data pre-processing

2.5.1.1 Definition of epochs for visual oddball task

Continuous data was segmented into epochs from 2000 ms, before the stimulus condition, to 1998 ms after stimulus onset of targets and non-targets.

For targets, only trials with correct responses were included. Non-target trials containing false responses (so-called commission errors) were rejected from further analysis.

The length of the epochs was chosen to minimize possible distortions of the analysed signal due to filter artefacts. The chosen time window enables the calculation of the baseline activation level between - 700 and - 300 ms before stimulus onset.

2.5.1.2 Artefact rejection

Each epoch was checked for artefacts caused by muscle tension, movements (e.g. eye blinks) or sweating as these artefacts disturb the baseline activity level or the actual reaction to a stimulus. Epochs were checked visually. For both the target and non-target stimuli, artefacts were rejected between 1000 ms before and 1000 ms after stimulus onset.

2.5.1.3 Check of channels

In parallel to the artefact rejection, electrodes exhibiting low conductance or those with stronger muscle artefacts were detected.

For two participants, one problematic electrode channel and for one participant two problematic electrode channels were interpolated by average of adjacent ones.

2.5.1.4 Adjusting the number of epochs between task conditions

Participants with fewer than 20 artefact-free epochs in one condition were excluded from further analysis (see section 2.1).

For each participant, the number of non-targets was matched to the number of targets by randomly drawing a subset of non-target epochs chosen from the entire experiment to ensure comparability between task conditions.

Participants with fewer than 20 artefact-free epochs in one condition were excluded from further analysis (see section 2.1).

For each participant, the number of non-targets was matched to the number of targets by randomly drawing a subset of non-target epochs chosen from the entire experiment to ensure comparability between task conditions.

A linear regression was conducted in order to detect age related correction effects (R^2 = .0658, F(1, 157) = 11.1, p = .0011), which were found to be significantly different from no correlation effect with age (slope of zero).

Table 2: Mean numbers of epochs included from each experimental condition for further analysis of the oddball task.

Task	Condition	Groups (Mean ± SD)
Visual Oddball	Target & Non-Target	30.70 ± 4.74

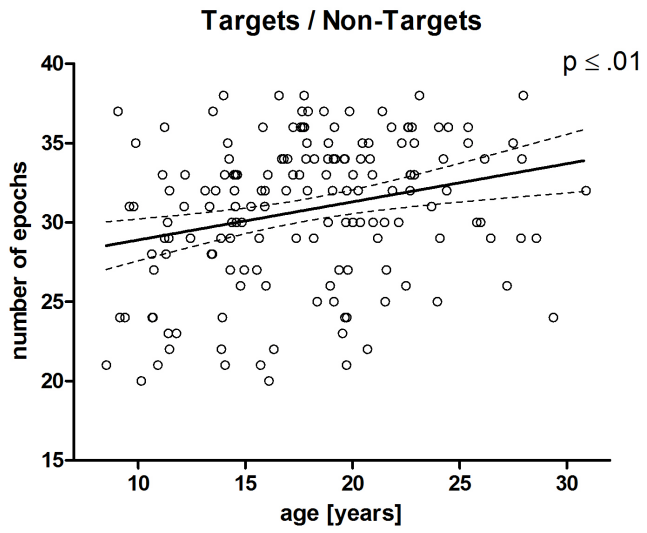

Figure 29: Linear regression of adjusted number of epochs for target and non-target trials after artefact rejection of the oddball task. Dashed lines indicate the 95 % confidence interval of the model.

2.5.2. ERP analysis

2.5.2.1 Analysis of the stimulus-locked P3b in the time domain

Artefact-free epochs for each participant were averaged separately for target and non-target trials. The averaged ERPs were digitally low-pass filtered with a finite impulse response at 20 Hz. Filtering of the ERP was performed to increase the signal-to-noise ratio by restricting the analysis to the frequency range for which significant P3b effects are normally reported.

2.5.2.2 Time windows and regions of interest for the P3b

The time window between 400 and 600 ms post-stimulus was determined to incorporate the P3b by visual inspection of the grand average and all single subject averages (separately for targets and non-targets; see Figure 30A&B). The chosen time window is in accordance with previous studies (Basar-Eroglu et al., 1992). For baseline correction, the mean amplitude between -700 and -300 ms before stimulus onset was subtracted from the ERP. The baseline period matches the time-frequency analyses (see below).

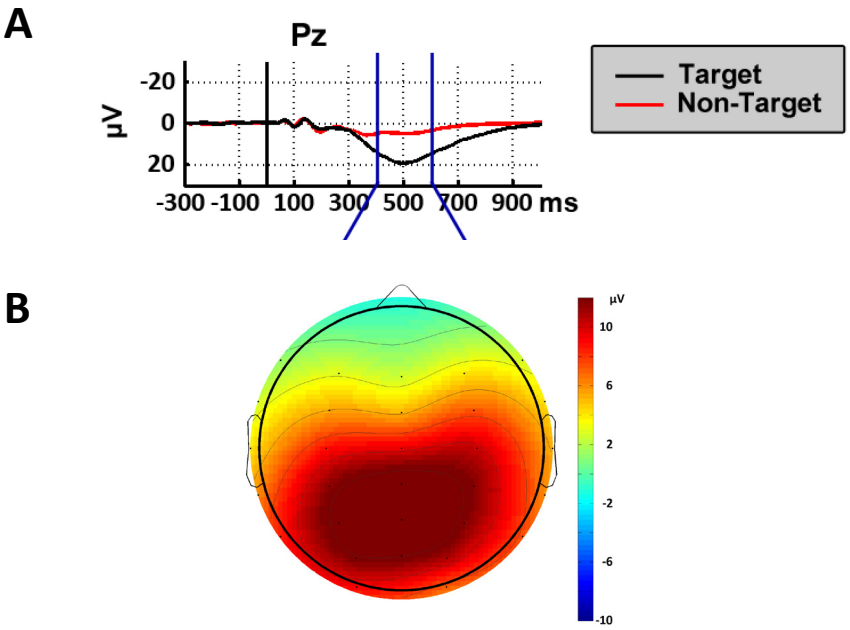

Figure 30: A: Time course of ERPs of the oddball task at electrode Pz averaged over all participants for target (black) and non-target (red) trials. The time window for analysis is depicted by blue lines.
B: Averaged topological distribution of P3b during 400 to 600 ms for target stimuli for all participants.

Mean ERP amplitude values were pooled into a frontal (F3, Fz, F4) and a parietal region of interest (ROI; P3, Pz, P4). These ROIs incorporated the posterior maximum of the P3b and allowed to estimate the contribution of frontal brain sites on the P3b (Polich, 2007; van Dinteren et al., 2014a).

The topographical plot in Figure 28 illustrates that the chosen electrode sites incorporated the maximal deflection of the P3b. Investigating a frontal and a parietal ROI reflects that trajectories of frontal and parietal P3b amplitudes differ over the lifespan (van Dinteren et al., 2014b) and that within the P3b time window, both frontal and parietal brain regions are activated during tasks requiring target detection (Bocquillon et al., 2011; Wronka, Kaiser, & Coenen, 2012).

The P3b latency was defined as the individual maximum peak between -300 and -700 ms within the parietal ROI (P3, Pz, P4). It was investigated for target trials only.

2.5.3. Time-frequency analysis

2.5.3.1 Time-frequency transformation of EEG data

Time-frequency analysis was applied by Morlet-wavelet-based time-frequency decomposition to each single artefact-free epoch described in detail in SECTION I.3.5. This was also analogous to the manner of previous studies of this institute (Mathes et al., 2014; Mathes et al., 2012). In the present study, time-frequency transformation was conducted at central frequencies of the delta and theta band. For this step, the toolbox of Torrence and Compo (1998) for MATLAB was utilised. Parameters used for the analysis of each frequency band of interest are given in Table 3.

Table 3: Parameters used for time-frequency analysis and their resulting resolution for studies I and II.

Frequency band	Centre frequency	Number of cycles	Time resolution	Frequency resolution
Delta	2.5 Hz	2.5	570 ms	1.5 – 3.6 Hz
Theta	5.5 Hz	5	500 ms	4.4 – 6.7 Hz

The wavelets were normalized to have unity energy. In order to enhance comparability with signal amplitude if calculated by a Fourier transform, the transformed data was multiplied by the square-root of the sampling interval (Mathes et al., 2014); Torrence and Compo (1998).

2.5.3.2 Pre-stimulus amplitude

As pre-stimulus amplitude, single-trial non-baseline-corrected amplitude (AMP) during a time window of -700 to -300 ms preceding the stimulus onset was calculated individually for all participants and each frequency band. Only the analysis of the pre-stimulus interval for target trials is presented after ruling out an effect of the stimulus category on the interval preceding the stimulus.

2.5.3.3 Post-stimulus amplitude modulation

To estimate stimulus-induced amplitude changes, so-called event-related spectral perturbations (ERSP; see SECTION I.3.6.4 for theory), the post-stimulus amplitude values

were baseline-corrected using the Z-transform (see SECTION I.3.6.3) for the pre-stimulus time window of -700 to -300 ms from each spectral estimate, producing a baseline-normalised-time-frequency distribution. The ERSP was averaged across trials for each participant and stimulus category.

2.5.3.4 Inter-trial phase coherence

The phase information obtained by the wavelet transform of single trials EEG data was averaged across trials for each participant and stimulus category. For theoretical explanation of this procedure see SECTION I.3.6.5.

2.5.3.5 Time-frequency windows and ROIs

Visual inspection of the grand average and all individual subject responses were used to determine time-frequency windows and ROIs, including the maximal response for each measure (Amplitude, ERSP and ITC) and frequency band (delta and theta).Figure 31 displays an exemplary time course of delta ERSP values for target stimuli. The chosen time window is indicated by blue dashed lines and includes the peak signal strength. A topological plot below shows the distribution of the signal strength over the head during the chosen time window. Table 4 sums the determined time windows and corresponding ROIs for both frequency bands (delta & theta) and both analysis conditions (ERSP & ITC; compare with plots in Figure 43).

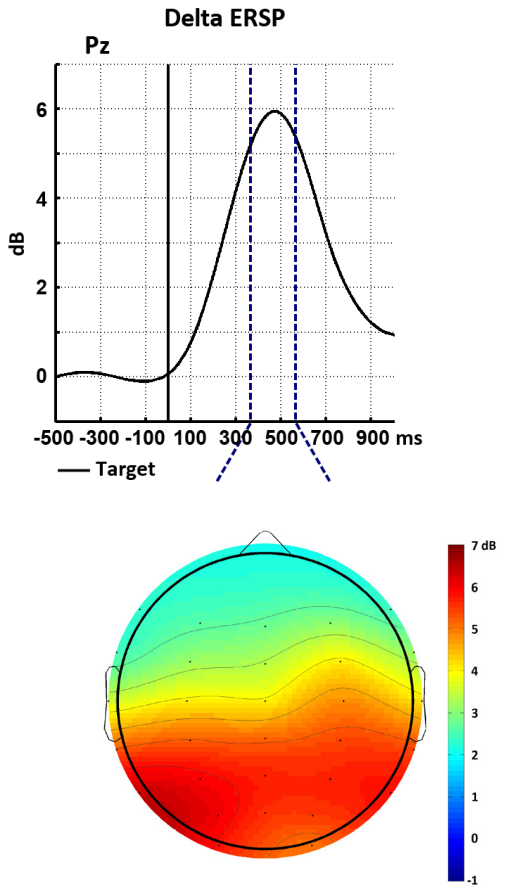

Figure 31: Overview of time-frequency analysis for target stimuli of the oddball task for baseline-corrected amplitude of the delta frequency band averaged over all participants. Top as line plot with blue lines indicating determined time window and below as topological plot during this time window

Table 4: Analysed frequency bands with corresponding time windows and ROIs for each analysis method for target stimuli of the oddball task.

Frequency band	Method	Analysis time window [ms]	ROI for analysis
Delta	AMP	-700 to -300	Fz, FCz, Cz, CPz, Pz
	ERSP	350 to 550	P3, Pz, P4, PO3, POz, PO4
	ITC	400 to 600	P3, Pz, P4, PO3, POz, PO4
Theta	AMP	-700 to -300	Fz, FCz, Cz
	ERSP	300 to 500	FCz, C3, Cz, C4, CPz
	ITC	150 to 350	PO3, POz, PO4

2.5.4. Spatial phase coherence analysis

Spatial phase coherence analysis was conducted using the WPLI (described in SECTION I.3.6.6) based on the Matlab script published by Cohen, M. X. (2015). The data was baseline-corrected by a z-transformation as described in SECTION I.3.6.3. Due to the type of baseline correction, the scaling of WPLI values is no longer restricted to values between zero and one.

There is special interest in the theta frequency band that spans from 4 - 7 Hz, as theta oscillations develop over adolescence and are of special importance for long-range network cooperation in the brain, especially in combination with fronto-parietal network activity (described by the FPN in SECTION I.2.7)

2.5.4.1 Grouping of electrodes

Data analysis in this thesis is focused on network activity of the frontal cortex as frontal theta oscillations are related to target detection (Demiralp & Basar, 1992). Further, the frontal cortex is of major interest due to the fact that this area in general and its frontal theta oscillations in particular, develop during adolescence (Amso, D. & Scerif, 2015; Uhlhaas et al., 2009).

Spatial distribution of the cerebral response to target stimuli was analysed through grouping and averaging the connectivity strengths originating from 48 connections across electrodes in order to reveal the time window of maximal response averaged over the full age range. Electrodes Fz, FCz, and Cz were defined as seed electrodes. Subsequently, connections from the seed electrodes to other seed electrodes and to electrodes F3, F4, FC3, FC4, C3 and C4 were assigned to fronto-central connections (FC) of rather local cerebral networks, while connections from the seed electrodes to electrodes P3, Pz, P4, PO3, POz, PO4, O1 and O2 were categorized as anterior-posterior connections (AP) of rather long-ranging brain networks. Connectivity strengths from seed to lateral electrodes were weak and were thus excluded from analysis. Figure 32 depicts the seed electrodes as well as the electrodes whose connections were taken into consideration for further connectivity analysis. The subdivision of connections from the seeds as FC and AP is indicated in Figure 32 by light blue and blue colour, respectively.

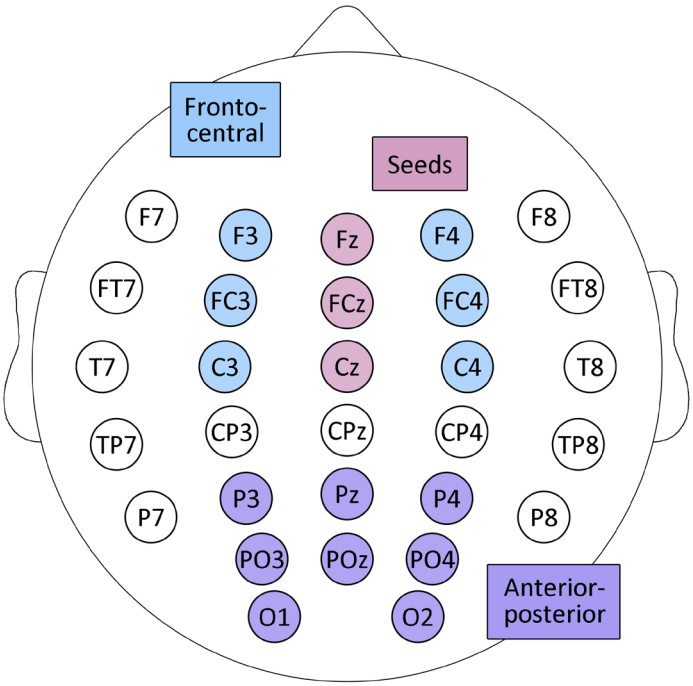

Figure 32: Electrode positions on topological plot. Head from above, nose upwards. Magenta indicates seed electrodes. Light blue to seed electrodes were taken into consideration for local cerebral networks assigned to fronto-central connections (FC), while purple to seed electrodes are categorized as anterior-posterior connections (AP) and stand for long-ranging networks.

2.5.4.2 Analysis time window

Similarly to the time-frequency analysis, the data set was inspected to determine the time window with overall maximum response strength in the theta frequency band. Figure 33 depicts the connectivity strength averaged over all participants and all connections for the target and non-target trials with the baseline window of -700 to -300 ms prior to stimulus onset. The time window of 300 to 500 ms post-stimulus was utilized for further statistical analysis, which fits to the relevant time window for the P3b component of the ERP (Basar-Eroglu et al., 1992).

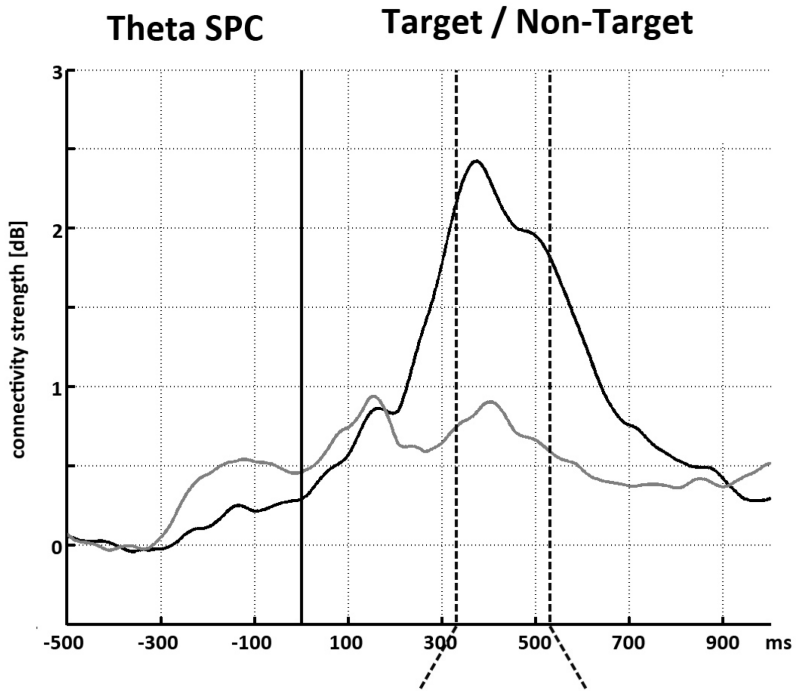

Figure 33: Line plot depicting connectivity strength of the theta frequency band of spatial phase connections. Connections originated from the electrode seeds Fz, FCz and Cz averaged over all participants. Data are separately averaged for the conditions target (black line) and non-target (grey line) in the oddball task. For further analysis, the time window 330 to 530 ms post-stimulus was taken into consideration (indicated by vertical ticks).

2.6. Statistical analysis

2.6.1. Statistical analysis of behavioural data

For correctly classified targets, mean, median, standard deviation and coefficient of variation of reaction time (RT) were determined to estimate the timing of the motor response and its trial-by-trial variability (McIntosh, Kovacevic, & Itier, 2008).

Linear regression models of mean values of omission, false positive rates, and median reaction times over the age range of all participants were conducted separately using Graphpad Prism 5.03.

For RT, the population's Coefficient of Variation was estimated by using the ratio of the sample standard deviation to the sample mean.

2.6.2. Statistical regression analysis of EEG-data

Regression analyses of individual latencies and mean amplitude values over the age range of all participants were conducted separately using Graphpad Prism 5.03. In a similar way, pre-stimulus amplitude, ERSP and ITC values for the delta and theta frequency band and for SPC values of FC and AP connections for only the theta frequency band were analysed by regression modelling over the age range of all participants.

There is an ongoing debate in literature of the maturational trajectory of brain development during the first decades of life between a linear versus a quadratic/non-linear age trend (Brown, Marsh, & LaRue, 1983). van Dinteren et al. (2014a, 2014b) assumed for the age-dependent trajectories of amplitude and latency, as well as concurrent slow frequency oscillations, a logarithmic Gaussian model over the life span. In comparison to van Dinteren's study of participants between age 6 and 87, the study analysed here is based on participants only aging between 8 and 30 years. Thus, the flattening behaviour of the log Gaussian trajectory exhibited with ongoing age is not represented by our data.

In line with the ongoing debate in literature, a linear regression model was fitted to the data and compared to a quadratic model.

A model containing more parameters (here the quadratic model) is able to provide improved data description; however, additional parameters might not significantly increase the model's precision while instead they add unnecessary complexity (overfitting the model – also describing random noise in data).

In order to obtain the model that describes the data in best manner, the extra-sum-of-squares F-test (implemented in Graphpad Prism) was utilized. It compares differences of the sum-of squares between models while taking into account the number of parameters (and therefore different numbers of degrees of freedom) ("GraphPad Prism Tutorial," 2015). The null hypothesis assumes that the simpler model (i.e., the linear model) is correct. Significance level was set to $p < .05$.

In the results section, each data set is presented by a scatter plot over age in combination with the chosen regression model. Linear curves are described by their slope (B0) and

intercept (B1), while quadratic curves are described by their parameters B0, B1 and B2 (see Table 5) and the vertex (peak) of the quadratic curve. The term convex quadratic model is used for a parabola with a positive second derivative, i.e. possessing a trough. Consequently, a quadratic model with opposite opening behaviour is termed concave in the following sections.

Residuals from the model were checked for Gaussian distribution by assessing the D'Agostino & Pearson omnibus K2 test implemented in Graphpad Prism 5.03. Regression analysis assumes its result to be Gaussian, distributed around the fit. Residuals are not supposed to cluster for a model to describe the data well. In parallel a runs-test was computed, testing whether the curve fit deviates systematically from the data. Both were assessed in order to check for the quality of the regression analysis result.

Table 5: Regression models and their corresponding equations chosen for analysis

Model	Equation		
Linear	$Y = B0 + B1 * X$	with	X:= age [years]
Quadratic	$Y = B0 + B1 * X + B2 * X^2$		Y:= data set to be described

3. Results

3.1. Behavioural data

3.1.1. Error rates

All participants, on average, showed low error rates (compare Table 6). No participant exceeded an error rate above 23.68 %. No relation with age could be found for the mean percentage of errors (p = .0433), as depicted in Figure 34. Residuals were not distributed Gaussian-shaped around the model ($p \leq .0001$).

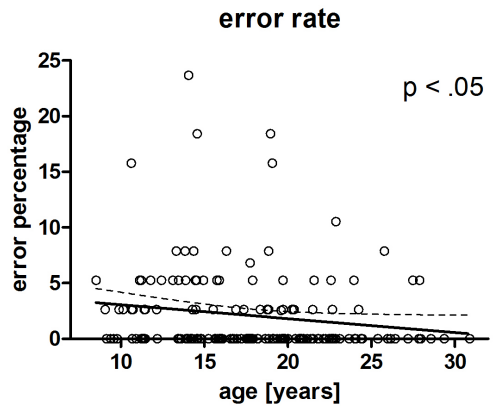

Figure 34: Linear regression model of mean error rate conducted by participants of the oddball experiment with dashed lines indicating the 95 % confidence interval of the model.

Figure 35A displays the number of omission errors (no button pressed upon appearance of target stimulus) over age. Regression analysis revealed a significant decreasing linear age trend (p = .0436).

Figure 35B shows the number of falsely positive reacted trials (button pressed upon appearance of non-target stimulus) over age. The error conduct exhibits no correlation effect with age (p = .3751).

The residuals of the models for omission and falsely positive errors were not distributed Gaussian-shaped around the fit ($p \leq .0001$, each).

For further details of the regression models see Table 7.

Table 6: Behavioural data of oddball task.

Mean error rate [%]		2.08
RT	Median [ms]	531.05
	Individual SD [ms]	98.73
	Coefficient of Variation	0.18

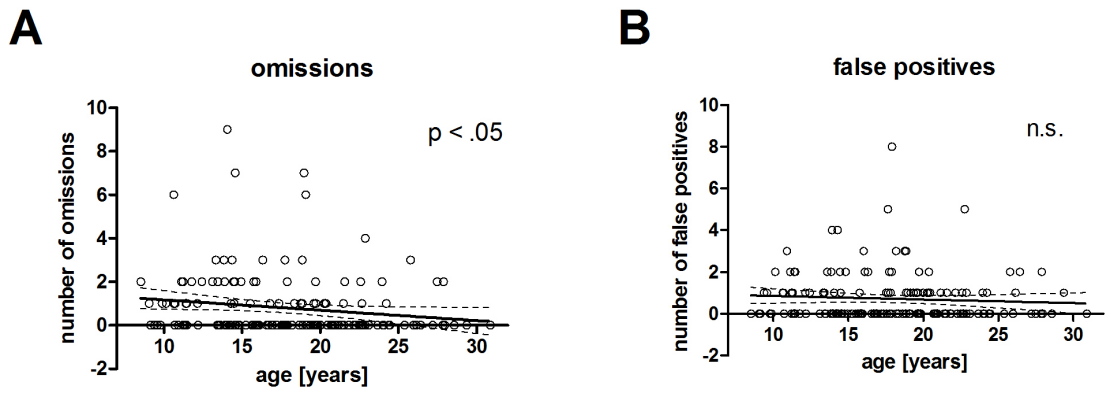

Figure 35: Linear regression of performance of oddball task with dashed lines indicating the 95 % confidence interval of the model.
A: Number of omission mistakes during performance.
B: Number of falsely responded trials.

Table 7: Description of best-fit regression models for behavioural data in the oddball task.

Target	Model	F-value (df)	B0	B1	B2	Normality of Residuals	Runs-Test	R^2
Number of epochs	L	(1, 157) 11.1**	26.5	.2	-	10.0***	n.s.	.0658
Error rate	L	(1, 157) 4.1*	4.3	-.1	-	121.5****	n.s.	.0258
Omissions	L	(1, 157) 4.1*	1.6	-.5	-	119.4****	n.s.	.0257
False positives	L	(1, 157) .8	1.0	.0	-	114.7****	n.s.	.0050
Median RT	Q	(1, 156) 22.8****	1017.0	-47.6	1.1	40.2****	n.s.	.2914

n.s.: not significant, * $p < .05$, ** $p \leq .01$, *** $p \leq .001$, **** $p \leq .0001$.

3.1.2. Reaction times

Individual median reaction time varied around 530 ms (see Table 6 for detailed information). Figure 36 displays the individual median reaction time over age. The data exhibits a significant convex quadratic age trend peaking at 22.46 years of age ($p \leq .0001$, also see Table 7). Residuals were not, however, distributed Gaussian-shaped around the fit ($p \leq .0001$).

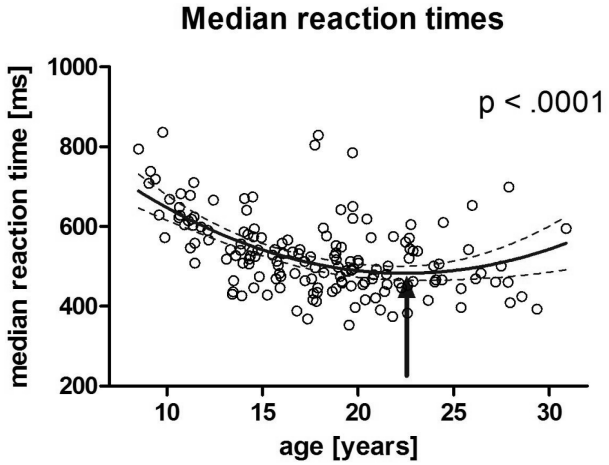

Figure 36: Quadratic regression of median reaction time plotted over age range for the oddball task. Dashed lines indicate the 95 % confidence interval of the model. The arrow indicates the minimum of the quadratic model at 22.46 years of age.

3.2. EEG-Data of Oddball task

3.2.1. Event-related potentials

Figure 37A depicts the time course of target and non-target ERP averaged over all participants of electrodes Fz, Cz, Pz and O2 along the midline. Target trials elicited a P3b response component peaking at electrode Pz 496 ms after stimulus appearance. Figure 37B displays a topological plot averaged over a time window from 400 to 600 ms showing maximal response strength over posterior brain areas.

A

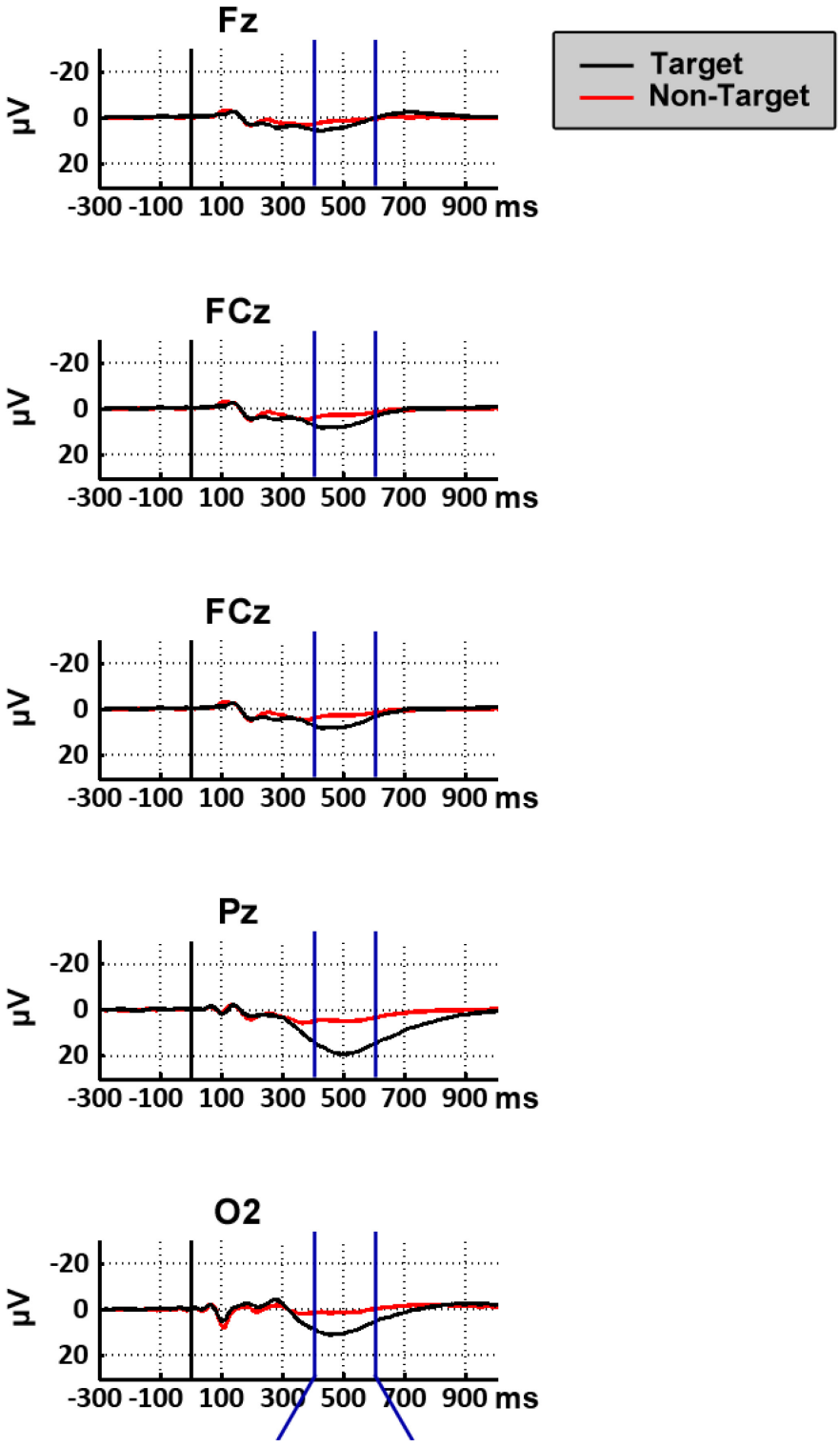
Fz
FCz
FCz
Pz
O2
μV
-20
0
20
-300 -100 100 300 500 700 900 ms
Target
Non-Target

B

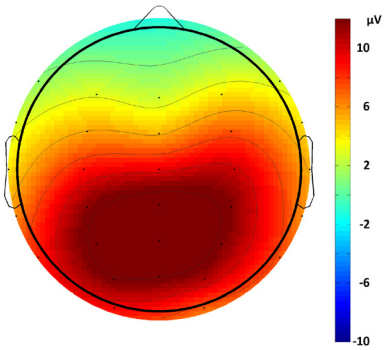

Figure 37: A: Time course of ERPs of the oddball task at electrodes Fz, FCz, Cz, Pz and O2 averaged over all participants for target (black) and non-target (red) trials. The time window for analysis is depicted by blue lines. B: Averaged topological distribution of P3b during 400 to 600 ms for target stimuli for all participants.

Individual peak analysis revealed a convex quadratic age-dependent effect of the P3b latency for the parietal brain region with its trough at 19.87 years of age (p = .0147), shown in Figure 38. For this model, the residuals are not scattered in Gaussian distribution around the curve (see test for normality of residuals in Table 8).

No age-dependent effect was found for P3b amplitude (p = .2161), depicted in Figure 39.

Table 8 provides a detailed description of the best-fit regression model parameters for latency and amplitude of the b component.

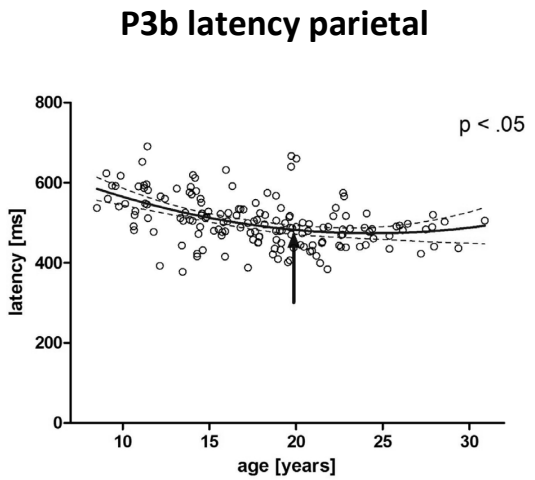

Figure 38: Quadratic regression of individual P3b latency of target stimuli during oddball task for a parietal (P3, Pz, P4) ROI assessed during 300 to 700 ms in relation to the age of participants. Dashed lines indicate the 95 % confidence interval of the model. The arrow indicates the minimum of the quadratic model at 19.87 years of age.

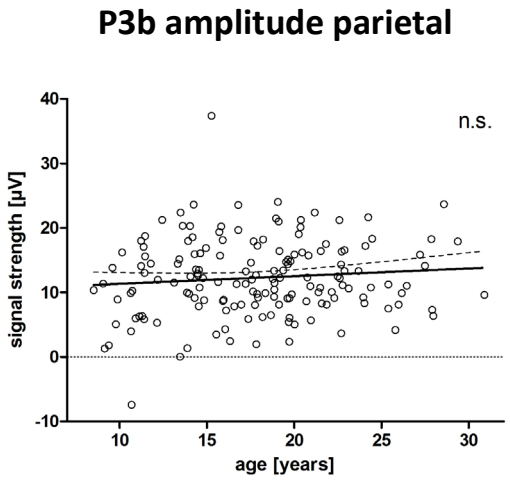

Figure 39: Linear regression of individual P3b amplitude of target stimuli during oddball task for a parietal (P3, Pz, P4) ROI averaged over a time window of 300 to 700 ms in relation to the age of participants. Dashed lines indicate the 95 % confidence interval of the model.

Table 8: Description of best-fit regression models for latency and amplitude of the P3b response component to target stimuli in the oddball task.

Target	Model	F-value (df)	B0	B1	B2	Normality of Residuals	Runs-Test	R^2
Latency	Q	(1, 156) 6.1 *	736.5	-21.6	.4	12.43 **	n.s.	.2154
Amplitude	L	(1, 157) 1.5	10.16	.1	-	11.53 **	n.s.	.0097

n.s.: not significant, * $p < .05$, ** $p \leq .01$, *** $p \leq .001$, **** $p \leq .0001$.

3.2.2. Event-related oscillations

3.2.2.1 Delta frequency band

Pre-stimulus interval

The topological distribution of the pre-stimulus amplitude of the delta frequency signals averaged over the baseline time window is depicted by a head map in the left part of Figure 40. The activity is distributed over the central line covering anterior to posterior regions of the brain.

Depicted on the right side of Figure 40, a convex quadratic age trend ($p \leq .0001$, minimum at 25.32 years) explained the age-dependent trajectory significantly well for the pre-stimulus delta amplitude.

Table 9 provides an overview of the parameters of all regression models described in section 3.2.2.

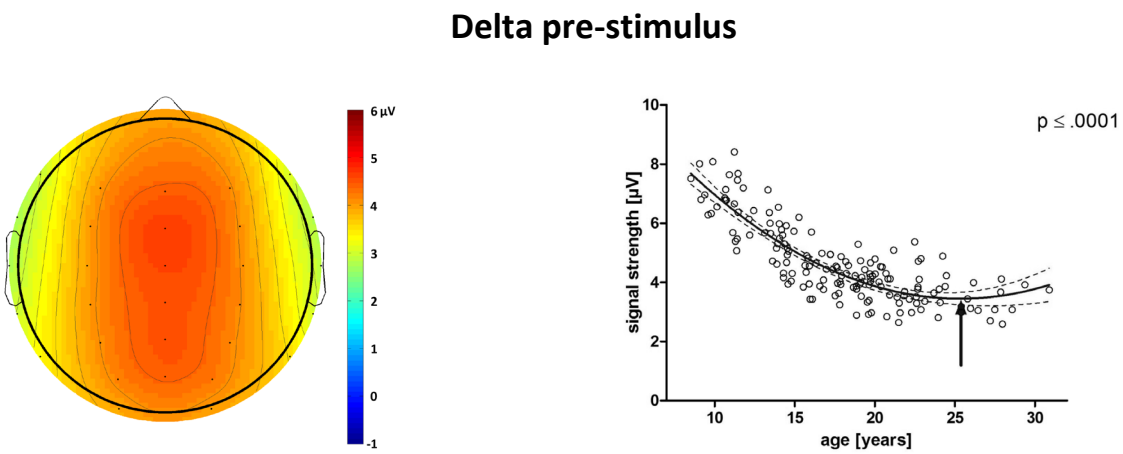

Figure 40: Left: Topological plot of non-baseline-corrected amplitude of delta frequency band during -700 to -300 ms before presentation of target stimuli of the oddball task.
Right: Quadratic regression model for pre-stimulus amplitude of the delta frequency band dependent on age for the ROI: Fz, FCz, Cz, CPz and Pz. Dashed lines indicate the 95 % confidence interval of the model. The arrow indicates the minimum of the quadratic model at 25.32 years of age.

Event-related spectral perturbation

On the left of Figure 41, the ERSP values of the delta frequency band over time in relation to baseline activity for target trials (A-C) and non-target trials (D) are depicted.

The time course of the grand average for targets is depicted for the electrode site Pz, with the peak at 472 ms. Around the maximum peak between 350 to 550 ms post-stimulus, the ERSP values are maximal over parietal areas of the brain.

The delta ERSP follows a significant concave quadratic age trend with its maximum peaking at 24.09 years ($p \leq 0.0001$), shown in graph C.

By contrast, graph D depicts the best-fit regression model for delta ERSP for non-target trials, which is significantly positively related with age in an increasing linear fashion ($p \leq .0001$).

Inter-trial coherence

The inter-trial coherence (ITC) of the delta frequency band over time is depicted in Figure 41A-C on the right for target trials and in D for non-target trials.

Graph A shows the ITC averaged over all participants as a continuous function over time for electrode Pz. An increase of ITC after stimulus presentation can be observed and it reaches its maximum at 512 ms. In graph B, the ITC is averaged for a time window of 400 to 600 ms and exhibits the maximal ITC over posterior regions of the brain.

The delta ITC shows a significant age trend when a concave quadratic model with a maximum peak at 24.29 years of age is applied as depicted in graph C ($p = 0.0002$).

Graph D depicts the regression model of delta ITC for non-target trials, which displays a significant positive linear age trend ($p = .0295$).

Delta frequency band

ERSP

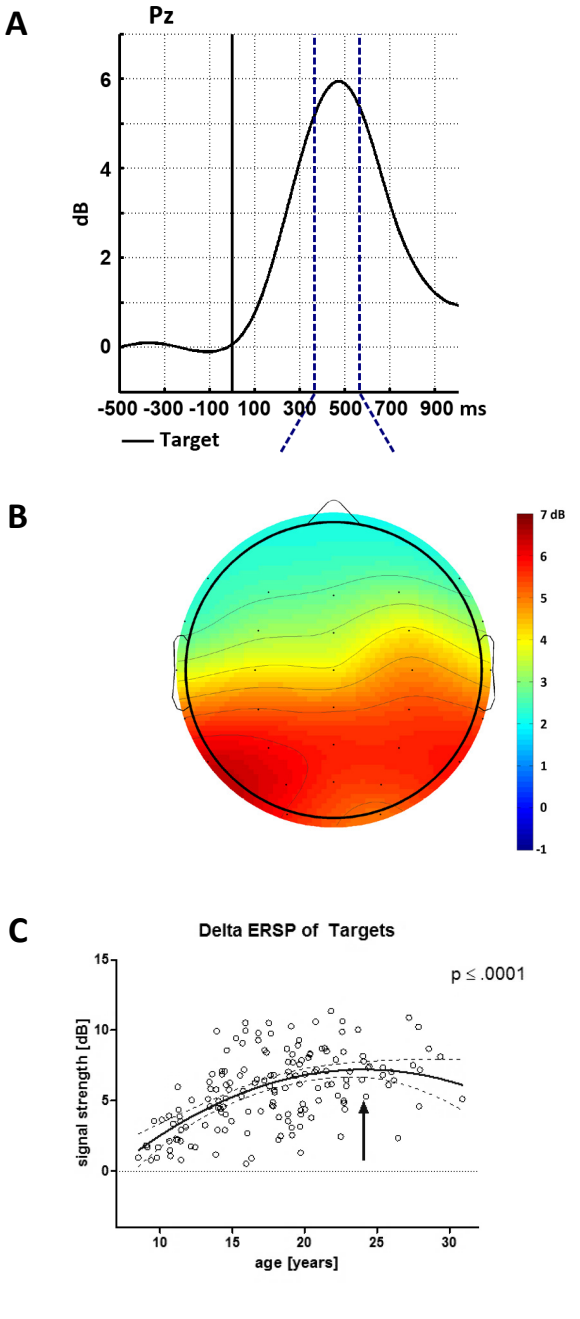

ITC

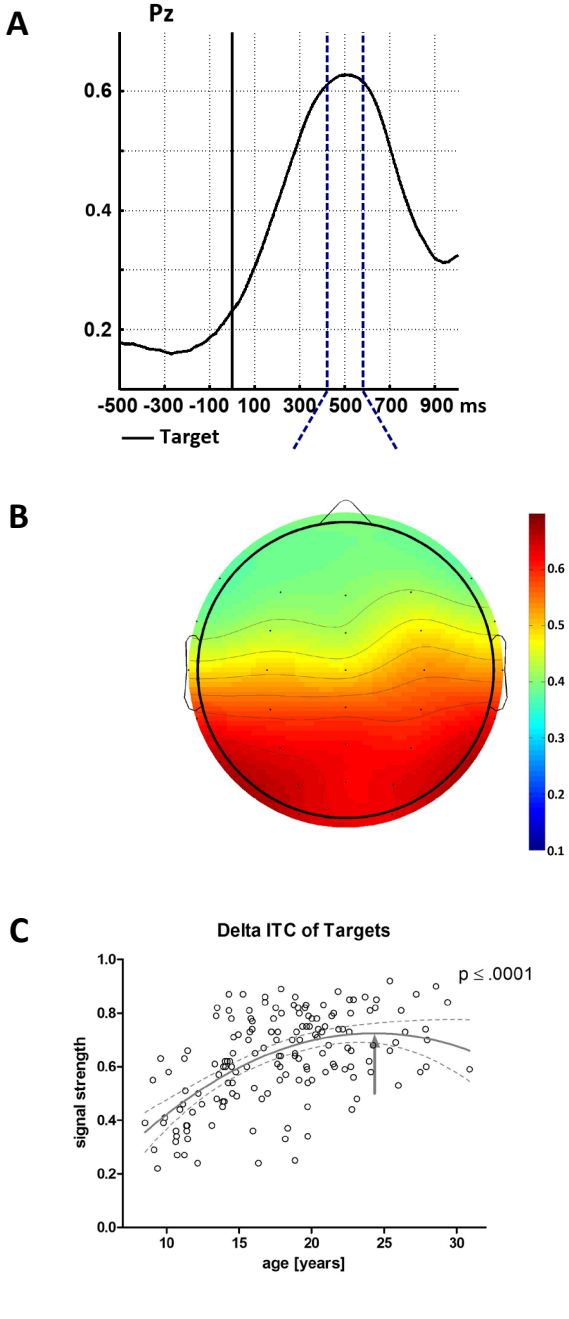

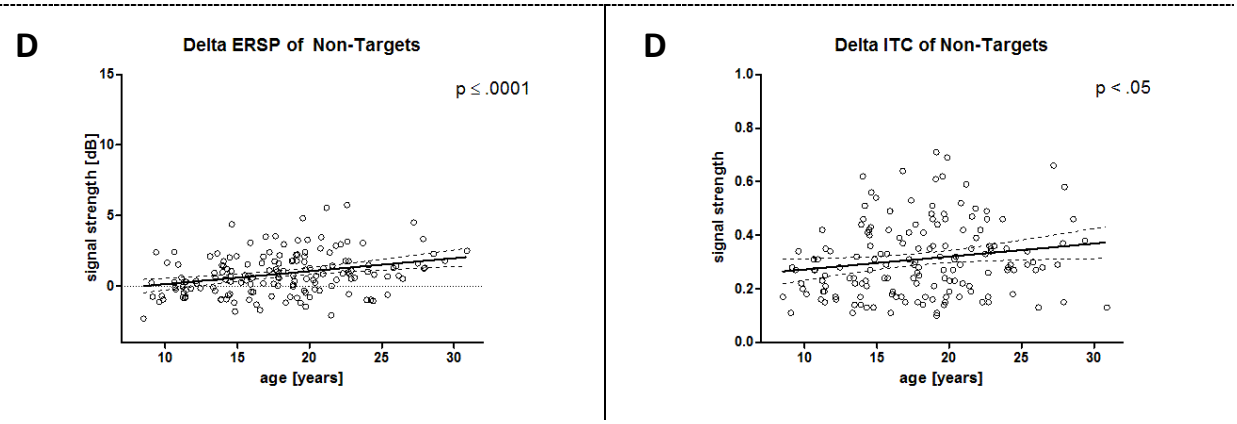

Figure 41: Overview of time-frequency analysis for the oddball task. Each condition is displayed averaged over all participants; top as a line plot with blue lines indicating determined time window and below as a topological plot during this time window. Below quadratic (C) and linear (D) regression of the age-dependent signal strength, averaged over the ROI for the target stimuli and of non-target stimuli (at the bottom) during the given time window, is plotted with key indicators of regression analysis. Dashed lines in graphs C and D indicate the 95 % confidence intervals of the regression models. Arrows indicate the maxima of the quadratic models at 24.09 years (C) and 24.29 years (D) of age.
A: Baseline-corrected amplitude of the delta frequency band.
B: ITC of the delta frequency band.

3.2.2.2 Theta frequency band

Pre-stimulus interval

The topological distribution of the pre-stimulus amplitude of the theta frequency response signal, averaged over the baseline time window, is depicted by a head map in the left part of Figure 42. The maximal strength of the signal is located over electrode FCz.

On the right side, Figure 42 displays the quadratic regression model for the theta baseline amplitude over age. Theta baseline amplitude showed a significant convex quadratic age trend with a minimum trough at 26.33 years of age ($p \leq 0.001$). The quality of the regression model, however, is not perfect, as indicated by its residuals not being scattered in a Gaussian distribution around the model (see Table 9, test for normality of residuals).

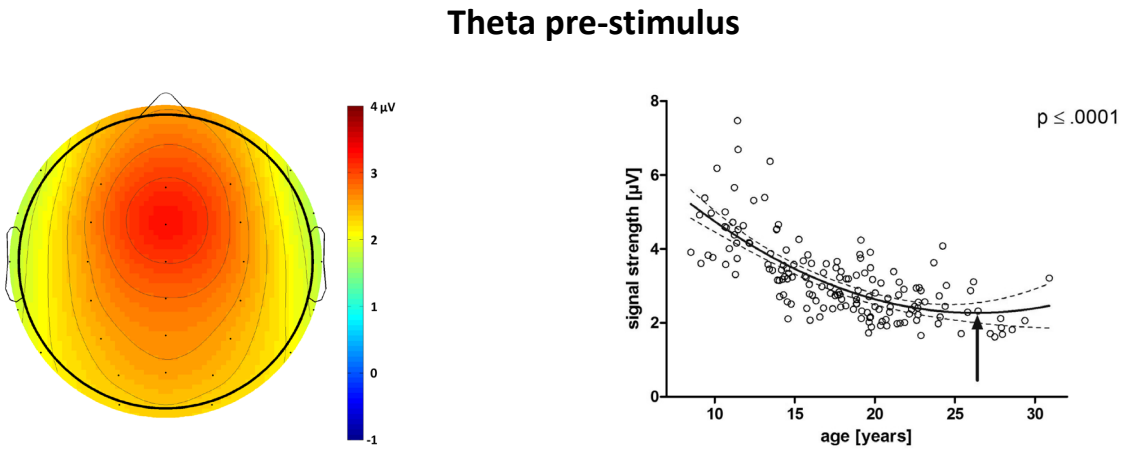

Figure 42: Left: Topological plot of non-baseline-corrected amplitude of theta frequency band during -700 to -300 ms before presentation of target stimuli of the oddball task.
Right: Quadratic regression model for pre-stimulus amplitude of the theta frequency band dependent on age for the ROI: Fz, FCz and Cz. Dashed lines indicate the 95 % confidence interval of the model. The arrow indicates the minimum of quadratic model at 26.33 years of age.

Event-related spectral perturbation

On the left, Figure 43 displays the ERSP of the theta frequency band over time in relation to baseline activity for target trials in A-C and non-target trials in D. Graph A shows the continuous course over time at the electrode of maximal response strength, Cz. Upon the appearance of target stimuli, the ERSP increases and reaches its maximum at 396 ms. Figure 43B depicts a topological plot of the theta ERSP averaged over 300 to 500 ms. The activity pattern manifests a broad peak over central areas of the brain.

The theta ERSP displayed a significant concave quadratic age trend with its maximum at 25.02 years (p = .0061), shown in graph C. The quality of the regression model, however, is not perfect, as indicated by a non-Gaussian distribution of the residuals around the fit (see Table 9).

By contrast, no age trend could be found for the theta ERSP of non-target trials (see graph D; p = .8113).

Inter-trial coherence

The inter trial coherence of the theta frequency band over time is depicted on the right of Figure 43 (in A-C for target and in D for non-target trials). Graph A shows the ITC averaged

over all participants as a continuous function over time of electrode POz. An increase of ITC after stimulus presentation can be observed and it reaches its maximum at 216 ms. In graph B, the ITC is averaged for 150 to 250 ms and is displayed as a topological distribution. The ITC is increased over central brain areas and simultaneously reaches its maximal ITC in a second peak located over posterior regions of the brain.

The theta ITC shows a significant positive linear age trend for targets ($p \leq .0001$), as depicted in graph C.

Graph D depicts the regression model of theta ITC for non-target trials, which displays a significant positive linear age trend ($p = .0004$).

For both target and non-target trials the regression models do not describe the data perfectly as is indicated by a non-Gaussian distribution of the residuals.

The linear regression model for target trials shows a steeper increase than for non-target trials (see Table 9); however, both models do not significantly alter from each other when slope and intercept are taken into account (H_0 = One curve for both data sets, $F_{(2, 314)} = 1.9$, $p = .1507$).

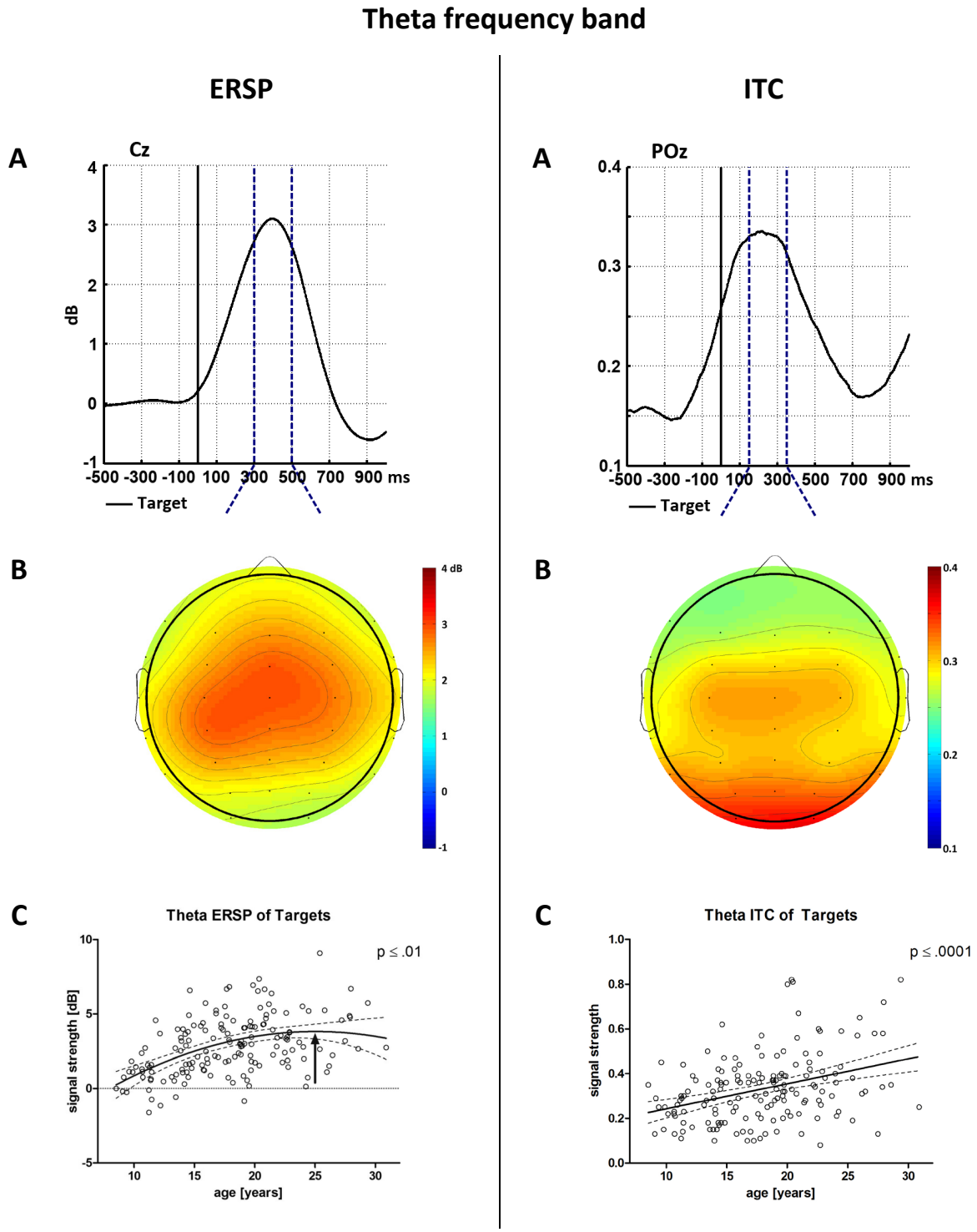
Theta frequency band
ERSP
ITC
A
Cz
dB
4
3
2
1
0
-1
-500 -300 -100 100 300 500 700 900 ms
Target
A
POz
0.4
0.3
0.2
0.1
-500 -300 -100 100 300 500 700 900 ms
Target
B
4 dB
3
2
1
0
-1
B
0.4
0.3
0.2
0.1
C
Theta ERSP of Targets
p ≤ .01
signal strength [dB]
10
5
0
-5
10 15 20 25 30
age [years]
C
Theta ITC of Targets
p ≤ .0001
signal strength
1.0
0.8
0.6
0.4
0.2
0.0
10 15 20 25 30
age [years]

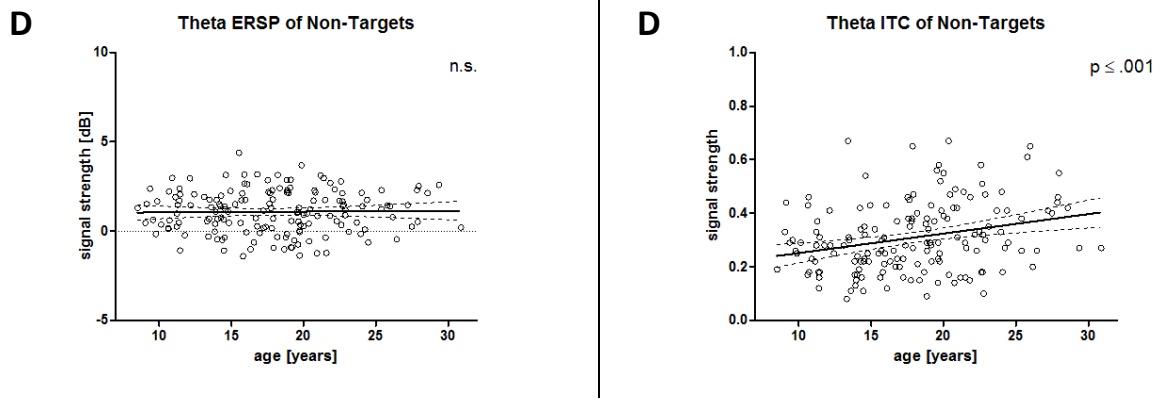

Figure 43: Overview of time-frequency analysis for the oddball task. Each condition displayed is averaged over all participants; top as a line plot with blue lines indicating the determined time window and below as a topological plot during this time window. Below, quadratic (IC) and linear (IIC, ID & IID) regression of the age-dependent signal strength, averaged over the ROI for the target stimuli and for non-target stimuli (at the bottom), during the given time window is plotted with key indicators of regression analysis. Dashed lines in graphs C and D indicate the 95 % confidence intervals of the regression models. The arrow in C indicates the maximum of the quadratic model at 25.02 years of age.
A: Baseline-corrected amplitude of the theta frequency band.
B: ITC of the theta frequency band.

Table 9: Description of best-fit regression models for the data of the delta and theta frequency band for target and non-target stimuli of the oddball task.

Target	condition	Model	F-value (df)	B0	B1	B2	Normality of Residuals	Runs-Test	R^2
Delta	AMP	Q	(1, 156) 63.8****	13.1	-.8	.0	2.8	n.s.	.7220
	ERSP	Q	(1, 156) 15.4****	-6.5	1.1	-.0	.06	n.s.	.3128
	ITC	Q	(1, 156) 14.9***	.3	.0	-	3.9	n.s.	.3168
Theta	AMP	Q	(1, 156) 21.4****	8.7	-.5	.0	39.1****	n.s.	.5255
	ERSP	Q	(1, 156) 7.7**	-4.4	.7	-.0	2.5	n.s.	.2262
	ITC	L	(1, 157) 23.5****	.1	.0	-	15.1***	n.s.	.1303
Non-Target									
Delta	ERSP	L	(1, 157) 16.0****	-.8	.1	-	9.7**	n.s.	.0950
	ITC	L	(1, 157) 4.8*	.2	.0	-	10.6	n.s.	.0496
Theta	ERSP	L	(1, 157) .1	1.0	.0	-	4.6	n.s.	.0004
	ITC	L	(1, 157) 12.9***	.2	.0	-	9.2*	n.s.	.0761

n.s.: not significant, * $p < .05$, ** $p \leq .01$, *** $p \leq .001$, **** $p \leq .0001$.

3.2.3. Spatial phase coherence

3.2.3.1 Pre-stimulus interval

Regression analysis of the spatial phase coherence of the theta frequency band, averaged for a time window before the appearance of target stimuli, is presented in Figure 44 for connections of fronto-central (A) and anterior-posterior (B) distribution.

Pre-stimulus SPC of FC connections follow a decreasing linear age trend (p = .0207). By contrast, no relation with age was found for AP connections (p = .6771).

The quality of the regression model for AP connections, however, is not perfect, as is indicated by a non-Gaussian distribution of its residuals ($p \leq .0001$).

Further parameters of the regression models for the pre- and post-stimulus intervals are listed in Table 10.

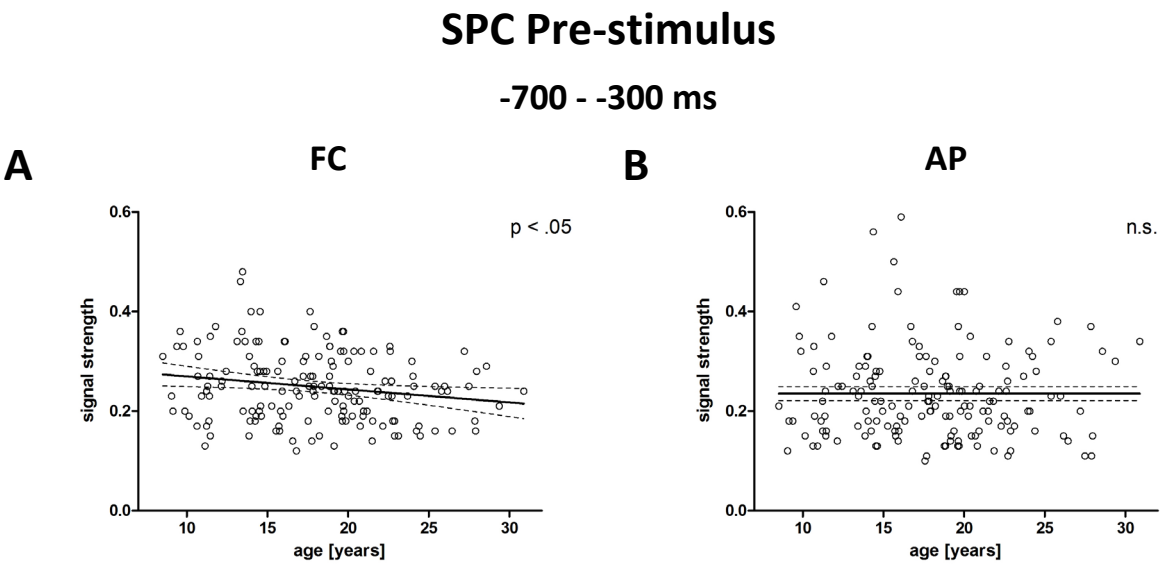

Figure 44: Best-fit regression models for the spatial phase coherence of FC (A) and AP (B) show connections from a frontal seed for theta oscillations during the pre-stimulus time window of -700 to -300 ms before presentation of target stimuli in the oddball task. Dashed lines indicate the 95 % confidence intervals of the models.

3.2.3.2 Target stimuli

Figure 45 displays the SPC of the theta frequency band averaged for connections of FC and AP distributions, together for all participants, and for target and non-target trials dependent on baseline activity. Upon appearance of target stimuli only, the strength of connectivity increases, reaching its maximum after 402 ms. Below, a topological plot displays the distribution of single connections with their connectivity strength during the maximal response from 300 to 500 ms.

Regression analysis of individual SPC during cerebral response to target stimulus presentation revealed an increasing linear trajectory for FC (see Figure 46A; $p \leq .0001$) and AP (see Figure 46B; $p = .0021$) connections as the best fit. Both models do not differ significantly from each other ($F_{(2, 314)} = .04$, $p = .9586$).

The quality of both regression models is not perfect, as indicated by a non-Gaussian distribution of the residuals. Additionally, for FC connections, the runs test revealed an uneven distribution of the scatter above and below the regression model.

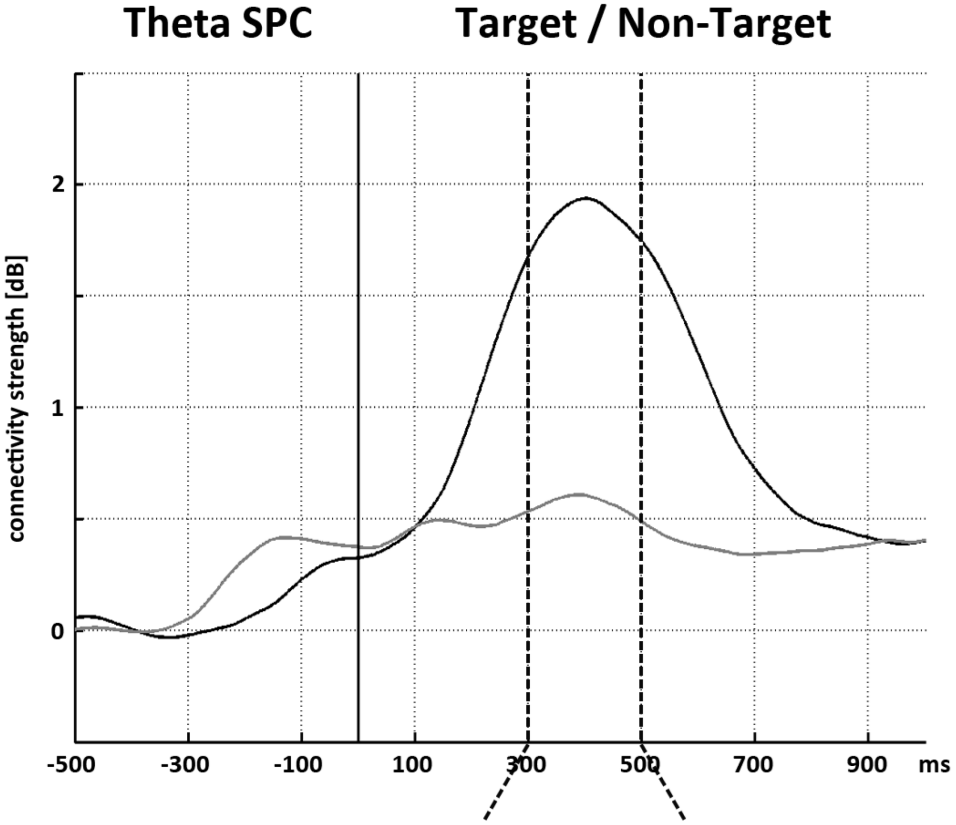
Theta SPC
Target / Non-Target
connectivity strength [dB]
2
1
0
-500
-300
-100
100
300
500
700
900
ms

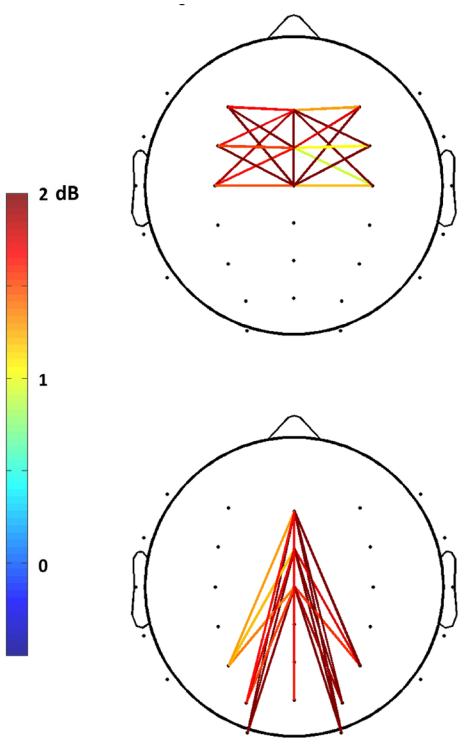

Figure 45: Top: Time course of spatial phase coherence of the theta frequency band averaged for fronto-central and anterior-posterior connections from a frontal seed (Fz, FCz and Cz; lateral electrodes and neighbouring electrode connections excluded) in relation to the baseline connectivity strength between -700 to -300 ms for target (black) and non-target (grey) stimuli presentation during the oddball task. A vertical black line (0 ms) indicates stimulus onset. Two dashed vertical lines display the analysis time window.
Bottom: Topological plots displaying single connections and their baseline-dependent spatial phase coherence, averaged over all participants 300 to 500 ms after the presentation of a target stimulus in the oddball task. The top plot shows fronto-central connections only, while the bottom displays only connections from anterior to posterior. Connections are depicted by lines between electrodes (black dots). The colour bar indicates the cerebral connectivity strength, with warm colours representing stronger connectivity.

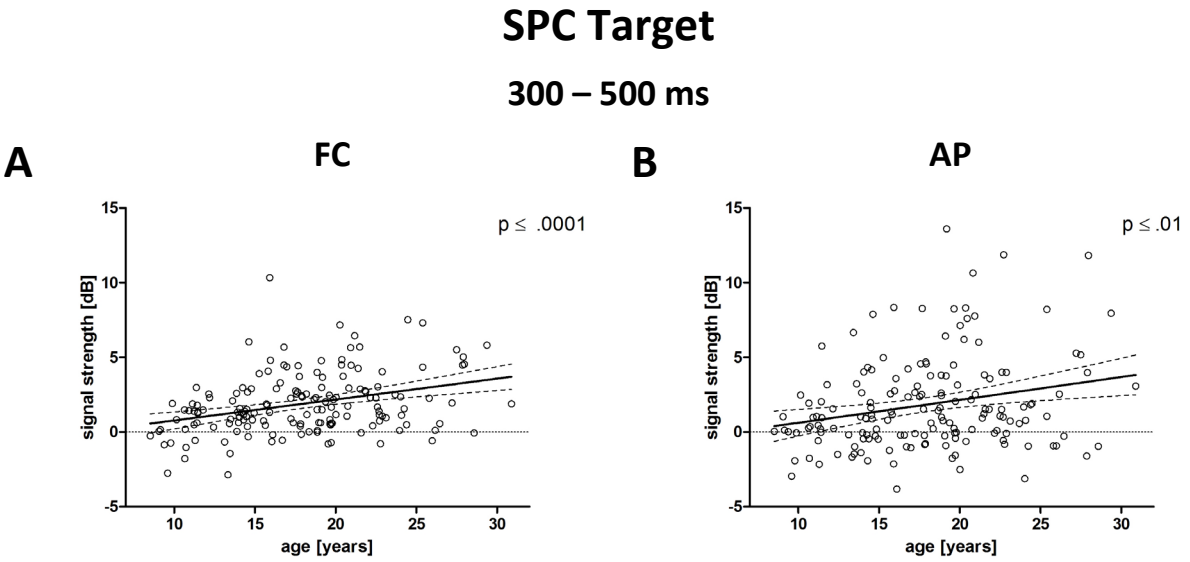

Figure 46: Best-fit regression models for the baseline-dependent spatial phase coherence of FC (A) and AP (B) connections from a frontal seed for theta oscillations, in response to target stimuli in the oddball task, averaged over a time window of 300 to 500 ms. Dashed lines indicate the 95 % confidence intervals of the models.

Table 10: Description of best-fit regression models for the baseline-dependent spatial phase coherence of the theta frequency band of FC and AP connections from a frontal seed, averaged from -700 to -300 ms before and for 300 to 500 ms after the appearance of target stimuli in the oddball task.

Stimulus	Distribution	Model	F-value (df)	B0	B1	B2	Normality of Residuals	Runs-Test	R^2
Pre-Stimulus	FC	L	(1, 157) 5.5 *	.3	.0	-	4.1	n.s.	.0336
	AP	L	(1, 157) .2	.2	.0	-	34.4****	n.s.	.0011
Target	FC	L	(1, 157) 20.0 *	-.6	.1	-	27.3****	**	.1129
	AP	L	(1, 157) 9.8 ***	-.9	.2	-	30.7****	n.s.	.0588

n.s.: not significant, * $p < .05$, ** $p \leq .01$, *** $p \leq .001$, **** $p \leq .0001$.

4. Discussion of results

The aim of the study was to investigate maturation of fronto-parietal brain networks during the transition from childhood through adolescence and into young adulthood. We focused on the P3b time window during target, non-target and novel processing and the concurrent time-frequency characteristics of delta and theta oscillations.

4.1. Behavioural data

The oddball task was simple enough for all participants to perform well. An improvement of performance over age was nevertheless detected as the error rate decreased over age. This effect based especially on the decrease of omission errors. This finding is in line with various studies on the development of performance improvement, showing a higher number of errors for younger participants in a variety of tasks (Booth et al., 2003; Rojas-Benjumea, Sauque-Poggio, Barriga-Paulino, Rodriguez-Martinez, & Gomez, 2015; Segalowitz, Santesso, Murphy, et al., 2010; Tamm et al., 2002; van Dinteren et al., 2014a). Younger participants might have insufficient abilities to sustain attention, explaining the omission in perception of response relevant stimuli. Increases in cognitive control, the ability to voluntarily guide our behaviour and to focus attention, throughout childhood and adolescence may play a prominent role in performance improvement with age (Luna et al., 2010).

Reaction times decreased over age and showed a slowing tendency towards the adult age of 22.46 years. In line, an increase in reaction speed with development is observed in a broad range of tasks in literature (Booth et al., 2003; Segalowitz, Santesso, Murphy, et al., 2010). Increased RTs for younger participants might base on a diversity of aspects, e.g. increased

uncertainty about the correctness of response, slower cerebral processing speed, due to longer encoding, longer processing steps from perception to action or decelerated motor response (cf. Kirino, Belger, Goldman-Rakic, & McCarthy, 2000) and are discussed in connection to concurrent structural changes found during adolescence (Blakemore & Choudhury, 2006).

4.2. EEG-Data

4.2.1. The P3b component

Target stimuli elicited a P3b component in the time window of 400 to 600 ms post-stimulus over parietal electrode sites. This finding is similar to many reports in literature (e.g. Basar-Eroglu et al., 1992; Basar-Eroglu et al., 2001; Polich, 2007).

Age related changes of the P3b during childhood and throughout adolescence are suggested to reflect changes in mental processing (Courchesne, 1983; Katsanis et al., 1996). The P3b is related to a variety of cognitive processes mainly associated with attention, stimulus processing, evaluation, memory and response preparation (Polich, 2007; Verleger, Jaśkowski, et al., 2005).

One general aspect is the association of the P3b with the formation of awareness of the necessity to react upon a target stimulus and thus, combining the perception to response preparation (Basar-Eroglu et al., 1992; Verleger, Jaśkowski, et al., 2005). Age related changes of the P3b may reflect differences in the validation of action necessity.

4.2.1.1 Latency

In this study, the P3b latency followed a decreasing trend with age slowing towards an age of 19.87 years. The decreasing P3b latency during childhood and adolescence is well observed in the literature (Polich et al., 1990; Rozhkov et al., 2009; Sangal et al., 1998; Tsai et al., 2012; Yordanova, J. & Kolev, 1997). In a large cross-sectional life span study, van Dinteren et al. (2014a, 2014b) reported that the P3b latency may decrease until the age of 25 years.

van Dinteren et al. (2014b) proposed a relation between myelination and P3b latency. Myelination is a major structural change in brain development and increases during adolescence as described in detail in SECTION I.2.5. Brickman et al. (2012) assessed fractional anisotropy for their cross-sectional life span study, as it is a diffusion tensor imaging measure for the degree of myelination and organisation of white matter bundles. Van Dinteren observed a strong similarity between his developmental course of P3b latency and Brickman's developmental course of myelination and thus, suggested a relation between both. Increases in myelination might explain decreasing P3b latency on the neuronal basis.

In line with the suggestion of increased myelination decreasing the P3b latency, van Dinteren et al. (2014b) among others further discussed the P3b latency to reflect neural speed or cerebral efficiency (e.g. Courchesne, 1978b). Shorter P3b latencies are discussed to be related to higher-order cognitive capabilities for many years (e.g. Polich et al., 1983). The speed with which subjects are able to allocate attentional resources seems to be a major aspect for P3b latency as well as superior cognitive performance (Polich, 2007). Furthermore, the brain is suggested to become more efficient throughout maturation (Segalowitz, Santesso, & Jetha, 2010; van Dinteren et al., 2014b). Accordingly, decreasing P3b latency over childhood and throughout adolescence and into young adulthood may be a correlate for increasing of cognitive capabilities for this age period, which are in general reported for many different tasks (Arain et al., 2013; Blakemore & Choudhury, 2006; Demetriou et al., 2002).

The age at which maturation of P3b reaches its minimal latency varies across studies. Sample size and age span differences may account for this variation. Different regression models have been applied and may further affect the observed age peak. Nonetheless, an overall trend of maturation of P3b latency well into adolescence and partly extending into young adulthood can be observed. Further, non-linear regression models indicate a slowing of decreasing P3b latency towards adulthood (Courchesne, 1978b; Polich et al., 1990; van Dinteren et al., 2014b). Our results are in line with this developmental phase in life and with a slowing regression trend towards maturation.

4.2.1.2 Amplitude

In contrast to the decreasing P3b latency with age, no age related effect was found for the P3b amplitude in this study.

Amplitude age-trends vary in literature

Observed developmental trends of the P3b amplitude strongly vary in literature. Similar to the results of this study, Johnstone et al. (1996) and Sangal et al. (1998) could not find an age related effect of parietal P3b amplitude. However, both an increase (Polich et al., 1990; Tsai et al., 2012; van Dinteren et al., 2014a, 2014b) as well as a decrease of P3b amplitude (Courchesne, 1978b; Katsanis et al., 1996; Pfueller et al., 2011) have been reported.

Possible reasons behind diversity of P3b amplitude development

Differences in age related P3b amplitude trends across studies might results from varying calculation methods. Amplitude can be assessed by simply stating peak amplitude values or by assessing mean amplitude through summation of the area under the curve. Additionally, data pre-processing might affect the ERP amplitudes, such as e.g. filtering (e.g. Duncan-Johnson & Donchin, 1979) or optional baseline correction (see SECTION I.3.6.3), and thus may further affect the results (Luck, 2005).

Different mental processing due to variations in task design or sensory modality might further explain why results for the development of the P3b component vary across studies (Courchesne, 1983; Polich, 2007).

Differences in task design or sensory modality may even affect other ERPs overlapping with the P3b. Different event-related components are thought to reflect different neuronal processes, which might follow different maturational trends. An overlapping of ERPs, thus, might cause a blur of the P3b amplitude with other ERPs for younger subjects (Polich et al., 1990).

Developmental dissociation between P3b amplitude and latency

Polich et al. (1990) stated that neural processing underlying the P3b are operating slower for children; however he suggested that the cognitive mechanisms are similar to adult P3b processing. As cognitive speed has been related to the P3b latency, this concept might explain our findings of P3b amplitude being unaffected by age.

EROs yield further insight into maturational brain processes

Investigating brain maturation solely on the basis of ERP signals is insufficient. As addressed in Mathes, Khalaidovski, et al. (2016), changes in the ERP signal co-occur with changes in spatial and temporal modulation of EROs. As described in SECTION I.4.4, oscillations may

strongly vary in characteristics, albeit resulting in similar averaged ERP signals. Maturational processes in the brain may account for and are reflected in such differences in oscillatory characteristics. EROs thus provide an additional approach for the investment of brain maturation.

4.2.1.3 Summary

Brain processes reflected in the P3b are still developing during adolescence. Developmental changes might decelerate with age and be more apparent for P3b latency than P3b amplitude (Pfueller et al., 2011; Polich et al., 1990). Maturational brain changes underlying the P3b might, however, be diminished due to a combination of increased spontaneous slow-wave oscillations and decreased task-related coordination of brain activity after stimulus onset in adolescents. Results of this study are, therefore, discussed in regard to slow-wave oscillations in the following section.

4.2.2. Event-related oscillations

4.2.2.1 Common maturational trends of delta and theta oscillations

Summary: Results of delta oscillations

Delta pre-stimulus amplitude had its maximum at central electrode sites and decreased with age until approximately 25 years of age. This trend was diminished with increasing age. By contrast, post-stimulus modulations of event-related delta responses within the P3b time window were maximal at posterior electrode sides and diminished for younger participants. The increase of post-stimulus amplitude modulations and ITC elicited by task-relevant, targets with age was apparent until approximately 24 years of age, although slowing down during the course of brain maturation. For non-relevant stimuli post-stimulus amplitude and ITC of delta responses slightly increased with age.

Summary: Results of theta oscillations

For theta amplitude, the signal was maximally located over fronto-central areas for pre- and post-stimulus responses. Similar to delta responses, pre-stimulus amplitude showed a decreasing trajectory with age until approximately 26 years of age. This trend slowed down with increasing age.

The maximal post-stimulus theta response occurred 100 ms prior to the time window of the P3b component. For theta ITC, the signal strength increased about 250 ms prior to the P3b time window. Task-related theta modulations exhibited a maximum over central to posterior electrode sites. Post-stimulus modulations of theta for target processing followed an increasing course with age peaking at approximately 25 years for amplitude and increasing linearly for ITC. Non-target stimuli exhibited a less pronounced linear increase than target stimuli for ITC (not significant). Post-stimulus theta amplitude of non-target trials showed no relation with age.

Pre-stimulus interval

The pre-stimulus interval reflects a measure of internal, endogenous neural processes of the brain similar to activity reflected in the spontaneous EEG. The post-stimulus brain response is affected by pre-stimulus activation patterns and its influence should be considered for the interpretation of cortical task processing (Raichle & Snyder, 2007).

Our findings of decreasing slow-wave activity in the pre-stimulus interval over childhood and adolescence are similar to results in other studies (Krause, Salminen, Sillanmaki, & Holopainen, 2001; Liu et al., 2014; Müller et al., 2009; Yordanova, J. & Kolev, 1997). The developmental trend is comparable to the general decrease of slow-wave oscillations in spontaneous EEG (Clarke et al., 2001; Cragg et al., 2011; Dustman et al., 1999; Segalowitz, Santesso, & Jetha, 2010). A reduction of the amplitude of slow-wave oscillations with co-occurring increase of faster rhythms in the spontaneous EEG from childhood throughout adolescence (John et al., 1980; Matousek & Petersen, 1973) is generally considered as a sign of healthy maturation (Barry & Clarke, 2009; Clarke et al., 2001).

Different studies indicate that amplified slow-wave activity during rest may relate to activity from a larger neuronal pool in children. Maturation during adolescence leads to a reduction in unnecessary neurons and synaptic connections as a consequence of pruning (Pfueller et al., 2011; Whitford et al., 2007). Therefore, the decrease in slow-wave oscillations during the pre-stimulus interval may reflect structural brain changes during development.

Event-related activity

Baseline correction was applied in order to investigate stimulus induced activity only for event-related brain responses.

Due to similar timing, modulation patterns and distribution, the results reflect an involvement of delta and theta oscillations to the P3b component, as often stated in literature (e.g. Basar-Eroglu et al., 2001).

The results implicate a steady decrease of pre-stimulus amplitudes of slow-wave oscillations into young adulthood; while post-stimulus modulations continuously increased with age (Liu et al., 2014; Yordanova, J. & Kolev, 1997). For target trials, delta and theta values decelerated until reaching young adulthood.

This age related trend of enhanced task-related slow-wave modulation might base on the same structural changes observed to affect brain oscillations at rest. Maturational synaptic pruning eliminates unneeded neurons and synapses and, thereby, increases coordination of brain activity within brain networks. This might account as one factor for enhanced neuronal plasticity and might offer to strengthen important neuronal connections (Blakemore & Choudhury, 2006; Jensen & Nutt, 2015).

Post-stimulus ITC enhancement of both delta and theta oscillations increase with age. An increase in slow-wave response precision of timing through childhood and adolescence has been reported in literature and was mainly associated with structural changes of the brain (Müller et al., 2009; Yordanova, J. & Kolev, 1998).

Developmental increase of precision in response timing has been linked to the white matter increase observed during adolescence (Uhlhaas & Singer, 2011; Whitford et al., 2007). Increase of myelination and axon sizes enable faster signal transmission. Additionally, brain connectivity becomes better structured and organised especially through improved long-range connections (Giedd, 2004; Giedd et al., 1999; Paus, 2010).

In general, the improvement in response precision of timing of slow-wave oscillations during adolescence might relate to the diminished trial-by-trial variability of reaction time (Bender et al., 2015; Papenberg et al., 2013). Further, it has been linked to behavioural performance in inhibition control, which was shown to improve during adolescence (Liu et al., 2014).

In our study, the trend of increasing response precision in timing seemed to slow down earlier for posterior delta compared to frontal theta oscillations, which increased continued linearly up to young adulthood. In line with our findings, Liu et al. (2014) concluded from their results a prolongation of maturation of frontal theta in comparison to posterior delta, especially in regard to neuronal response precision of timing, emphasizing the immaturity of frontal cortex during adolescence.

Thus, the pre-stimulus amplitude decrease combined with the post-stimulus enhancement of amplitude and ITC indicate a more precise modulation of slow-wave oscillatory neuronal response only upon task demands. This effect was also observed for higher frequency bands (Werkle-Bergner et al., 2009) and time-windows preceding the P3b (Barry & De Blasio, 2012; Yordanova, Juliana & Kolev, 2009). Thus, maturation of event-related neural responses, together with increase in precision and accompanied by an increase in correct and faster response behaviour may index an increase in efficiency of the brain (Durston & Casey, 2006; Durston et al., 2006; Segalowitz, Santesso, & Jetha, 2010), even though maturational pace may differ between frequency bands (Krause et al., 2001), post-stimulus amplitude modulations and ITC (Nanova, Kolev, & Yordanova, 2011).

4.2.2.2 Maturation of the FP-network as indicated by ERO

Delta oscillations

Delta oscillations are thought to play a role various cognitive tasks (Basar et al., 2001; Harmony et al., 1996; Knyazev, 2012; Mathes et al., 2012). In the visual oddball paradigm, delta oscillations are suggested to be related to signal detection and decision-making processes. Delta oscillations seem to link cognitive processes from stimulus perception, evaluation over decision-making and response initiation (Basar-Eroglu et al., 1992; Basar et al., 2000; Verleger, Jaśkowski, et al., 2005). Coherent delta oscillations between frontal and parietal brain areas were found to correlate with decision-making during a somatosensory discrimination task (Nácher et al., 2013). The fronto-parietal network was found to be modulated by stimulus' characteristics (e.g. discrimination difficulty) during decision-making (White, Mumford, & Poldrack, 2012). Evidence is given that decision-making processes continue to develop well past childhood and throughout adolescence (Pammi & Srinivasan, 2013). Developmental enhancement of task-related parietal delta modulation with age found in this study might indicate the maturational progress of decision-making abilities and related cognitive processes during target detection on account of immature connectivity patterns within the fronto-parietal network.

Theta oscillations

The anterior theta response to target stimuli has been related to focused attention and signal detection (Basar-Eroglu et al., 1992; Basar-Eroglu & Demiralp, 2001; Mathes et al., 2014) and was suggested to play a role in cognitive top-down processes (Basar-Eroglu &

Demiralp, 2001; Basar et al., 2001). Fronto-medial theta has been associated with a variety of tasks assessing cognitive control, e.g. focus of attention (Cohen, M. X. & Ridderinkhof, 2013; for an overview: van Noordt et al., 2017) and is suggested as an integrative tool in fronto-parietal network communication (Buzsaki & Draguhn, 2004; Klimesch, 1999).

The trend of increasing enhancement and local phase coherency of task-related theta oscillations during childhood and throughout adolescence revealed in this study were consistent with results from several tasks related to the fronto-parietal network (Crowley et al., 2014; Krause et al., 2001; Liu et al., 2014; Müller et al., 2009; Papenberg et al., 2013; Uhlhaas et al., 2009; Yordanova, J. & Kolev, 1997). The enhancement of task-related theta activation with age was linked to improvement of cognitive abilities and may reflect an ongoing maturational progress of the fronto-parietal network and correlated cognitive functions, such as focus of attention necessary for signal detection.

Summary

In summary, the findings obtained in this study of increased event-related modulation and temporal precision of slow-wave oscillatory brain activity may serve as an indicator of cerebral maturation during adolescence and may explain concurrent improvements in cognitive performance. The findings are in line with the current literature. Furthermore, the results demonstrate the collaborative relationship of posterior delta and anterior theta oscillations in target processing. The results indicate the ongoing maturational progress of the fronto-parietal network and confirm the assumption of brain development reaching into the third decade of life.

4.2.3. Spatial phase coherence

Target stimulus processing leads to an increase in SPC for FC and AP connections, which both exhibit a similar, linear increasing trend with age. The time window of maximal response strength matches the maximum of the theta ERSP time interval. Pre-stimulus SPC of theta oscillations decreases with age for FC connections, but was not related with age for AP connections. Even for FC connections was the magnitude of the developmental decrease minor (B0 = .3) when compared to the trajectories of the task-related post-stimulus connectivity strength (FC: B0 = -.6 and AP: B0 = -.9). Therefore, age-related changes of SPC seem to mainly affect event-related brain processes during target detection.

Findings from spontaneous EEG and resting-state MRI

Brain maturation has been related to a general increase in the diversity of cortical states. Improved sophistication of information processing from childhood to young adulthood has been suggested as cause.

Functional brain connectivity measured by resting state fMRI has been shown to progress during development from a more local organization to an increasingly integrated and spatially distributed architecture (Betzel et al., 2014; Fair et al., 2009; Fair et al., 2007; Hagmann et al., 2010; Johnson, 2001; Kelly et al., 2009; Michels et al., 2013; Smit, de Geus, Boersma, Boomsma, & Stam, 2016; Supekar, Musen, & Menon, 2009). These studies propose that functional connectivity decreases on a short-range, local level, while increasing in distant, global connectivity over childhood and adolescence.

Hwang, Hallquist, and Luna (2013) utilized graph theory measures of efficiency. They proposed that frontal hubs reach a stable nature by late childhood. Wide-spread connectivity, however, continues to increase during adolescence leading to improved information flow and, thus, possibly improved cognitive function with age.

Dosenbach et al. (2010) utilized multivariate pattern analysis to establish a functional maturation curve based on their resting fMRI data. Their model predicts increase in individual brain maturity depending on the higher degree of functional segregation within local brain regions and integration of distant cortical regions through connections along the anterior-posterior axis. Brain maturation seems to relate primarily to increased functional connectivity for both, between different task-related networks (Dosenbach et al., 2010) and between different resting state networks (Betzel et al., 2014). Connectivity within resting-state networks is proposed to increase with age, as well (Fair et al., 2007).

In accordance, evidence from coherence measures of spontaneous EEG data indicates individual regions to become more specialised, while integration of distributed networks increases (Bunge & Wright, 2007; Luna & Sweeney, 2004; Michels et al., 2013; Smit et al., 2016). (Vakorin et al., 2013) estimated the number and duration of cognitive states during resting-state EEG within a longitudinal study of 11 – 13 year olds. With age, the EEG pattern becomes more non-stationary, resulting from an increasing number and decreasing duration of functional brain states. The changes in the pattern of brain states indicate that maturation leads to increased global integration and a greater repertoire of functional cortical states (McIntosh et al., 2008; Miskovic et al., 2015; Vakorin, Lippe, & McIntosh, 2011; Vakorin et

al., 2013). These implications, in turn, could indicate the maturing brain and its functions to become more variable and flexible (Vakorin et al., 2013).

These findings might be associated with the increase in cognitive abilities with age. McIntosh et al. (2008) strongly supports this idea: According to them a brain constituting of a greater repertoire exhibits greater variability. Therefore, the brain yields a greater complexity and this comes along with a greater capacity to process information, which ultimately may explain the higher cognitive capacities of the adult brain. These implications can be corroborated and reinforced by both MRI data yielding high spatial precision and EEG data enabling measurement of brain networks with a high temporal precision, thereby, offering to investigate dynamic global brain communication in real time.

Enhanced frontal theta SPC during target detection

In our study, increased neural communication with age became specifically apparent for event-related SPC measures during target detection. This effect coincides with the increase of theta ERSP and ITC during target processing and was reported in similar by Ehlers, Wills, Desikan, Phillips, and Havstad (2014). This strengthens the association of frontal theta oscillations involved in target detection on a local and global level and the contribution of fronto-temporal network activation is suggested.

Our findings further suggest a coinciding, equivocal maturation of local (FC) and global (AP) network communication. This contradicts the various findings of resting-state fMRI functional connectivity suggesting a local connectivity decline with concurrent increase of global connectivity (Betzel et al., 2014; Fair et al., 2009; Fair et al., 2007; Hagmann et al., 2010; Johnson, 2001; Kelly et al., 2009; Michels et al., 2013; Smit et al., 2016; Supekar et al., 2009). Compared to implications of resting-state EEG studies (Bunge & Wright, 2007; Luna & Sweeney, 2004; Michels et al., 2013; Smit et al., 2016), our finding of increasing task-related FC connectivity with age might indicate that the frontal cortex becomes more specialised to target detection during brain maturation. In general, literature on developmental changes of brain networks is scarce, especially in regard to task-related spatial phase coherence of the theta frequency band.

Our results indicate a continuous strengthening of both FC and AP connections originating from the frontal cortex with age. This indicates that with age theta phase is found to exhibit a stronger precision of timing within frontal network activity. This effect coincides with the

developmental increase of theta ERSP and ITC during target processing, which was maximal at frontal electrode sites.

In accordance with our study, Ehlers et al. (2014) measured an auditory oddball task comparing 10 – 14 and 18 – 25 year olds by calculating phase difference locking index (PDLI) between Fz and Pz. They observed a general increase of neuronal synchrony across frequencies with age upon target processing.

Similarly demonstrated Hwang, Velanova, and Luna (2010) that the number of frontal connections involved in top-down control increases over adolescence; by contrast, strong connectivity within parietal regions decreased from childhood to adolescence. They assessed MRI measurement of a cognitive control task of 8 to 27 year old participants.

Increasing precision of theta phase timing on a global level may, hence, indicate maturation of the frontal cortex and its integration into the FPN.

Possible relation between functional connectivity and brain structure during development

Developmental increases of connectivity strength have, in general, been related to the structural changes of the developing brain through a variety of measures and observations such as EEG spatial coherence, MRI functional coherence or diffusion tensor imaging (DTI) measures and also graph theory analysis assessed through EEG or MRI (Casey et al., 2000; Hagmann et al., 2010; Kelly et al., 2009; Luna & Sweeney, 2004; Paus et al., 1999; Smit et al., 2016).

Up until now, few studies assessed brain maturation with more than one imaging method at the time, albeit their results corroborate the current hypothesised correlation between EEG coherence measures and structural changes during development. Their results suggest that EEG measures reproduce structural integrity indicated by MRI measures of white matter tracts (Chu et al., 2015; Teipel et al., 2009; Thatcher, Biver, McAlaster, & Salazar, 1998).

Extensive myelination of cortical pathways during childhood and adolescence improves signal transmission along the axon, especially over longer distances (Giedd, 2004; Giedd et al., 1999; Paus, 2010). Alongside, grey matter is reduced in the development leading to a reduction of redundant synapses. Pruning is considered to decrease the number of neurons and synapses (Paus et al., 2008). Elimination of connections and concurrent strengthening of important connections have been associated to support white matter integrity (Huttenlocher, 1979) and are considered to transform the brain from an immature organised

towards a highly efficient communication system (Hagmann et al., 2010; Hwang et al., 2010; Luna & Sweeney, 2004).

A higher number of neurons and synapses in children, thus, do not relate to higher connectivity strengths. Pre-stimulus SPC in this study was (nearly) similar across age. This finding is in accordance with Miskovic et al. (2015), who reported no changes of theta connectivity for spontaneous EEG recordings between 7 and 11 years of age.

Increasing phase coherence upon cognitive task performance during maturation may relate to structural improvement of white matter integrity allowing for more efficient neuronal communication.

Summary

Taken together, our findings suggest that in addition to developmental changes reflected in localized EEG measures, task-related spatial phase coherence of the frontal cortex continues to mature throughout adolescence for fronto-central and fronto-parietal connections.

Our results, in connection to several findings in the literature, indicate that brain networks are reorganised during development and that especially connectivity strength of the frontal cortex increases.

The fronto-parietal network has been associated with top-down processes utilized during target detection. Both the maturation of localized brain functions and improved coordination of cognitive processes may relate to increasing brain efficiency and processing speed alongside with improvements in task performance.

SECTION III.

Study II: Visual Novelty Oddball Task

1. Aim of the study

The selected experimental paradigm of a novelty oddball task in the present study demands the detection of target stimuli, similar to the classic oddball design presented in study I. In order to understand maturational changes during adolescence several executive functions involving the frontal cortex und its associated brain networks need to be investigated. The novelty oddball paradigm, therefore, extents the classic oddball task design by including a further stimulus class, which demands additional cognitive processes in order for task accomplishment. A number of novel stimuli are presented within the sequence of target and non-target stimuli demanding cognitive processing in form of attention control. Although these novel stimuli are highly salient and should automatically catch the attention of observer, they are not relevant for task accomplishment, and therefore, serve as distractors. A great deflection of the concentration, i.e., away from the actual task, is a disadvantage for quick and correct execution of the task. Adolescents are still more prone to be sidetracked by emotional or rewarding stimuli when compared to adults (Heim & Keil, 2012; Isler et al., 2008; Prada et al., 2014; Steinberg, 2014). The selected experimental design is intended to show how young people deal with novel stimuli, how strongly these stimuli affect adolescent behaviour and how the neuronal processing of these stimuli proceeds in parallel.

In the following, details about the employed methods are outlined. Thereafter, results of the behavioural and EEG data are presented. At the end, a discussion highlighting the differences due to adaption of task difficulty from study I to study II and underlining the novel aspects of study II is given.

2. Methods

The methods for participant recruitment, the data acquisition, the set-up, the recording of the EEG and the methods for data analysis used in Study II were similar to those of Study I (see SECTION II.2) and were therefore not described in detail again.

2.1. Participants

Participants were recruited through a similar process and by the same criteria. They underwent the same procedure before and after EEG measurement in accordance with the details of study I described in SECTION II.2.1. Several participants took part in both studies, which were then combined into one EEG session. Therefore, in study II as well, one participant stated having experienced an epileptic seizure during young childhood, but reported no further seizures and being free of medical intake for at least one year. Three participants reported to have reading and writing difficulties and one participant stated to have arithmetical weakness. Except for three participants, all older pupils were attending a secondary school that aims for a-level graduation (German: Abitur).

For the analysis, two participants had to be excluded due to poor data quality resulting in a low number of artefact-free epochs (see also SECTION II.2.5.1). One further participant had to be excluded for the same reason, although for only one of two analysis conditions.

84 participants with an age span ranging from 8 to 28 years were considered for further analysis.

As described in SECTION II.2.1, participants completed a d2-test after the EEG session. Also, in this section, exclusion criteria are discussed. Three participants were not able to conduct

any further demanding psychological test due to symptoms of fatigue. Two young participants scored poorly on the d2-test (KL PR*<5%), with one of them being only eight years old. None of the participants were excluded from further analysis due to low scores on the d2-test, as all considered participants were solving the task during the EEG session well.

Demographic information of participants included for analysis (e.g. age span, its variation, gender and handedness) is given in Table 11.

Table 11: Characteristics of participants included in the analysis of the novelty oddball experiment.

Number of participants	84
Age span:	8 to 28 years
Mean age ± SD:	16.56 ± 4.74
Male/female	35/49
Right-/left-handed	82/2

2.2. Visual Novelty Oddball Paradigm

One major process during brain maturation is the development of global frontal networks (e.g. Uhlhaas et al., 2009). The paradigm of Study II is a variation of the simple visual oddball task presented in Study I. In order to increase the involvement of frontal brain processes, the visual novelty oddball paradigm was assessed. The design not only provides infrequent target stimuli embedded in a sequence of frequent non-target stimuli, but also includes a third class of stimuli: novels. The task design allows for studying of the neuronal response to new, unknown stimuli (novels), which draw attention and serve as distractions during the task. This process is known to involve the fronto-parietal network, due to processes of attention shifting and the assessment of stimulus relevance (e.g. Isler et al., 2008).

Task design and stimuli for this study were elaborated in cooperation with Prof. Dr. John Polich and based on his study Polich and Comerchero (2003). Figure 47 outlines the task schedule (A), as well as the stimulus categories (B & C). In order to reduce eye movements throughout the experiment, a green dot in each stimulus picture serves as the fixation point.

All stimuli are presented on a grey screen (50% white, 50% black). The stimulus types that were used are explained in the following.

0. Inter-stimulus intervals: ISI serve as a pause in between the presentation of the other stimuli. As ISI only the grey background with the green fixation dot was presented. The presentation time of the ISI varied randomly between 1500 and 1900 ms. This was to prevent rhythmic adaptation of the subject to the temporal characteristics of the experimental sequence, which would have led to expectations and habituation, as well as the separated presentation of targets and non-targets.

1. Non-Target: A small blue circle is presented frequently with an appearance rate of 76% (273 presented non-targets). It is not relevant to respond to it.

2. Target: Upon the appearance of target stimuli (12 % appearance rate; 42 presented targets), which are in the form of a larger blue circle, the subject is supposed to respond via pressing a button using the right index finger. Target stimuli are of slightly larger circle diameter compared to non-targets. Therefore, discrimination between target and non-target stimuli demands attentional awareness.
In order to adapt the difficulty level to age-dependent task abilities, an adjustment of circle size difference between targets and non-targets was introduced in this study. Four target sizes constitute four difficulty levels (with the smallest target circle being the hardest level). For an assessment of personal abilities, each participant conducted a training phase (see further below).

3. Novels (new, unknown stimuli): Novels differ upon each presentation and strongly deviate from standard and target stimuli. Novels appear rarely at the same frequency as targets (12 % appearance rate; 42 presented novels). In contrast to target stimuli, however, the appearance of Novels is not linked to a task. This stimulus category - even though it is not relevant for action - draws attention from the actual task in order to process the new, unknown stimulus. Pre-tests have shown that colourful, comic-like animals with positive, smiling faces gazing straight ahead achieve the desired effect (Figure 47C; all novel stimuli were adapted from open accessible clipart from https://openclipart.org).

For emphasis of characteristic EEG response signals to novel stimuli, the task schedule involves known results in the literature:

1. **Similarity between standard and target stimuli:** Previous studies were able to show that with higher difficulty to discriminate between standard and target stimuli, the resultant

level of attention was also high. Thus, a distraction of attention caused by the appearance of random and unexpected novel stimuli is accentuated (Daffner, K. R., Mesulam, et al., 2000; Polich & Comerchero, 2003).

2. **Novels:** Previous studies emphasize that especially conspicuous and rare stimuli, as well as positive images and faces gazing directly at the observer, attract attention (Hahn & Perrett, 2014; Horstmann, 2015). The novel stimuli were specifically adapted to meet these findings (see Figure 47). Since the novels were not task-relevant, their rare appearance embedded in a sequence between standard and target stimuli should be particularly suitable for studying the fronto-parietal network and its involvement in task distraction.

The paradigm was divided into three runs, with equal appearance frequency for each stimulus category in each run. The runs were separated by a pause of 20 seconds. During the pause, participants saw an instruction to relax and wait for the next block. Additionally, task instructions were displayed as a reminder. Stimuli were presented in a pseudo-random order for 100 ms each. Each presentation of a target or novel stimulus was followed by a non-target stimulus.

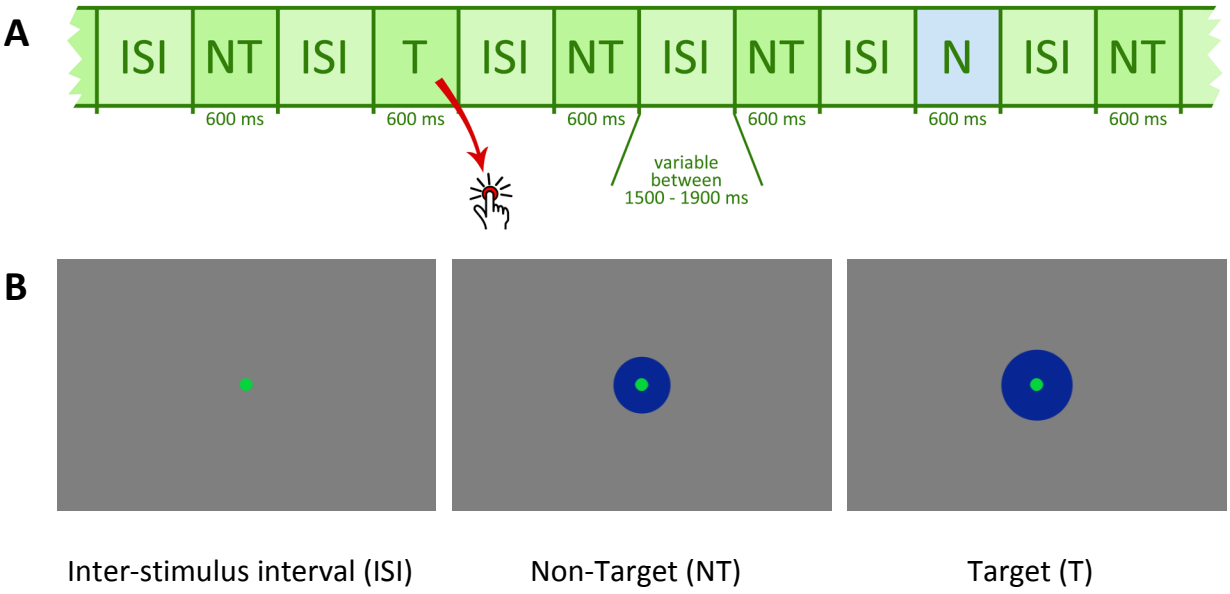

C

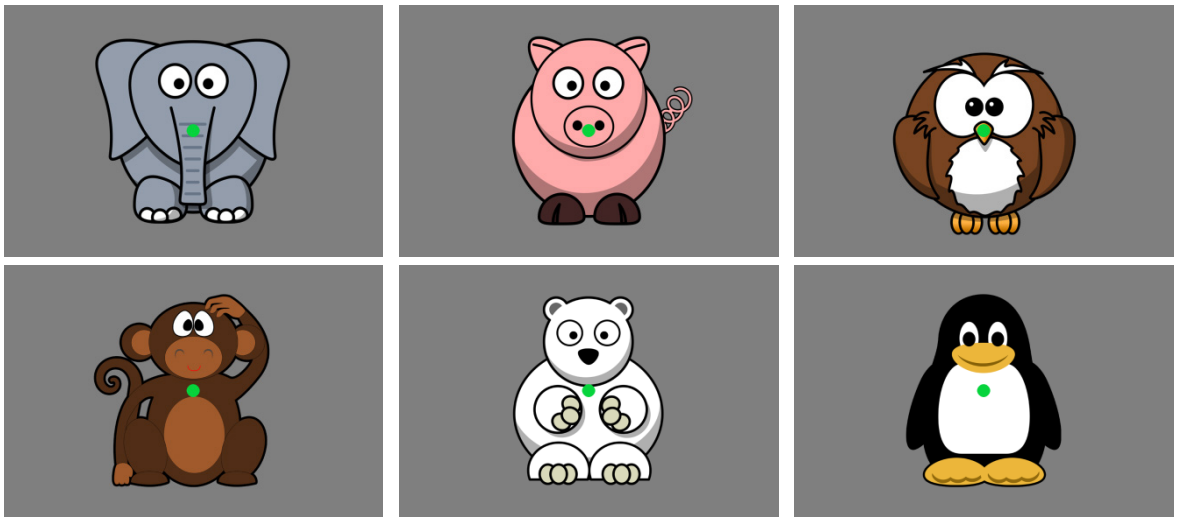

Figure 47: (A) Schematic presentation of stimulus sequence and presentation times of the visual novelty oddball task with all four stimulus categories: inter-stimulus interval (ISI), non-target (NT), target (T; relevance for response), and novels (N; attention drawing)
(B) Presented standard and target stimuli as well as pause stimulus in between (ISI) of novelty oddball task
(C) Six different novel stimuli, which appear surprisingly and distracting, however are not relevant for task accomplishment.

Training phase: In order to assess the personal abilities, each participant conducted a training phase, in which a simple oddball design was presented (no novels were shown during the training phase). This phase consisted of four blocks of each 273 non-targets and 42 targets (12 %), separated by a pause of 20 seconds. During the pause, participants saw an instruction to relax and wait for the next block. Additionally, task instructions were displayed as a reminder.

In each block, one difficulty level was presented. Throughout all blocks and also for the later acquired task, standard stimuli were kept equal (see above). The training phase, however, utilized four different circle sizes for target stimuli (with all target circles being larger than non-targets).

Participants were instructed to respond quickly but calmly upon the appearance of a larger circle (target). Participants were informed that at the beginning and after each pause at least three non-target stimuli are presented first, in order to allow reassessment of non-target circle size. The sequence of blocks began with the simplest level, consisting of the target stimulus with the largest circle diameter. The instructor stayed to make certain that the task was understood and left the measuring chamber during the

presentation of the first block. After each pause, the difficulty level was increased. Subsequently, results of the training phase were analysed and the smallest target stimulus, with at least 80% detection rate and less than 10 % of false positive responses during the same block, was chosen for the novelty oddball task combined with the EEG measurement. Each participant was also asked for his or her personal opinion of task difficulty and how comfortable he or she felt with the chosen level. The goal was to pick a small target in order to ensure a high level of attentional awareness throughout the whole task. This was done while also ensuring that no participant was overstrained to keep this awareness level for several minutes.

2.3. EEG session

After completion of the questionnaire, first the training phase for the visual novelty oddball experiment was conducted in order to measure the appropriate difficulty level for each participant. Thereafter, participants were seated in the measuring chamber and the EEG cap was put on. The measurement protocol followed the same steps as for study I (see SECTION II.2.3).

Following the spontaneous EEG measurement, the participant was reminded of the task during the training phase, the level for the novelty oddball task was reiterated and the new stimulus category (novels) was introduced. Participants were asked not to respond to novels. Participants were asked to stay relaxed and to reduce eye blinks, if possible. Once they understood the task, the instructor left the measurement chamber and started the task and the EEG measurement.

The total time it took to set up and record an EEG was approximately 90 minutes.

Following the EEG session, participants answered a questionnaire regarding difficulties or comments on the previous tasks.

2.4. EEG data analysis

2.4.1. EEG data pre-processing

EEG data pre-processing of study II followed the same steps as of study I. For detailed description see SECTION II.2.5.1.

After EEG data pre-processing, data sets of 79 out of 84 participants were further analysed for novel stimuli and 80 data sets for target stimuli.

As presented in Table 12, the average number of artefact-free epochs plus/minus standard deviation of the further-analysed participants is 29.44 ± 6.08 for novels. For targets and non-targets, on average 30.78 ± 5.23 artefact-free epochs were further analysed.

Table 12: Mean numbers of epochs included from each experimental condition for further analysis of the novelty oddball task.

Condition	Groups (Mean ± SD)
Novels	29.44 ± 6.08
Target & Non-Target	30.78 ± 5.23

Figure 48 displays the number of epochs per participant plotted over the age range for (A) novels and (B) targets and non-targets. For all participants, at least 20 epochs were considered for analysis. A linear regression was conducted for all stimuli conditions in order to detect age related correction effects. For all stimuli, the number of epochs is not significantly related to the age of participants (novels: p = .5295; targets / non-targets: p = .5142). For further details of the regression models see Table 17.

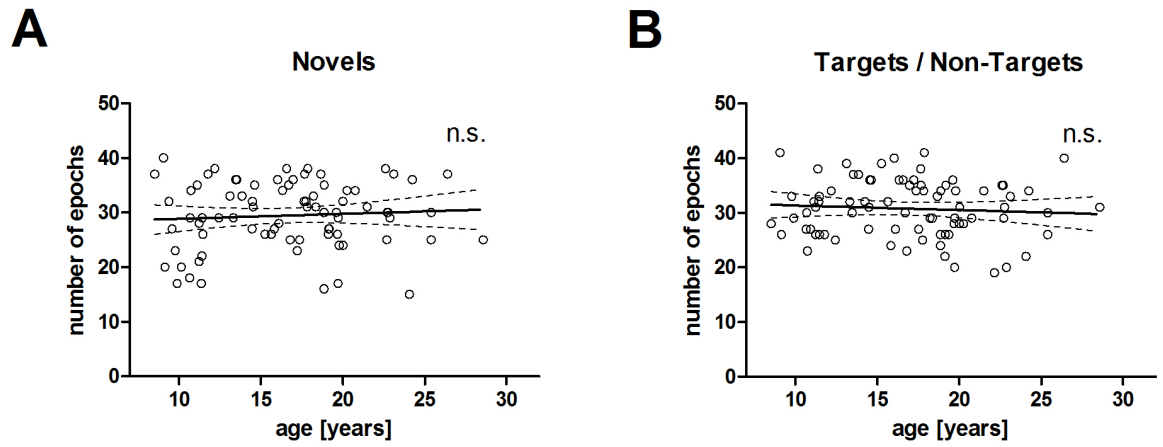

Figure 48: Linear regression of adjusted number of epochs for (A) novel trials and (B) target and non-target trials after artefact rejection of the novelty oddball task. Dashed lines indicate the 95 % confidence interval of the model.

2.4.2. ERP analysis

2.4.2.1 Analysis of the stimulus-locked P3b in the time domain

Before statistical analysis, epochs for each participant were averaged separately for novels, targets and non-targets. Data filtering of study II was conducted analogously to study I. For a detailed description see SECTION II.2.5.2.1.

2.4.2.2 Time windows and regions of interest for the P3b

The time windows incorporating the P3b, P3a and N2 were determined by visual inspection of the grand average and all single subject averages (separately for each stimulus condition; see Figure 49 to Figure 51). These time windows are reported in the literature for each of the components (Bocquillon et al., 2014; Polich, 2007). The time window for the P3b component is chosen analogously to that of study I (see section 2.5.2.2).

For all ERP components, baseline correction was applied by the mean amplitude between -700 and -300 ms before stimulus onset and was subtracted from the ERP before analysis. The baseline period matches the time-frequency analyses (see SECTION II.2.5.3.2 & 2.4.3.2).

To estimate the components' amplitude, age-related latency differences of the maximum P3a and the minimum N2 were taken into account. This procedure was chosen to ensure that the maximum P3a and minimum N2 were reflected equally among the age range, even if processing time was still prolonged in the younger participants. For details of the chosen time windows see Table 13.

Mean ERP amplitude values and peak latencies were pooled into frontal (F3, Fz, F4) and parietal ROIs (P3, Pz, P4). The frontal region incorporated the minimum of the N2 (Folstein & van Petten, 2008; Polich, 2007). The posterior region incorporated the maximum of the P3b (Polich, 2007; van Dinteren et al., 2014a). The P3a component was maximal at posterior electrode sites (Bocquillon et al., 2011; Ferrari, Bradley, Codispoti, & Lang, 2010; Hagen, Gatherwright, Lopez, & Polich, 2006; Oades et al., 1997). In accordance with the literature, occurred the Novel-P3a earlier and with larger amplitudes at fronto-central electrode sites than the P3b elicited by targets. This emphasizing the role of anterior brain regions of underlying novelty processing and cognitive control of distractors (cf. Friedman et al., 2001; Polich, 2007; Polich & Criado, 2006).

Time windows and ROIs of latency and amplitude analyses for all stimulus categories and their examined ERP components are listed in Table 13.

Table 13: Time windows and regions of interest for P3a and P3b analysis of the novelty oddball task

Stimulus condition	ERP component	Time window for analysis [ms]			ROI
		average analysis	individual latency	individual amplitude	
Novel	N2	200 - 300	200 - 500	8 to 16.6 years: 250 – 300 16.6 to 30 years: 200 – 250	frontal
	P3a	300 – 500	300 – 500	8 to 13.5 years: 400 – 500 13.5 to 30 years: 300 – 400	frontal
Target	P3b	400 - 600	300 - 700	300 - 700	parietal

The topographical plot in Figure 49B illustrates that the chosen electrode sites incorporated the maximal deflection of the P3b. Investigating a frontal and a parietal ROI reflects that trajectories of frontal P3a and N2, and parietal P3b amplitude differ over the lifespan (van

Dinteren et al., 2014a) and that within the P3a, N2 and P3b time window, both frontal and parietal brain regions are activated during tasks requiring novel processing and target detection (Bocquillon et al., 2011; Wronka et al., 2012).

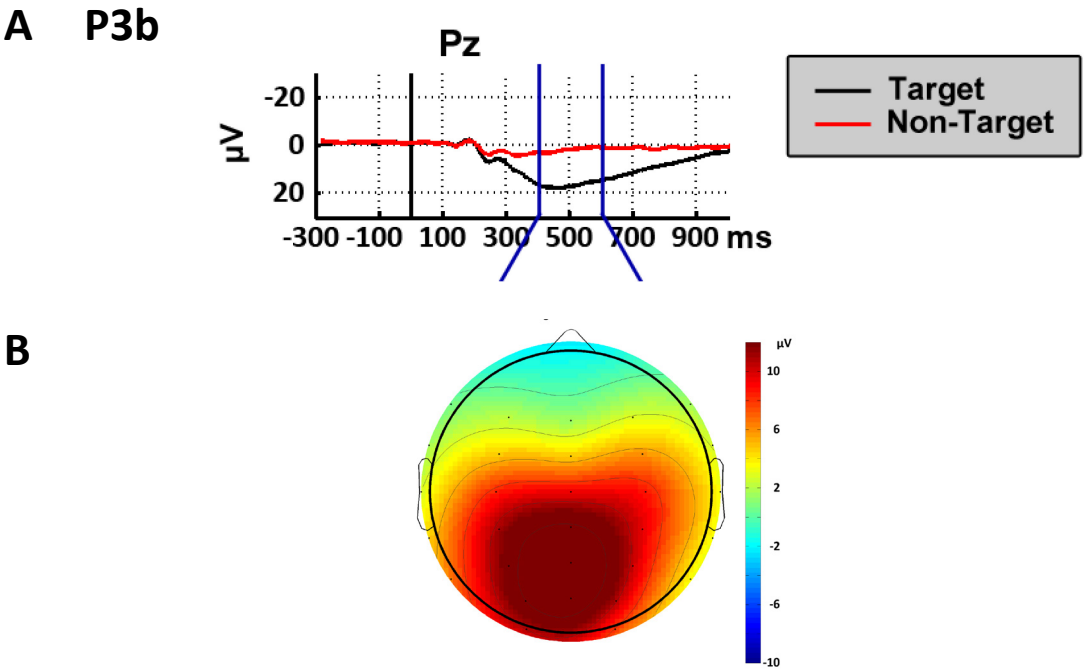

Figure 49: A: Time course of ERPs of target stimuli of the novelty oddball task at electrode Pz averaged over all participants. The time window for the P3b analysis is depicted by blue lines.
B: Averaged topological distribution of P3b during 400 to 600 ms for target stimuli for all participants.

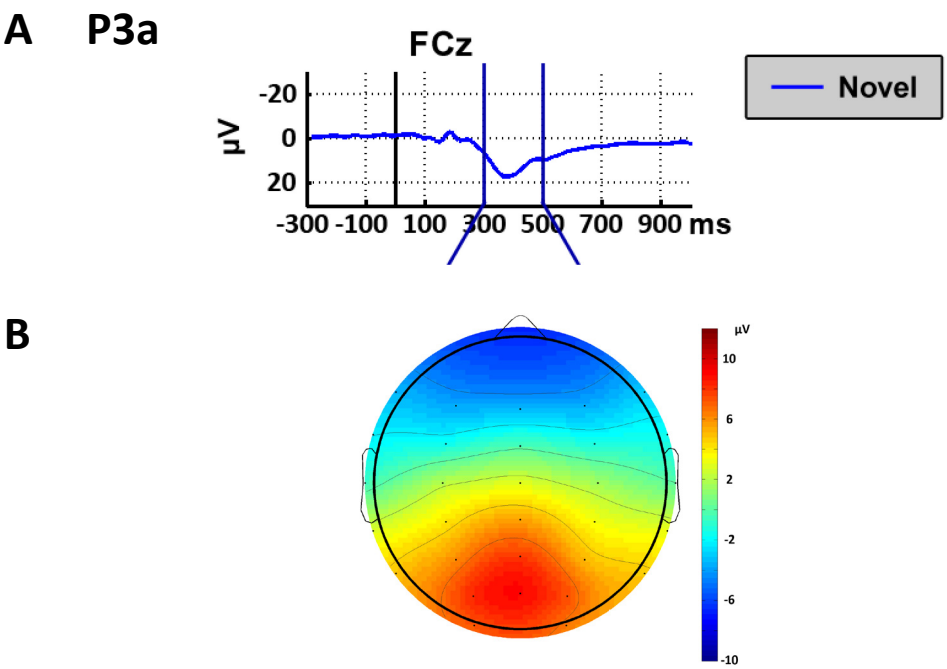

Figure 50: A: Time course of ERPs of novel stimuli of the novelty oddball task at electrode FCz averaged over all participants. The time window for the P3a analysis is depicted by blue vertical lines.
B: Averaged topological distribution of P3a during 300 to 500 ms for novel stimuli for all participants.

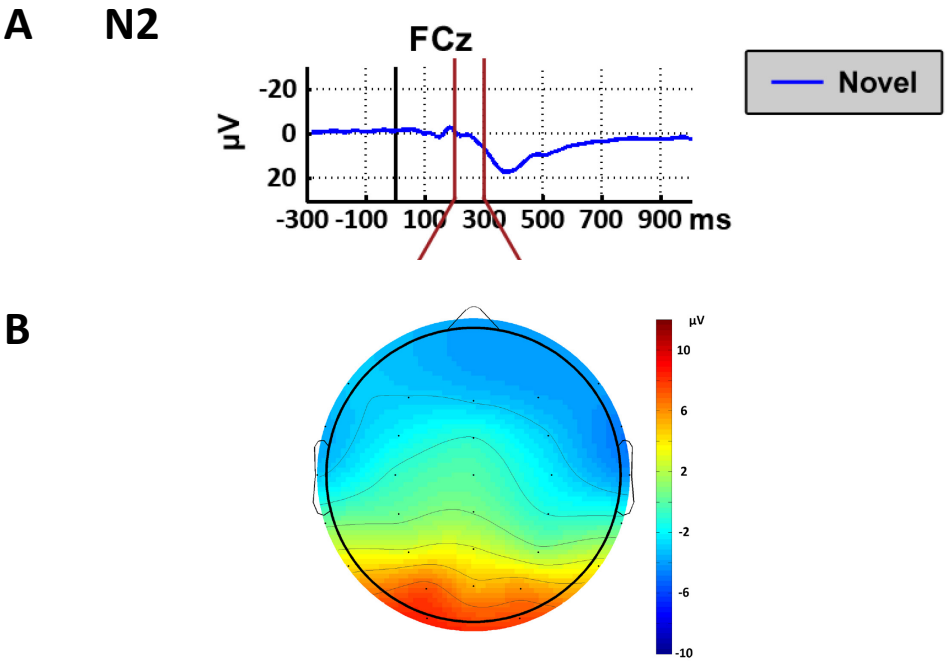

Figure 51: A: Time course of ERPs of novel stimuli of the novelty oddball task at electrode FCz averaged over all participants. The time window for the N2 analysis is depicted by red vertical lines.
B: Averaged topological distribution of N2 during 200 to 300 ms for novel stimuli for all participants

2.4.3. Time-frequency analysis

2.4.3.1 Time-frequency transformation of EEG data

Time–frequency analysis for study II was applied analogously as in study I. For a detailed description see SECTION II.2.5.3.1

2.4.3.2 Pre-stimulus amplitude

Single-trial amplitude (AMP) was calculated individually for all participants as well as for each frequency band of interest and all conditions (novels, target and non-target).

2.4.3.3 Event-related spectral perturbation

To estimate amplitude changes induced by the stimulus onset, the data was baseline-corrected. Baseline correction for study II was applied analogously as in study I. For a detailed description see SECTION II.2.5.3.3.

2.4.3.4 Inter-trial phase coherence

The inter-trial phase coherence (ITC) of study II was applied analogously as in study I. For a detailed description see SECTION II.2.5.3.4

2.4.3.5 Time-frequency windows and ROIs

In accordance with the analysis of study I (see SECTION II.2.5.3.5), for each frequency band and each before described analysis method, visual inspection of the grand average and all single-subject maximal response strengths (resulting peak times were rounded) were used to determine time-frequency windows of range 200 ms and their corresponding ROIs. Since the topographical distributions of all response patterns (averaged over all participants) displayed no strong lateralisation effect, time windows were fit to the maximal response strength of an electrode along the central line.

Table 4 sums the determined time windows and corresponding ROIs for both frequency bands (delta & theta) and both analysis conditions (ERSP & ITC).

Table 14: Analysed frequency bands, according time windows and ROIs for each analysis method in the novelty oddball task.

Condition/ Stimulus	Frequency band	Method	Analysis time window [ms]	ROI for analysis
Novels	Delta	AMP	-700 to -300	Fz, FCz, Cz, CPz, Pz
		ERSP	250 to 450	FCz, C3, Cz, C4, CP3, CPz, CP4
		ITC	200 to 400	CP3, CPz, CP4, P3, Pz, P4
	Theta	AMP	-700 to -300	Fz, FCz, Cz
		ERSP	200 to 400	Fz, FC3, FCz, FC4, Cz
		ITC	200 to 400	Fz, FC3, FCz, FC4, Cz
Target &Non-target	Delta	AMP	-700 to -300	Fz, FCz, Cz, CPz, Pz
		ERSP	300 to 500	P3, Pz, P4, PO3, POz, PO4
		ITC	300 to 500	P3, Pz, P4, PO3, POz, PO4, O1, O2
	Theta	AMP	-700 to -300	Fz, FCz, Cz
		ERSP	250 to 450	Fz, FC3, FCz, FC4, Cz
		ITC	150 to 350	Fz, FC3, FCz, FC4, Cz

2.4.4. Spatial phase coherence analysis

Analysis of the spatial phase coherence followed the described method of SECTION II.2.5.4. The chosen time windows for all stimulus categories of the novelty oddball task are summed in Table 15.

Table 15: Analysis time windows for SPC of the theta frequency band for all stimulus categories of the novelty oddball task.

Stimuli	Time window
Novels	200 – 400 ms
Target & Non-Target	300 – 500 ms

2.5. Statistical analysis

Behavioural and EEG-data of the novelty oddball task were analysed equally, as described in SECTION II.2.6 for the data of the oddball task with additionally observing one further stimulus class: novel stimuli.

Due to the behavioural data, no participant was excluded for excessively long reaction times (861.62 ms on personal average being the slowest RT) or too many errors (28.57 % being the highest personal error rate).

3. Results

3.1. Behavioural data

3.1.1. Error rates

All participants, on average, showed low error rates (compare Table 16). No participants reached an error rate above 28.57 %. No relation with age could be found for the mean percentage of errors (p = .6397), as depicted in Figure 52.

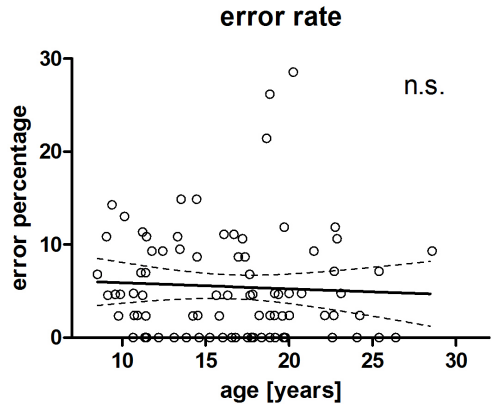

Figure 52: Linear regression model of mean error rate conducted by participants of the novelty oddball experiment with dashed lines indicating the 95 % confidence interval of the model.

Figure 53A displays the number of omission errors over age. The omission error conduct exhibits no correlation effect with age (p = .5957).

Figure 53B shows the number of falsely positive reacted trials over age. Regression analysis revealed no linear age trend (p = .2368).

For further details of the regression models see Table 17.

Table 16: Behavioural data of novelty oddball task.

Mean error rate [%]		5.48
RT	Median [ms]	503.42
	Individual SD [ms]	86.42
	Coefficient of Variation	0.17

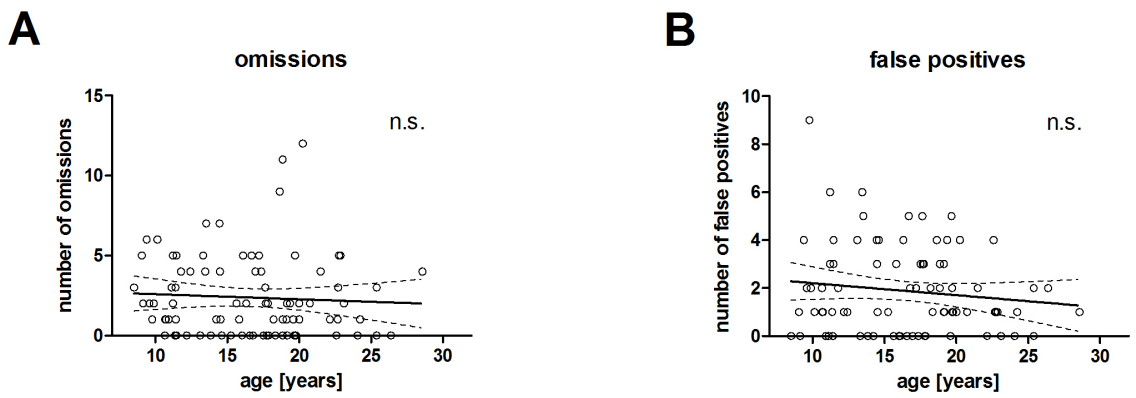

Figure 53: Linear regression of performance of novelty oddball task with dashed lines indicating the 95 % confidence interval of the model.
A: Number of omission mistakes during performance.
B: Number of falsely responded trials.

Table 17: Description of best-fit regression models for number of epochs and behavioural data of the novelty oddball task.

	Model	F-value (df)	B0	B1	B2	Normality of Residuals	Runs-Test	R^2
Number of epochs Novel	L	$^{(1, 77)}$ .4	27.9	.1	-	3.2	n.s.	.0052
Number of epochs Target / Non-Target	L	$^{(1, 78)}$ .4	32.2	-.1	-	3.2	n.s.	.0055
Omissions	L	$^{(1, 82)}$ .3	2.9	.0	-	30.8****	n.s.	.0034
False positives	L	$^{(1, 82)}$ 1.4	2.7	-.1	-	15.4 ***	n.s.	.0170
Median RT	Q	$^{(1, 81)}$ 7.7**	844.2	-36.6	.9	45.7****	n.s.	.2140

n.s.: not significant, * $p < .05$, ** $p \leq .01$, *** $p \leq .001$, **** $p \leq .0001$.

3.1.2. Reaction times

Individual median reaction time variated around 503 ms (see Table 16 for detailed information). Figure 54 displays the individual median reaction time over age. The data exhibits a significant convex quadratic age trend with its minimum at 20.64 years of age (p = .0067, also see Table 17). The regression model is not perfectly describing the data, as indicated by a non-Gaussian distribution of its residuals.

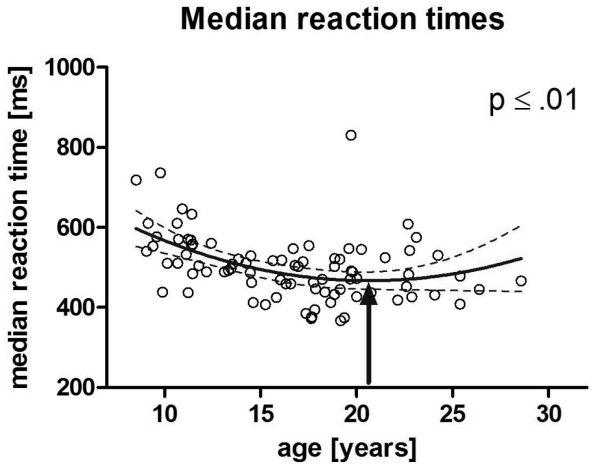

Figure 54: Quadratic regression of median reaction time plotted over age range for the novelty oddball task. Dashed lines indicate the 95 % confidence interval of the model. The arrow indicates the minimum of the quadratic model at 20.64 years of age.

3.2. EEG-Data of Novelty Oddball Paradigm

3.2.1. Event-related potentials

3.2.1.1 P3b component

Figure 55A depicts the ERP over time for target and non-target trials for electrodes Fz, FCz, Cz, Pz and O2. In Figure 55B, the topological distribution for only target trials is averaged over the time window of interest for the P3b component. Upon target presentation, a positive deflection can be observed after around 300 ms, reaching its maximum at Pz after 466 ms. The P3b is located over posterior regions of the brain.

Regression analysis of the P3b revealed no relation with age for latency (see Figure 56; p = .0513) and amplitude (Figure 57; p = .4001).

Table 18 provides further detail of both regression models.

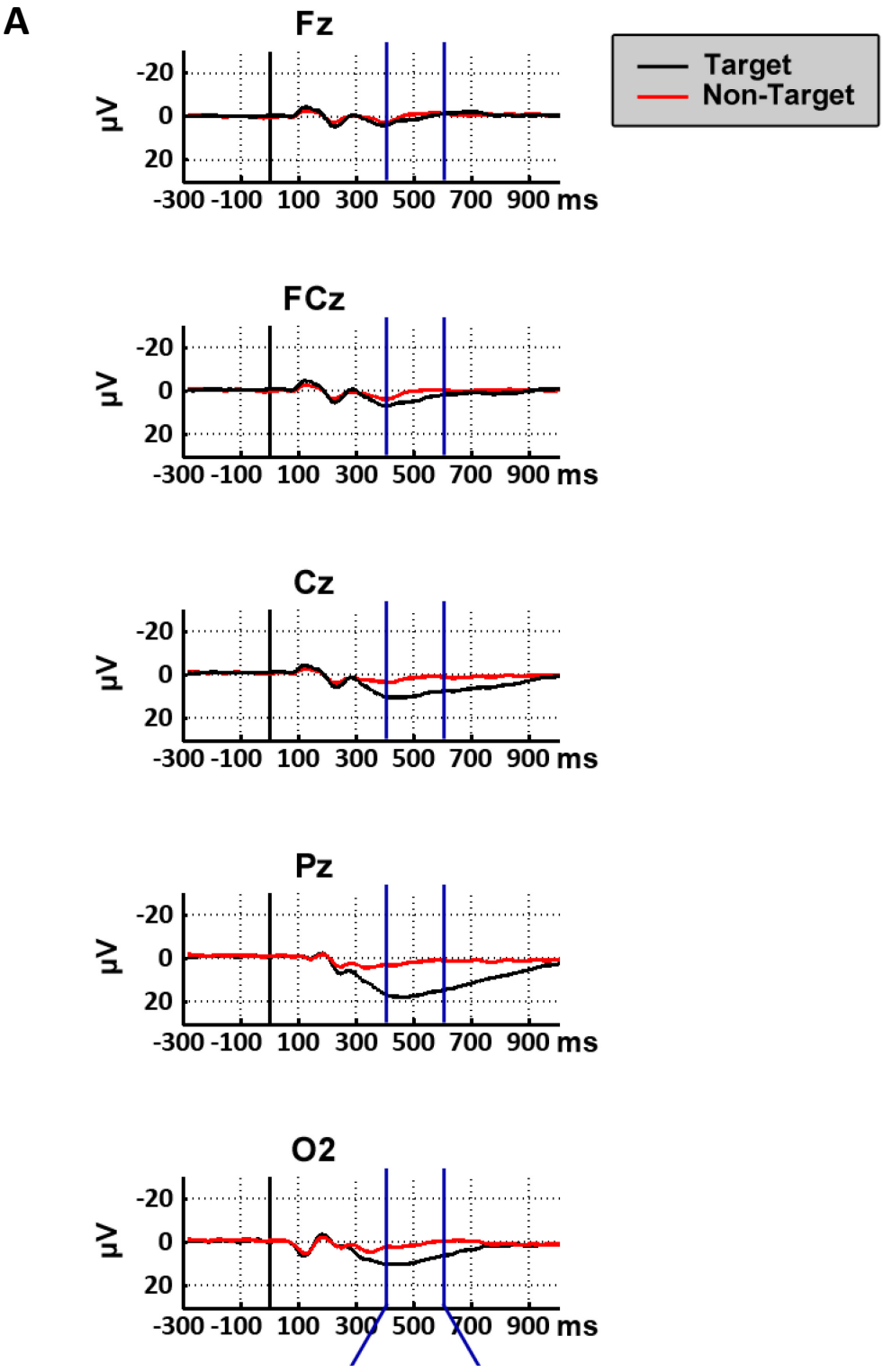
A
Fz
FCz
Cz
Pz
O2
μV
-20
0
20
-300 -100 100 300 500 700 900 ms
Target
Non-Target

B

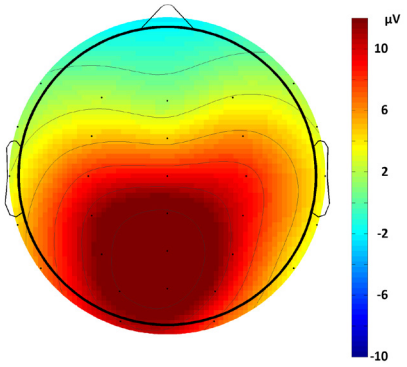

Figure 55: A: Time course of ERPs for the novelty oddball task at electrodes Fz, FCz, Cz, Pz and O2 averaged over all participants for target (black) and non-target (red) trials. The time window for analysis is depicted by blue lines. B: Averaged topological distribution of P3b during 400 to 600 ms for target stimuli for all participants.

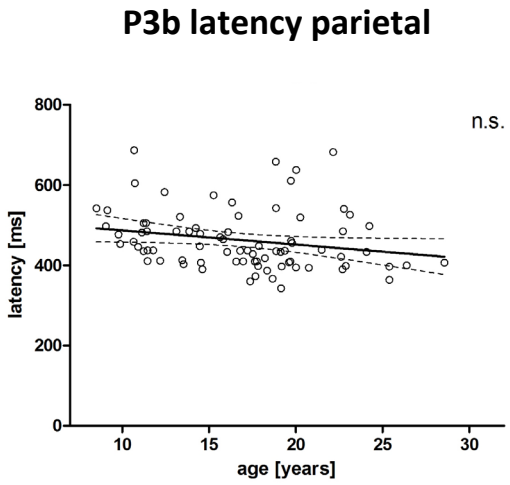

Figure 56: Linear regression of individual P3b latency of target stimuli during novelty oddball task for a parietal ROI (P3, Pz, P4) assessed from 300 to 700 ms in relation to the age of participants. Dashed lines indicate the 95 % confidence interval of the model.

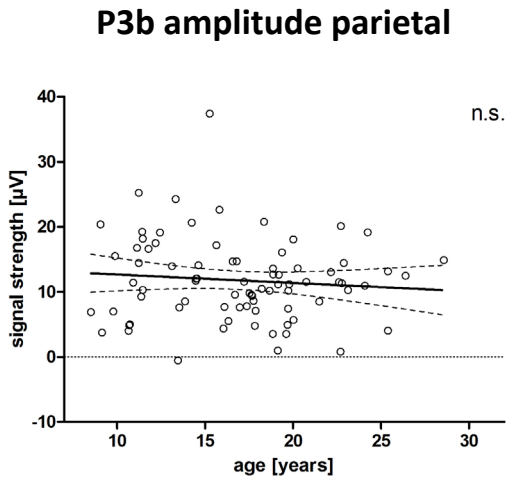

Figure 57: Linear regression of individual P3b amplitude of target stimuli during novelty oddball task for a parietal ROI (P3, Pz, P4) averaged over a time window of 300 to 700 ms in relation to the age of participants. Dashed lines indicate the 95 % confidence interval of the model.

3.2.1.2 P3a component

The ERP of novel stimuli is presented in Figure 58A for electrodes Fz, FCz, Cz, Pz and O2. The time window of interest for the P3a component is indicated by vertical blue lines from 300 to 500 ms. The P3a reaches its maximum at electrode FCz 248 ms after stimulus presentation, with a distribution over frontal brain areas.

Regression analysis of the P3a's latency indicated a decreasing linear effect with age ($p \leq .0001$), as depicted in Figure 59.

An increasing linear effect was found for the amplitude of the P3a over age (see Figure 60; $p \leq .0001$).

See Table 18 for further details of the regression models.

A

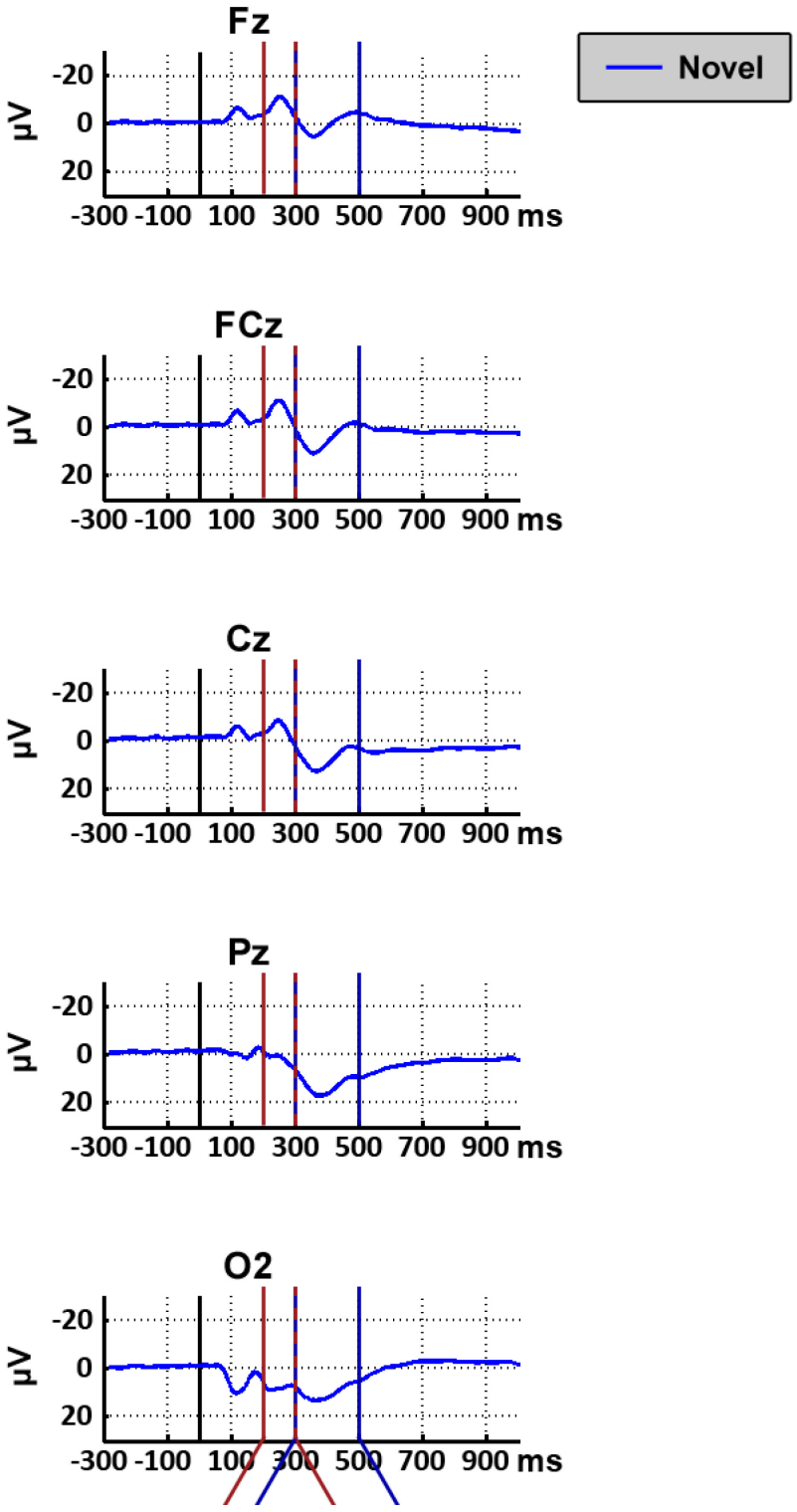

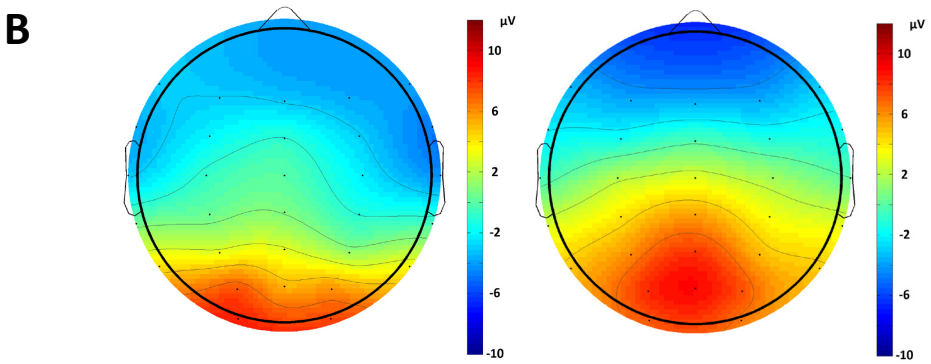

Figure 58: A: Time course of ERPs of the novelty oddball task at electrodes Fz, FCz, Cz, Pz and O2 averaged over all participants for novel trials. The time windows for analysis are depicted by red (N2) and blue (P3a) vertical lines. B: Averaged topological distributions of N2 (left) during 200 to 300 ms and P3a (right) during 300 to 500 ms for novel stimuli for all participants.

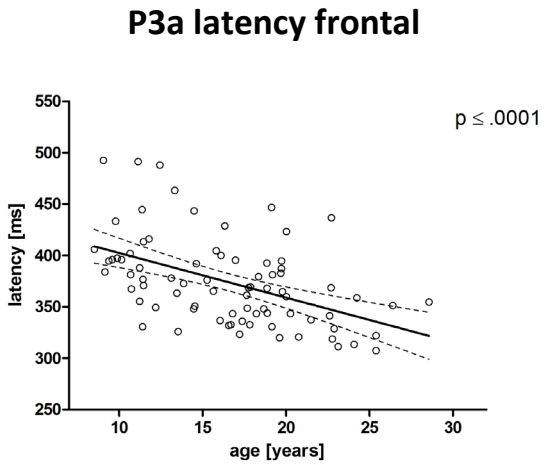

Figure 59: Linear regression of individual P3a latency of novel stimuli during novelty oddball task for a frontal ROI (F3, Fz, F4), assessed from 300 to 500 ms in relation to the age of participants. Dashed lines indicate the 95 % confidence interval of the model.

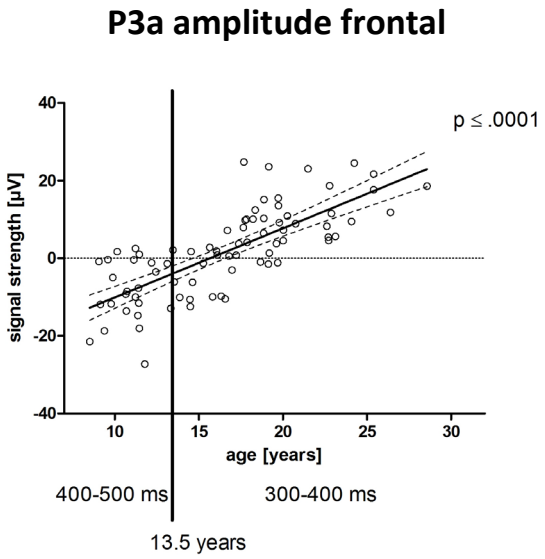

Figure 60: Linear regression of individual P3a amplitude of novel stimuli during novelty oddball task for a frontal ROI (F3, Fz, F4) averaged over a time window of 400 to 500 ms for participants until age 13.5 years and 300 to 400 ms for older participants. Dashed lines indicate the 95 % confidence interval of the model.

3.2.1.3 Novelty N2 complex

Figure 58A depicts the time window of interest for the N2 complex from 200 to 300 ms elicited during novel presentation by vertical red lines. The N2 reaches its minimum at electrode FCz after 358 ms. Its topological distribution is shown in the left plot of Figure 58B. The negative deflection is minimal over frontal brain regions.

As shown in Figure 61, the latency of the N2 complex follows a convex quadratic trajectory with a minimum at an age of 17.36 years of age (p = .0033). The model is not, however, describing the data perfectly, as indicated by its residuals being distributed in a non-Gaussian fashion around the fit.

The magnitude of the frontal N2 amplitude decreases with age in a linear fashion ($p \leq .0001$), as depicted in Figure 62.

Details of both regression models are listed in Table 18.

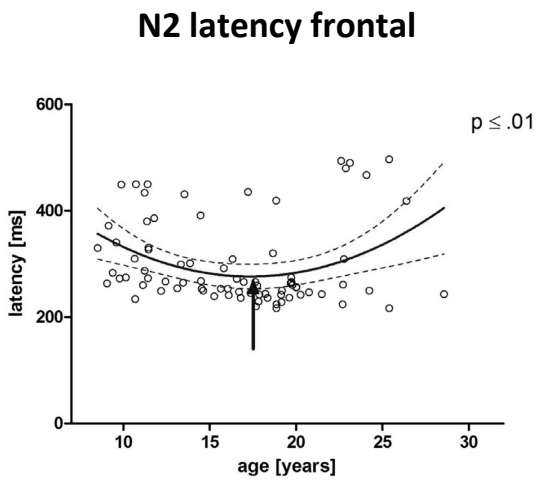

Figure 61: Quadratic regression of individual N2 latency of novel stimuli during novelty oddball task for a frontal ROI (F3, Fz, F4) assessed during 200 to 500 ms in relation to the age of participants. Dashed lines indicate the 95 % confidence interval of the model. The arrow indicates the minimum of the quadratic model at 17.36 years of age.

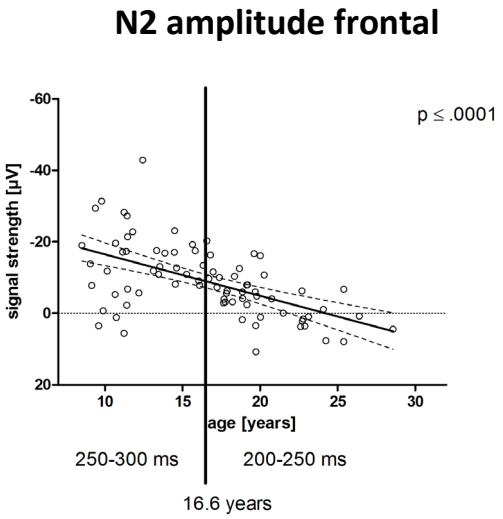

Figure 62: Linear regression of individual N2 amplitude of novel stimuli during novelty oddball task for a frontal ROI (F3, Fz, F4) in relation to the age of participants averaged over a time window of 250 to 300 ms for participants until age 16.6 years and 200 to 250 ms for older participants. Dashed lines indicate the 95 % confidence interval of the model. The y-axis was reversed for a simplified presentation, as the N2 stands for a negatively deflected ERP component.

Table 18: Description of best-fit regression models for latency and amplitude of the P3b, P3a and N2 response components during the novelty oddball task.

component	characteristics	Model	F-value (df)	B0	B1	B2	Normality of Residuals	Runs-Test	R^2
P3b	Lat	L	(1, 78) 3.9	522.5	-3.5	-	22.4****	n.s.	.0478
	Amp	L	(1, 78) .7	14.0	.2	-	16.3****	n.s.	.0091
P3a	Lat	L	(1, 77) 24.1****	445.9	-4.3	-	10.3**	n.s.	.2384
	Amp	L	(1, 77) 103.5****	.27.9	1.8	-	1.0	n.s.	.5733
N2	Lat	Q	(1, 76) 9.2**	586.5	-35.7	1.0	12.5**	n.s.	.1093
	Amp	L	(1, 77) 34.5****	-28.1	1.2	-	5.0	n.s.	.3092

n.s.: not significant, * $p < .05$, ** $p \leq .01$, *** $p \leq .001$, **** $p \leq .0001$.

3.2.2. Event-related oscillations

3.2.2.1 Delta frequency band

Pre-stimulus interval

The left of Figure 63 depicts a topological distribution of the delta frequency amplitude during the interval before the presentation of target stimuli. The signal is maximal over the central line of electrodes.

Regression analysis shown on the right of Figure 63 revealed a convex quadratic trend with a trough at 25.35 years of age ($p \leq .0001$).

Further details for all best-fit regression models of the delta frequency band are listed in Table 19.

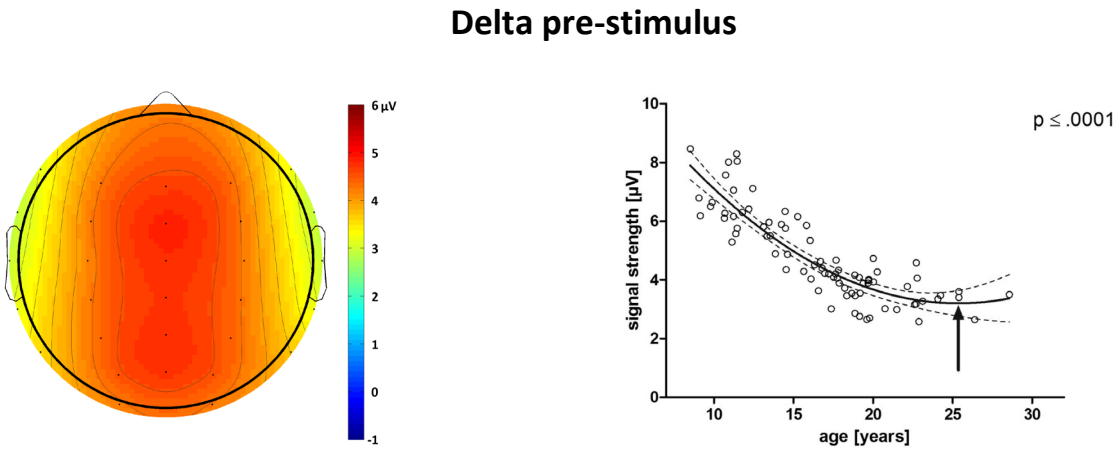

Figure 63: Left: Topological plot of non-baseline-corrected amplitude of the delta frequency band during -700 to -300 ms before presentation of target stimuli of the novelty oddball task.
Right: The best-fit quadratic regression model for pre-stimulus amplitude of the delta frequency band, dependent on age, of target stimuli for the ROI: Fz, FCz, Cz, CPz and Pz. Dashed lines indicate the 95 % confidence interval of the regression model. The arrow indicates the minimum of the quadratic model at 25.35 years of age.

Novel stimuli

Event-related spectral perturbation

The ERSP for the baseline-corrected amplitude of the delta frequency band for novel stimuli is shown on the left of Figure 64 with A depicting the time course and B depicting the topological distribution. Upon stimulus presentation, the delta ERSP increases, reaching its peak along the central line of electrodes at Cz after 332 ms and showing its maximal deflection over central brain areas.

With age, the delta ERSP follows an increasing linear trend ($p \leq .0001$), as visualized in Figure 64C.

Inter-trial coherence

On the right of Figure 64A, the delta ITC is shown as the time course for novel stimuli, while in B the signal distribution over the head is depicted. The delta ITC increases after stimulus presentation, reaching maximum occurrence at electrode CPz after 320 ms. Similar to the delta ERSP of novel stimuli, the ITC has a topological distribution spreading over central brain areas. Its maximum is located over central-parietal areas.

The best-fit model for the ITC over age is a linear trajectory ($p \leq .0001$), as shown in Figure 64C.

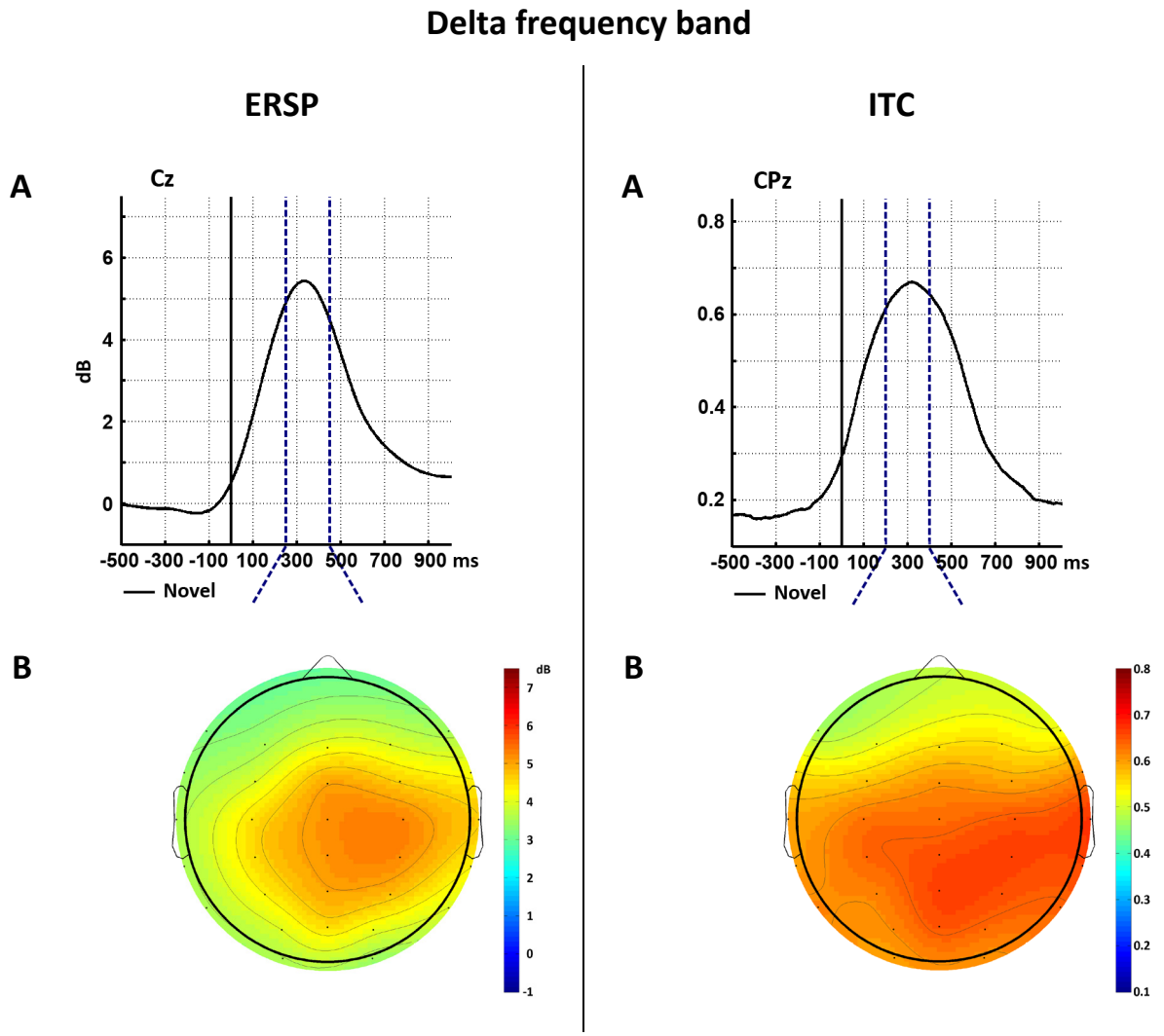

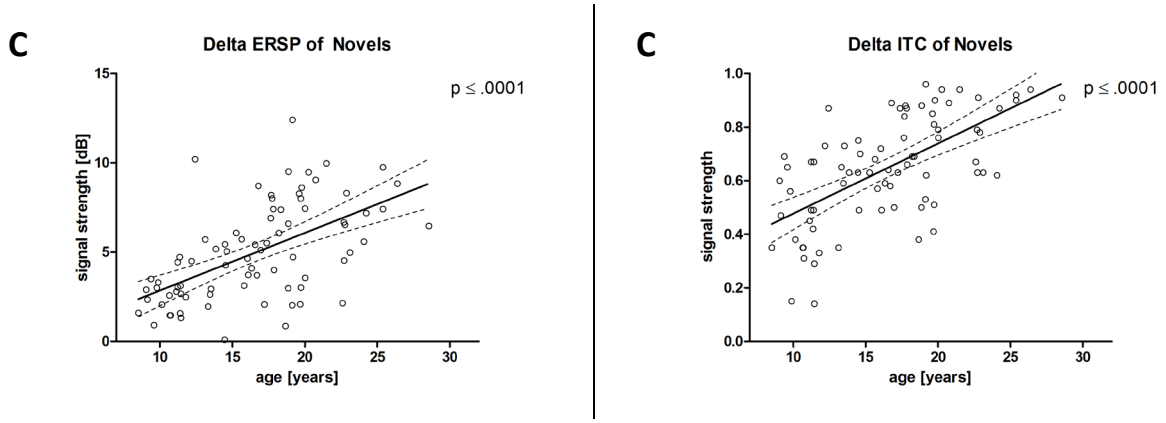

Figure 64: Overview of time-frequency analysis for the novelty oddball task for novel stimuli. Each condition is displayed averaged over all participants; top as a line plot with blue lines indicating determined time window (A) and below as a topological plot during this time window (B). Plotted below is a linear regression of the age-dependent signal strength averaged over the ROI for the novel stimuli during the given time window with key indicators of regression analysis (C). Dashed lines in the C graphs indicate the 95 % confidence intervals of the regression models.
A: Baseline-corrected amplitude of the delta frequency band.
B: ITC of the delta frequency band.

Target and non-target stimuli

Event-related spectral perturbation

Figure 65 displays on the left the ERSP for the delta frequency band averaged for target trials, as time course (A) and topological plot (B). The ERSP increases after stimulus appearance, peaking after 388 ms at electrode POz, with a distribution over posterior brain regions.

Quadratic regression analysis revealed a concave trend for target ERSP over age with a maximum peak at 21.58 years of age (p = .0330; see Figure 65C).

By contrast, for non-target trials, the ERSP followed an increasing linear age course (p = .0058), as depicted in Figure 65D.

Inter-trial coherence

On the right side of Figure 65, the ITC is plotted for the delta frequency band of target trials over time (A) and as a head plot (B). After 394 ms, the ITC reaches its peak at electrode POz, exhibiting a posterior distribution over the head.

The ITC follows an increasing linear age trend for target (p = .0472) and non-target trials (p = .0269), as displayed by graphs C and D, respectively. The increase of ITC for target trials is steeper when compared to non-target trials. Both regression models significantly differ from one another (H_0 = One curve for both data sets, $F_{(2, 156)}$ 41.1, $p \leq .0001$).

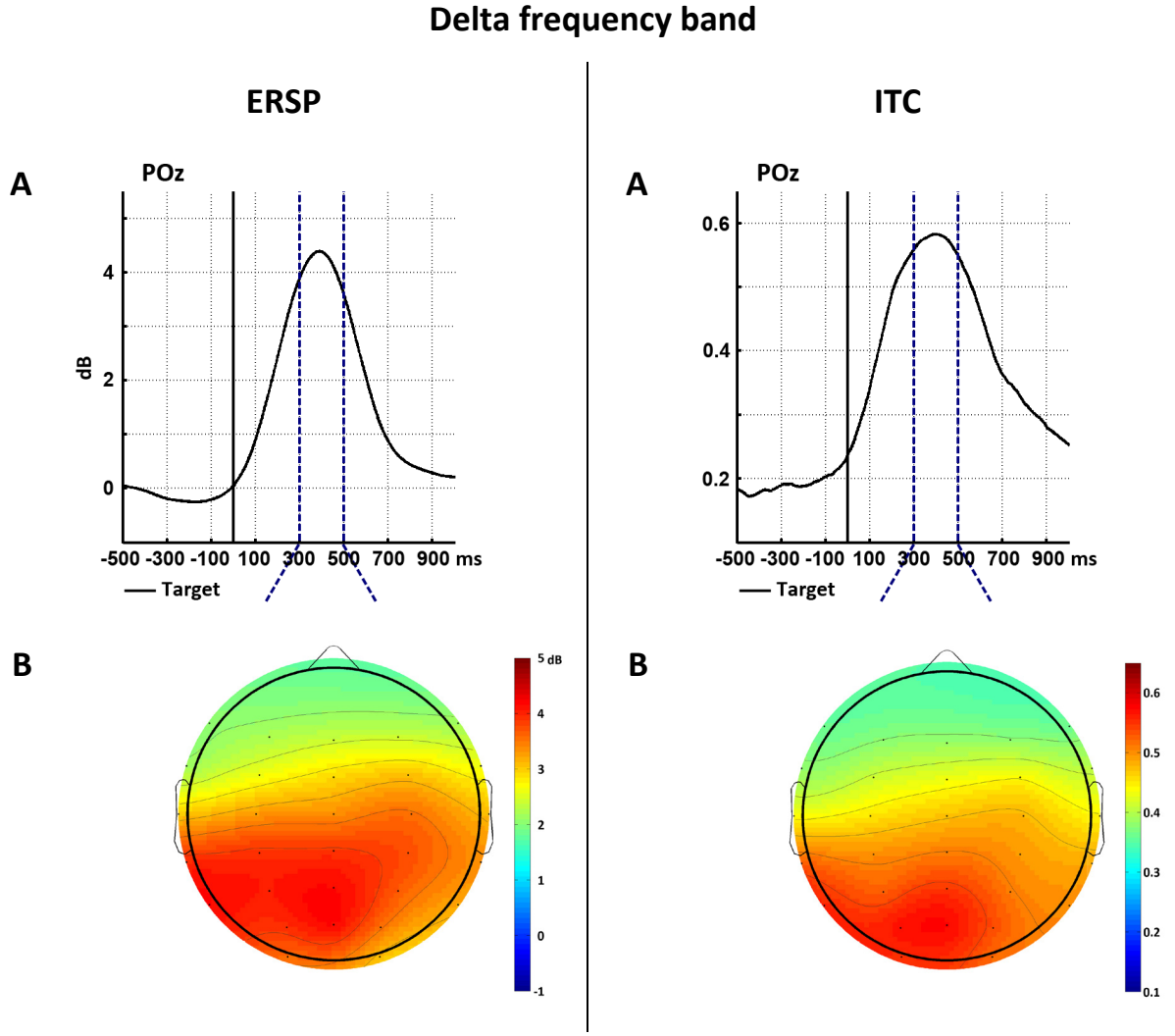

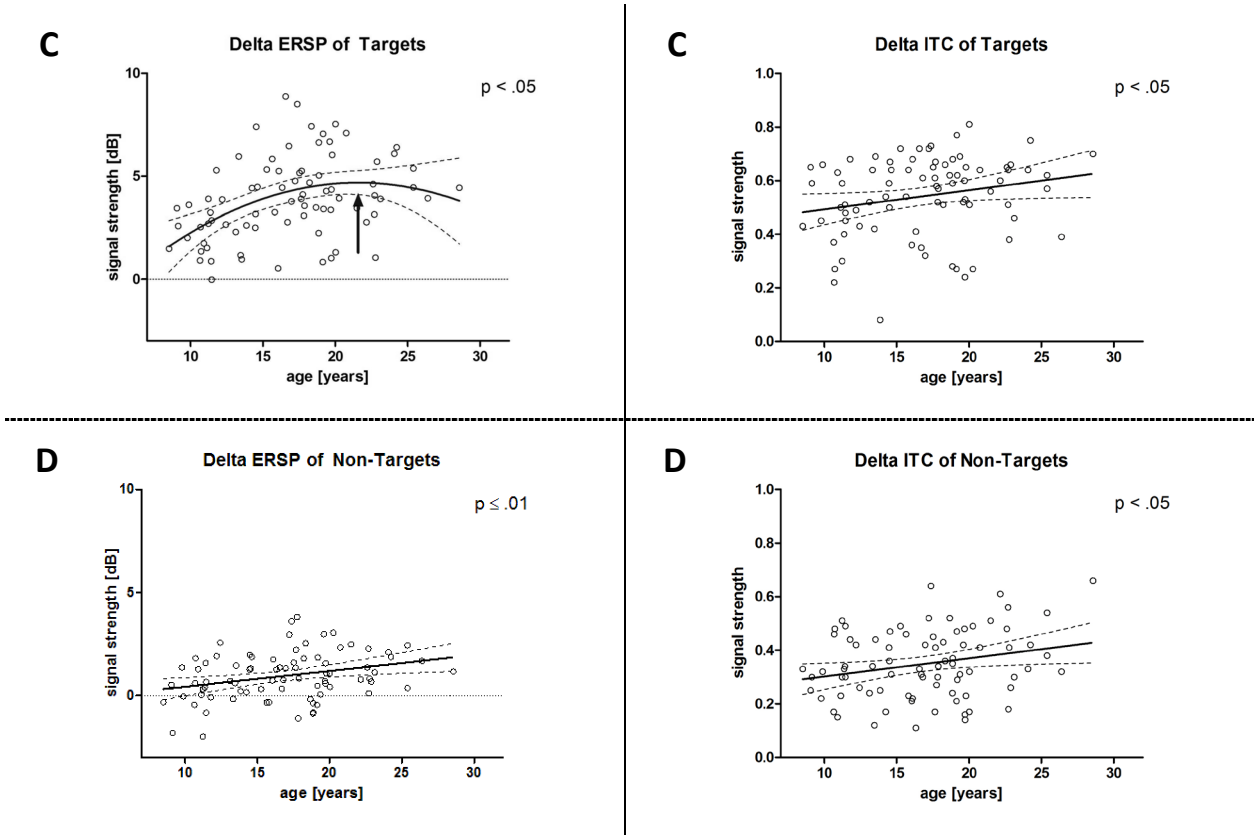

Figure 65: Overview of time-frequency analysis for the novelty oddball task for target stimuli. Each condition is displayed averaged over all participants; top as a line plot with blue lines indicating determined time window (A) and below as a topological plot during this time window (B). Plotted below are quadratic (left, C) and linear (left, D & right, C & D) regressions of the age-dependent signal strength averaged over the ROI for the target stimuli (C) and of non-target stimuli (D) during the given time window with key indicators of regression analysis. Dashed lines in graphs C and D indicate the 95 % confidence intervals of the regression models. The arrow in C indicates the maximum of the quadratic model at 21.58 years of age.
A: Baseline-corrected amplitude of the delta frequency band.
B: ITC of the delta frequency band.

3.2.2.2 Theta frequency band

Pre-stimulus interval

The theta frequency amplitude measured before presentation of target stimuli is depicted in a head plot on the left of Figure 66. The distribution is maximal over fronto-central brain regions. Over age, a significant linear decrease of the amplitude can be observed ($p \leq .0001$), as depicted on the right of Figure 66. The model is not, however, describing the data

perfectly, as indicated by its residuals not being not scattered Gaussian-shaped around the model ($p \leq .0001$).

Table 19 provides further details for all regression models of the theta frequency band described in this section.

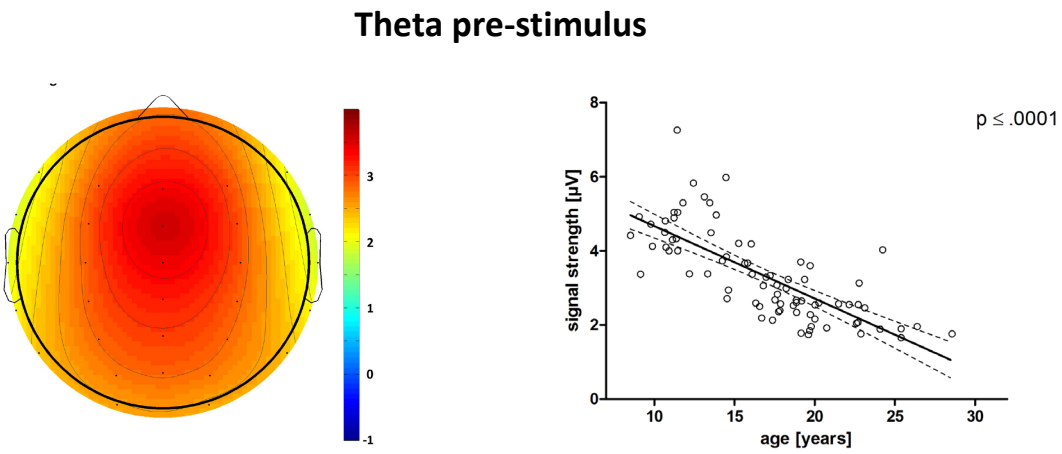

Figure 66: Left: Topological plot of non-baseline-corrected amplitude of the theta frequency band during -700 to -300 ms before presentation of target stimuli of the novelty oddball task.
Right: Linear regression model for pre-stimulus amplitude of the theta frequency band dependent on age for the ROI: Fz, FCz and Cz. Dashed lines indicate the 95 % confidence interval of the regression model.

Novel stimuli

Event-related spectral perturbation

The left of Figure 67 shows the baseline-corrected theta ERSP of novel stimuli as a time course in A and as a topological plot in B. Upon stimulus presentation, the ERSP increases until 310 ms, peaking at electrode FCz; hence, it is distributed over fronto-central brain areas.

As depicted in Figure 67C, the ERSP exhibits a significant concave quadratic trend with age peaking maximally at 21.48 years of age ($p = .0005$).

Inter-trial coherence

The theta ITC of novel trials is displayed in Figure 67A over time and in B over the head. The ITC increases, peaking at electrode FCz 300 ms after presentation of the novel stimuli. For

the time window of interest, the distribution is maximal over fronto-central areas of the brain.

With age, the ITC follows a concave quadratic trajectory with its maximum at 24.71 years of age (p = .0336), as shown in Figure 67C.

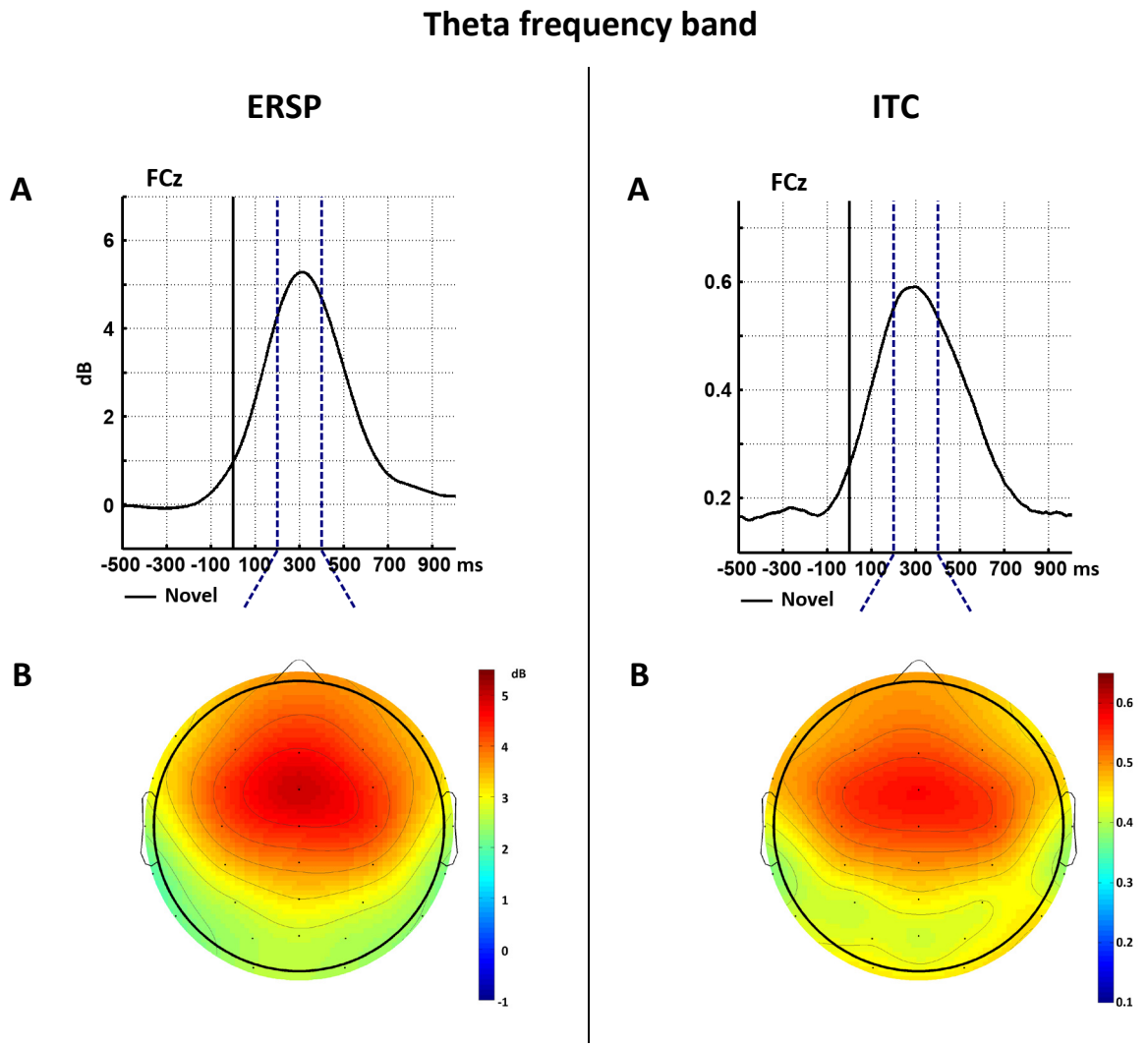

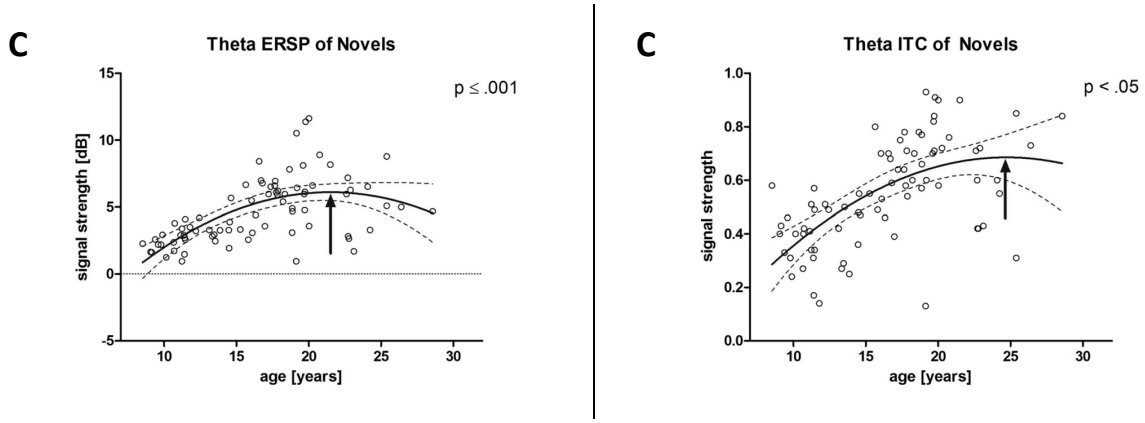

Figure 67: Overview of time-frequency analysis for the novelty oddball task for novel stimuli. Each condition is displayed averaged over all participants; top as a line plot with blue lines indicating determined time window (A) and below as a topological plot during this time window (B). Plotted below is a quadratic regression of the age-dependent signal strength averaged over the ROI for the novel stimuli during the given time window with key indicators of regression analysis (C). Dashed lines in the C graphs indicate the 95 % confidence intervals of the regression models. The arrows indicate the maxima of the quadratic models at 21.48 years (C) and 24.71 years (D) of age.
A: Baseline-corrected amplitude of the theta frequency band.
B: ITC of the theta frequency band.

Target and non-target stimuli

Event-related spectral perturbation

Displayed on the left of Figure 68A is the baseline-corrected theta ERSP for target trials as a course over time, showing an increase upon stimulus appearance and peaking after 352 ms at electrode FCz. In Figure 68B, the ERSP is shown as a topological plot with maximal distribution over fronto-central brain areas.

Regression analysis revealed a significant increasing linear age trend (p = .0045), depicted in Figure 68C.

By contrast no effect with age was found for the ERSP of the non-target trials (p = .8730), plotted in graph D.

Inter-trial coherence

The ITC for the theta frequency band is displayed on the right side of Figure 68. In A to C, the ITC is displayed for target trials as line, topological and scatter plot, respectively. Upon stimulus appearance, the ITC strength increases until its peak at 220 ms at electrode FCz.

The increased signal is distributed over fronto-central brain areas as well as on the left and right side of occipital areas.

In comparison to a linear age effect, both for target (p = .2565) and non-target trials (p = .2596), no significant age related effect could be found, as depicted in Figure 68C and D, respectively.

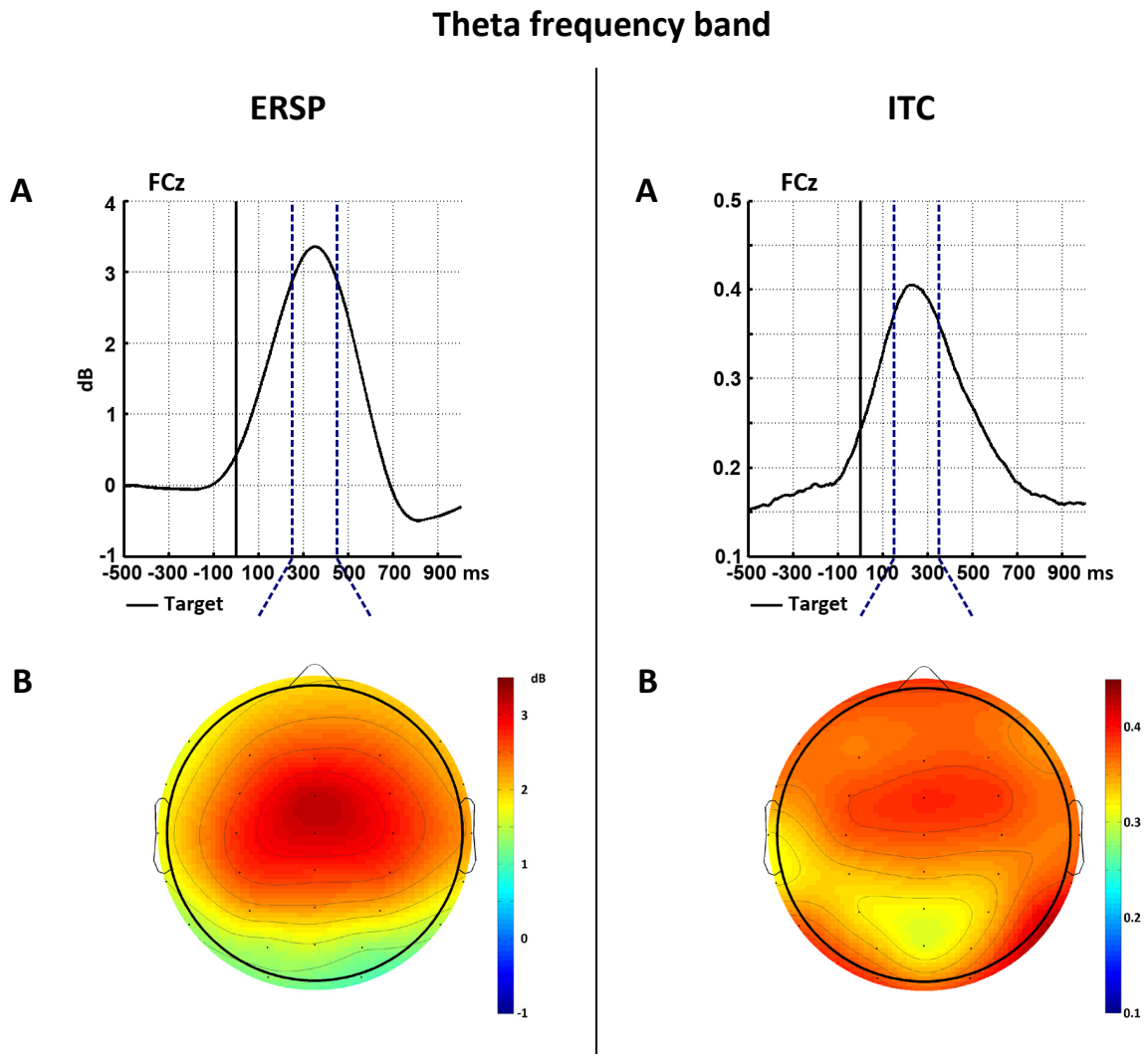

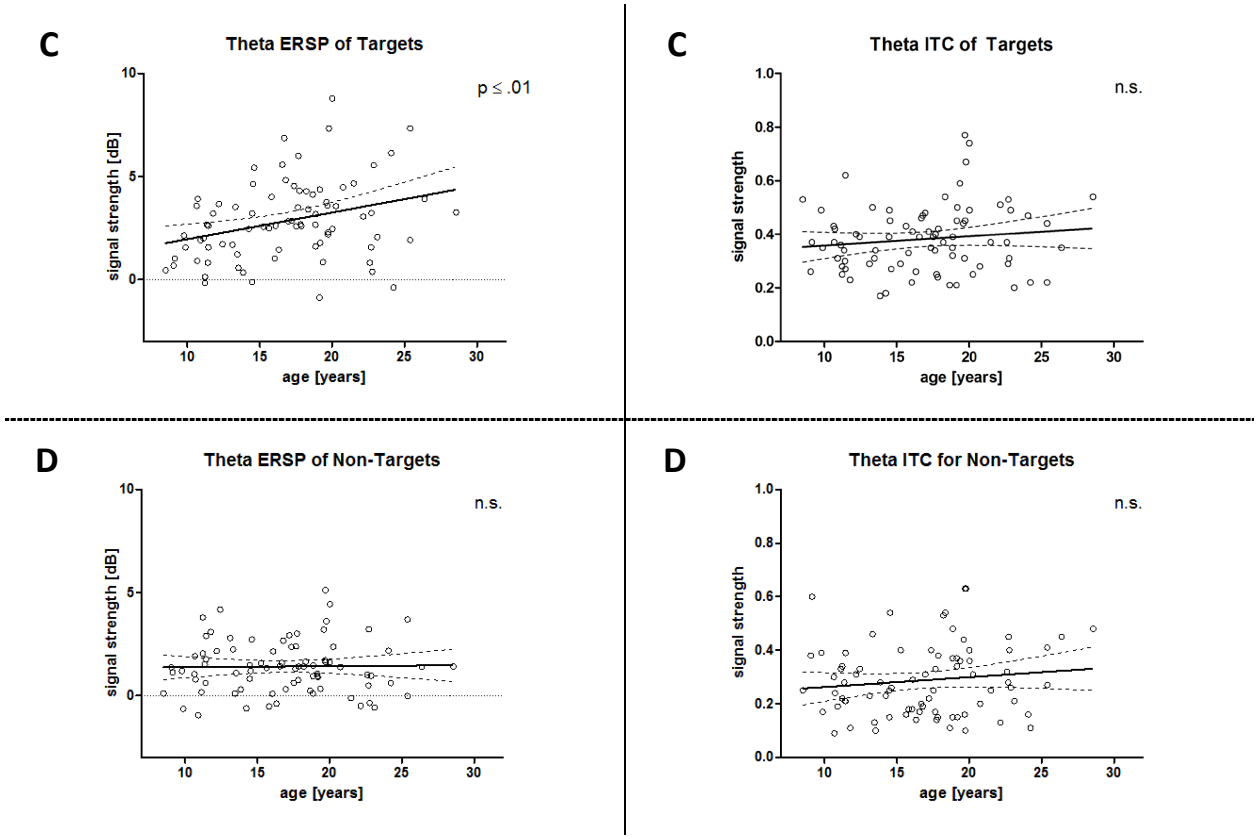

Figure 68: Overview of time-frequency analysis for the novelty oddball task for target stimuli. Each condition is displayed averaged over all participants; top as a line plot with blue lines indicating determined time window and below as a topological plot during this time window. Plotted below is a linear regression of the age-dependent signal strength averaged over the ROI for the target stimuli and of non-target stimuli (at the bottom) during the given time window with key indicators of regression analysis. Dashed lines in graphs C and D indicate the 95 % confidence intervals of the regression models.

A: Baseline-corrected amplitude of the theta frequency band.

B: ITC of the theta frequency band.

Table 19: Description of best-fit regression models for the data of the delta and theta frequency bands for all three stimulus types of the novelty oddball task.

Novel	condition	Model	F-value (df)	B0	B1	B2	Normality of Residuals	Runs-Test	R^2
Delta	ERSP	L	$_{(1, 77)}$ 36.6****	-.4	.3	-	3.7	n.s.	.3224
	ITC	L	$_{(1, 77)}$ 49.4****	.2	.0	-	2.9	n.s.	.3907
Theta	ERSP	Q	$_{(1, 76)}$ 13.4***	-8.3	1.3	.0	5.5	n.s.	.3984
	ITC	Q	$_{(1, 76)}$ 4.7*	-.2	.1	.0	6.2*	n.s.	.3633
Target									
Delta	AMP	Q	$_{(1, 77)}$ 26.1****	13.9	-.8	.0	1.9	n.s.	.7751
	ERSP	Q	$_{(1, 77)}$ 4.7*	-3.7	.8	.0	.2	n.s.	.1809
	ITC	Q	$_{(1, 77)}$ 4.1*	.3	.0	.0	9.0	n.s.	.0526
Theta	AMP	L	$_{(1, 78)}$ 100.4****	6.6	-.2	-	19.2****	n.s.	.5627
	ERSP	L	$_{(1, 78)}$ 8.6**	.7	.1	-	3.6	n.s.	.0989
	ITC	L	$_{(1, 78)}$ 1.3	.3	.0	-	7.4*	n.s.	.0164

Non-Target	condition	Model	F-value (df)	B0	B1	B2	Normality of Residuals	Runs-Test	R^2
Delta	ERSP	L	$_{(1, 78)}$ 8.1 **	-.3	.1	-	.2	n.s.	.0937
	ITC	L	$_{(1, 78)}$ 5.1 *	.2	.0	-	3.4	n.s.	.0612
Theta	ERSP	L	$_{(1, 78)}$ .0	1.3	.0	-	3.9	*	.0003
	ITC	L	$_{(1, 77)}$ 1.3	.2	.0	-	5.2	n.s.	.0162

n.s.: not significant, * $p < .05$, ** $p \leq .01$, *** $p \leq .001$, **** $p \leq .0001$.

3.2.3. Spatial phase coherence

3.2.3.1 Pre-stimulus interval

Figure 69 displays the spatial phase coherence of the theta frequency band, averaged for a time window before the appearance of target stimuli over age, for connections of fronto-central (A) and anterior-posterior (B) distribution.

Regression analysis revealed no relation with age for both FC ($p = .4530$) and AP ($p = .3129$) connections during the pre-stimulus interval.

The regression model for AP connections does not describe the data perfectly, as indicated by a non-Gaussian distribution of its residuals ($p = .0131$) and an uneven distribution of the data above and below the model ($p = .0027$).

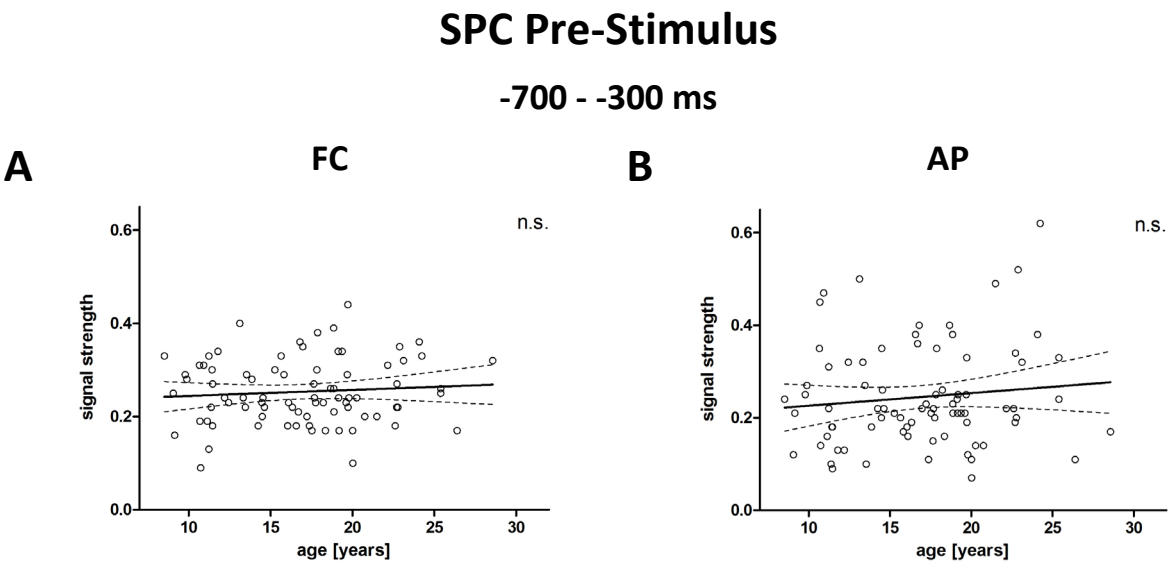

Figure 69: Best-fit regression models for the baseline-dependent spatial phase coherence of FC (A) and AP (B) connections from a frontal seed for theta oscillations during the pre-stimulus time window of -700 to -300 ms before presentation of target stimuli in the novelty oddball task. Dashed lines indicate the 95 % confidence intervals of the models.

3.2.3.2 Novel stimuli

On the top of Figure 70, the time course of the baseline-corrected theta SPC during novel trials, averaged for all participants, is displayed. Upon stimulus appearance, connectivity strength increases as a broad peak from approximately 220 to 420 ms. On the lower part of Figure 70, head plots show single connections averaged for the analysis time window and for connections of FC and AP range, separately.

Figure 71 depicts the regression analysis over age for both FC and AP connections. Rising linear regression models were fitting the data for FC (A; $p \leq .0001$) and AP (B; $p = .0055$). No difference between both regression models could be found ($F_{(2, 154)} = .1$, $p = .8661$).

Both regression models are not perfectly describing the data, as indicated by the model's residuals not being Gaussian distributed around the fit.

Regression models for the SPC of novel and target trials are described in further detail in Table 20.

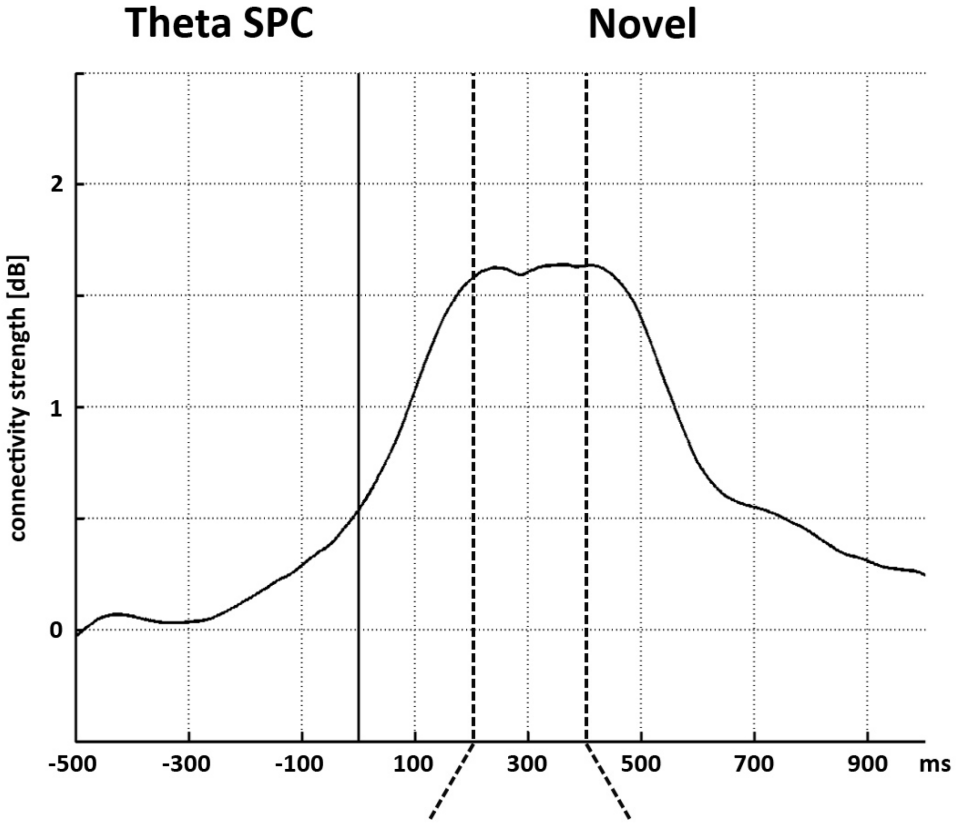
Theta SPC
Novel
connectivity strength [dB]
2
1
0
-500
-300
-100
100
300
500
700
900
ms

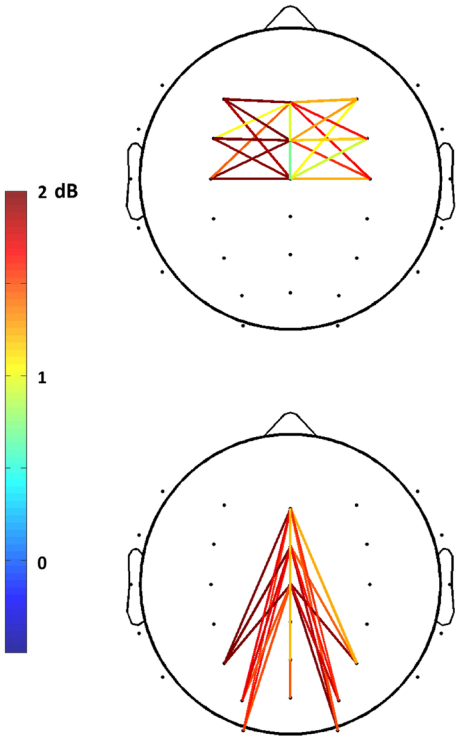

Figure 70: Top: Time course of spatial phase coherence of the theta frequency band averaged for fronto-central and anterior-posterior connections from a frontal seed (Fz, FCz and Cz; lateral electrodes and neighbouring electrode connections excluded) in relation to the baseline connectivity strength between -700 to -300 ms for novel stimulus presentation during the novelty oddball task. A vertical black line (0 ms) indicates stimulus onset. Dashed vertical lines display the analysis time window.
Bottom: Topological plots displaying single connections and their baseline-dependent spatial phase coherence are averaged over all participants for the time windows of 200 to 400 ms after the presentation of a novel stimulus in the novelty oddball task, separately. The top plot shows fronto-central connections only, while the bottom displays only connections from anterior to posterior. Connections are depicted by lines between electrodes (black dots). The colour bar indicates the cerebral connectivity strength, with warm colours representing stronger connectivity strength.

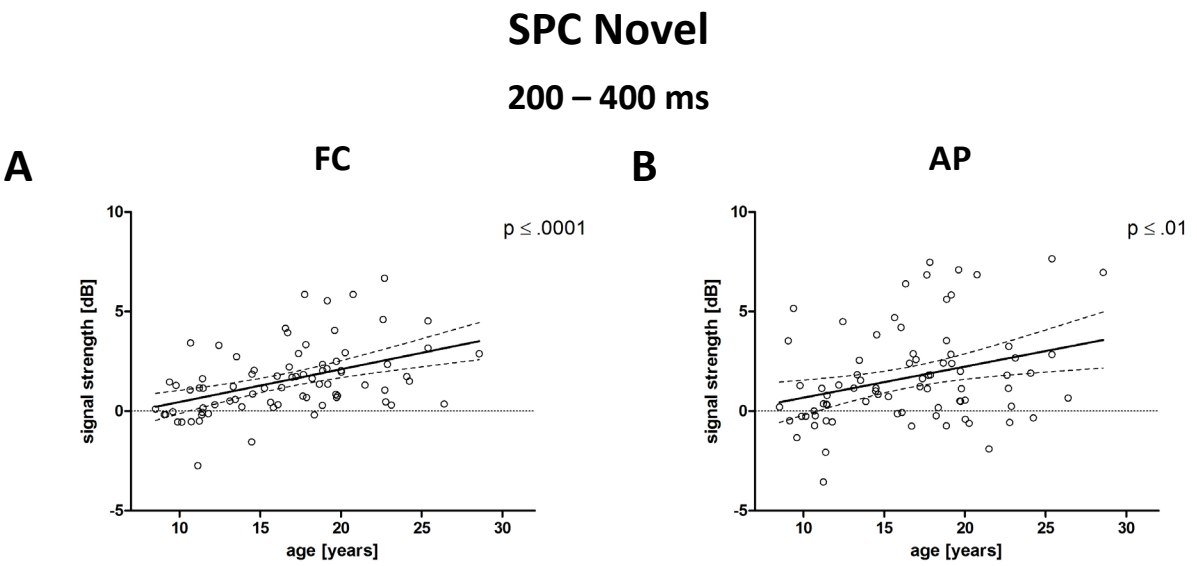

Figure 71: Best-fit regression models for the baseline-dependent spatial phase coherence of FC (A) and AP (B) connections from a frontal seed for theta oscillations in response to novel stimuli in the novelty oddball task, averaged over a time window of 200 to 400 ms. Dashed lines indicate the 95 % confidence intervals of the models.

3.2.3.3 Target stimuli

The baseline-corrected theta SPC of FC and AP connections averaged for target and non-target trials are displayed in the upper part of Figure 72. Upon target presentation, connectivity strength increases, reaching its maximum after 376 ms. Below in Figure 72, head plots show single connections for the analysis time window of maximal connectivity strength of 300 to 500 ms, separately for FC and AP connections of target trials.

Regression analysis revealed a significant concave quadratic age trend with an age peak at 18.52 years for theta SPC for FC connections (p =.0271) and for AP connections with an age peak at 17.97 years (p = .0482). The model for AP connections does not, however, describe the data perfectly, as indicated by the model's residuals not being distributed Gaussian-shaped around the fit. No difference between both regression models could be found ($F_{(3, 154)}$ = .1, p = .9441).

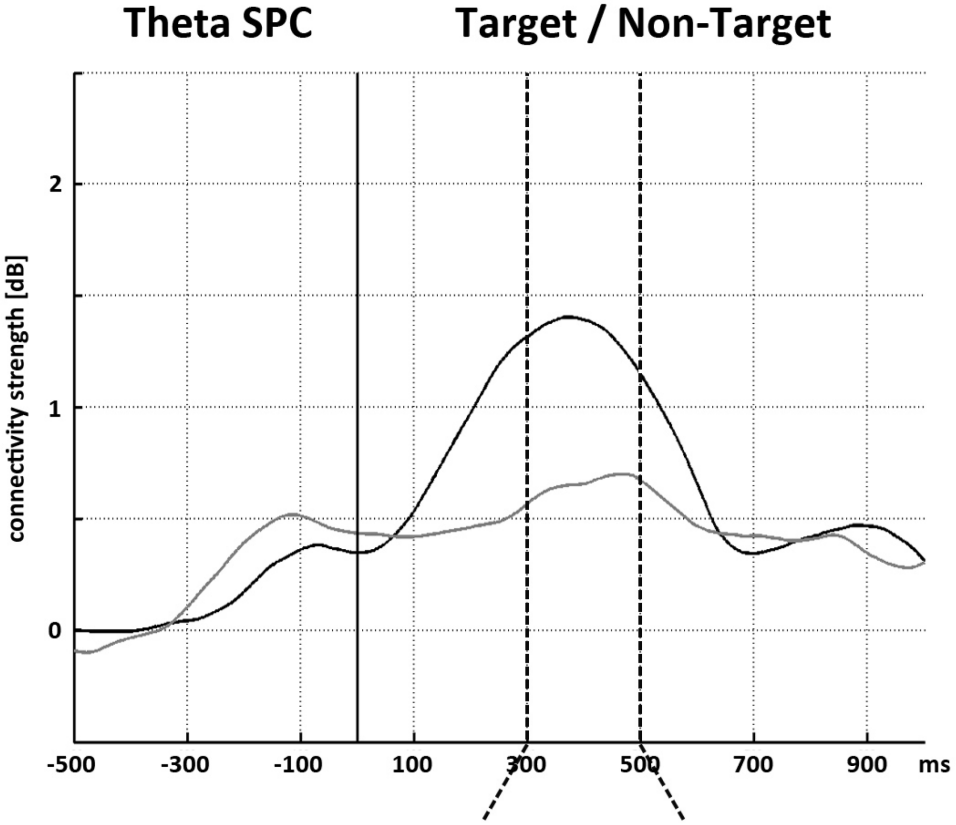
Theta SPC
Target / Non-Target
connectivity strength [dB]
2
1
0
-500
-300
-100
100
300
500
700
900
ms

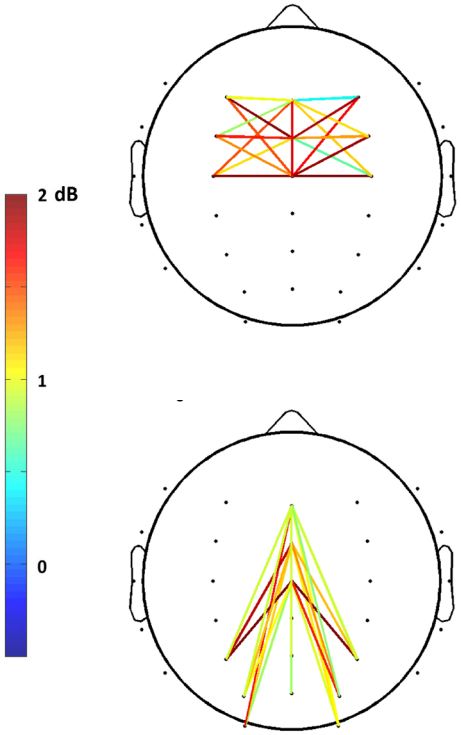

Figure 72: Top: Time course of spatial phase coherence of the theta frequency band averaged for fronto-central and anterior-posterior connections from a frontal seed (Fz, FCz and Cz; lateral electrodes and neighbouring electrode connections excluded), in relation to the baseline connectivity strength between -700 to -300 ms for target (black) and non-target (grey) stimulus presentation during the novelty oddball task. A vertical black line (0 ms) indicates stimulus onset. Two dashed vertical lines display the analysis time window.
Bottom: Topological plots displaying single connections and their baseline-dependent spatial phase coherence averaged over all participants 300 to 500 ms after the presentation of a target stimulus in the novelty oddball task. The top plot shows fronto-central connections only, while the bottom displays only connections from anterior to posterior. Connections are depicted by lines between electrodes (black dots). The colour bar indicates the cerebral connectivity strength, with warm colours representing stronger connectivity strength.

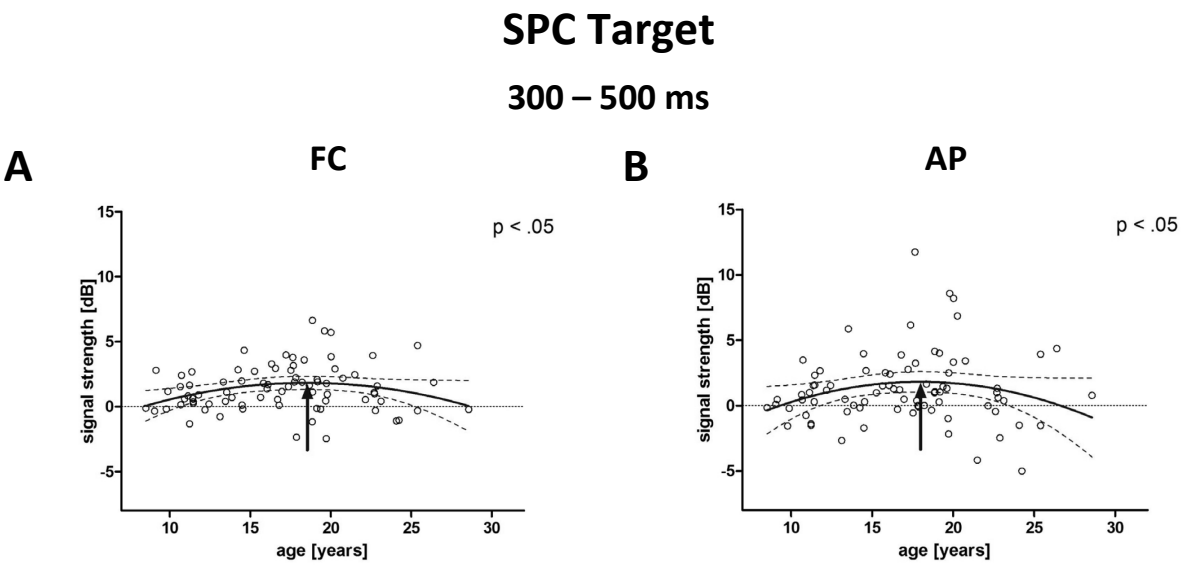

Figure 73: Best-fit regression models for the baseline-dependent spatial phase coherence of FC (A) and AP (B) connections from a frontal seed for theta oscillations, in response to target stimuli in the novelty oddball task, averaged over a time window of 300 to 500 ms. Dashed lines indicate the 95 % confidence intervals of the models. The arrows indicate the maxima of the quadratic models at 18.52 years (A) and 17.97 years (B) of age.

Table 20: Description of best-fit regression models for the baseline-dependent spatial phase coherence of the theta frequency band of FC and AP connections from a frontal seed upon the appearance of novel and target stimuli in the novelty oddball task.

Stimulus	Time window [ms]	Distribution	Model	F-value (df)	B0	B1	B2	Normality of Residuals	Runs-Test	R^2
Pre-Stimulus	-700 - -300	FC	L	$^{(1, 78)}$ .6	.2	.0	-	1.0	n.s.	.0072
		AP	L	$^{(1, 78)}$ 1.0	.2	.0	-	13.7**	**	.0131
Novel	200 - 400	FC	L	$^{(1, 77)}$ 20.6****	-1.2	.2	-	8.5*	n.s.	.2107
		AP	L	$^{(1, 77)}$ 8.2***	-.9	.2	-	6.1*	n.s.	.0958
Target	300 - 500	FC	Q	$^{(1, 77)}$ 5.1*	-4.2	.7	.0	n.s.	n.s.	.0742
		AP	Q	$^{(1, 77)}$ .5*	-6.0	.9	.0	22.2****	n.s.	.0529

n.s.: not significant, * $p < .05$, ** $p \leq .01$, *** $p \leq .001$, **** $p \leq .0001$.

4. Discussion of results

In the following, the results of study II are discussed in detail. Results that are comparable to the findings of study I are not described. Differences between both studies result from the introduction of a third stimulus category (novel stimuli) and due to adaption of task difficulty to individual abilities. The latter affects behavioural performance and influences the P3b component to target stimuli. Both aspects are discussed in the subsequent section. Developmental brain changes measured during novelty processing are discussed subsequently.

A combined discussion emphasizing the results from both studies can be found in SECTION IV.

4.1. Adaption of task difficulty to individual abilities

4.1.1. Behavioural data

One difference between study I and II was the adaption of task difficulty to individual abilities and hence, simplifying the task for younger participants.

No age related effect was found for error rates. Task difficulty, thus, was successfully adapted to individual abilities (see 2.2). This was done in order to correct for an age dependent error rate to ensure individual task feasibility.

Nevertheless, reaction times decreased with age slowing until an age of 20.64 years. This observation indicates latency decreases of response behaviour with age to be a quite robust

parameter of development independent of task difficulty. A deceleration between perception and action is thereby indicated. A general trend of reduced RT with age is in line with and well established in across a variety of tasks literature (Blakemore & Choudhury, 2006).

4.1.2. EEG data

4.1.2.1 Target P3b component

Similar to study I, no relation with age was revealed for P3b amplitude. P3b latency, in contrast, exhibited a decreasing effect with age in study I, but no relation with age in study II. Developmental differences affecting the P3b latency seem to be compensated by the adaption of task difficulty to age.

As described before, given P3b amplitude may reflect target expectancy and P3b latency stimulus evaluation time during an oddball paradigm (Picton, 1992; Strüber & Polich, 2002; Twomey, Murphy, Kelly, & O'Connell, 2015). Our results imply that in regard to this concept, adaption of task difficulty affected stimulus evaluation time.

Especially for children and young adolescents, differences between the stimulus categories target and non-target were increased simplifying stimulus differentiation. This facilitated stimulus evaluation processes enabling faster target detection.

Neuronal speed

As described prior, P3b latency is suggested to reflect speed of neuronal processing (e.g. Courchesne, 1978b; van Dinteren et al., 2014b). Our results imply that during development, limits of neuronal speed can be compensated by lowering task demands.

Cerebral processing capacities

Taken together processing capacities seem to evolve with development. The attentional resource allocation model described the relation between P3b amplitude and latency. If the task design is adapted to age-related capabilities of attentional resource capacity younger participants are able to produce similar P3b response component characteristics. However, this does not exclude developmental differences underlying P3b generation.

P3b latency and RT

Changes in task design mainly affected P3b latency, but the decreasing trend of RT with age was preserved. This implies that P3b latency and RT do not represent equal aspects in development. Stimulus evaluation time, neuronal speed and processing capacities are not the only factors accounting for decreased reaction time of younger participants. Together, these findings may indicate a slowed implementation of response related motor activity, or an increased uncertainty about the correctness of response, or a decelerated motor response accounting for decreases of RT.

Summary

Taken together, our results of study II support the idea of developmental dissociation of the two cognitive abilities, target expectancy and stimulus evaluation, during adolescence. In addition, task difficulty affects especially the associated cognitive processes of younger participants. A mature human brain's efficiency is reflected by its ability to accomplish difficult tasks while still assuring speed and accuracy of required responses.

4.1.2.2 Frontal theta oscillations elicited by targets

In study I, an increasing developmental trend for theta phase-locking upon target processing was observed. By contrast, in study II, no relation between theta phase-locking and age could be found for target processing. Adaption of task-demands to individual abilities indicates that theta phase response timing is able to work on adult level already at early adolescence, albeit for increased task-difficulty deteriorations on behavioural level arise for younger participants.

Interestingly, theta SPC for target processing also differed between study I and II. Theta SPC increased linearly with age for both, FC and AP connections, indicating its general protracted maturation during study I. This increase, however, accelerated during adolescence (with a peak at approximately 18 years), possibly indicating the specific nature of the adolescence in life (see also SECTION IV.2) and the specific challenges in this age period to focus on targets when distractors may interfere.

Theta oscillations have been associated with signal detection (Basar-Eroglu et al., 1992; Basar-Eroglu & Demiralp, 2001; Mathes et al., 2014). Simplification of discrimination between target and non-target might have facilitated signal detection for younger

participants. This emphasizes the importance of theta phase-locking for signal detection and its sensitivity to task-demands during development.

4.2. Processing of novel stimuli

4.2.1. Event-related potentials

4.2.1.1 The novelty N2 complex

The N2 is a commonly observed component in tasks requiring focused attention to stimuli and cognitive control. The N2 complex has been observed in a variety of tasks. Results indicate the existence of several N2-like components, which are assumed to reflect divergent cognitive processes and asses deviating cerebral sources (for a review see Folstein & van Petten, 2008). The three stimulus categories in the novelty oddball task may elicit three variations of the N2 (Bocquillon et al., 2014). In the course of this thesis, only the anterior N2 upon novelty stimulus presentation was further investigated. The novelty N2 possess a frontal distribution as frontal brain areas connected to the FPN play a major role in the related attentional and cognitive control processes upon novel stimulus occurrence (Folstein & van Petten, 2008). Developmental effects reflected in the novelty N2 are expected due to the immature frontal cortex in adolescence.

The novelty N2 latency declined with age that slows towards approximately 17 years, in parallel the magnitude of the N2 amplitude decreased linearly with age.

Developmental studies investigating novelty processing with an oddball task and reporting maturational changes of the N2 complex are scarce, albeit Courchesne already observed maturational differences regarding novelty oddball N2 amplitude in 1978 (Courchesne, 1978b).

N2 amplitude

The high inter-individual variability depicted in Figure 62 indicates that until approximately 13 years of age the occurrence of the N2 and P3a during novelty processing was inconsistent. The N2 occurred prior to the P3a component and had a fronto-central maximum.

Over the age range, a maturational impact on the N2 amplitude was indicated by a linearly decreasing magnitude with age. Similar to our results, Courchesne (1978b) reported a large N2-like response characterizing the ERP in young children (age 6 – 8 years) upon novel processing, which was not as prominent for adults. He suggested an age-related difference in processes corresponding to content evaluation of unexpected deviant events.

Attentional processing

Developmental changes of the novelty N2 might be associated with immature attentional processing. As reviewed by Folstein and van Petten (2008), a fronto-central N2 in a visual novelty oddball task seems to be sensitive to the degree of perceptual deviation of novel stimuli in contrast to target and non-target stimuli rather than to task difficulty. Further, the N2 is increased through complexity of novel stimuli (Daffner, K. R., Mesulam, et al., 2000). Saliency of novel stimuli is generally higher for rare and unexpected events and is either based on its high unfamiliarity or of its great difference to frequently presented stimulus categories; thus, from deviance in long-term or short-term context, respectively (Folstein & van Petten, 2008). The N2 may therefore reflect increased attentional processing due to interference of strongly salient novel stimuli (Bocquillon et al., 2014).

Novel stimuli represent strong mismatch or deviance in the sequence of target and non-target stimuli in regard to their physical appearance and, hence, imply conflict between the rarely presented novels and stored representations or templates of frequently presented stimuli. The N2 could therefore reflect mismatch detection (Falkenstein, 2006; Folstein, van Petten, & Rose, 2008; Polich, 2007).

Further, the N2 is discussed in the context of orientation (Friedman et al., 2001; Halgren et al., 1995; Knight, R. T., 1984; Snyder & Hillyard, 1976) and Suwazono et al suggested the novelty N2 to reflect a “general alerting system” (Suwazono, Machado, & Knight, 2000, p. 38). The orienting response is attributed to an involuntary focus of one’s attention to novel, unexpected events (Sokolov, 1963). Orientation and mismatch detection might reflect similar, not distinguishable processes (Folstein & van Petten, 2008). This attention system assessed for novelty processing might not yet have reached maturity by adolescence, which could be accompanied by slower and stronger activation reflected in the N2.

Involvement of the ACC

Studies indicate an involvement of the anterior cingulate cortex (ACC) in mediation of the N2 (Bocquillon et al., 2014; Kropotov, Ponomarev, Hollup, & Mueller, 2011; Wessel, Danielmeier, Morton, & Ullsperger, 2012). Upon stimulus presentation, the ACC is suggested to be necessary for increasing attentional resources in order for an implementation of a following stimulus categorisation (Bocquillon et al., 2014). Already in 1998, Badgaiyan and Posner assumed the involvement of the ACC in cognitive control for tasks with competing stimuli (Badgaiyan & Posner, 1998). In addition, the superior and medial frontal lobes seem to be involved in generation of the N2 (Bocquillon et al., 2014). Both are part of the fronto-parietal attention network indicating the network's role in stimulus evaluation.

Consequently, age-related differences in N2 complex might relate to differences in attentional processes and/or processing capacities and an immature fronto-parietal network. Further, the ACC might play a role in maturational processes reflected in the N2 amplitude during adolescence.

Inhibitory control as a cognitive control function

N2 amplitude decrease over adolescence may reflect a more efficient inhibitory control system with age, which is also discussed in regard to other cognitive tasks (cf. Casey et al., 2000).

Cognitive control composes of two aspects: interference suppression and response inhibition. Children are known to be more susceptible to interference and less able to inhibit responses than adults as cognitive control develops gradually over childhood. While generally cognitive control is associated with prefrontal areas for adults (Kawashima et al., 1996; Ridderinkhof, van den Wildenberg, Segalowitz, & Carter, 2004; Rubia et al., 2001), both aspects of control are processed by more posterior cortical regions in children indicating immature prefrontal brain areas and suggesting the PFC as limiting factor for the development of cognitive control (Bunge, Dudukovic, Thomason, Vaidya, & Gabrieli, 2002).

With increasing age, maturation of frontal brain areas enables better focus of attention in order to reduce novel processing minimizing the distracting effect of novel stimuli and hence, minimizing the active processing (Amso, D. & Scerif, 2015; Crone, 2009). This process is likely not reached through active inhibitory processes and is not linked to motor inhibition in order to supress the urge of a button press, as tasks demanding this control elicit a different kind of N2 complex (Folstein & van Petten, 2008). It rather reflects a general

tendency for a more focused attention on task demands related to inference suppression (Braver et al., 2001; Chan et al., 2008; Coderre et al., 2011; Niendam et al., 2012). The resulting minimization of orientation towards novel stimuli might be reflected in the decreasing N2 amplitude with age.

Remembered animals

In line with the argumentation that children and young adolescents seem to allocate more attention to novel stimuli and show a higher rate of stimulus processing, younger participants in this study stated to remember several novel stimuli. Older participants rather stated they had masked out the stimuli and thus, are not able to name the presented animals. However, this effect was not assessed and could therefore not be quantified in this study.

N2 Latency

In this study, N2 latency decreased over adolescence exhibiting a slowing tendency towards adulthood. Up to date, no study describing developmental trends for N2 latency upon novel stimulus presentation were found. However, a general developmental decreasing tendency of N2 latency for target N2 and N2 in the Go/NoGo task have been reported (Johnstone, Pleffer, Barry, Clarke, & Smith, 2005; Lewis, Lamm, Segalowitz, Stieben, & Zelazo, 2006; Tsai et al., 2012).

In parallel to P3a and P3b latency decrease, a tendency of N2 latency decrease over childhood and adolescence might reflect increasing neuronal speed and efficiency as underlying processing networks mature.

Summary

These data support the view that the novelty N2 amplitude and latency are affected by brain development during childhood and into adolescence. Immature attention system and hampered neural speed might cause these developmental differences of the N2.

4.2.1.2 The P3a component

Novel stimuli that occurred rare and unexpected within a stimulus sequence elicited a P3a component. The P3a occurred earlier and with larger amplitude than the P3b elicited by targets at fronto-central electrode sites (cf. Friedman et al., 2001; Polich, 2007; Polich &

Criado, 2006). The P3a topography may vary with stimulus and task design (Conroy & Polich, 2007; Courchesne, 1978b; Cycowicz, Friedman, & Rothstein, 1996) and may result in a parietal maximum, as found in our study (Bocquillon et al., 2011; Ferrari et al., 2010; Hagen et al., 2006; Oades et al., 1997).

Friedman et al. (2001) identified a frontal and a parietal activation to underlie the P3a upon presentation of novel stimuli. The frontal P3a-like aspect was associated to orienting, whereas the posterior aspect might play a role in categorization of new stimuli (cf. Courchesne, Hillyard, & Galambos, 1975).

Polich (2007) proposed that the P3 is composed of two subcomponents, which contribute to greater extent depending on stimulus category: Novel stimuli elicit a P3 with enhanced P3a aspect, albeit incorporate a posterior aspect. With repetition of the same novel stimuli within one experimental run the novelty P3 shifts to parietal brain areas, while the frontal amplitude decreases. This shift might reflect the formation of a new stimulus category, which is then assessed for stimulus comparison upon representation in order for rapid stimulus classification. By contrast, presentation of novel stimuli that are not repeated within on experimental run impedes stimulus classification demanding the contribution of frontal brain areas (Friedman et al., 2001).

The manifestation of the frontal P3a has been shown to also relate to the discrimination difficulty between target and non-target stimuli. This might indicate an indirect relation of available attention resources to the contribution of frontal brain regions to novel processing Polich (2007).

The variation in brain topography of the P3a elicited by novel stimuli may, hence, be explained by the contribution of an anterior and posterior subsystem and depends on the overall experimental design.

Two P3a sub-components in time: The early and the late P3a

Further, in some studies the P3a was suggested to consist of two subcomponents in time, an early and a late part and was found for novel stimuli of the auditory modality (Brinkman & Stauder, 2008; Čeponienė et al., 2004; Escera et al., 1998; Flores, Goméz, & Meneres, 2010; Segalowitz & Davies, 2004). In the study of Escera et al. (1998), auditory stimuli were presented in a passive manner (no reaction to stimulation was requested). The early P3a reached its peak around 200 – 250 ms after auditory novel presentation in adults and was maximal over fronto-central brain areas. The late auditory P3a peaked around 250 – 300 ms

and exhibited a more anterior to the early P3a. The early P3a was suggested to reflect automatic detection of stimulus irregularity and is relatively insensitive to attentional manipulations (Escera et al., 1998; Yamaguchi & Knight, 1991). The late P3a is enhanced by attention and habituates due to stimulus repetition. The late P3a may reflect the actual attention switch of conscious awareness towards the stimulus (Courchesne, 1978a; Cycowicz & Friedman, 1997; Escera et al., 1998).

Results indicate a maturation of early P3a by early adolescence, while the late P3a seems to continue maturation. The late P3a seems to still lack frontality, a characteristic in adults, in in the late phase of childhood (Čeponienė et al., 2004; Escera et al., 1998).

In this study, no separation between early and late P3a component were investigated for our visual novel stimuli. Only presentation of auditory novel stimuli seems to elicit separate early and late P3a components. Auditory processing takes place on a faster scale compared to visual processing (Kihara et al., 2010) and might, hence, lead to the dissociation between these two sub-components indicating that, concordantly, two sub-processes underlie P3a generation. Due indication of delate maturation for the late P3a component in auditory processing, this might also account for visual processing and would indicate, that especially the aspect of the attention switch and conscious awareness towards novel stimuli continues to mature.

Maturation of the P3a

Indicated by negative mean P3a amplitudes until approximately 15 years of age depicted in Figure 60, younger participants elicited an inconsistent P3a component. Between approximately age 13 to 15 years a large N2 complex was pulling the signal towards the negative and hence, interspersing the P3a component and making it difficult to analyse it due to its resulting small size.

Several studies reported similar findings: Segalowitz and Davies (2004) also reported inconsistent P3a patterns until an age of 13 years in their auditory novelty oddball task. Courchesne (1983) described the P3a to be too small to distinguish it from noise in seven year olds in a visual paradigm. Oades et al. (1997) reported a large N2 in children to intersperse into the P3a component. By contrast, several studies could detect a P3a component already in young children (e.g. Courchesne, 1978b; Kihara et al., 2010), albeit entailing inconsistency of the direction of maturational P3a trends.

Our results indicated an increase of P3a amplitude with age during adolescence. This finding is in line with several studies in literature (e.g. Cycowicz & Friedman, 1997; Kihara et al., 2010; Oades et al., 1997). Some studies, however, found a large P3a component decreasing with increasing age for childhood and adolescence (Courchesne, 1978b, 1983; Stige et al., 2007).

Variations in task design and modality might account for different findings for the P3a amplitude. Similar, they might account for differences in evocation of novelty N2, which intersperses with the P3a to an altered amount during development. The pattern of a decreasing N2 and increasing P3a amplitude in children and young adolescents may reciprocally obscure developmental changes of these ERPs (cf. Oades et al., 1997). The ambiguities regarding N2 and P3a development demonstrate the need for further investigation, moreover looking at the level of concurrent EROs. These issues are further addressed in the following section 4.2.1

The N2-P3a complex

Cognitive processes underlying the P3a component are likely to be related to and intermingled with the novelty N2 suggesting a unified novelty N2-P3a complex (Brinkman & Stauder, 2008; Daffner, K. R., Mesulam, et al., 2000; Daffner, K. R., Scinto, et al., 2000).

Upon novel stimulus presentation, an initial orienting response to the deviant stimulus is induced. As also described before (section 4.2.1.1), this attention driven process is suggested to be reflected in the novelty N2. The subsequent top-down attention shifting is associated with the P3a component and may indicate the actual distraction (Courchesne, 1978b; Escera et al., 1998; Friedman et al., 2001; Gumenyuk et al., 2001; Polich, 2007).

However, a separation between both processes is not clear (Brinkman & Stauder, 2008). The orienting response as an involuntary attention allocation is discussed to relate to both processes and is, thus, also discussed in regard to the P3a component (Cycowicz & Friedman, 1997; Debener et al., 2005; Friedman et al., 2001).

Both N2 and P3a are associated with cognitive control functions related to an attention control system (Conroy & Polich, 2007; Daffner, K. R., Scinto, et al., 2000). This system is strongly associated with frontal brain areas involved in the FPN and generators both for N2 and P3a are, thus, found within the frontal cortex (Bocquillon et al., 2011).

The mediation of novelty N2 is suggested to evolve from activation in the ACC (Bocquillon et al., 2014; Kropotov et al., 2011; Wessel et al., 2012). The ACC likely is involved in increasing attentional resources towards a presented stimulus, especially upon novelty stimuli (Bocquillon et al., 2014).

The P3a is associated with activity of the prefrontal cortex (Cycowicz & Friedman, 1997; Folstein & van Petten, 2008). Lesion studies demonstrate the importance of frontal brain areas for P3a generation upon novel processing (Daffner, K. R. et al., 2003; Knight, R. T., 1984).

As described earlier (in the theoretical introduction and section 4), frontal brain areas play a critical role in cognitive control functions. Especially attention control is critical for novel stimulus processing and demands the prefrontal cortex (Daffner, K. R., Scinto, et al., 2000; Knight, R. T., 1984). Further, the prefrontal cortex is suggested to be involved in formation of a working memory template upon repeated stimulus presentation, which can then be processed in more parietal brain areas. After template formation stimulus processing relies more heavily on parietal brain areas. This explains the habituation effect of a P3a towards a P3b upon stimulus repetition explained above (Cycowicz, 2000).

Since the P3a reflects frontal brain functions, developmental effects found for the P3a amplitude may reflect immaturity of the frontal cortex (e.g. Čeponienė et al., 2004; Cycowicz et al., 1996; Flores et al., 2010). Increasing P3a amplitude with age might reflect an increase in activity of an attentional control system related to prefrontal brain areas inhibiting the shift of attention towards distractor stimuli. This is in line with the conclusion Segalowitz and Davies (2004), Wetzel, Widmann, Berti, and Schroger (2006) and Wetzel, Schroger, and Widmann (2016) drew from their studies of children paying more attention to distractor stimuli. Further, Lackner, Santesso, Dywan, Wade, and Segalowitz (2013) suggested that the ability to disengage attention from distractors during early stimulus processing is also related to executive functioning abilities, while executive functions continue to mature into young adulthood. Thus, both the shift of attention towards and the disengagement of attention from distracting stimuli might not have reached mature level in children and young adolescence being reflected in reduced P3a amplitude.

Opposing maturational trend of N2-P3a complex

The novelty N2 and the P3a seem to follow an opposing maturational trend. With increasing age the novelty N2 decreases while the P3a increases. As cognitive processes underlying the

N2-P3a complex are strongly related, an increased novelty N2 might reflect a compensatory mechanism for immature P3a-related cognitive functions. By contrast, immature frontal lobes might lead to the assessment of different cognitive strategies in younger participants leading to differences in the N2-P3a complex. The N2-P3a complex, thus, might reflect variation in maturity of causal brain regions and/or reflect different forms of cognitive strategy assessed for novelty processing.

P3a latency

In this study, P3a latency decreased with increasing age into young adulthood. This is in line with findings from across a variety of studies (Courchesne, 1978b; Cycowicz et al., 1996; Oades et al., 1997; Ponton, Eggermont, Kwong, & Don, 2000), albeit also Stige et al. (2007) reported an increase of P3a latency with age. The cross-sectional life span study of Stige et al., however, applied a linear regression analysis from childhood to old age. The data indicated no age related changes of P3a latency when observed over childhood and adolescence, only.

Similar to P3b and N2 latency decrease with age described before (SECTION II.4.2.1.1 & 4.2.1.1), P3a latency decrease is associated with improvements of neuronal speed and efficiency due to maturation of underlying brain networks (e.g. Courchesne, 1978b; Oades et al., 1997).

Summary

Changes in P3a amplitude and latency reflect maturation of the brain during adolescence. A larger P3a component with earlier onset with age at frontal brain areas might reflect an increasing involvement of the frontal cortex in novelty processing and might reflect maturation of frontal lobes during adolescence and into young adulthood. Similar cognitive processes seem to correlate to the novelty N2 suggesting also similarities in developmental processes underlying age related changes of the novelty N2. Consideration of a unified N2-P3a complex in developmental investigations taking into account the distinct developmental trajectories for N2 and P3a activation pattern separately is suggested.

4.2.2. Event-related oscillations

The involvement of slow-wave oscillations to the P3a component are reflected by their similar timing, modulation patterns and distribution as reported in literature (Isler et al., 2008; Prada et al., 2014).

In general, increases of amplitude modulation and precision in timing of delta and theta oscillations over development were observed in this study. Up to date, not many studies investigating developmental changes in slow-wave oscillations during novelty processing can be found. Similar to the results of our study, Müller et al. (2009) reported a general increase of phase-locking of slow-wave oscillations for an age range from 9 to 13 years compared to young adults for the processing of novel sounds in a passive oddball design (no target stimulus). However, opposite to our findings, he observed a simultaneous decrease of slow-wave power compared to baseline-activity.

Delta oscillations

The pre-stimulus amplitude of delta activation decreased with age slowing towards approximately 25 years of age. Upon target processing, delta ERSP increased with age until slowing at approximately 22 years of age. Delta ITC increased in a linear fashion with age. For non-target trials ERSP and ITC slightly increased with age. During novel processing, delta ERSP and ITC followed an increasing linear age trajectory.

The delta pre-stimulus amplitude was maximal at central electrode sites, while post-stimulus amplitude and ITC were maximal over posterior electrode sites for target processing and centrally located for novel processing. The time window of maximal response to target stimuli matched the time window of the P3b component for amplitude, while for ITC occurring 100 ms earlier in time. Maximal delta amplitude and ITC response during novel processing occurred 50 to 100 ms earlier than the P3a component.

Prada et al. (2014) and Isler et al. (2008) found enhanced delta oscillations with increase phase synchronization co-occurring with the P3a response to be associated with attentional processing of novelty. Delta oscillations have been associated with the assessment of contextual novelty, which includes detection of distracting stimuli and novelty upon introduction of new task rules.

The P3a has been related to an orienting response towards novel stimuli (Friedman et al., 2001). Isler et al. (2008) concluded from their results that especially delta oscillations, both

increased power and phase-locking, play an important role in the orienting response. Global synchronization of delta combined with more local phase-coupling to higher frequencies might reflect a mechanism for involuntary bottom-up attention capture during the orienting response.

Given the enhanced distractibility in children and young adolescents reported in literature, decreased delta oscillations might not reflect a decreased orienting response. Studies indicate that novel stimuli are recognized by children to great extent (Heim & Keil, 2012; Isler et al., 2008; Prada et al., 2014). Our study did not assess the degree of recognition of novel stimuli. Upon interrogation, young participants stated to remember several novel stimuli in contrast to older participants. A systematic follow-up study is required for investigation of this issue.

Even though task-related delta activation is reduced in children and young adolescents an attention capture of novel stimuli is, thus, suggested and, indicated by greater their distractibility, might even be stronger than for older participants. Our findings of increasing delta activation with age might, therefore, reflect a general difference in novel processing, which might base on differences in the neuronal mechanisms underlying attention capture during the orienting response towards novel stimuli.

Theta oscillations

Pre-stimulus amplitude of theta oscillations decreased linearly with age. During target processing theta ERSP increased with age, while ITC was not related to age. Non-targets processing exhibited no relation with age for theta oscillations. Theta ERSP and ITC during novel processing followed an increasing age trajectory peaking at approximately 21.5 years for amplitude and at 25 years for ITC. The theta activation was maximal over fronto-central electrode sites pre- and post-stimulus. The time window of maximal response of theta ERSP matched the P3b time window, while the maximal theta ITC response occurred 150 ms earlier. Theta activation of novel processing co-occurred with the P3a component.

Prior to stimulus presentation theta SPC of FC and AP connections show no relation with age. Upon novel presentation, theta SPC increases similarly for FC and AP connections in a linear fashion with age. The time window of maximal response to novel stimuli reflects both ERSP and ITC of the theta frequency band. Theta SPC for target stimulus processing also increases with age; however, peaking at an age of 18.5 and 18 years for FC and AP

connections, respectively, followed by a slight decrease for ongoing age. The time window of maximal response to target stimuli matches the time window of theta ERSP activity.

Theta oscillations are related to attentional processes demanding the focus of attention (Buzsaki, 2005). Cognitive control is needed to focus attention especially in regard to distraction minimization needed in the novelty oddball task upon novel stimulus presentation. The FPN has been linked to control of attention (Amso, D. & Scerif, 2015; Dosenbach et al., 2008; Naghavi & Nyberg, 2005). Frontal theta oscillations are discussed as communication tool for the fronto-parietal network in cognitive control (Clayton, Yeung, & Cohen Kadosh, 2015). In this context, theta oscillations are not only related to the P3a component, but also the novelty N2 (Hajihosseini & Holroyd, 2013; Isler et al., 2008). In line, the enhancement of theta oscillations upon novel processing occurs slightly earlier in time than delta oscillations and also the P3a component found in our results and indicated by Müller et al. (2009).

With regard to the developmental trends revealed in our study, enhanced theta amplitude modulation and phase-locking upon novel processing with age might reflect inferior abilities of attention control at younger age linked to immature frontal brain areas.

Further, upon novel presentation, theta SPC increases linearly with age for FC and AP connections. In accordance with our results, Ehlers et al. (2014) reported fronto-parietal theta connectivity to be similar for target and novel processing. The time window of the maximal theta connectivity co-occurs with the maxima of frontal theta ERSP and ITC. The involvement of both local and global theta activity is, thereby, indicated for target detection and novel processing.

Summary

Slow-wave oscillations are involved in novelty processing and are likely to reflect attentional processes related to involuntary orienting towards distractors and attentional control to focus attention on proper task performance despite distraction. These processes are associated with wide-spanning brain network communication, in which frontal brain areas are thought to play a lead role. Decreased task-related slow-wave modulation and precision timing might reflect immaturity of these neuronal assemblies and our results indicate associated maturational changes reaching into young adulthood.

SECTION IV.

General discussion

Brain maturation is proposed to continue until the third decade of life (Paus et al., 2008). Adolescence may constitute a unique phase of enhanced brain plasticity in life as it entails the opportunity to adapt to growing cognitive challenges required for reaching independence as an adult (Amso, Dima, Haas, McShane, & Badre, 2014; Lourenco & Casey, 2013). The frontal cortex is among one of the last structures to mature during adolescence (Hedman et al., 2012; Sowell, Thompson, Holmes, Jernigan, & Toga, 1999). It plays a central role in an array of higher-order cognitive functions and its integration into brain-spanning networks leads to the advanced cognitive performance of the adult brain (Crone, 2009).

1. EEG-Data in perspective of maturational changes

1.1. Main outcome of study I & II

Children and young adolescents exhibited P3b components similar to adults. Using time-frequency analysis, however, major developmental changes of concurrent slow-wave oscillations in the delta and theta band could be revealed. With age, spontaneous EEG amplitudes of slow-oscillations decreased, while task-related amplitude enhancements increased and time precision, as indicated by trial-by-trial phase-consistency of the post-stimulus response, improved. Notably, these tendencies are diminished in non-targets. Therefore, increasing behavioural performance may be attributed to the maturation of task-related modulation of slow brain oscillations. Differentiation between linear and quadratic age trends revealed only minor differences between most measures. No quadratic trend reached its peak or trough before an age of 17.5 years, indicating prolonged brain maturation until early adulthood. This also indicates that brain maturation occurred in a continuous fashion until early adulthood; however, this may be different for higher frequency bands (Uhlhaas et al., 2009).

Pre-experimental adjustments of task demands between participants in study II enabled younger participants to perform with a similar error rate and response timing as adults during the main task. Consequentially, theta ITC did not change with age, although an age-related increase of theta ITC was detected otherwise (see study I). Adjusting task difficulty did not, however, eliminate the other developmental changes described above. These

results imply that throughout development, some cerebral mechanisms may already work on an adult-like level; however for adolescents, even these mechanisms seem to be less effective than in adults as they require a lowering of task difficulty. Furthermore, the developing brain does not reach adult levels of task-related brain modulation for all brain mechanisms when task demands are adjusted between participants.

In the time domain, precision of response timing increased with age. Lowering the task demands to account for lower individual abilities of younger participants enabled them to perform on adult levels for behavioural measures and response timing.

Furthermore, an impact of task demands on theta phase response timing could be detected, indicating that younger participants have the ability to elicit adult-like theta phase-locking when task demands are lowered.

The results imply that throughout development some cerebral mechanisms already work on an adult-like level for low task demands; however, the system is not functioning as effectively when tasks become difficult. On other levels, the developing brain is not able to compensate for immature neuronal circuits even for low task demands.

Occurrences of similar developmental effects in both studies I and II indicate the robustness of these findings. These findings also confirmed the age-group analysis of Mathes, Khalaidovski, et al. (2016), which are based partly on the same data as study I. Defining the ranges for age group analysis is, to some extent, arbitrary during adolescence. With increased sample size in this study, by contrast, advantageous regression analysis was feasible without the need of age group definition. The new analysis method further enabled better descriptions of age-related trajectories in brain changes, e.g., by the determination of deceleration, acceleration or linear consistency in developmental trends. Furthermore, expanding the age range allowed the investigation of not only the transition from adolescence into adulthood, but also the transition from late childhood into adolescence. In addition, data analysis was expanded by the incorporation of global measures for the maturation of brain networks. Additionally, study II introduced the opportunity to study the processing of novel stimuli in regard to developmental changes of the brain. Novel stimuli were hypothesized to play a major role in the maturation of the adolescent brain.

Taken together, the findings of studies I and II indicate cerebral development during adolescence, which leads to a general increase in the precision and efficiency of both local and global oscillatory network activity.

1.2. Development of brain oscillations in relation to brain structure

Up until now, a strong association has been suggested in the literature between the changes found in EEG measurements and the structural brain changes during development.

Pruning leads to a reduction of grey matter, meaning the elimination of unnecessary neurons and synapses (cf. Paus et al., 2008). A smaller number of neurons that fire together are associated with a reduction of slow-wave EEG power (Whitford et al., 2007)

Reduction of grey matter occurs in concert with an increase of white matter through the myelination of neurons, thereby facilitating faster signal transmission across brain regions (Giedd, 2004; Giedd et al., 1999; Paus, 2010). This process allows for faster reactions and more precise signalling especially on the level of phase response timing (Segalowitz, Santesso, & Jetha, 2010).

Our findings support the general idea of the reduction of unnecessary synapses, which is indicated by the reductions of pre-stimulus delta and theta amplitudes combined with increased signalling speed and precision during development. The latter is indicated by an increase in post-stimulus amplitude power, ITC and coordination of the frontal cortex with other brain regions, as well as decreasing the latency of late cognitive ERP components. On the behavioural level, task performance improves and reaction times decrease with age.

Overall, structural changes enable brain plasticity and thereby create the opportunity for enhanced learning. The structural changes of the brain augment processing speed, response consistency, and thus, efficiency, which are all of special importance in regard to improvements of cognitive control functions during adolescence (Segalowitz, Santesso, & Jetha, 2010).

1.3. Functional networks

Developmental changes may not be solely based on anatomical growth factors and structural changes of the brain, but they are accompanied by maturation of brain processes within functional networks (Segalowitz, Santesso, & Jetha, 2010).

Brain maturation mainly progresses from posterior to anterior brain regions and increasingly allows for the incorporation of distant brain areas into wide-spanning functional networks. The frontal lobe reflects a major hub in higher-order cognition. It is the last to mature, thereby delineating the phase of adolescence (Cole et al., 2014; Naghavi & Nyberg, 2005).

The FPN is involved in a broad variety of tasks, mainly those in conjunction with higher-order cognitive control functions (Naghavi & Nyberg, 2005; Ridderinkhof et al., 2004; van Noordt et al., 2017). A variety of overlapping sub-systems is suggested to be flexibly connected to the FPN and flexible hub sub-systems are organized and activated on demand (Chein, J. M. & Schneider, 2005; Cole et al., 2014; Dosenbach et al., 2010; Fedorenko et al., 2013; Hwang et al., 2013; Zanto & Gazzaley, 2013). For the FPN, the frontal cortex is thought of as a main region for integration and organization of top-down control within connected neuronal assemblies that span the brain (Naghavi & Nyberg, 2005; Scolari et al., 2015).

Adolescence is shaped by a fundamental reorganisation of the entire brain, especially with regard to connections to and from the frontal cortex. These maturational processes have been associated with an increase in cognitive performance in many tasks and a general increase of intellectual abilities (Konrad, Firk, & Uhlhaas, 2013).

Our findings indicate that this developmental reorganisation also involves the FPN, which is important for cognitive control processes assessed for both target detection and novel processing. This indicates that reorganisation of the FPN is related to various cognitive control functions. Furthermore, our results imply a relation between maturation the FPN and improvement of task-related performance.

1.4. Combined investigation of EEG measures

The findings of studies I and II demonstrate the importance of the joint investigation of maturational brain changes in the time and frequency domains and for both local and global measures.

Latency differences are best investigated using ERPs, since filtering procedures for time-frequency analysis reduce temporal precision (Cohen, M. X., 2014). ERPs are also good indicators for time-frequency changes that co-occur in different frequency bands. Opposing developmental changes in the time-frequency domain might, however, cancel each other out in the ERP (Cohen, M. X., 2014). Our data indicated: for young participants, a larger

phase jitter between responses was accompanied by enhanced slow-wave amplitudes and the combined impact of both effects in ERP analysis resulted in similar P3b amplitudes across the investigated age-range (see also Figure 26 in SECTION I.4.3).

ERSP and ITC measures are suitable to differentiate between induced amplitude modulation (ERSP) and consistency of neural timing across trials (as indexed by ITC), since the latter measure is independent of amplitude values. Amplitude and latency, as well as power and trial-by-trial phase-locking measures, focus on local brain activity. Several studies, however, strongly propose developmental changes within widely distributed brain networks (Segalowitz, Santesso, & Jetha, 2010). Measures like the SPC enable the investigation of network dynamics, as reflected in the EEG. Thus, spatial coherency measures are specifically suitable for studying developmental changes in event-related functional brain connectivity, as developmental studies on brain connectivity are still piloting and implicating extensive neural reorganisation (Uhlhaas et al., 2009).

Taken together, ERPs and local and global time-frequency measures complement each other for the investigation of selective neurodevelopmental changes throughout the adolescence.

2. Assessment of life-long cerebral plasticity

Age-related studies generally enable a distinction between different stages of development and aging (Daffner, Kirk R., Alperin, Mott, Tusch, & Holcomb, 2015; Fjell & Walhovd, 2003; Lindenberger, Li, & Backman, 2006; Müller & Lindenberger, 2012; Smit et al., 2016) differentially for healthy and patient groups, and, thus, indicate life-long brain changes. Life-long brain plasticity seems to enable life-long learning and adaption to current life circumstances. It may also indicate age-related cognitive decline or illnesses of the brain (Basar-Eroglu, Schmiedt-Fehr, Marbach, Brand, & Mathes, 2008; Basar, 2013; Basar, Emek-Savas, Güntekin, & Yener, 2016; Mathes, Schmiedt-Fehr, et al., 2016; Schmiedt-Fehr & Basar-Eroglu, 2011; Schmiedt-Fehr, Mathes, Kedilaya, Krauss, & Basar-Eroglu, 2016). Taking age into account is, therefore, important to understand the neurocognitive basement of human behaviour and variations in socio-cognitive abilities (Dahl, 2004; Lindenberger, Wenger, & Lovden, 2017; Steinberg, 2013).

Age-related changes of ERPs van Dinteren et al. (2014a, 2014b) and EROs can be observed over the entire lifespan (Bache et al., 2015; Mathes, Khalaidovski, et al., 2016; Müller et al., 2009; Schmiedt-Fehr & Basar-Eroglu, 2011). Many studies, however, observe only a certain age range and investigations are restricted to a certain period of life.

Applying regression models requires careful consideration of the investigated age range, since possible trajectories may differ between life periods. The best model solution may additionally depend on the length of the age range incorporated by the model.

Both, van Dinteren et al. (2014a, 2014b) and Brickman et al. (2012) assessed a logarithmic Gaussian model in order to describe their data from large cross-sectional studies spanning from childhood to old age. P3b latency, for example, seems to decrease during brain maturation, reaching a trough at approximately of 25 years of age followed by a slow increase for the rest of the life span (see Figure 74). These studies provide strong evidence for a life-long plasticity of the brain and indicate segregation of maturational (first decades of life) from degenerative stages associated with aging processes (last decades of life).

Nonetheless, a logarithmic Gaussian model might not constitute the optimal choice for a life span study, as it always consists of a peak or a trough. Changes of the brain during the life span might encompass a plateau between maturation and degeneration, for which a simpler model only consists of a peak or a trough.

Looking only at a section of this data, different models may describe the data best. In the example of van Dinteren's study of P3b latency, a linear decrease might be suitable for the first phase during childhood, while a quadratic model would be a better option to describe the steady deceleration of this decreasing trend towards the trough at young adulthood. For later decades of life, a linearly increasing model might fit the trend of the data.

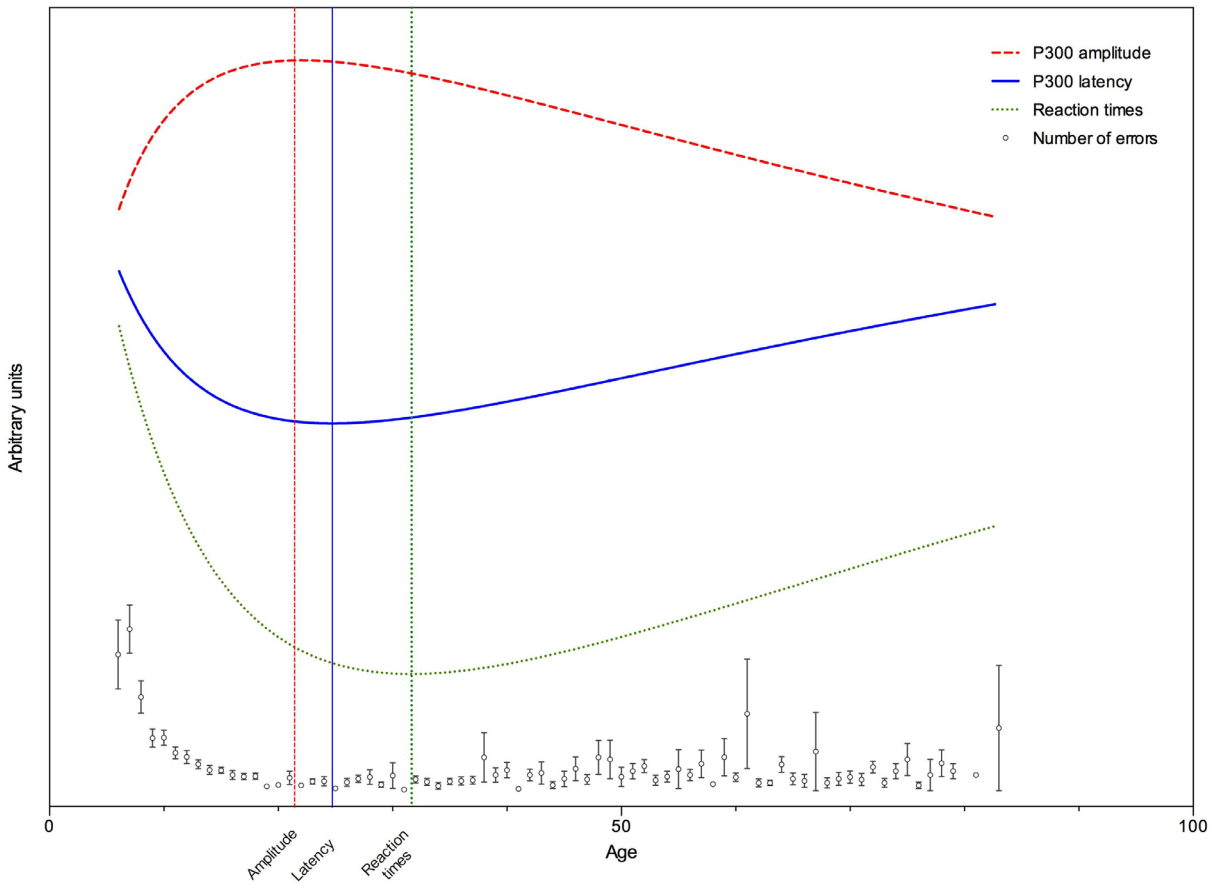

Figure 74: Regression model for reaction times (green) and P3b measures (amplitude in red, latency in blue) and number of errors (whiskers indicate SEM) across the human life span of a cross-sectional dataset (van Dinteren et al., 2014b).

Our data also only describes a section of the life span (8 to 30 years). Quadratic regression models were compared to linear models in order to differentiate between a deceleration and an ongoing age trend, respectively. It was determined that for this age span, a logarithmic Gaussian model would not yield different results than reported for the application of a quadratic model.

Developmental aspects that exhibit a peak or a trough in their trajectories during young adulthood imply a decelerating effect during late adolescence. As depicted by the presented data of van Dinteren's study in Figure 74 this applies, e.g., for reaction times during adolescence. In our studies, e.g. P3a amplitude and latency exhibited linear age trends indicating a prolonged maturation into young adulthood.

By contrast, developmental aspects may peak during adolescence, indicating an 'overshoot' (or an 'undershoot' for a trough). During the period of adolescence several factors are found to follow a U-shaped or inverted U-shaped pattern:
These trends are reflected in behavioural peaks such as risk-taking behaviour or sensation-seeking (Steinberg, 2010) and are suggested to relate to an immature socioemotional, incentive-processing system (Steinberg, 2013). This trend also applies for a trough in reaction times during adolescence in the study by Uhlhaas et al. (2009). On the structural level of the brain, U-shaped trajectories are suggested for the reduction of grey matter (Giedd et al., 1999) and total cerebellum size (Tiemeier et al., 2010). Oscillatory brain networks might excessively increase in connectivity during adolescence, but may be reorganised and cleared in a later process (Uhlhaas et al., 2009).

These trajectories imply that the youth phase may reflect a peculiarity - a special nature – both differing from childhood and adulthood (Steinberg, 2014).

Findings of our studies possibly reflecting adolescent-specific developmental states were exhibited for study II, only, for novel N2 latency (trough at ~17.5 years) and theta SPC during target detection (FC: peak at ~18.5 years; AP: peak at ~18 years); hence, still relatively late during adolescence.

The point of deflection for one developmental aspect is hard to precisely define due to differences between studies and applied models: The minimal value for P3b latency, for example, has been observed for an age as early as 12 years by Fuchigami et al. (1995), whereas the data of van Dinteren's study determined an age of 25 years as the minimal latency (see Figure 74).

Studies spanning a larger age range provide more information about the overall developmental trend and indicate in which phase of life a deflection is to be expected. An early peak or trough indicates a process that reaches maturity earlier than one at a later time in life. Data, which are described best by a linear model, strongly indicate a process with continuing maturational progress. Short-term changes might, however, be underestimated when modelling a continuous life span trajectory.

3. Limitations and future prospects for developmental EEG studies

Physical growth

Physical growth during development leads to an increase in head circumference until about 12 years of age accompanied by a thickening of the skull and an increase in skull density that extends into young adulthood (Adeloye, Kattan, & Silverman, 1975; Whitford et al., 2007). Furthermore, Beauchamp et al. (2011) observed an increasing brain scalp distance over child development. A reduction in EEG and ERP amplitude with age was suggested to be a consequence of developmental skull changes (Frodl et al., 2001; Segalowitz, Santesso, & Jetha, 2010). Pulighеddu et al. (2005) measured a decrease of spontaneous theta oscillations with development via MEG, which is not affected by skull thickness and density, thus attributing the main effect to structural brain changes. Therefore, it is unlikely that age differences in skull thickness would fully account for age differences in EEG power. Furthermore, utilization of baseline correction for ERSP measures is thought to reduce the influence of skull density as well as other perturbations on amplitude measures (Cohen, M. X., 2014).

Choice of novel stimuli

Novel stimuli assessed in this study consisted of animals facing the participant. The animal's face was not, however, always centred at the fixation dot. As a natural tendency, one's gaze shifts to faces as they contain essential social information in the daily life (Wahl, Michel, Pauen, & Hoehl, 2013). In study II, a gaze shift would further strengthen the distracting effect of novel stimuli as it draws the participant's focus from the centre of the monitor where subsequent stimuli were presented. Additionally, movement of the eyes causes artefacts in the EEG, which need to be excluded from further analysis minimizing the amount of comparable data.

Repetition of the study while measuring the gaze shift (e.g. by eye-tracking), in order to exclude non-attended stimuli or assessment of novel stimuli without faces, may help to circumvent this issue.

Lateralization effects

Statistical analyses of our presented studies were performed for regions of interest defined over brain areas along the central line. No statement about lateralization of cerebral responses can be made.

Thatcher, Walker, and Giudice (1987) observed different rates of continuous growth processes determined by changes in EEG coherence for hemispheric development from early childhood until adult age. A lateralisation effect should, therefore, be taken into consideration for investigation of brain development. In this study, averaged data exhibited maxima over central electrode lines, suggesting no strong effect of lateralization.

Inter-individual differences

Investigation of brain development yields the issue of separating individual developmental aspects from general developmental trends (Blakemore, Burnett, & Dahl, 2010). Inter-individual differences resulting from biological events, such as the onset of puberty, were not taken into consideration in the studies presented here. Separated analysis for gender may help to reduce the effect of this issue, albeit demanding increased sample sizes (Clarke et al., 2001; Nanova et al., 2011; Sumich et al., 2012; Yuan, Ju, Yang, Chen, & Li, 2014). Furthermore, determination of pubertal status from blood samples may support the disentangling of developmental effects of biological events and brain maturation (Dorn, 2006; Shirtcliff, Dahl, & Pollak, 2009).

A longitudinal study design yields the advantage of studying individual developmental trajectories and thus balances inter-individual differences in the investigation of developmental changes.

Increases in sample size

Increasing sample sizes may balance inter-individual differences to a higher degree.

A greater relation of number of participants per age-span further improves the application of regression analysis. Several regression models measured in the presented studies, exhibited a non-Gaussian distribution of residuals around the model and, additionally, a significant runs-test indicated a low reliability of the calculated model due to low sample size.

Investigation of a larger age range would improve the assessment of developmental trajectories.

Different measures of cognitive performance

In order to understand brain development entirely, investigation of the comparison of a variety of cognitive abilities and correlated functional networks is necessary.

One suggestion of an extensive test for the novelty oddball task presented in this thesis would be to add a memory test of novel stimuli:

As already mentioned in the discussion of novel stimulus processing, quantification of remembered novel stimuli was not assessed. A greater distractibility of children and young adolescents was indicated in this study and in the literature (Isler et al., 2008; Prada et al., 2014). The quantification of remembered novel stimuli would reveal whether younger participants processed novel stimuli to a degree that the stimuli could be remembered. In combination with the general error rate, this information could serve as an estimate of encoding depth, and thus distractibility, since in-depth encoding of novels is not required during the tasks.

Combined analysis of all frequency bands

The presented studies demonstrate that the maturation of the frontal cortex and its involvement in the FPN relate to developmental changes in delta and theta oscillations. In accordance with this statement, a correlation is suggested between these changes and the development of higher cognitive functions during adolescence.

According to Basar's theory of oscillatory information transmission, sensory and cognitive processes may only be realized in their complexity through the dynamic interplay of all frequency bands (Basar, 2011). In accordance with this view, frequency bands other than delta and theta have been found to play an important role in the FPN and during associated cognitive functions. For example, Modulations of alpha oscillations play a role in the generation of the P3 component and are suggested to relate to the FPN through a correlation with theta oscillations during tasks involving cognitive control (van Noordt et al., 2017).

Imaging techniques for network investigation

In order to understand brain development in more detail, different imaging techniques should be combined. For example, fMRI may yield more information about source localization. Of special interest for the investigation of local and global brain network maturation are DTI measures identifying fibre tracks along the brain, as indicated, e.g., by Hagmann et al. (2010) during resting-state fMRI. MRI measures yield only low temporal resolution and need to be combined with EEG findings in order to understand the dynamic functioning of brain networks.

Determination of directed SPC

In order to understand dynamic functional connectivity in more detail, network connectivity should be further analysed. Measures indicating the direction of information flow within brain networks, such as the directed WPLI (Stam & van Straaten, 2012), may, for instance, enable the investigation of the frontal cortex in its control role of top-down processes within the FPN as indicated by (2015).

Taken together, the standard and novelty oddball paradigm constitute simple cognitive tasks, which are easy to implement; however, studies of neurodevelopmental changes are still scarce, especially in relation to event-related brain oscillations. Despite their limitations, these studies demonstrate the potential of their combined utilization to investigate brain maturation and concurrent changes in task-related behaviour and distractibility.

SECTION V.

Conclusion

In conclusion, our findings imply that improved abilities for target detection and reduced distractibility coincide with developmental changes in frontal brain areas within the fronto-parietal network throughout adolescence.

The results indicate an increase of task-related modulation and coordination of slow-wave brain activity during adolescence, which can be related to the maturation of the fronto-parietal network.

These developmental changes indicate an increased plasticity of the brain during adolescence leading to more precise and efficient communication that coincides with an increase, with age, in task performance and speed.

The studies demonstrate the potential of investigation of the processing of novel impressions through time-frequency analysis. They especially highlight the strength of spatial phase coherence analysis in the observation of brain network maturation relating to higher-order cognitive processes, e.g. the control of attention.

It is essential to extend our understanding of healthy brain maturation, as excessive brain plasticity during adolescence yields great opportunities to raise the personal potential, although this heightened plasticity increases the vulnerability to disruption of normal development and mental health.

List of figures

List of tables

List of equations

Abbreviations

µV	Microvolt
ACC	Anterior Cingulate Cortex
Ag	Silver
AgCl	Silverchlorid
ANOVA	Analysis of variance
AP	Anterior-Posterior
C	Central
cf.	lat. confer
dB	Decibel
dlPFC	Dorso lateral Prefrontal Cortex
DTI	Diffusion Tensor Imaging
dWPLI	Debiased Weighted Phase Lag Index
e.g.	Example given
EEG	Electroencephalogram
EOG	Electrooculogram
ERO	Event-Related Oscillation
ERP	Event-Related Potential
ERSP	Event-Related Perturbation
F	Frontal
FC	Fronto-Central
fMRI	Functional Magnetic Resonance Imaging
FPN	Fronto-parietal network
	here: number of participants per group
Hz	Hertz
i.e.	lat. id est
IC	Imaginary coherence
Im	Imaginary part
ISI	Inter-Stimulus Interval
ITC	Inter-trial Phase Coherence
kΩ	Kilo-Ohm
MFC	Medial Frontal Cortex
MFG	Medial Frontal Gyrus
MRI	Magnetic Resonance Imaging
ms	Milliseconds
n	Sample size
n.s.	Not significant
NT	Non-target
O	Occipital
SD	Standard Deviation

P	Parietal
PFC	Prefrontal Cortex
PLI	Phase Lag Index
PLV	Phase Locking Value
Re	Real part
RT	Reaction Time
SE	Standard Error
SPC	Spatial Phase Coherence
T	Target
T	Temporal
WPLI	Weighted Phase Lag Index

Appendix

A. Flyer A

Universität Bremen

Neugierig auf Forschung?

Teilnehmer gesucht
für wissenschaftliches Projekt
Die Entwicklung des Gehirns im Schulalter

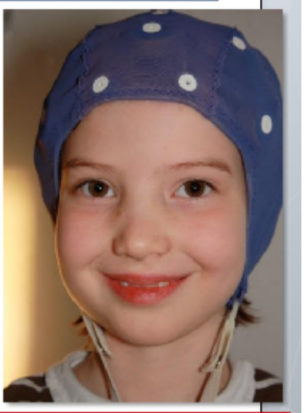

Liebe Schülerinnen und Schüler, liebe Eltern,

Die Entwicklung des Gehirns ist noch immer ein Rätsel. Wir wollen herausfinden, wie neue Herausforderungen die Entwicklung des Gehirns im Schulalter beeinflussen.

Interessierte Kinder und Jugendliche von 9 bis 18 Jahren möchten wir einladen, an unserer Studie teilzunehmen.

Unser Forschungsziel

Kindheit und Jugend haben langfristige Bedeutung für die Gesundheit, soziale Eingebundenheit und Leistungsfähigkeit eines Menschen.

Das Interesse an neuen Erfahrungen spielt eine tragende Rolle für das Entwicklungspotential von Kindern und Jugendlichen. Doch insbesondere während der Jugend kann der Drang nach neuen Erfahrungen auch dazu führen, Gefahren zu unterschätzen.

Unser Ziel ist es, die Gehirnentwicklung, die dem Interesse an neuen Situationen und Handlungsplanungen bei Kindern und Jugendlichen zugrunde liegt, besser zu verstehen.

Unsere Forschung soll helfen, zukünftig gesunde Entwicklungsprozesse zu unterstützen und potentielle Gefährdungen erkennen zu können.

Daher wären wir für Ihre Unterstützung unserer wissenschaftlichen Arbeit sehr dankbar.

Unsere Forschungsmethode

Es werden Bilder gezeigt. Auf einige Bilder soll mit einem Knopfdruck reagiert werden. Das obige Foto zeigt, wie dabei gleichzeitig über eine Kappe die Gehirnaktivität gemessen werden kann. Viele Arztpraxen benutzen diese ungefährliche Methode (EEG-Messung) routinemäßig. Sie ermöglicht uns die Gehirnaktivität in Echtzeit – das heißt im Millisekundenbereich – zu messen.

Die Teilnahme

Für die Teilnahme an der Untersuchung wird eine Aufwandsentschädigung in Höhe von 20 Euro bezahlt. Die Untersuchung dauert, inklusive Pausen, ungefähr 2 Stunden.

Eltern dürfen während der Untersuchung natürlich dabei bleiben.

Kontakt

Für Rückfragen und Terminabsprachen stehen wir Ihnen gerne zur Verfügung.

PD Dr. Birgit Mathes & Annika Wienke (M.Sc.)
Institut für Psychologie & Kognitionsforschung der Universität Bremen
Email: annika.wienke@uni-bremen.de
Telefon: 0421 - 218 68707

B. Flyer B

Universität Bremen

Forschungs- & Lehrprojekt

„Wie kommt die Welt in den Kopf?“

Institut für Psychologie & Kognitionsforschung

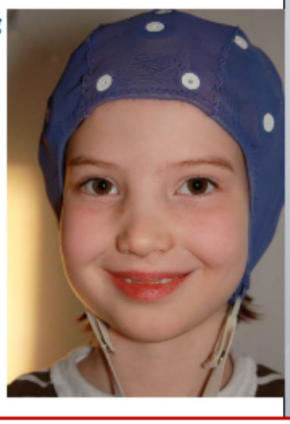

Unser Forschungsinteresse

Die Entwicklung des Gehirns ist noch immer ein Rätsel. Wir wollen herausfinden, wie neue Herausforderungen die Entwicklung des Gehirns im Schulalter beeinflussen. Wir hoffen dadurch Methoden zur Stabilisierung von gesunden Entwicklungsverläufen zu finden.

Interessierte Schüler*innen möchten wir einladen an unserer Studie teilzunehmen.

Unser Lehrprojekt

Wir möchten Ihre Schüler*innen überzeugen, dass sie einen wichtigen Forschungsbeitrag leisten können. Uns ist wichtig, dass Ihre Schüler*innen verstehen, wie und warum wir forschen. Daher möchten wir Ihre Schüler*innen über unsere Forschung direkt aufklären.

In einer Doppelstunde würden wir Ihren Schüler*innen gerne die Entwicklung von Wahrnehmung und Denken näherbringen. Das Lernziel ist, zu verstehen, dass Wahrnehmung durch die Sinne aber auch durch eigene Interessen und Erfahrungen bestimmt ist. Das Verstehen dieses Zusammenhangs soll das Erleben von Selbstbestimmtheit stärken.

Wir bieten spannendes Unterrichtsmaterial, geben einen kurzen theoretischen Überblick und arbeiten viel in Kleingruppen. Hierbei passen wir Inhalt und Umfang altersentsprechend an. Wir freuen uns über Ideen, um unser Lehrprojekt optimal in Ihren Unterricht einzugliedern.

Mögliche Eingliederungen:

- Klasse 4: Sachunterricht – Entwicklung & Persönlichkeit
- Klasse 6: Naturwissenschaften – Erwachsen werden
- Klasse 8: Naturwissenschaften – Von Sinnen
- Oberstufe: Kurse zur Biologie, Psychologie & Pädagogik

Unsere Forschungsmethode

Die Heranwachsenden bekommen eine Aufgabe auf einem Computermonitor präsentiert und lösen diese durch einen Knopfdruck. Das obige Foto zeigt wie dabei gleichzeitig über eine Kappe die Gehirnaktivität gemessen werden kann. Viele Arztpraxen benutzen diese Methode routinemäßig. Sie ermöglicht uns die Gehirnaktivität in Echtzeit – das heißt im Millisekundenbereich – zu messen.

Kontakt

Für Rückfragen stehen wir Ihnen gerne zur Verfügung.

PD Dr. Birgit Mathes,
Institut für Psychologie & Kognitionsforschung der Universität Bremen
Email: *birgit.mathes@uni-bremen.de*
Telefon: 0421 218 68707

C. Consent forms

Einwilligungserklärung

Projekt: „Entwicklung ereigniskorrelierter Gehirnoszillationen bis zum jungen Erwachsenenalter"

Name:_____, Geburtsdatum:_____

Über die geplante EEG-**Untersuchung** im Rahmen einer wissenschaftlichen Studie hat mich Frau / Herr ..... in einem Aufklärungsgespräch ausführlich informiert. Auch habe ich das entsprechende Informationsblatt gelesen und den Fragebogen zu möglichen Ausschlusskriterien ausgefüllt.

Ich konnte alle mir wichtig erscheinenden Fragen, z.B. über die in meinem Fall speziellen Risiken und möglichen Komplikationen und über die Neben- und Folgemaßnahmen stellen, die zur Vorbereitung oder während der Untersuchung erforderlich sind.

Ich habe verstanden, dass es sich bei dieser Studie nicht um eine medizinische Untersuchung handelt und daher aus der EEG-Messung auch keine Informationen über den gesundheitlichen Zustand abgeleitet können.

Die mir erteilten Informationen habe ich inhaltlich verstanden. Mir ist bekannt, dass ich meine Einwilligung jederzeit ohne Angaben von Gründen und ohne persönlichen Nachteil widerrufen kann.

Ich weiß, dass die bei Untersuchungen mit mir gewonnenen Daten auf der Basis elektronischer Datenverarbeitung weiterverarbeitet und eventuell für wissenschaftliche Veröffentlichungen verwendet werden sollen.

Ich gebe hiermit meine Einwilligung, dass bei mir im Rahmen eines Forschungsvorhabens eine EEG-Untersuchung des Gehirns durchgeführt wird.

Ich erkläre mich damit einverstanden, dass meine persönlichen Daten pseudonymisiert in einer für die Öffentlichkeit nicht zugänglichen Datenbank erfasst werden. Pseudonymisiert bedeutet, dass die persönlichen Daten durch Zuteilung von Buchstaben und Zahlencodes gespeichert werden. Eine Zuordnung von Untersuchungsbefunden und personenbezogenen Teilnehmerdaten ist somit für Fremde nicht möglich. Informationen zu meiner Person werden im Rahmen datenschutzrechtlicher Bedingungen verwaltet. Die Speicherung meiner persönlichen Daten dient ausschließlich der Möglichkeit einer erneuten Kontaktaufnahme des Instituts zum Zwecke der Vereinbarung weiterer Untersuchungen. Um Folgeuntersuchungen zu ermöglichen wird die pseudoanonymisierte Zuordnung meiner Daten und mir bis zehn Jahre nach dem heutigen Untersuchungstag möglich sein. Danach wird sie, so nicht schriftlich neu vereinbart, unwiderruflich gelöscht.

_____	_____	_____
Ort, Datum	Unterschrift Teilnehmer	Unterschrift Untersucher

Einwilligungserklärung

für die Teilnahme am Projekt
„Entwicklung ereigniskorrelierter Gehirnoszillationen bis zum jungen Erwachsenenalter"

Name:_____, Geburtsdatum:_____

Mir ist bekannt, dass die Teilnahme meines Kindes an der wissenschaftlichen Studie freiwillig ist und er/sie diese jederzeit ohne Angabe von Gründen und ohne persönlichen Nachteil widerrufen kann. Die Daten werden dann vollständig gelöscht. Hierüber erhalte ich, als Erziehungsberichtigter, eine Nachricht.

Über die geplante EEG-Untersuchung im Rahmen einer wissenschaftlichen Studie hat mich und mein Kind Frau / Herr ..... in einem Aufklärungsgespräch ausführlich informiert. Auch habe ich das entsprechende Informationsblatt gelesen und den Fragebogen zu möglichen Ausschlusskriterien ausgefüllt.

Mein Kind und ich konnten alle uns wichtig erscheinenden Fragen, z.B. über die in Fall meines Kindes speziellen Risiken und möglichen Komplikationen und über die Neben- und Folgemaßnahmen stellen, die zur Vorbereitung oder während der Untersuchung erforderlich sind.

Ich habe verstanden, dass es sich bei dieser Studie nicht um eine medizinische Untersuchung handelt und daher aus der EEG-Messung auch keine Informationen über den gesundheitlichen Zustand abgeleitet werden können.

Ich weiß, dass die bei Untersuchungen gewonnenen Daten meines Kindes auf der Basis elektronischer Datenverarbeitung weiterverarbeitet und eventuell für wissenschaftliche Veröffentlichungen verwendet werden sollen.

Ich gebe hiermit meine Einwilligung, dass im Rahmen eines Forschungsvorhabens eine EEG-Untersuchung des Gehirns meines Kindes durchgeführt wird. Die mir erteilten Informationen habe ich inhaltlich verstanden.

Ich erkläre mich damit einverstanden, dass die persönlichen Daten meines Kindes pseudonymisiert in einer für die Öffentlichkeit nicht zugänglichen Datenbank erfasst werden. Pseudonymisiert bedeutet, dass die persönlichen Daten durch Zuteilung von Buchstaben und Zahlencodes gespeichert werden. Eine Zuordnung von Untersuchungsbefunden und personenbezogenen Teilnehmerdaten ist somit für Fremde nicht möglich. Die Speicherung der persönlichen Daten meines Kindes dient ausschließlich der Möglichkeit einer erneuten Kontaktaufnahme des Instituts zum Zwecke der Vereinbarung weiterer Untersuchungen.

Informationen zu meiner Person und die meines Kindes werden im Rahmen datenschutzrechtlicher Bedingungen verwaltet. Um Folgeuntersuchungen zu ermöglichen wird die pseudoanonymisierte Zuordnung der Daten meines Kindes und meiner Familie bis zehn Jahre nach dem heutigen Untersuchungstag möglich sein. Danach wird sie, so nicht schriftlich neu vereinbart, unwiderruflich gelöscht.

_____	_____	_____
Ort, Datum	Erziehungsberechtigter	Untersucher

D. Questionaire

Ablaufplan

Versuchsleiter: _____ **Datum:** _____ **Probandencode:** _____

Informationsblatt..... Bemerkungen: _____
Einverständniserklärung ..... _____
Versuchspersonenstunden..... Ja Nein _____

Alter: _____ **geb.:** _____ **Muttersprache** _____ **Geschlecht** _____

Bildungsstand: **Schüler, Klasse:** _____, **Schulzweig:** Grund Oberschule FOS/BOS Gymnasium;
Erlangung des Abiturs möglich? Ja Nein
Bereits erlangter Schulabschluss: Haupt Real FOS/BOS Abitur
Ausbildung: Bereits erlangter Abschluss: Ja Nein
Studium: > 2 Semester; **Bereits erlangter Abschluss:** Bachelor Master Promotion
Besondere Lernschwierigkeiten: Ja Nein **Welche?** _____

Nikotin: Ja Nein; **Anz. pro Tag?** _____
Koffein: Ja Nein; **zuletzt?** _____ **wie viel?** _____ **wie häufig?** _____
Alkohol: Ja Nein; **zuletzt?** _____ **wie viel?** _____ **wie häufig?** _____
Drogenkonsum: Ja Nein; **Welche?** _____ **wie häufig?** _____

Brille oder Kontaktlinsen: Ja Nein **Dioptrien:** LI _____ RE _____
Augen- oder Hörprobleme? Ja Nein _____
Platzangst? Ja Nein
Hirntraumatische Vorgeschichte? Ja Nein _____
Neurologische Vorgeschichte? Ja Nein _____ **Familie?** Ja Nein _____
Psychiatrische Vorgeschichte? Ja Nein _____ **Familie?** Ja Nein _____
Weitere Erkrankungen? Ja Nein _____ **Familie?** Ja Nein _____
Medikation? Ja Nein _____
Pille? Ja Nein **Periode?** Ja Nein

Schlaf in der letzten Nacht (Stunden): _____
Wie viele Stunden schlafen sie gewöhnlich? _____
Wann letzte Mahlzeit? _____

Körperliches Wohlbefinden (1 = sehr schlecht, 10 = sehr gut)? .....**1 - 2 - 3 - 4 - 5 - 6 - 7 - 8 - 9 - 10**
Psychisches Wohlbefinden (1 = sehr schlecht, 10 = sehr gut)?.....**1 - 2 - 3 - 4 - 5 - 6 - 7 - 8 - 9 - 10**
Stressbelastung (1 = gering, 10 = hoch)?.....**1 - 2 - 3 - 4 - 5 - 6 - 7 - 8 - 9 - 10**

Händigkeit (nach Oldfield, 1997)
Bitte machen Sie einmal vor, wie Sie ...

...schreiben ... r ... zeichnen ... r ... einen Ball werfen ... r ... mit einer Schere schneiden ... r ...
...sich die Zähne putzen ... r ... mit dem Messer Brot schneiden ... r ... mit dem Löffel essen ... r
...mit dem Besen fegen ... r ... ein Streichholz anzünden ... r ... den Deckel von einer Dose schrauben ... r

Händigkeit der Mutter? ... r ...des Vaters? ... r ...einer Linkshänder in der Familie? Ja Nein
LQ=(R-L) / (R+L) x 100 → Links- Rechts- **Händig**

Farbseh-Test: Ja Nein **Sehtest:** Ja Nein

Kopfumfang: _____ **cm**

Bibliography

Adeloye, A., Kattan, K. R., & Silverman, F. N. (1975). Thickness of the normal skull in the American Blacks and Whites. *Am J Phys Anthropol, 43*(1), 23-30.

Adrian, E. D., & Matthews, B. H. C. (1934). The berger rhythm: potential changes from the occipital lobes in man. *Brain, 57*(4), 355-385.

Ahnert, L. (2013). *Theorien in der Entwicklungspsychologie*. Berlin Heidelberg: Springer-Verlag.

Amso, D., Haas, S., McShane, L., & Badre, D. (2014). Working memory updating and the development of rule-guided behavior. *Cognition, 133*(1), 201-210.

Amso, D., & Scerif, G. (2015). The attentive brain: insights from developmental cognitive neuroscience. *Nat Rev Neurosci, 16*(10), 606-619.

Anderson, V. A., Anderson, P., Northam, E., Jacobs, R., & Catroppa, C. (2001). Development of executive functions through late childhood and adolescence in an Australian sample. *Dev Neuropsychol, 20*(1), 385-406.

Arain, M., Haque, M., Johal, L., Mathur, P., Nel, W., Rais, A., . . . Sharma, S. (2013). Maturation of the adolescent brain. *Neuropsychiatric Disease and Treatment, 9*, 449-461.

Arnett, J. (1992). Reckless behavior in adolescence: A developmental perspective. *Developmental Review, 12*(4), 339-373.

Arnett, J. (1999). Adolescent storm and stress, reconsidered. *Am Psychol, 54*(5), 317-326.

Bache, C., Kopp, F., Springer, A., Stadler, W., Lindenberger, U., & Werkle-Bergner, M. (2015). Rhythmic neural activity indicates the contribution of attention and memory to the processing of occluded movements in 10-month-old infants. *Int J Psychophysiol, 98*(2 Pt 1), 201-212.

Badgaiyan, R. D., & Posner, M. I. (1998). Mapping the cingulate cortex in response selection and monitoring. *Neuroimage, 7*(3), 255-260.

Barry, R. J., & Clarke, A. R. (2009). Spontaneous EEG oscillations in children, adolescents, and adults: Typical development, and pathological aspects in relation to AD/HD. *Journal of Psychophysiology, 23*(4), 157-173.

Barry, R. J., & De Blasio, F. M. (2012). EEG–ERP phase dynamics of children in the auditory Go/NoGo task. *International Journal of Psychophysiology, 86*(3), 251-261.

Basar-Eroglu, C., Basar, E., Demiralp, T., & Schürmann, M. (1992). P300-response: possible psychophysiological correlates in delta and theta frequency channels. A review. *Int J Psychophysiol, 13*(2), 161-179.

Basar-Eroglu, C., & Demiralp, T. (2001). Event-related theta oscillations: an integrative and comparative approach in the human and animal brain. *Int J Psychophysiol, 39*(2-3), 167-195.

Basar-Eroglu, C., Demiralp, T., Schürmann, M., & Basar, E. (2001). Topological distribution of oddball 'P300' responses. *Int J Psychophysiol, 39*(2-3), 213-220.

Basar-Eroglu, C., Schmiedt-Fehr, C., Marbach, S., Brand, A., & Mathes, B. (2008). Altered oscillatory alpha and theta networks in schizophrenia. *Brain Res, 1235*, 143-152.

Basar-Eroglu, C., Strüber, D., Schürmann, M., Stadler, M., & Basar, E. (1996). Gamma-band responses in the brain: a short review of psychophysiological correlates and functional significance. *International Journal of Psychophysiology, 24*(1), 101-112.

Basar, E. (1998). *Brain Function and Oscillations*. Berlin Heidelberg: Springer-Verlag.

Basar, E. (2011). *Brain-Body-Mind in the Nebulous Cartesian System : A holistic Approach by Oscillations*. New York: Springer.

Basar, E. (2013). Brain oscillations in neuropsychiatric disease. *Dialogues Clin Neurosci, 15*(3), 291-300.

Basar, E., Basar-Eroglu, C., Karakas, S., & Schürmann, M. (1999). Are cognitive processes manifested in event-related gamma, alpha, theta and delta oscillations in the EEG? *Neurosci Lett, 259*(3), 165-168.

Basar, E., Basar-Eroglu, C., Karakas, S., & Schürmann, M. (2000). Brain oscillations in perception and memory. *Int J Psychophysiol, 35*(2-3), 95-124.

Basar, E., Basar-Eroglu, C., Karakas, S., & Schürmann, M. (2001). Gamma, alpha, delta, and theta oscillations govern cognitive processes. *Int J Psychophysiol, 39*(2-3), 241-248.

Basar, E., Emek-Savas, D. D., Güntekin, B., & Yener, G. G. (2016). Delay of cognitive gamma responses in Alzheimer's disease. *Neuroimage Clin, 11*, 106-115.

Basar, E., & Güntekin, B. (2008). A review of brain oscillations in cognitive disorders and the role of neurotransmitters. *Brain Res, 1235*, 172-193.

Basar, E., & Güntekin, B. (2009). Darwin's evolution theory, brain oscillations, and complex brain function in a new "Cartesian view". *Int J Psychophysiol, 71*(1), 2-8.

Bastiaansen, M., & Hagoort, P. (2003). Event-induced theta responses as a window on the dynamics of memory. *Cortex, 39*(4-5), 967-992.

Bastos, A. M., & Schoffelen, J. M. (2015). A Tutorial Review of Functional Connectivity Analysis Methods and Their Interpretational Pitfalls. *Front Syst Neurosci, 9*, 175.

Bates, M. E., & Lemay, E. P., Jr. (2004). The d2 Test of attention: construct validity and extensions in scoring techniques. *J Int Neuropsychol Soc, 10*(3), 392-400.

Beauchamp, M. S., Beurlot, M. R., Fava, E., Nath, A. R., Parikh, N. A., Saad, Z. S., . . . Oghalai, J. S. (2011). The developmental trajectory of brain-scalp distance from birth through childhood: implications for functional neuroimaging. *PLoS One, 6*(9), e24981.

Bender, S., Banaschewski, T., Roessner, V., Klein, C., Rietschel, M., Feige, B., . . . Laucht, M. (2015). Variability of single trial brain activation predicts fluctuations in reaction time. *Biol Psychol, 106*, 50-60.

Berns, G. S., Cohen, J. D., & Mintun, M. A. (1997). Brain regions responsive to novelty in the absence of awareness. *Science, 276*(5316), 1272-1275.

Betzel, R. F., Byrge, L., He, Y., Goni, J., Zuo, X. N., & Sporns, O. (2014). Changes in structural and functional connectivity among resting-state networks across the human lifespan. *Neuroimage, 102 Pt 2*, 345-357.

Birbaumer, N., & Schmidt, R. F. (2010). *Biologische Psychologie* (7 ed.). Heidelberg: Springer Medizin Verlag.

Blakemore, S. J. (2008). The social brain in adolescence. *Nat Rev Neurosci, 9*(4), 267-277.

Blakemore, S. J. (2012). Imaging brain development: the adolescent brain. *Neuroimage, 61*(2), 397-406.

Blakemore, S. J., Burnett, S., & Dahl, R. E. (2010). The Role of Puberty in the Developing Adolescent Brain. *Human Brain Mapping, 31*(6), 926-933.

Blakemore, S. J., & Choudhury, S. (2006). Development of the adolescent brain: implications for executive function and social cognition. *J Child Psychol Psychiatry, 47*(3-4), 296-312.

Bledowski, C., Prvulovic, D., Goebel, R., Zanella, F. E., & Linden, D. E. (2004). Attentional systems in target and distractor processing: a combined ERP and fMRI study. *Neuroimage, 22*(2), 530-540.

Bocquillon, P., Bourriez, J. L., Palmero-Soler, E., Betrouni, N., Houdayer, E., Derambure, P., & Dujardin, K. (2011). Use of swLORETA to localize the cortical sources of target- and distracter-elicited P300 components. *Clinical Neurophysiology, 122*(10), 1991-2002.

Bocquillon, P., Bourriez, J. L., Palmero-Soler, E., Molaee-Ardekani, B., Derambure, P., & Dujardin, K. (2014). The spatiotemporal dynamics of early attention processes: a high-resolution electroencephalographic study of N2 subcomponent sources. *Neuroscience, 271*, 9-22.

Booth, J. R., Burman, D. D., Meyer, J. R., Lei, Z., Trommer, B. L., Davenport, N. D., . . . Mesulam, M. M. (2003). Neural development of selective attention and response inhibition. *Neuroimage, 20*(2), 737-751.

Bösel, R. (2001). Aufmerksamkeitswechsel und Konzentration: Von den Funktionen zum Mechanismus. *Zeitschrift für Psychologie, 209*(1), 34-53.

Bosman, C. A., Lansink, C. S., & Pennartz, C. M. (2014). Functions of gamma-band synchronization in cognition: from single circuits to functional diversity across cortical and subcortical systems. *Eur J Neurosci, 39*(11), 1982-1999.

Botvinick, M. M., Braver, T. S., Barch, D. M., Carter, C. S., & Cohen, J. D. (2001). Conflict monitoring and cognitive control. *Psychol Rev, 108*(3), 624-652.

Botvinick, M. M., Cohen, J. D., & Carter, C. S. (2004). Conflict monitoring and anterior cingulate cortex: an update. *Trends Cogn Sci, 8*(12), 539-546.

Braver, T. S., Barch, D. M., Gray, J. R., Molfese, D. L., & Snyder, A. (2001). Anterior cingulate cortex and response conflict: effects of frequency, inhibition and errors. *Cerebral Cortex, 11*(9), 825-836.

Brickenkamp, R. (2002). *Test d2 - Aufmerksamkeits-Belastungs-Test (9. Aufl.)*. Göttingen: Hogrefe, Verl. für Psychologie.

Brickman, A. M., Meier, I. B., Korgaonkar, M. S., Provenzano, F. A., Grieve, S. M., Siedlecki, K. L., . . . Zimmerman, M. E. (2012). Testing the white matter retrogenesis hypothesis of cognitive aging. *Neurobiol Aging, 33*(8), 1699-1715.

Brinkman, M. J., & Stauder, J. E. (2008). The development of passive auditory novelty processing. *Int J Psychophysiol, 70*(1), 33-39.

Brown, W. S., Marsh, J. T., & LaRue, A. (1983). Exponential electrophysiological aging: P3 latency. *Electroencephalogr Clin Neurophysiol, 55*(3), 277-285.

Bunge, S. A., & Crone, E. A. (2009). Neural correlates of the development of cognitive control. In Rumsey, J. M. & Ernst, M. (Eds.), *Neuroimaging in Developmental Clinical Neuroscience* (pp. 22-37). Cambridge: Cambridge University Press.

Bunge, S. A., Dudukovic, N. M., Thomason, M. E., Vaidya, C. J., & Gabrieli, J. D. (2002). Immature frontal lobe contributions to cognitive control in children: evidence from fMRI. *Neuron, 33*(2), 301-311.

Bunge, S. A., & Wright, S. B. (2007). Neurodevelopmental changes in working memory and cognitive control. *Curr Opin Neurobiol, 17*(2), 243-250.

Busch, N. A., Dubois, J., & van Rullen, R. (2009). The phase of ongoing EEG oscillations predicts visual perception. *J Neurosci, 29*(24), 7869-7876.

Buzsaki, G. (2002). Theta oscillations in the hippocampus. *Neuron, 33*(3), 325-340.

Buzsaki, G. (2005). Theta rhythm of navigation: link between path integration and landmark navigation, episodic and semantic memory. *Hippocampus, 15*(7), 827-840.

Buzsaki, G., & Draguhn, A. (2004). Neuronal oscillations in cortical networks. *Science, 304*(5679), 1926-1929.

Buzsaki, G., Logothetis, N., & Singer, W. (2013). Scaling brain size, keeping timing: evolutionary preservation of brain rhythms. *Neuron, 80*(3), 751-764.

Carstensen, L. L., & Mikels, J. A. (2005). At the Intersection of Emotion and Cognition: Aging and the Positivity Effect. *Current Directions in Psychological Science, 14*(3), 117-121.

Casey, B. J., Giedd, J. N., & Thomas, K. M. (2000). Structural and functional brain development and its relation to cognitive development. *Biol Psychol, 54*(1-3), 241-257.

Casey, B. J., Jones, R. M., Levita, L., Libby, V., Pattwell, S. S., Ruberry, E. J., . . . Somerville, L. H. (2010). The storm and stress of adolescence: insights from human imaging and mouse genetics. *Dev Psychobiol, 52*(3), 225-235.

Čeponienė, R., Lepistö, T., Soininen, M., Aronen, E., Alku, P., & Näätänen, R. (2004). Event-related potentials associated with sound discrimination versus novelty detection in children. *Psychophysiology, 41*(1), 130-141.

Chaix, Y., Albaret, J. M., Brassard, C., Cheuret, E., de Castelnau, P., Benesteau, J., . . . Demonet, J. F. (2007). Motor impairment in dyslexia: the influence of attention disorders. *Eur J Paediatr Neurol, 11*(6), 368-374.

Chan, R. C., Shum, D., Toulopoulou, T., & Chen, E. Y. (2008). Assessment of executive functions: review of instruments and identification of critical issues. *Arch Clin Neuropsychol, 23*(2), 201-216.

Chassin, L., Fora, D. B., & King, K. M. (2004). Trajectories of alcohol and drug use and dependence from adolescence to adulthood: the effects of familial alcoholism and personality. *J Abnorm Psychol, 113*(4), 483-498.

Chatrian, G. E., Lettich, E., & Nelson, P. L. (1988). Modified nomenclature for the "10%" electrode system. *J Clin Neurophysiol, 5*(2), 183-186.

Chein, J., Albert, D., O'Brien, L., Uckert, K., & Steinberg, L. (2011). Peers increase adolescent risk taking by enhancing activity in the brain's reward circuitry. *Dev Sci, 14*(2), F1-10.

Chein, J. M., & Schneider, W. (2005). Neuroimaging studies of practice-related change: fMRI and meta-analytic evidence of a domain-general control network for learning. *Brain Res Cogn Brain Res, 25*(3), 607-623.

Cho, R. Y., Walker, C. P., Polizzotto, N. R., Wozny, T. A., Fissell, C., Chen, C. M., & Lewis, D. A. (2015). Development of sensory gamma oscillations and cross-frequency coupling from childhood to early adulthood. *Cerebral Cortex, 25*(6), 1509-1518.

Chu, C. J., Tanaka, N., Diaz, J., Edlow, B. L., Wu, O., Hämäläinen, M., . . . Kramer, M. A. (2015). EEG functional connectivity is partially predicted by underlying white matter connectivity. *Neuroimage, 108*(Supplement C), 23-33.

Clarke, A. R., Barry, R. J., McCarthy, R., & Selikowitz, M. (2001). Age and sex effects in the EEG: development of the normal child. *Clin Neurophysiol, 112*(5), 806-814.

Clayton, M. S., Yeung, N., & Cohen Kadosh, R. (2015). The roles of cortical oscillations in sustained attention. *Trends in cognitive sciences, 19*(4), 188-195.

Coderre, E., Conklin, K., & van Heuven, W. J. (2011). Electrophysiological measures of conflict detection and resolution in the Stroop task. *Brain Res, 1413*, 51-59.

Cohen, J., & Stewart, I. (1994). *The collapse of chaos: discovering simplicity in a complex world*: Viking.

Cohen, J. R., Asarnow, R. F., Sabb, F. W., Bilder, R. M., Bookheimer, S. Y., Knowlton, B. J., & Poldrack, R. A. (2010). A unique adolescent response to reward prediction errors. *Nat Neurosci, 13*(6), 669-671.

Cohen, M. X. (2014). *Analyzing neural time series data : theory and practice* (1 ed.): MIT Press, Massachusetts Institute of Technology.

Cohen, M. X. (2015). Effects of time lag and frequency matching on phase-based connectivity. *J Neurosci Methods, 250*, 137-146.

Cohen, M. X., & Ridderinkhof, K. R. (2013). EEG source reconstruction reveals frontal-parietal dynamics of spatial conflict processing. *PLoS One, 8*(2), e57293.

Cohen, M. X., & van Gaal, S. (2013). Dynamic interactions between large-scale brain networks predict behavioral adaptation after perceptual errors. *Cerebral Cortex, 23*(5), 1061-1072.

Cole, M. W., Repovs, G., & Anticevic, A. (2014). The frontoparietal control system: a central role in mental health. *Neuroscientist, 20*(6), 652-664.

Cole, M. W., Reynolds, J. R., Power, J. D., Repovs, G., Anticevic, A., & Braver, T. S. (2013). Multi-task connectivity reveals flexible hubs for adaptive task control. *Nat Neurosci, 16*(9), 1348-1355.

Conroy, M. A., & Polich, J. (2007). Normative Variation of P3a and P3b from a Large Sample. *Journal of Psychophysiology, 21*(1), 22-32.

Correa, A., Lupianez, J., Madrid, E., & Tudela, P. (2006). Temporal attention enhances early visual processing: a review and new evidence from event-related potentials. *Brain Res, 1076*(1), 116-128.

Coull, J. T. (1998). Neural correlates of attention and arousal: insights from electrophysiology, functional neuroimaging and psychopharmacology. *Prog Neurobiol, 55*(4), 343-361.

Courchesne, E. (1978a). Changes in P3 waves with event repetition: long-term effects on scalp distribution and amplitude. *Electroencephalogr Clin Neurophysiol, 45*(6), 754-766.

Courchesne, E. (1978b). Neurophysiological correlates of cognitive development: Changes in long-latency event-related potentials from childhood to adulthood. *Electroencephalography and Clinical Neurophysiology, 45*(4), 468-482.

Courchesne, E. (1983). 15 Cognitive Components of the Event-Related Brain Potential: Changes Associated with Development. In Gaillard, A. W. K. & Ritter, W. (Eds.), *Advances in Psychology* (Vol. 10, pp. 329-344): North-Holland.

Courchesne, E., Hillyard, S. A., & Galambos, R. (1975). Stimulus novelty, task relevance and the visual evoked potential in man. *Electroencephalogr Clin Neurophysiol, 39*(2), 131-143.

Cragg, L., Kovacevic, N., McIntosh, A. R., Poulsen, C., Martinu, K., Leonard, G., & Paus, T. (2011). Maturation of EEG power spectra in early adolescence: a longitudinal study. *Dev Sci, 14*(5), 935-943.

Crone, E. A. (2009). Executive functions in adolescence: inferences from brain and behavior. *Dev Sci, 12*(6), 825-830.

Crowley, M. J., van Noordt, S. J., Wu, J., Hommer, R. E., South, M., Fearon, R. M., & Mayes, L. C. (2014). Reward feedback processing in children and adolescents: medial frontal theta oscillations. *Brain Cogn, 89*, 79-89.

Cycowicz, Y. M. (2000). Memory development and event-related brain potentials in children. *Biol Psychol, 54*(1-3), 145-174.

Cycowicz, Y. M., & Friedman, D. (1997). A developmental study of the effect of temporal order on the ERPs elicited by novel environmental sounds. *Electroencephalogr Clin Neurophysiol, 103*(2), 304-318.

Cycowicz, Y. M., Friedman, D., & Rothstein, M. (1996). An ERP developmental study of repetition priming by auditory novel stimuli. *Psychophysiology, 33*(6), 680-690.

Daffner, K. R., Alperin, B. R., Mott, K. K., Tusch, E. S., & Holcomb, P. J. (2015). Age-related differences in early novelty processing: Using PCA to parse the overlapping anterior P2 and N2 components. *Biological Psychology, 105*(Supplement C), 83-94.

Daffner, K. R., Mesulam, M. M., Scinto, L. F. M., Calvo, V., Faust, R., & Holcomb, P. J. (2000). An electrophysiological index of stimulus unfamiliarity. *Psychophysiology, 37*(6), 737-747.

Daffner, K. R., Scinto, L. F., Calvo, V., Faust, R., Mesulam, M. M., West, W. C., & Holcomb, P. J. (2000). The influence of stimulus deviance on electrophysiologic and behavioral responses to novel events. *J Cogn Neurosci, 12*(3), 393-406.

Daffner, K. R., Scinto, L. F., Weitzman, A. M., Faust, R., Rentz, D. M., Budson, A. E., & Holcomb, P. J. (2003). Frontal and parietal components of a cerebral network mediating voluntary attention to novel events. *J Cogn Neurosci, 15*(2), 294-313.

Dahl, R. E. (2004). Adolescent brain development: a period of vulnerabilities and opportunities. Keynote address. *Ann N Y Acad Sci, 1021*, 1-22.

Danielmeier, C., & Ullsperger, M. (2011). Post-error adjustments. *Front Psychol, 2*, 233.

de Borst, A. W., Sack, A. T., Jansma, B. M., Esposito, F., de Martino, F., Valente, G., . . . Formisano, E. (2012). Integration of "what" and "where" in frontal cortex during visual imagery of scenes. *Neuroimage, 60*(1), 47-58.

Debener, S., Makeig, S., Delorme, A., & Engel, A. K. (2005). What is novel in the novelty oddball paradigm? Functional significance of the novelty P3 event-related potential as revealed by independent component analysis. *Brain Res Cogn Brain Res, 22*(3), 309-321.

Delorme, A., & Makeig, S. (2004). EEGLAB: an open source toolbox for analysis of single-trial EEG dynamics including independent component analysis. *J Neurosci Methods, 134*(1), 9-21.

Demetriou, A., Christou, C., Spanoudis, G., & Platsidou, M. (2002). The development of mental processing: efficiency, working memory, and thinking. *Monogr Soc Res Child Dev, 67*(1), i-viii, 1-155; discussion 156.

Demiralp, T., Ademoglu, A., Istefanopulos, Y., Basar-Eroglu, C., & Basar, E. (2001). Wavelet analysis of oddball P300. *Int J Psychophysiol, 39*(2-3), 221-227.

Demiralp, T., & Basar, E. (1992). Theta rhythmicities following expected visual and auditory targets. *Int J Psychophysiol, 13*(2), 147-160.

DiClemente, R. J., Hansen, W. B., & Ponton, L. E. (1996). *Handbook of Adolescent Health Risk Behavior*. New York: Springer Science & Business Media.

Donchin, E. (1981). Surprise!...Surprise? *Psychophysiology, 18*(5), 493-513.

Dorn, L. D. (2006). Measuring puberty. *J Adolesc Health, 39*(5), 625-626.

Dosenbach, N. U., Fair, D. A., Cohen, A. L., Schlaggar, B. L., & Petersen, S. E. (2008). A dual-networks architecture of top-down control. *Trends Cogn Sci, 12*(3), 99-105.

Dosenbach, N. U., Nardos, B., Cohen, A. L., Fair, D. A., Power, J. D., Church, J. A., . . . Schlaggar, B. L. (2010). Prediction of individual brain maturity using fMRI. *Science, 329*(5997), 1358-1361.

Duncan-Johnson, C. C., & Donchin, E. (1979). The Time Constant in P300 Recording. *Psychophysiology, 16*(1), 53-55.

Duncan-Johnson, C. C., & Donchin, E. (1982). The P300 component of the event-related brain potential as an index of information processing. *Biol Psychol, 14*(1-2), 1-52.

Duncan, J. (2010). The multiple-demand (MD) system of the primate brain: mental programs for intelligent behaviour. *Trends Cogn Sci, 14*(4), 172-179.

Duncan, J., & Owen, A. M. (2000). Common regions of the human frontal lobe recruited by diverse cognitive demands. *Trends Neurosci, 23*(10), 475-483.

Durston, S., & Casey, B. J. (2006). What have we learned about cognitive development from neuroimaging? *Neuropsychologia, 44*(11), 2149-2157.

Durston, S., Davidson, M. C., Tottenham, N., Galvan, A., Spicer, J., Fossella, J. A., & Casey, B. J. (2006). A shift from diffuse to focal cortical activity with development. *Dev Sci, 9*(1), 1-8.

Dustman, R. E., Shearer, D. E., & Emmerson, R. Y. (1999). Life-span changes in EEG spectral amplitude, amplitude variability and mean frequency. *Clin Neurophysiol, 110*(8), 1399-1409.

Ehlers, C. L., Wills, D. N., Desikan, A., Phillips, E., & Havstad, J. (2014). Decreases in energy and increases in phase locking of event-related oscillations to auditory stimuli occur during adolescence in human and rodent brain. *Dev Neurosci, 36*(3-4), 175-195.

Engel, A. K., & Fries, P. (2010). Beta-band oscillations--signalling the status quo? *Curr Opin Neurobiol, 20*(2), 156-165.

Ernst, M., Pine, D. S., & Hardin, M. (2006). Triadic model of the neurobiology of motivated behavior in adolescence. *Psychol Med, 36*(3), 299-312.

Escera, C., Alho, K., Winkler, I., & Näätänen, R. (1998). Neural mechanisms of involuntary attention to acoustic novelty and change. *J Cogn Neurosci, 10*(5), 590-604.

Fair, D. A., Cohen, A. L., Power, J. D., Dosenbach, N. U., Church, J. A., Miezin, F. M., . . . Petersen, S. E. (2009). Functional brain networks develop from a "local to distributed" organization. *PLoS Comput Biol, 5*(5), e1000381.

Fair, D. A., Dosenbach, N. U., Church, J. A., Cohen, A. L., Brahmbhatt, S., Miezin, F. M., . . . Schlaggar, B. L. (2007). Development of distinct control networks through segregation and integration. *Proc Natl Acad Sci U S A, 104*(33), 13507-13512.

Falkenstein, M. (2006). Inhibition, conflict and the Nogo-N2. *Clin Neurophysiol, 117*(8), 1638-1640.

Fedorenko, E., Duncan, J., & Kanwisher, N. (2013). Broad domain generality in focal regions of frontal and parietal cortex. *Proc Natl Acad Sci U S A, 110*(41), 16616-16621.

Fehr, T. (2013). A hybrid model for the neural representation of complex mental processing in the human brain. *Cogn Neurodyn, 7*(2), 89-103.

Fell, J., Klaver, P., Lehnertz, K., Grunwald, T., Schaller, C., Elger, C. E., & Fernandez, G. (2001). Human memory formation is accompanied by rhinal-hippocampal coupling and decoupling. *Nat Neurosci, 4*(12), 1259-1264.

Ferrari, V., Bradley, M. M., Codispoti, M., & Lang, P. J. (2010). Detecting Novelty and Significance. *Journal of Cognitive Neuroscience, 22*(2), 404-411.

Fjell, A. M., & Walhovd, K. B. (2003). On the topography of P3a and P3b across the adult lifespan--a factor-analytic study using orthogonal procrustes rotation. *Brain Topogr, 15*(3), 153-164.

Flores, A. B., Goméz, C. M., & Meneres, S. (2010). Evaluation of spatial validity-invalidity by the P300 component in children and young adults. *Brain Res Bull, 81*(6), 525-533.

Folstein, J. R., & van Petten, C. (2008). Influence of cognitive control and mismatch on the N2 component of the ERP: A review. *Psychophysiology, 45*(1), 152-170.

Folstein, J. R., van Petten, C., & Rose, S. A. (2008). Novelty and conflict in the categorization of complex stimuli. *Psychophysiology, 45*(3), 467-479.

Friedman, D., Cycowicz, Y. M., & Gaeta, H. (2001). The novelty P3: an event-related brain potential (ERP) sign of the brain's evaluation of novelty. *Neurosci Biobehav Rev, 25*(4), 355-373.

Fries, P. (2015). Rhythms For Cognition: Communication Through Coherence. *Neuron, 88*(1), 220-235.

Frodl, T., Meisenzahl, E. M., Müller, D., Leinsinger, G., Juckel, G., Hahn, K., . . . Hegerl, U. (2001). The effect of the skull on event-related P300. *Clinical Neurophysiology, 112*(9), 1773-1776.

Fuchigami, T., Okubo, O., Ejiri, K., Fujita, Y., Kohira, R., Noguchi, Y., . . . Harada, K. (1995). Developmental changes in P300 wave elicited during two different experimental conditions. *Pediatr Neurol, 13*(1), 25-28.

Fuster, J. M. (2006). The cognit: a network model of cortical representation. *Int J Psychophysiol, 60*(2), 125-132.

Gaeta, H., Friedman, D., & Hunt, G. (2003). Stimulus characteristics and task category dissociate the anterior and posterior aspects of the novelty P3. *Psychophysiology, 40*(2), 198-208.

Galvan, A., Hare, T. A., Parra, C. E., Penn, J., Voss, H., Glover, G., & Casey, B. J. (2006). Earlier development of the accumbens relative to orbitofrontal cortex might underlie risk-taking behavior in adolescents. *J Neurosci, 26*(25), 6885-6892.

Galvan, A., Hare, T. A., Voss, H., Glover, G., & Casey, B. J. (2007). Risk-taking and the adolescent brain: who is at risk? *Dev Sci, 10*(2), F8-f14.

Gardner, M., & Steinberg, L. (2005). Peer influence on risk taking, risk preference, and risky decision making in adolescence and adulthood: an experimental study. *Dev Psychol, 41*(4), 625-635.

Gasser, T., Jennen-Steinmetz, C., Sroka, L., Verleger, R., & Mocks, J. (1988). Development of the EEG of school-age children and adolescents. II. Topography. *Electroencephalogr Clin Neurophysiol, 69*(2), 100-109.

Gasser, T., Verleger, R., Bacher, P., & Sroka, L. (1988). Development of the EEG of school-age children and adolescents. I. Analysis of band power. *Electroencephalogr Clin Neurophysiol, 69*(2), 91-99.

Gibbs, F. A., Davis, H. H., & Lennox, W. G. (1935). The electro-encephalogram in epilepsy and in conditions of impaired consciousness. *Archives of Neurology & Psychiatry, 34*(6), 1133-1148.

Giedd, J. N. (2004). Structural magnetic resonance imaging of the adolescent brain. *Ann N Y Acad Sci, 1021*, 77-85.

Giedd, J. N., Blumenthal, J., Jeffries, N. O., Castellanos, F. X., Liu, H., Zijdenbos, A., . . . Rapoport, J. L. (1999). Brain development during childhood and adolescence: a longitudinal MRI study. *Nat Neurosci, 2*(10), 861-863.

Gogtay, N., Giedd, J. N., Lusk, L., Hayashi, K. M., Greenstein, D., Vaituzis, A. C., . . . Thompson, P. M. (2004). Dynamic mapping of human cortical development during childhood through early adulthood. *Proceedings of the National Academy of Sciences of the United States of America, 101*(21), 8174-8179.

Goldstein, A., Spencer, K. M., & Donchin, E. (2002). The influence of stimulus deviance and novelty on the P300 and novelty P3. *Psychophysiology, 39*(6), 781-790.

GraphPad Prism Tutorial. (2015). Retrieved from https://www.graphpad.com/guides/prism/6/curve-fitting/

Gray, C. M., König, P., Engel, A. K., & Singer, W. (1989). Oscillatory responses in cat visual cortex exhibit inter-columnar synchronization which reflects global stimulus properties. *Nature, 338*(6213), 334-337.

Greene, J. D., Nystrom, L. E., Engell, A. D., Darley, J. M., & Cohen, J. D. (2004). The neural bases of cognitive conflict and control in moral judgment. *Neuron, 44*(2), 389-400.

Grunwald, T., Lehnertz, K., Heinze, H. J., Helmstaedter, C., & Elger, C. E. (1998). Verbal novelty detection within the human hippocampus proper. *Proc Natl Acad Sci U S A, 95*(6), 3193-3197.

Gumenyuk, V., Korzyukov, O., Alho, K., Escera, C., Schroger, E., Ilmoniemi, R. J., & Näätänen, R. (2001). Brain activity index of distractibility in normal school-age children. *Neurosci Lett, 314*(3), 147-150.

Güntekin, B., & Basar, E. (2007). Emotional face expressions are differentiated with brain oscillations. *Int J Psychophysiol, 64*(1), 91-100.

Güntekin, B., & Basar, E. (2014). A review of brain oscillations in perception of faces and emotional pictures. *Neuropsychologia, 58*, 33-51.

Güntekin, B., & Basar, E. (2016). Review of evoked and event-related delta responses in the human brain. *Int J Psychophysiol, 103*, 43-52.

Hagen, G. F., Gatherwright, J. R., Lopez, B. A., & Polich, J. (2006). P3a from visual stimuli: task difficulty effects. *Int J Psychophysiol, 59*(1), 8-14.

Hagmann, P., Sporns, O., Madan, N., Cammoun, L., Pienaar, R., Wedeen, V. J., . . . Grant, P. E. (2010). White matter maturation reshapes structural connectivity in the late developing human brain. *Proc Natl Acad Sci U S A, 107*(44), 19067-19072.

Hahn, A. C., & Perrett, D. I. (2014). Neural and behavioral responses to attractiveness in adult and infant faces. *Neurosci Biobehav Rev, 46 Pt 4*, 591-603.

Hajihosseini, A., & Holroyd, C. B. (2013). Frontal midline theta and N200 amplitude reflect complementary information about expectancy and outcome evaluation. *Psychophysiology, 50*(6), 550-562.

Halgren, E., Baudena, P., Clarke, J. M., Heit, G., Liegeois, C., Chauvel, P., & Musolino, A. (1995). Intracerebral potentials to rare target and distractor auditory and visual stimuli. I. Superior temporal plane and parietal lobe. *Electroencephalogr Clin Neurophysiol, 94*(3), 191-220.

Hall, G. S. (1904). *Adolescence: Its Psychology and Its Relations to Physiology, Anthropology, Sociology, Sex, Crime, Religion and Education*. New York: D. Appleton.

Hansen, J. C., & Hillyard, S. A. (1980). Endogenous brain potentials associated with selective auditory attention. *Electroencephalogr Clin Neurophysiol, 49*(3-4), 277-290.

Hanslmayr, S., Gross, J., Klimesch, W., & Shapiro, K. L. (2011). The role of alpha oscillations in temporal attention. *Brain Res Rev, 67*(1-2), 331-343.

Hardmeier, M., Hatz, F., Bousleiman, H., Schindler, C., Stam, C. J., & Fuhr, P. (2014). Reproducibility of functional connectivity and graph measures based on the phase lag index (PLI) and weighted phase lag index (wPLI) derived from high resolution EEG. *PLoS One, 9*(10), e108648.

Harmony, T. (2013). The functional significance of delta oscillations in cognitive processing. *Front Integr Neurosci, 7*, 83.

Harmony, T., Fernandez, T., Silva, J., Bernal, J., Diaz-Comas, L., Reyes, A., . . . Rodriguez, M. (1996). EEG delta activity: an indicator of attention to internal processing during performance of mental tasks. *Int J Psychophysiol, 24*(1-2), 161-171.

Hedman, A. M., van Haren, N. E., Schnack, H. G., Kahn, R. S., & Hulshoff Pol, H. E. (2012). Human brain changes across the life span: a review of 56 longitudinal magnetic resonance imaging studies. *Hum Brain Mapp, 33*(8), 1987-2002.

Heim, S., & Keil, A. (2012). Developmental trajectories of regulating attentional selection over time. *Front Psychol, 3*, 277.

Herrmann, C. S., & Demiralp, T. (2005). Human EEG gamma oscillations in neuropsychiatric disorders. *Clin Neurophysiol, 116*(12), 2719-2733.

Herrmann, C. S., Grigutsch, M., & Busch, N. A. (2005). EEG oscillations and wavelet analysis. In Handy, T. C. (Ed.), *Event-related potentials: A methods handbook* (pp. 229 - 259). Cambridge, MA: MIT Press.

Herrmann, C. S., Munk, M. H., & Engel, A. K. (2004). Cognitive functions of gamma-band activity: memory match and utilization. *Trends Cogn Sci, 8*(8), 347-355.

Herrmann, C. S., Rach, S., Vosskuhl, J., & Strüber, D. (2014). Time-frequency analysis of event-related potentials: a brief tutorial. *Brain Topogr, 27*(4), 438-450.

Herrmann, C. S., Strüber, D., Helfrich, R. F., & Engel, A. K. (2016). EEG oscillations: From correlation to causality. *Int J Psychophysiol, 103*, 12-21.

Hillyard, S. A. (1985). Electrophysiology of human selective attention. *Trends in Neurosciences, 8*(Supplement C), 400-405.

Hopf, J.-M., Schoenfeld, M. A., & Heinze, H.-J. (2005). The temporal flexibility of attentional selection in the visual cortex. *Current Opinion in Neurobiology, 15*(2), 183-187.

Horstmann, G. (2015). The surprise-attention link: a review. *Ann N Y Acad Sci, 1339*, 106-115.

Horvitz, J. C. (2000). Mesolimbocortical and nigrostriatal dopamine responses to salient non-reward events. *Neuroscience, 96*(4), 651-656.

Hughes, S. W., Lorincz, M., Cope, D. W., Blethyn, K. L., Kekesi, K. A., Parri, H. R., . . . Crunelli, V. (2004). Synchronized oscillations at alpha and theta frequencies in the lateral geniculate nucleus. *Neuron, 42*(2), 253-268.

Huttenlocher, P. R. (1979). Synaptic density in human frontal cortex - developmental changes and effects of aging. *Brain Res, 163*(2), 195-205.

Hwang, K., Ghuman, A. S., Manoach, D. S., Jones, S. R., & Luna, B. (2016). Frontal preparatory neural oscillations associated with cognitive control: A developmental study comparing young adults and adolescents. *Neuroimage, 136*, 139-148.

Hwang, K., Hallquist, M. N., & Luna, B. (2013). The development of hub architecture in the human functional brain network. *Cerebral Cortex, 23*(10), 2380-2393.

Hwang, K., Velanova, K., & Luna, B. (2010). Strengthening of top-down frontal cognitive control networks underlying the development of inhibitory control: a functional magnetic resonance imaging effective connectivity study. *J Neurosci, 30*(46), 15535-15545.

Isler, J. R., Grieve, P. G., Czernochowski, D., Stark, R. I., & Friedman, D. (2008). Cross-frequency phase coupling of brain rhythms during the orienting response. *Brain Res, 1232*, 163-172.

Jann, K., Dierks, T., Boesch, C., Kottlow, M., Strik, W., & Koenig, T. (2009). BOLD correlates of EEG alpha phase-locking and the fMRI default mode network. *Neuroimage, 45*(3), 903-916.

Jasper, H. H. (1958). The ten-twenty electrode system of the International Federation. *Electroencepheph. clin. Neurophysiol.*(10), 371-175.

Jasper, H. H., & Carmichael, L. (1935). Electrical potentials from the intact human brain. *Science, 81*(2089), 51-53.

Jensen, F. E., & Nutt, A. E. (2015). *The Teenage Brain*. London: HarperCollins.

John, E. R., Ahn, H., Prichep, L., Trepetin, M., Brown, D., & Kaye, H. (1980). Developmental equations for the electroencephalogram. *Science, 210*(4475), 1255-1258.

Johnson, M. H. (2001). Functional brain development in humans. *Nat Rev Neurosci, 2*(7), 475-483.

Johnstone, S. J., Barry, R. J., Anderson, J. W., & Coyle, S. F. (1996). Age-related changes in child and adolescent event-related potential component morphology, amplitude and latency to standard and target stimuli in an auditory oddball task.

Johnstone, S. J., Pleffer, C. B., Barry, R. J., Clarke, A. R., & Smith, J. L. (2005). Development of Inhibitory Processing During the Go/NoGo Task. *Journal of Psychophysiology, 19*(1), 11-23.

Kahneman, D. (1973). *Attention and effort* (Vol. 1063): Prentice-Hall Englewood Cliffs, NJ.

Kaiser, J., & Gruzelier, J. H. (1999). Effects of pubertal timing on EEG coherence and P3 latency. *Int J Psychophysiol, 34*(3), 225-236.

Katsanis, J., Iacono, W. G., & McGue, M. K. (1996). The association between P300 and age from preadolescence to early adulthood. *Int J Psychophysiol, 24*(3), 213-221.

Kawasaki, M., Kitajo, K., & Yamaguchi, Y. (2014). Fronto-parietal and fronto-temporal theta phase synchronization for visual and auditory-verbal working memory. *Front Psychol, 5*, 200.

Kawashima, R., Satoh, K., Itoh, H., Ono, S., Furumoto, S., Gotoh, R., . . . Fukuda, H. (1996). Functional anatomy of GO/NO-GO discrimination and response selection--a PET study in man. *Brain Res, 728*(1), 79-89.

Kayser, C., Ince, R. A., & Panzeri, S. (2012). Analysis of slow (theta) oscillations as a potential temporal reference frame for information coding in sensory cortices. *PLoS Comput Biol, 8*(10), e1002717.

Kelly, A. M., Di Martino, A., Uddin, L. Q., Shehzad, Z., Gee, D. G., Reiss, P. T., . . . Milham, M. P. (2009). Development of anterior cingulate functional connectivity from late childhood to early adulthood. *Cerebral Cortex, 19*(3), 640-657.

Khader, P., Heil, M., & Rösler, F. (2009). Verfahren zur Registrierung elektrischer und magnetischer Hirnaktivität. In Sturm, W., Herrmann, M., & Münte, T. F. (Eds.), *Lehrbuch der Klinischen Neuropsychologie* (pp. 260–274). Heidelberg: Spektrum Akademischer Verlag.

Kihara, M., Hogan, A. M., Newton, C. R., Garrashi, H. H., Neville, B. R., & de Haan, M. (2010). Auditory and visual novelty processing in normally-developing Kenyan children. *Clin Neurophysiol, 121*(4), 564-576.

Kilavik, B. E., Zaepffel, M., Brovelli, A., MacKay, W. A., & Riehle, A. (2013). The ups and downs of beta oscillations in sensorimotor cortex. *Exp Neurol, 245*, 15-26.

Kirino, E., Belger, A., Goldman-Rakic, P., & McCarthy, G. (2000). Prefrontal activation evoked by infrequent target and novel stimuli in a visual target detection task: an event-related functional magnetic resonance imaging study. *J Neurosci, 20*(17), 6612-6618.

Klimesch, W. (1996). Memory processes, brain oscillations and EEG synchronization. *Int J Psychophysiol, 24*(1-2), 61-100.

Klimesch, W. (1997). EEG-alpha rhythms and memory processes. *Int J Psychophysiol, 26*(1-3), 319-340.

Klimesch, W. (1999). EEG alpha and theta oscillations reflect cognitive and memory performance: a review and analysis. *Brain Res Brain Res Rev, 29*(2-3), 169-195.

Klimesch, W., Freunberger, R., & Sauseng, P. (2010). Oscillatory mechanisms of process binding in memory. *Neurosci Biobehav Rev, 34*(7), 1002-1014.

Klimesch, W., Schack, B., Schabus, M., Doppelmayr, M., Gruber, W., & Sauseng, P. (2004). Phase-locked alpha and theta oscillations generate the P1-N1 complex and are related to memory performance. *Brain Res Cogn Brain Res, 19*(3), 302-316.

Klingberg, T. (2014). Childhood cognitive development as a skill. *Trends Cogn Sci, 18*(11), 573-579.

Knight, R. (1996). Contribution of human hippocampal region to novelty detection. *Nature, 383*(6597), 256-259.

Knight, R. T. (1984). Decreased response to novel stimuli after prefrontal lesions in man. *Electroencephalogr Clin Neurophysiol, 59*(1), 9-20.

Knyazev, G. G. (2012). EEG delta oscillations as a correlate of basic homeostatic and motivational processes. *Neurosci Biobehav Rev, 36*(1), 677-695.

Kolev, V., Demiralp, T., Yordanova, J., Ademoglu, A., & Isoglu-Alkac, U. (1997). Time-frequency analysis reveals multiple functional components during oddball P300. *Neuroreport, 8*(8), 2061-2065.

Konrad, K., Firk, C., & Uhlhaas, P. J. (2013). Brain Development During Adolescence: Neuroscientific Insights Into This Developmental Period. *Deutsches Ärzteblatt International, 110*(25), 425-431.

Krause, C. M., Salminen, P. A., Sillanmaki, L., & Holopainen, I. E. (2001). Event-related desynchronization and synchronization during a memory task in children. *Clin Neurophysiol, 112*(12), 2233-2240.

Krause, C. M., Sillanmaki, L., Koivisto, M., Saarela, C., Haggqvist, A., Laine, M., & Hamalainen, H. (2000). The effects of memory load on event-related EEG desynchronization and synchronization. *Clin Neurophysiol, 111*(11), 2071-2078.

Kropotov, J. D., Ponomarev, V. A., Hollup, S., & Mueller, A. (2011). Dissociating action inhibition, conflict monitoring and sensory mismatch into independent components of event related potentials in GO/NOGO task. *Neuroimage, 57*(2), 565-575.

Kuba, M., Kubová, Z., Kremláček, J., & Langrová, J. (2007). Motion-onset VEPs: Characteristics, methods, and diagnostic use. *Vision Research, 47*(2), 189-202.

Labate, D., Foresta, F., Mammone, N., & Morabito, F. C. (2015). Effects of Artifacts Rejection on EEG Complexity in Alzheimer's Disease. In Bassis, S., Esposito, A., & Morabito, C. F. (Eds.), *Advances in Neural Networks: Computational and Theoretical Issues* (pp. 129-136). Cham: Springer International Publishing.

Lackner, C. L., Santesso, D. L., Dywan, J., Wade, T. J., & Segalowitz, S. J. (2013). Electrocortical indices of selective attention predict adolescent executive functioning. *Biological Psychology, 93*(2), 325-333.

Lahat, A., & Fox, N. A. (2013). Chapter 23 - The Neural Correlates of Cognitive Control and the Development of Social Behavior A2 - Rubenstein, John L.R. In Rakic, P. (Ed.), *Neural Circuit Development and Function in the Brain* (pp. 413-427). Oxford: Academic Press.

Lee, S., & Kruse, J. (2008). *Biopotential Electrode Sensors in ECG/EEG/EMG Systems*. Norwood.

Lee, T. G., & D'Esposito, M. (2012). The dynamic nature of top-down signals originating from prefrontal cortex: a combined fMRI-TMS study. *J Neurosci, 32*(44), 15458-15466.

Lerner, R. M., & Steinberg, L. (2004). *Handbook of Adolescent Psychology* (2 ed.). New Jersey: John Wiley & Sons, Inc.

Lewis, M. D., Lamm, C., Segalowitz, S. J., Stieben, J., & Zelazo, P. D. (2006). Neurophysiological correlates of emotion regulation in children and adolescents. *J Cogn Neurosci, 18*(3), 430-443.

Lindenberger, U., Li, S. C., & Backman, L. (2006). Delineating brain-behavior mappings across the lifespan: substantive and methodological advances in developmental neuroscience. *Neurosci Biobehav Rev, 30*(6), 713-717.

Lindenberger, U., Wenger, E., & Lovden, M. (2017). Towards a stronger science of human plasticity. *Nat Rev Neurosci, 18*(5), 261-262.

Liu, Z. X., Woltering, S., & Lewis, M. D. (2014). Developmental change in EEG theta activity in the medial prefrontal cortex during response control. *Neuroimage, 85 Pt 2*, 873-887.

Lopes da Silva, F. H., Gonçalves, S. I., & De Munck, J. C. (2010). Elektroencephalograpy (EEG). In Binder, M. D., Hirokawa, N., & Windhorst, U. (Eds.), *Encyclopedia of Neuroscience* (pp. 849–855). Berlin: Springer.

Lopes da Silva, F. (2013). EEG and MEG: Relevance to Neuroscience. *Neuron, 80*(5), 1112-1128.

Lourenco, F., & Casey, B. J. (2013). Adjusting behavior to changing environmental demands with development. *Neurosci Biobehav Rev, 37*(9 Pt B), 2233-2242.

Luck, S. J. (2005). *An Introduction to the Event-related Potential Technique*: MIT Press.

Luck, S. J., & Hillyard, S. A. (1994). Electrophysiological correlates of feature analysis during visual search. *Psychophysiology, 31*(3), 291-308.

Luck, S. J., Mathalon, D. H., O'Donnell, B. F., Hamalainen, M. S., Spencer, K. M., Javitt, D. C., & Uhlhaas, P. J. (2011). A roadmap for the development and validation of event-related potential biomarkers in schizophrenia research. *Biol Psychiatry, 70*(1), 28-34.

Luna, B., Padmanabhan, A., & O'Hearn, K. (2010). What has fMRI told us about the development of cognitive control through adolescence? *Brain Cogn, 72*(1), 101-113.

Luna, B., & Sweeney, J. A. (2004). The emergence of collaborative brain function: FMRI studies of the development of response inhibition. *Ann N Y Acad Sci, 1021*, 296-309.

Mangun, G. R. (1995). Neural mechanisms of visual selective attention. *Psychophysiology, 32*(1), 4-18.

Marcuse, L. V., Schneider, M., Mortati, K. A., Donnelly, K. M., Arnedo, V., & Grant, A. C. (2008). Quantitative analysis of the EEG posterior-dominant rhythm in healthy adolescents. *Clin Neurophysiol, 119*(8), 1778-1781.

Mathes, B., Khalaidovski, K., Schmiedt-Fehr, C., & Basar-Eroglu, C. (2014). Frontal theta activity is pronounced during illusory perception. *Int J Psychophysiol, 94*(3), 445-454.

Mathes, B., Khalaidovski, K., Wienke, A. S., Schmiedt-Fehr, C., & Basar-Eroglu, C. (2016). Maturation of the P3 and concurrent oscillatory processes during early and late adolescence. *Clinical Neurophysiology, 127*, 2599-2609.

Mathes, B., Schmiedt-Fehr, C., Kedilaya, S., Strüber, D., Brand, A., & Basar-Eroglu, C. (2016). Theta response in schizophrenia is indifferent to perceptual illusion. *Clin Neurophysiol, 127*(1), 419-430.

Mathes, B., Schmiedt, J., Schmiedt-Fehr, C., Pantelis, C., & Basar-Eroglu, C. (2012). New rather than old? For working memory tasks with abstract patterns the P3 and the single-trial delta response are larger for modified than identical probe stimuli. *Psychophysiology, 49*(7), 920-932.

Mathewson, K. E., Basak, C., Maclin, E. L., Low, K. A., Boot, W. R., Kramer, A. F., . . . Gratton, G. (2012). Different slopes for different folks: alpha and delta EEG power predict subsequent video game learning rate and improvements in cognitive control tasks. *Psychophysiology, 49*(12), 1558-1570.

Matousek, M., & Petersen, I. (1973). Automatic evaluation of EEG background activity by means of age-dependent EEG quotients. *Electroencephalogr Clin Neurophysiol, 35*(6), 603-612.

McCarley, R. W., Faux, S. F., Shenton, M. E., Nestor, P. G., & Adams, J. (1991). Event-related potentials in schizophrenia: their biological and clinical correlates and a new model of schizophrenic pathophysiology. *Schizophr Res, 4*(2), 209-231.

McGlashan, T. H., & Hoffman, R. E. (2000). Schizophrenia as a disorder of developmentally reduced synaptic connectivity. *Arch Gen Psychiatry, 57*(7), 637-648.

McIntosh, A. R., Kovacevic, N., & Itier, R. J. (2008). Increased brain signal variability accompanies lower behavioral variability in development. *PLoS Comput Biol, 4*(7), e1000106.

Merchant, H., Harrington, D. L., & Meck, W. H. (2013). Neural basis of the perception and estimation of time. *Annu Rev Neurosci, 36*, 313-336.

Michels, L., Muthuraman, M., Luchinger, R., Martin, E., Anwar, A. R., Raethjen, J., . . . Siniatchkin, M. (2013). Developmental changes of functional and directed resting-state connectivities associated with neuronal oscillations in EEG. *Neuroimage, 81*, 231-242.

Miskovic, V., Ma, X., Chou, C. A., Fan, M., Owens, M., Sayama, H., & Gibb, B. E. (2015). Developmental changes in spontaneous electrocortical activity and network organization from early to late childhood. *Neuroimage, 118*, 237-247.

Müller, V., Brehmer, Y., von Oertzen, T., Li, S. C., & Lindenberger, U. (2008). Electrophysiological correlates of selective attention: a lifespan comparison. *BMC Neurosci, 9*, 18.

Müller, V., Gruber, W., Klimesch, W., & Lindenberger, U. (2009). Lifespan differences in cortical dynamics of auditory perception. *Dev Sci, 12*(6), 839-853.

Müller, V., & Lindenberger, U. (2012). Lifespan differences in nonlinear dynamics during rest and auditory oddball performance. *Dev Sci, 15*(4), 540-556.

Murakami, S., & Okada, Y. (2006). Contributions of principal neocortical neurons to magnetoencephalography and electroencephalography signals. *J Physiol, 575*(Pt 3), 925-936.

Myers, D. G. (2008). *Psychologie* (Reiss, M., Trans. Reiss, M. & Wahl, S. Eds. 2 ed.). Heidelberg: Springer Medizin Verlag.

Nácher, V., Ledberg, A., Deco, G., & Romo, R. (2013). Coherent delta-band oscillations between cortical areas correlate with decision making. *Proceedings of the National Academy of Sciences of the United States of America, 110*(37), 15085-15090.

Naghavi, H. R., & Nyberg, L. (2005). Common fronto-parietal activity in attention, memory, and consciousness: shared demands on integration? *Conscious Cogn, 14*(2), 390-425.

Nanova, P., Kolev, V., & Yordanova, J. (2011). Developmental gender differences in the synchronization of auditory event-related oscillations. *Clin Neurophysiol, 122*(5), 907-915.

Neundörfer, B. (1990). *EEG-Fibel: Das EEG in der ärztlichen Praxis*. Stuttgart: Gustav Fischer.

Neuper, C., & Pfurtscheller, G. (2001). Event-related dynamics of cortical rhythms: frequency-specific features and functional correlates. *Int J Psychophysiol, 43*(1), 41-58.

Niendam, T. A., Laird, A. R., Ray, K. L., Dean, Y. M., Glahn, D. C., & Carter, C. S. (2012). Meta-analytic evidence for a superordinate cognitive control network subserving diverse executive functions. *Cogn Affect Behav Neurosci, 12*(2), 241-268.

Nigbur, R., Cohen, M. X., Ridderinkhof, K. R., & Sturmer, B. (2012). Theta dynamics reveal domain-specific control over stimulus and response conflict. *J Cogn Neurosci, 24*(5), 1264-1274.

Nobre, A., Correa, A., & Coull, J. (2007). The hazards of time. *Curr Opin Neurobiol, 17*(4), 465-470.

Nuechterlein, K. H., Ventura, J., Subotnik, K. L., & Bartzokis, G. (2014). The early longitudinal course of cognitive deficits in schizophrenia. *J Clin Psychiatry, 75 Suppl 2*, 25-29.

Oades, R. D., Dittmann-Balcar, A., & Zerbin, D. (1997). Development and topography of auditory event-related potentials (ERPs): mismatch and processing negativity in individuals 8-22 years of age. *Psychophysiology, 34*(6), 677-693.

Okamoto, M., Dan, H., Sakamoto, K., Takeo, K., Shimizu, K., Kohno, S., . . . Dan, I. (2004). Three-dimensional probabilistic anatomical cranio-cerebral correlation via the international 10-20 system oriented for transcranial functional brain mapping. *Neuroimage, 21*(1), 99-111.

Oldfield, R. C. (1971). The assessment and analysis of handedness: the Edinburgh inventory. *Neuropsychologia, 9*(1), 97-113.

Orekhova, E. V., Stroganova, T. A., & Posikera, I. N. (2001). Alpha activity as an index of cortical inhibition during sustained internally controlled attention in infants. *Clin Neurophysiol, 112*(5), 740-749.

Ozgoren, M., Basar-Eroglu, C., & Basar, E. (2005). Beta oscillations in face recognition. *Int J Psychophysiol, 55*(1), 51-59.

Pammi, V. S. C., & Srinivasan, N. (2013). *Decision Making: Neural and Behavioural Approaches* (1 ed. Vol. 202). Oxford: Elsevier B. V.

Pantelis, C., Yucel, M., Bora, E., Fornito, A., Testa, R., Brewer, W. J., . . . Wood, S. J. (2009). Neurobiological markers of illness onset in psychosis and schizophrenia: The search for a moving target. *Neuropsychol Rev, 19*(3), 385-398.

Papenberg, G., Hämmerer, D., Müller, V., Lindenberger, U., & Li, S. C. (2013). Lower theta inter-trial phase coherence during performance monitoring is related to higher reaction time variability: a lifespan study. *Neuroimage, 83*, 912-920.

Paus, T. (2010). Growth of white matter in the adolescent brain: myelin or axon? *Brain Cogn, 72*(1), 26-35.

Paus, T., Keshavan, M., & Giedd, J. N. (2008). Why do many psychiatric disorders emerge during adolescence? *Nat Rev Neurosci, 9*(12), 947-957.

Paus, T., Zijdenbos, A., Worsley, K., Collins, D. L., Blumenthal, J., Giedd, J. N., . . . Evans, A. C. (1999). Structural maturation of neural pathways in children and adolescents: in vivo study. *Science, 283*(5409), 1908-1911.

Pfueller, U., Oelkers-Ax, R., Gmehlin, D., Parzer, P., Roesch-Ely, D., Weisbrod, M., & Bender, S. (2011). Maturation of P300 amplitude and short-term learning as reflected by P300 habituation between trial blocks in children. *International Journal of Psychophysiology, 79*(2), 184-194.

Pfurtscheller, G., & Lopes da Silva, F. H. (1999). Event-related EEG/MEG synchronization and desynchronization: basic principles. *Clin Neurophysiol, 110*(11), 1842-1857.

Picton, T. W. (1992). The P300 wave of the human event-related potential. *J Clin Neurophysiol, 9*(4), 456-479.

Plowman, S. A., Dustman, K., Walicek, H., Corless, C., & Ehlers, G. (1999). The effects of ENDUROX on the physiological responses to stair-stepping exercise. *Res Q Exerc Sport, 70*(4), 385-388.

Polich, J. (2007). Updating P300: an integrative theory of P3a and P3b. *Clin Neurophysiol, 118*(10), 2128-2148.

Polich, J., & Comerchero, M. D. (2003). P3a from visual stimuli: typicality, task, and topography. *Brain Topogr, 15*(3), 141-152.

Polich, J., & Criado, J. R. (2006). Neuropsychology and neuropharmacology of P3a and P3b. *Int J Psychophysiol, 60*(2), 172-185.

Polich, J., Howard, L., & Starr, A. (1983). P300 latency correlates with digit span. *Psychophysiology, 20*(6), 665-669.

Polich, J., Ladish, C., & Burns, T. (1990). Normal variation of P300 in children: Age, memory span, and head size. *International Journal of Psychophysiology, 9*(3), 237-248.

Ponton, C. W., Eggermont, J. J., Kwong, B., & Don, M. (2000). Maturation of human central auditory system activity: evidence from multi-channel evoked potentials. *Clin Neurophysiol, 111*(2), 220-236.

Posner, M. I., & Petersen, S. E. (1990). The attention system of the human brain. *Annu Rev Neurosci, 13*, 25-42.

Posner, M. I., & Rothbart, M. K. (2007). Research on attention networks as a model for the integration of psychological science. *Annu Rev Psychol, 58*, 1-23.

Prada, L., Barceló, F., Herrmann, C. S., & Escera, C. (2014). EEG delta oscillations index inhibitory control of contextual novelty to both irrelevant distracters and relevant task-switch cues. *Psychophysiology, 51*(7), 658-672.

Ptak, R. (2012). The frontoparietal attention network of the human brain: action, saliency, and a priority map of the environment. *Neuroscientist, 18*(5), 502-515.

Puligheddu, M., de Munck, J. C., Stam, C. J., Verbunt, J., de Jongh, A., van Dijk, B. W., & Marrosu, F. (2005). Age distribution of MEG spontaneous theta activity in healthy subjects. *Brain Topogr, 17*(3), 165-175.

Raichle, M. E., & Snyder, A. Z. (2007). A default mode of brain function: a brief history of an evolving idea. *Neuroimage, 37*(4), 1083-1090; discussion 1097-1089.

Ridderinkhof, K. R., van den Wildenberg, W. P. M., Segalowitz, S. J., & Carter, C. S. (2004). Neurocognitive mechanisms of cognitive control: The role of prefrontal cortex in action selection, response inhibition, performance monitoring, and reward-based learning. *Brain and Cognition, 56*(2), 129-140.

Rojas-Benjumea, M. A., Sauque-Poggio, A. M., Barriga-Paulino, C. I., Rodriguez-Martinez, E. I., & Gomez, C. M. (2015). Development of behavioral parameters and ERPs in a novel-target visual detection paradigm in children, adolescents and young adults. *Behav Brain Funct, 11*, 22.

Rothbart, M. K., Ellis, L. K., Rueda, M. R., & Posner, M. I. (2003). Developing mechanisms of temperamental effortful control. *J Pers, 71*(6), 1113-1143.

Rozhkov, V. P., Sergeeva, E. G., & Soroko, S. I. (2009). Age dynamics of evoked brain potentials in involuntary and voluntary attention to a deviant stimulus in schoolchildren from the northern region. *Neurosci Behav Physiol, 39*(9), 851-863.

Rubenstein, J. L. R., & Rakic, P. (2013). *Neural Circuit Development and Function in the Brain: Comprehensive Developmental Neuroscience* (1 ed.). San Diego: Elsevier Academic Press.

Rubia, K., Russell, T., Overmeyer, S., Brammer, M. J., Bullmore, E. T., Sharma, T., . . . Taylor, E. (2001). Mapping motor inhibition: conjunctive brain activations across different versions of go/no-go and stop tasks. *Neuroimage, 13*(2), 250-261.

Sadaghiani, S., Scheeringa, R., Lehongre, K., Morillon, B., Giraud, A.-L., D'Esposito, M., & Kleinschmidt, A. (2012). Alpha-band phase synchrony is related to activity in the fronto-parietal adaptive control network. *The Journal of neuroscience : the official journal of the Society for Neuroscience, 32*(41), 14305-14310.

Sanei, S., & Chambers, J. A. (2007). *EEG Signal Processing*. Chichester: John Wiley & Sons Ltd.

Sangal, R. B., Sangal, J. M., & Belisle, C. (1998). P300 latency and age: a quadratic regression explains their relationship from age 5 to 85. *Clin Electroencephalogr, 29*(1), 1-6.

Sauseng, P., Klimesch, W., Freunberger, R., Pecherstorfer, T., Hanslmayr, S., & Doppelmayr, M. (2006). Relevance of EEG alpha and theta oscillations during task switching. *Exp Brain Res, 170*(3), 295-301.

Schmiedt-Fehr, C., & Basar-Eroglu, C. (2011). Event-related delta and theta brain oscillations reflect age-related changes in both a general and a specific neuronal inhibitory mechanism. *Clin Neurophysiol, 122*(6), 1156-1167.

Schmiedt-Fehr, C., Mathes, B., Kedilaya, S., Krauss, J., & Basar-Eroglu, C. (2016). Aging differentially affects alpha and beta sensorimotor rhythms in a go/nogo task. *Clinical Neurophysiology, 127*(10), 3234-3242.

Scolari, M., Seidl-Rathkopf, K. N., & Kastner, S. (2015). Functions of the human frontoparietal attention network: Evidence from neuroimaging. *Current Opinion in Behavioral Sciences, 1*, 32-39.

Segalowitz, S. J., & Davies, P. L. (2004). Charting the maturation of the frontal lobe: an electrophysiological strategy. *Brain Cogn, 55*(1), 116-133.

Segalowitz, S. J., Santesso, D. L., & Jetha, M. K. (2010). Electrophysiological changes during adolescence: a review. *Brain Cogn, 72*(1), 86-100.

Segalowitz, S. J., Santesso, D. L., Murphy, T. I., Homan, D., Chantziantoniou, D. K., & Khan, S. (2010). Retest reliability of medial frontal negativities during performance monitoring. *Psychophysiology, 47*(2), 260-270.

Shirtcliff, E. A., Dahl, R. E., & Pollak, S. D. (2009). Pubertal development: correspondence between hormonal and physical development. *Child Dev, 80*(2), 327-337.

Shulman, E. P., Smith, A. R., Silva, K., Icenogle, G., Duell, N., Chein, J., & Steinberg, L. (2016). The dual systems model: Review, reappraisal, and reaffirmation. *Dev Cogn Neurosci, 17*, 103-117.

Silveri, M. M., Tzilos, G. K., Pimentel, P. J., & Yurgelun-Todd, D. A. (2004). Trajectories of adolescent emotional and cognitive development: effects of sex and risk for drug use. *Ann N Y Acad Sci, 1021*, 363-370.

Simons-Morton, B., Lerner, N., & Singer, J. (2005). The observed effects of teenage passengers on the risky driving behavior of teenage drivers. *Accid Anal Prev, 37*(6), 973-982.

Simons, D. J. (2000). Attentional capture and inattentional blindness. *Trends Cogn Sci, 4*(4), 147-155.

Smit, D. J., de Geus, E. J., Boersma, M., Boomsma, D. I., & Stam, C. J. (2016). Life-Span Development of Brain Network Integration Assessed with Phase Lag Index Connectivity and Minimum Spanning Tree Graphs. *Brain Connect, 6*(4), 312-325.

Smith, A. R., Chein, J., & Steinberg, L. (2014). Peers increase adolescent risk taking even when the probabilities of negative outcomes are known. *Dev Psychol, 50*(5), 1564-1568.

Snyder, E., & Hillyard, S. A. (1976). Long-latency evoked potentials to irrelevant, deviant stimuli. *Behav Biol, 16*(3), 319-331.

Sokolov, E. N. (1963). Higher nervous functions; the orienting reflex. *Annu Rev Physiol, 25*, 545-580.

Soltani, M., & Knight, R. T. (2000). Neural origins of the P300. *Crit Rev Neurobiol, 14*(3-4), 199-224.

Somerville, L. H., & Casey, B. J. (2010). Developmental neurobiology of cognitive control and motivational systems. *Curr Opin Neurobiol, 20*(2), 236-241.

Sowell, E. R., Peterson, B. S., Thompson, P. M., Welcome, S. E., Henkenius, A. L., & Toga, A. W. (2003). Mapping cortical change across the human life span. *Nat Neurosci, 6*(3), 309-315.

Sowell, E. R., Thompson, P. M., Holmes, C. J., Jernigan, T. L., & Toga, A. W. (1999). In vivo evidence for post-adolescent brain maturation in frontal and striatal regions. *Nat Neurosci, 2*(10), 859-861.

Spear, L. P. (2000). The adolescent brain and age-related behavioral manifestations. *Neuroscience & Biobehavioral Reviews, 24*(4), 417-463.

Stam, C. J., Nolte, G., & Daffertshofer, A. (2007). Phase lag index: assessment of functional connectivity from multi channel EEG and MEG with diminished bias from common sources. *Hum Brain Mapp, 28*(11), 1178-1193.

Stam, C. J., & van Straaten, E. C. (2012). Go with the flow: use of a directed phase lag index (dPLI) to characterize patterns of phase relations in a large-scale model of brain dynamics. *Neuroimage, 62*(3), 1415-1428.

Stein, V., & Nicoll, R. A. (2003). GABA generates excitement. *Neuron, 37*(3), 375-378.

Steinberg, L. (2008). A Social Neuroscience Perspective on Adolescent Risk-Taking. *Dev Rev, 28*(1), 78-106.

Steinberg, L. (2010). A dual systems model of adolescent risk-taking. *Dev Psychobiol, 52*(3), 216-224.

Steinberg, L. (2013). The influence of neuroscience on US Supreme Court decisions about adolescents' criminal culpability. *Nat Rev Neurosci, 14*(7), 513-518.

Steinberg, L. (2014). *Age of Opportunity: Lessons from the New Science of Adolescence*: Houghton Mifflin Harcourt.

Steinberg, L., Albert, D., Cauffman, E., Banich, M., Graham, S., & Woolard, J. (2008). Age differences in sensation seeking and impulsivity as indexed by behavior and self-report: evidence for a dual systems model. *Dev Psychol, 44*(6), 1764-1778.

Stephenson, M. T., Hoyle, R. H., Palmgreen, P., & Slater, M. D. (2003). Brief measures of sensation seeking for screening and large-scale surveys. *Drug Alcohol Depend, 72*(3), 279-286.

Steriade, M. (2000). Corticothalamic resonance, states of vigilance and mentation. *Neuroscience, 101*(2), 243-276.

Steriade, M., Mccormick, D. A., & Sejnowski, T. J. (1993). Thalamocortical Oscillations in the Sleeping and Aroused Brain. *Science, 262*(5134), 679-685.

Stige, S., Fjell, A. M., Smith, L., Lindgren, M., & Walhovd, K. B. (2007). The development of visual P3a and P3b. *Dev Neuropsychol, 32*(1), 563-584.

Strüber, D., & Polich, J. (2002). P300 and slow wave from oddball and single-stimulus visual tasks: inter-stimulus interval effects. *Int J Psychophysiol, 45*(3), 187-196.

Sumich, A. L., Sarkar, S., Hermens, D. F., Ibrahimovic, A., Kelesidi, K., Wilson, D., & Rubia, K. (2012). Sex differences in brain maturation as measured using event-related potentials. *Dev Neuropsychol, 37*(5), 415-433.

Supekar, K., Musen, M., & Menon, V. (2009). Development of large-scale functional brain networks in children. *PLoS Biol, 7*(7), e1000157.

Suwazono, S., Machado, L., & Knight, R. T. (2000). Predictive value of novel stimuli modifies visual event-related potentials and behavior. *Clin Neurophysiol, 111*(1), 29-39.

Tamm, L., Menon, V., & Reiss, A. L. (2002). Maturation of brain function associated with response inhibition. *J Am Acad Child Adolesc Psychiatry, 41*(10), 1231-1238.

Teipel, S. J., Pogarell, O., Meindl, T., Dietrich, O., Sydykova, D., Hunklinger, U., . . . Hampel, H. (2009). Regional networks underlying interhemispheric connectivity: An EEG and DTI study in healthy ageing and amnestic mild cognitive impairment. *Human Brain Mapping, 30*(7), 2098-2119.

Thatcher, R. W., Biver, C., McAlaster, R., & Salazar, A. (1998). Biophysical Linkage between MRI and EEG Coherence in Closed Head Injury. *Neuroimage, 8*(4), 307-326.

Thatcher, R. W., Walker, R. A., & Giudice, S. (1987). Human cerebral hemispheres develop at different rates and ages. *Science, 236*(4805), 1110-1113.

Tiemeier, H., Lenroot, R. K., Greenstein, D. K., Tran, L., Pierson, R., & Giedd, J. N. (2010). Cerebellum development during childhood and adolescence: a longitudinal morphometric MRI study. *Neuroimage, 49*(1), 63-70.

Tong, S., & Thakor, N. V. (2009). *Quantitative EEG Analysis Methods and Clinical Applications* (1 ed.). Norwood: Artech House.

Torrence, C., & Compo, G. P. (1998). A Practical Guide to Wavelet Analysis. *Bulletin of the American Meteorological Society, 79*(1), 61-78.

Tsai, M. L., Hung, K. L., Tao-Hsin Tung, W., & Chiang, T. R. (2012). Age-changed normative auditory event-related potential value in children in Taiwan. *J Formos Med Assoc, 111*(5), 245-252.

Twomey, D. M., Murphy, P. R., Kelly, S. P., & O'Connell, R. G. (2015). The classic P300 encodes a build-to-threshold decision variable. *Eur J Neurosci, 42*(1), 1636-1643.

Uhlhaas, P. J., Linden, D. E., Singer, W., Haenschel, C., Lindner, M., Maurer, K., & Rodriguez, E. (2006). Dysfunctional long-range coordination of neural activity during Gestalt perception in schizophrenia. *J Neurosci, 26*(31), 8168-8175.

Uhlhaas, P. J., Roux, F., Singer, W., Haenschel, C., Sireteanu, R., & Rodriguez, E. (2009). The development of neural synchrony reflects late maturation and restructuring of functional networks in humans. *Proc Natl Acad Sci U S A, 106*(24), 9866-9871.

Uhlhaas, P. J., & Singer, W. (2011). The development of neural synchrony and large-scale cortical networks during adolescence: relevance for the pathophysiology of schizophrenia and neurodevelopmental hypothesis. *Schizophr Bull, 37*(3), 514-523.

Ursu, S., Clark, K. A., Aizenstein, H. J., Stenger, V. A., & Carter, C. S. (2009). Conflict-related activity in the caudal anterior cingulate cortex in the absence of awareness. *Biol Psychol, 80*(3), 279-286.

Vakorin, V. A., Lippe, S., & McIntosh, A. R. (2011). Variability of brain signals processed locally transforms into higher connectivity with brain development. *J Neurosci, 31*(17), 6405-6413.

Vakorin, V. A., McIntosh, A. R., Misic, B., Krakovska, O., Poulsen, C., Martinu, K., & Paus, T. (2013). Exploring age-related changes in dynamical non-stationarity in electroencephalographic signals during early adolescence. *PLoS One, 8*(3), e57217.

van Dinteren, R., Arns, M., Jongsma, M. L. A., & Kessels, R. P. C. (2014a). Combined frontal and parietal P300 amplitudes indicate compensated cognitive processing across the lifespan. *Frontiers in Aging Neuroscience, 6*(294).

van Dinteren, R., Arns, M., Jongsma, M. L. A., & Kessels, R. P. C. (2014b). P300 Development across the Lifespan: A Systematic Review and Meta-Analysis. *PLoS One, 9*(2), e87347.

van Duijvenvoorde, A. C., Peters, S., Braams, B. R., & Crone, E. A. (2016). What motivates adolescents? Neural responses to rewards and their influence on adolescents' risk taking, learning, and cognitive control. *Neurosci Biobehav Rev, 70*, 135-147.

van Noordt, S. J. R., Desjardins, J. A., Gogo, C. E. T., Tekok-Kilic, A., & Segalowitz, S. J. (2017). Cognitive control in the eye of the beholder: Electrocortical theta and alpha modulation during response preparation in a cued saccade task. *Neuroimage, 145*(Part A), 82-95.

van Straaten, E. C., den Haan, J., de Waal, H., van der Flier, W. M., Barkhof, F., Prins, N. D., & Stam, C. J. (2015). Disturbed phase relations in white matter hyperintensity based vascular dementia: an EEG directed connectivity study. *Clin Neurophysiol, 126*(3), 497-504.

Verleger, R. (1988). Event-related potentials and cognition: A critique of the context updating hypothesis and an alternative interpretation of P3. *Behavioral and Brain Sciences, 11*(3), 343-356.

Verleger, R., Gorgen, S., & Jaskowski, P. (2005). An ERP indicator of processing relevant gestalts in masked priming. *Psychophysiology, 42*(6), 677-690.

Verleger, R., Jaśkowski, P., & Wascher, E. (2005). Evidence for an Integrative Role of P3b in Linking Reaction to Perception. *Journal of Psychophysiology, 19*(3), 165-181.

Vinck, M., Oostenveld, R., van Wingerden, M., Battaglia, F., & Pennartz, C. M. (2011). An improved index of phase-synchronization for electrophysiological data in the presence of volume-conduction, noise and sample-size bias. *Neuroimage, 55*(4), 1548-1565.

Vogel, E. K., & Luck, S. J. (2000). The visual N1 component as an index of a discrimination process. *Psychophysiology, 37*(2), 190-203.

von Stein, A., Chiang, C., & Konig, P. (2000). Top-down processing mediated by interareal synchronization. *Proc Natl Acad Sci U S A, 97*(26), 14748-14753.

von Stein, A., & Sarnthein, J. (2000). Different frequencies for different scales of cortical integration: from local gamma to long range alpha/theta synchronization. *Int J Psychophysiol, 38*(3), 301-313.

Wahl, S., Michel, C., Pauen, S., & Hoehl, S. (2013). Head and eye movements affect object processing in 4-month-old infants more than an artificial orientation cue. *Br J Dev Psychol, 31*(Pt 2), 212-230.

Wang, J., Gao, D., Li, D., Desroches, A. S., Liu, L., & Li, X. (2014). Theta-gamma coupling reflects the interaction of bottom-up and top-down processes in speech perception in children. *Neuroimage, 102 Pt 2*, 637-645.

Werkle-Bergner, M., Shing, Y. L., Müller, V., Li, S.-C., & Lindenberger, U. (2009). EEG gamma-band synchronization in visual coding from childhood to old age: Evidence from evoked power and inter-trial phase locking. *Clinical Neurophysiology, 120*(7), 1291-1302.

Wessel, J. R., Danielmeier, C., Morton, J. B., & Ullsperger, M. (2012). Surprise and error: common neuronal architecture for the processing of errors and novelty. *J Neurosci, 32*(22), 7528-7537.

Wetzel, N., Schroger, E., & Widmann, A. (2016). Distraction by Novel and Pitch-Deviant Sounds in Children. *Front Psychol, 7*, 1949.

Wetzel, N., Widmann, A., Berti, S., & Schroger, E. (2006). The development of involuntary and voluntary attention from childhood to adulthood: a combined behavioral and event-related potential study. *Clin Neurophysiol, 117*(10), 2191-2203.

White, C. N., Mumford, J. A., & Poldrack, R. A. (2012). Perceptual Criteria in the Human Brain. *The Journal of Neuroscience, 32*(47), 16716-16724.

Whitford, T. J., Rennie, C. J., Grieve, S. M., Clark, C. R., Gordon, E., & Williams, L. M. (2007). Brain maturation in adolescence: concurrent changes in neuroanatomy and neurophysiology. *Hum Brain Mapp, 28*(3), 228-237.

Windmann, S., Wehrmann, M., Calabrese, P., & Gunturkun, O. (2006). Role of the prefrontal cortex in attentional control over bistable vision. *J Cogn Neurosci, 18*(3), 456-471.

Wittmann, B. C., Bunzeck, N., Dolan, R. J., & Düzel, E. (2007). Anticipation of novelty recruits reward system and hippocampus while promoting recollection. *Neuroimage, 38*(1-9), 194-202.

Wrobel, A. (2000). Beta activity: a carrier for visual attention. *Acta Neurobiol Exp (Wars), 60*(2), 247-260.

Wronka, E., Kaiser, J., & Coenen, A. M. (2012). Neural generators of the auditory evoked potential components P3a and P3b. *Acta Neurobiol Exp (Wars), 72*(1), 51-64.

Yamaguchi, S., & Knight, R. T. (1991). Anterior and posterior association cortex contributions to the somatosensory P300. *J Neurosci, 11*(7), 2039-2054.

Yordanova, J., Falkenstein, M., Hohnsbein, J., & Kolev, V. (2004). Parallel systems of error processing in the brain. *Neuroimage, 22*(2), 590-602.

Yordanova, J., & Kolev, V. (1997). Developmental changes in the event-related EEG theta response and P300. *Electroencephalogr Clin Neurophysiol, 104*(5), 418-430.

Yordanova, J., & Kolev, V. (1998). Developmental changes in the theta response system: a single sweep analysis. *Psychophysiology, 12*, 113-126.

Yordanova, J., & Kolev, V. (2009). Event-Related Brain Oscillations. *Journal of Psychophysiology, 23*(4), 174-182.

Yordanova, J., & Kolev, V. N. (1996). Developmental changes in the alpha response system. *Electroencephalogr Clin Neurophysiol, 99*(6), 527-538.

Yuan, J., Ju, E., Yang, J., Chen, X., & Li, H. (2014). Different patterns of puberty effect in neural oscillation to negative stimuli: sex differences. *Cogn Neurodyn, 8*(6), 517-524.

Zanto, T. P., & Gazzaley, A. (2013). Fronto-parietal network: flexible hub of cognitive control. *Trends Cogn Sci, 17*(12), 602-603.

Zanto, T. P., Rubens, M. T., Thangavel, A., & Gazzaley, A. (2011). Causal role of the prefrontal cortex in top-down modulation of visual processing and working memory. *Nat Neurosci, 14*(5), 656-661.

Zimring, F. E. (1998). Toward a Jurisprudence of Youth Violence. *Crime and Justice, 24*, 477-501.

Zschocke, S. (2012). *Klinische Elektroenzephalographie* (3 ed.). Heidelberg: Springer-Verlag.

Zuckerman, M. (1994). *Behavioral Expressions and Biosocial Bases of Sensation Seeking*. New York: Cambridge University Press.

Acknowledgements

This work would not have become what it is without a great number of people supporting me.

First of all, I would like to express my sincere gratitude to my supervisors PD Dr. Birgit Mathes and Prof. Dr. Canan Başar-Eroğlu for granting me the opportunity to conduct my Ph.D. at the Institute of Psychology and Cognition Research (IPK) of the University of Bremen. I would like to thank both, for their extraordinary support, their endless encouragement and their strong belief in my abilities. The advice and care of Prof. Dr. Canan Başar-Eroğlu has always been of great help. I cannot thank PD Dr. Birgit Mathes enough for her enormous help throughout the entire time of the Ph.D. No question was left unanswered and she has always been there for me supporting and guiding me to become a better scientist.

Furthermore, I would like to thank the University of Bremen for financial support. I am very grateful for the scholarship and the opportunity to discuss my data with the scientific community.

Special thanks are directed to Prof. Dr. Dr. Gerhard Roth, Gisela Gründl, Anja Krüger and Henrike Welpinghus for the chance to get in contact with several schools and teachers in order for PD Dr. Birgit Mathes and me to lecture about brain development and further, enabling us to recruit children and adolescents for our study.

I would like to thank all participants for their interest in our study and their motivated involvement. Also, I would like to thank all children and their parents for their great commitment even on weekends and holidays.

Thank you to all members of the IPK for the extraordinary atmosphere of this institute:
Prof. Dr. Christina Schmiedt-Fehr, Prof Dr. Dietmar Heubrock, Dr. Andreas Brand, Evgenij

Coromaldi, Christiane Degering-Machirus, Edwin Hoff, Janna Krauss, Prof. Dr. Gerhard Meyer, Dr. Tobias Hayer, Tim Brosowski, Marc von Meduna.

Great thanks to Wilfried Alexander for all the technical support inside and outside of the institute, for all the entertainment and his great (technical) gadgets.

Thank you to Dr. Linda Rürup for the company, all the nice talks and the great support she offered me.

I would also like to mention Dr. Ksenia Khalaidovski and thank her for the opportunity to directly start working with EEG data of a great sample, which has helped to form a profound fundament for this thesis.

Great thanks to Prof. Dr. John Polich for help with the study design based on his many years of experience with the Oddball task.

Finally, I would like to thank my family, my friends and Stefan for always supporting me through thick and thin days despite the rare visits, the constant lack of time and the increasing tension.

Declaration of authorship

Eidesstattliche Erklärung

gem. §6 Absatz 5 der Promotionsordnung Dr.rer.nat. des Fachbereichs 11

der Universität Bremen vom 06.07.2011

Hiermit versichere ich, dass die Arbeit ohne unerlaubte fremde Hilfe angefertigt wurde, keine anderen als die angegebenen Quellen und Hilfsmittel benutzt wurden und die den benutzten Werken wörtlich oder inhaltlich entnommenen Stellen als solche kenntlich gemacht worden sind.

Bremen, 10.01.2018

_____

Annika S. Wienke